AD-A085 128 CALIFORNIA UNIV LIVERMORE LAWRENCE LIVERMORE LAB F/G 21/5
POTENTIAL ENVIRONMENTAL EFFECTS OF AIRCRAFT EMISSIONS.(U)
OCT 79 F M LUTHER, J S CHANG, W H DUEWER W-7405-ENG-48
UNCLASSIFIED UCRL-52861 FAA/EE-79-23 NL

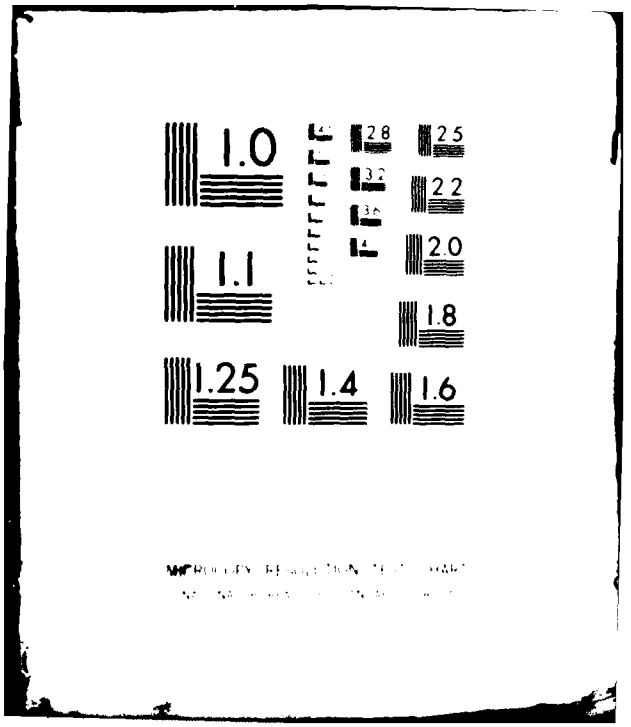
1.0
1.1
1.25
1.4
1.6
1.8
2.0
2.2
2.5
2.8
3.2
3.6

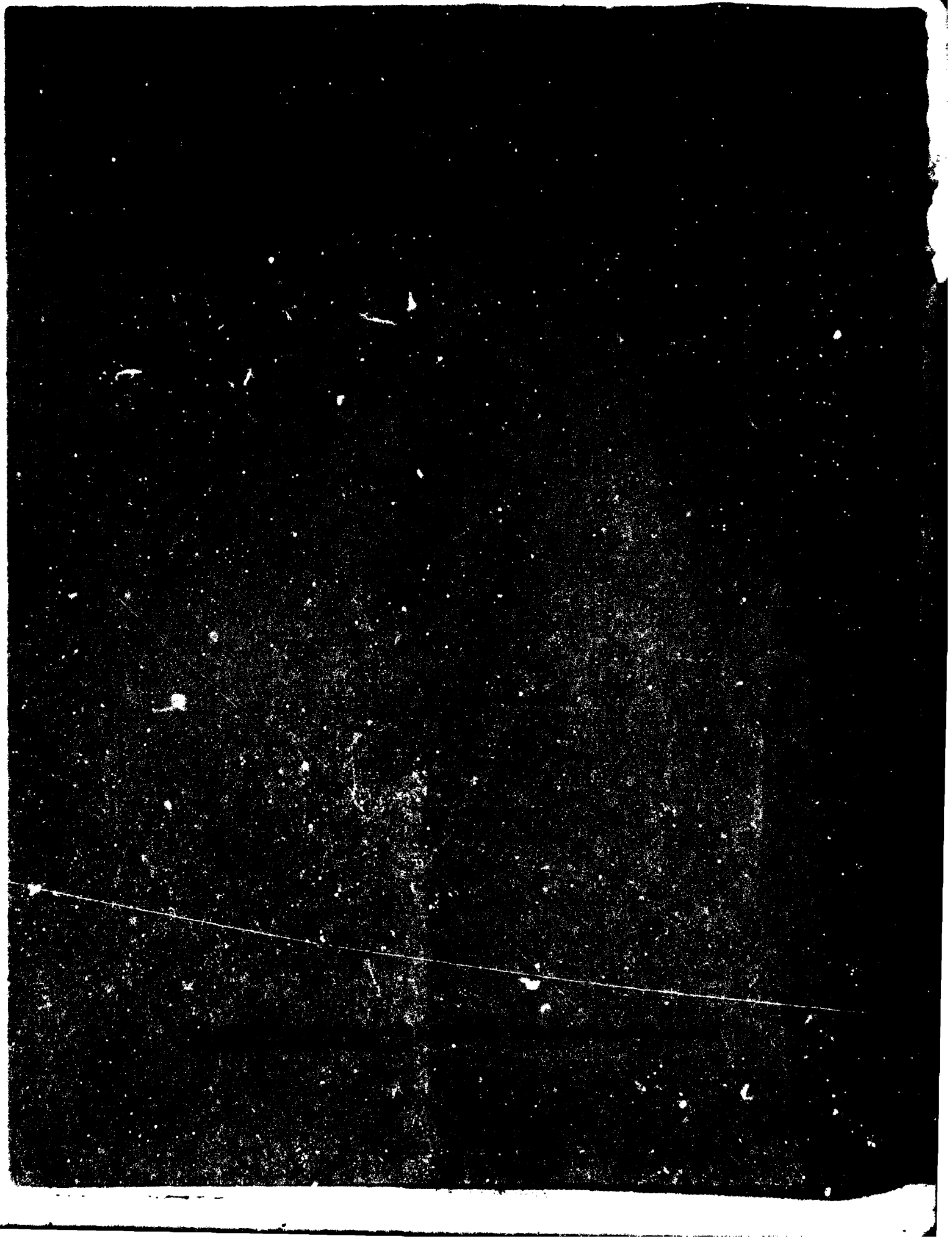

Technical Report Documentation Page

1. Report No.	2. Government Accession No.	3. Recipient's Catalog No.
(19) (18) FAA-EE-79-23	AD-A085 128	

4. Title and Subtitle	5. Report Date
(6) Potential Environmental Effects of Aircraft Emissions	October 15, 1979
	6. Performing Organization Code

7. Author(s)	8. Performing Organization Report No.
(10) F.M. Luther, J.S. Chang, W.H. Duewer, J.E. Penner, R.L. Tarp, and D.J. Wuebbles	(14) UCRL-52861

9. Performing Organization Name and Address	10. Work Unit No. (TRAIS) / 11. Contract or Grant No.
Lawrence Livermore Laboratory University of California Livermore, California 94550	(15) W-7405-eng-48, DOT-FA79WAI-034

12. Sponsoring Agency Name and Address	13. Type of Report and Period Covered
U.S. Department of Transportation, Federal Aviation Administration, Office of Environment and Energy, High Altitude Pollution Program Washington, D.C. 20591	(9) Final Report,
(11) 15 Oct 79	14. Sponsoring Agency Code (12) 234

15. Supplementary Notes

16. Abstract

An assessment is provided of the potential environmental effects of fleets of subsonic, supersonic, and hypersonic aircraft. A general discussion of photochemical and transport modeling techniques is included along with a description of the LLL one-dimensional transport-kinetics model that was used in the assessment. Model simulations of the natural and perturbed stratosphere are used to compare theory with observations as a means of verification of model processes. A review is provided of engine emission indexes amd 1990 fleet projections. Assessments of the potential effects of subsonic and supersonic aircraft fleets indicate a small increase in total ozone. However, the change in total ozone is the net difference between regions of ozone increase (in the lower stratosphere and upper troposphere) and ozone decrease (in the upper stratosphere). The percent change in the local ozone concentration is much larger than the change in total ozone. The effect of a proposed hydrogen fueled hypersonic transport fleet is a small reduction in total ozone. A study is made of the effect on these results of uncertainties in chemical rate coefficients, speculative chemical reactions, temperature feedback, hydrostatic adjustment, and various model parameters. The potential effect on ozone of aircraft emissions is compared with potential changes due to other anthropogenic perturbations.

17. Key Words	18. Distribution Statement
Ozone perturbations, Climate perturbations, NO_x injections, Stratospheric model, Aircraft emissions	Available to the public through National Technical Information Service, Springfield, Virginia 22161.

19. Security Classif. (of this report)	20. Security Classif. (of this page)	21. No. of Pages	22. Price
Unclassified	Unclassified	234	

Form DOT F 1700.7 (8-72) Reproduction of completed page authorized

390999

UCRL-52861
Distribution Category UC-11

Potential environmental effects of aircraft emissions

F. M. Luther
J. S. Chang
W. H. Duewer
J. E. Penner
R. L. Tarp
D. J. Wuebbles

Manuscript date: October 15, 1979

LAWRENCE LIVERMORE LABORATORY
University of California • Livermore, California • 94550

Available from: National Technical Information Service • U.S. Department of Commerce
5285 Port Royal Road • Springfield, VA 22161 • $14.00 per copy • (Microfiche $3.50)

ABSTRACT

An assessment is provided of the potential environmental effects of fleets of subsonic, supersonic, and hypersonic aircraft. A general discussion of photochemical and transport modeling techniques is included along with a description of the LLL one-dimensional transport-kinetics model that was used in the assessment. Model simulations of the natural and perturbed stratosphere are used to compare theory with observations as a means of verification of model processes. A review is provided of engine emission indexes and 1990 fleet projections. Assessments of the potential effects of subsonic and supersonic aircraft fleets indicate a small increase in total ozone. However, the change in total ozone is the net difference between regions of ozone increase (in the lower stratosphere and upper troposphere) and ozone decrease (in the upper stratosphere). The percent change in the local ozone concentration is much larger than the change in total ozone. The effect of a proposed hydrogen fueled hypersonic transport fleet is a small reduction in total ozone. A study is made of the effect on these results of uncertainties in chemical rate coefficients, speculative chemical reactions, temperature feedback, hydrostatic adjustment, and various model parameters. The potential effect on ozone of aircraft emissions is compared with potential changes due to other anthropogenic perturbations.

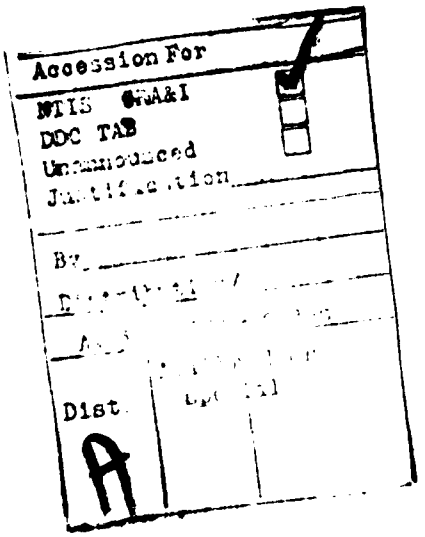

CONTENTS

	Page
ABSTRACT	ii
ACKNOWLEDGMENTS	v
EXECUTIVE SUMMARY	vi
1. INTRODUCTION	1
2. COUPLED TRANSPORT AND CHEMICAL KINETICS MODELS	3
2.1 Chemistry of the Stratosphere	4
2.2 Modeling Photochemical and Transport Processes	9
Classification of Models	11
Transport Representation	13
Radiative Processes	15
Physical Domain and Boundary Conditions	18
Averaging Processes	19
Sources and Sinks	19
Other Physical Data	20
Time-Dependent and Steady-State Solutions	20
3. MODEL SIMULATIONS OF STRATOSPHERIC OBSERVATIONS	21
3.1 Stratospheric Composition	21
$O(^3P)$	22
O_3	22
OH, HO_2	23
NO	24
NO_2	26
HNO_3	27
Total NO_y	27
HNO_3/NO_2	30
N_2O_5	31
Cl, ClO	31
Cl/ClO Ratio	33
HCl	33
$ClONO_2$	34
Total ClX	36
3.2 Model Simulations of Past Perturbations	37
Possible Long-Term Solar Variations and the Effects on Temperature and Ozone	37
The Atmospheric Nuclear Tests of the 1950's and 1960's	38
Polar Cap Absorption Events	41
The Solar Eclipse on February 26, 1979	42

		Page
4.	POTENTIAL CHANGES IN OZONE CAUSED BY AIRCRAFT EMISSIONS	44
4.1	Emission Indexes and Fleet Projections	44
	1990 Fleets	44
	SST Fleets of Commercially Viable Size	45
	Hypersonic Transport Emissions	46
4.2	Current Assessment Results	48
	Subsonic and Supersonic Aircraft Fleets	49
	Hypersonic Transport Fleet	56
4.3	Sensitivity Studies	57
	Effect of Variations in K_z	57
	Effect of Variations in Background ClX	59
	Effects of Speculative Reactions and Mechanisms	60
	Effects of Uncertainties in Chemical Rate Coefficients	71
	Effect of Temperature Feedback and Hydrostatic Adjustment	73
4.4	Comparison with Other Results	81
5.	POTENTIAL CHANGES IN OZONE RESULTING FROM OTHER PERTURBATIONS	86
5.1	Chlorofluoromethanes	86
5.2	Change in Stratospheric H_2O	93
5.3	Increase in N_2O	99
5.4	Doubling of CO_2	102
5.5	Increase in CH_3CCl_3	105
	REFERENCES	108
	APPENDIX A. Description of the LLL One-Dimensional Transport-Kinetics Model	117
	APPENDIX B. Effect of Changes in Ozone on UV Dose and Skin Cancer Incidence	139
	APPENDIX C. Potential Climatic Effects of Stratospheric Perturbations	151
	APPENDIX D. The Relation Between Atmospheric Trace Species Variabilities and Solar UV Variability	161
	APPENDIX E. A Theoretical Study of Stratospheric Trace Species Variations During a Solar Eclipse	181
	APPENDIX F. The Atmospheric Nuclear Tests of the 1950's and 1960's: A Possible Test of Ozone Depletion Theories	190

ACKNOWLEDGMENTS

This document was prepared for the High Altitude Pollution Program of the Federal Aviation Administration's Office of Environment and Energy. This work was performed under the auspices of the U. S. Department of Energy by the Lawrence Livermore Laboratory under contract No. W-7405-Eng-48, and supported in part by the High Altitude Pollution Program of the Federal Aviation Administration under contract DOT-FA79WAI-034.

EXECUTIVE SUMMARY

The purpose of this report is to review the major changes in the aircraft emission assessments since the end of the Climatic Impact Assessment Program in 1975 and to provide a comprehensive discussion of the current modeling results. Assessments are made of the potential effects of subsonic and supersonic aircraft fleets and of a proposed hydrogen-fueled hypersonic transport fleet. Studies are made of the effects on the results of uncertainties in chemical rate coefficients, vertical transport coefficients, speculative chemical reactions, temperature feedback, hydrostatic adjustment, and various model parameters. A summary of the conclusions and recommendations resulting from these studies follows.

Assessment Results

- Subsonic aircraft fleets projected for the year 1990 are estimated to cause an increase in hemispheric mean total ozone of nearly 2%. Because of uncertainties in the treatment of poorly understood phenomena in the troposphere, these results are suggestive but not definitive.
- Supersonic transport fleets of commercially viable size are estimated to cause an increase in total ozone of less than 1.5%, depending on the altitude of injection, the NO_x emission index, and a number of model parameters (see below).
- Emissions from a hypothesized commercially viable fleet of hypersonic transports are estimated to cause up to a 2% reduction in total ozone.
- For subsonic and supersonic transport fleets, reductions in the NO_x emission rate have a greater effect on ΔO_3 than does a similar percent reduction of the H_2O emission rate.
- The increase in total ozone caused by an NO_x injection increases as the background ClX concentration increases.
- An analysis of the effect on model sensitivity of speculative reactions and photochemical mechanisms not included in the basic model shows that it is plausible that stratospheric injections of NO_x could lead to a slight decrease in total ozone rather than an increase as predicted with the

current model. These speculative reactions and mechanisms, although plausible, are not highly probable, but the fact that they have a significant effect on model sensitivity indicates that they are worthy of careful attention and further study.

- Changes in evaluated recommendations for chemical rate coefficients over the last five years have resulted in substantial changes in the model-predicted response to perturbations. Even recent rate recommendations appearing a few months apart carry a significant amount of uncertainty. The uncertainty limits for reactions in the various evaluations have generally become smaller when individual reactions are considered. However, over the same time period, new and often highly uncertain reactions have been recognized, and it is far from obvious that the error that might be associated with reactions actually included in models has gotten smaller over the last decade. Moreover, new reactions have been introduced to the models at a fluctuating but not obviously decreasing rate. Thus, past variations in model predictions may provide a reasonable estimator of the magnitude of possible future variations in similar predictions.
- Temperature feedback and hydrostatic adjustment have a small, but not insignificant, effect on the computed change in total ozone. Both of these feedback mechanisms tend to increase the value of ΔO_3 when the net effect is an increase in total ozone. Temperature feedback and hydrostatic adjustment have a much more significant effect on the computed change in local ozone concentration, particularly at higher altitudes (>35 km). This has important implications for monitoring programs that are directing their attention to certain altitude regions as a means of detecting early trends in ozone due to anthropogenic perturbations.

Model Comparisons with Observational Data

- There is good agreement between model-calculated distributions of $O(^3P)$ and the few available measurements.

- The unperturbed O_3 profile computed by the model falls within the range of rocket and balloon measurements at middle latitudes.
- There appears to be reasonable agreement between theoretical calculations and the few available measurements of OH and HO_2 in the stratosphere. Comparison of the total OH column does not indicate significant differences in annual-average column content.
- Theoretical models calculate approximately a factor of 2 more NO_y at high altitude than has been measured. Part of the reason for this difference (among others) may be that the model predicts too much N_2O in the upper stratosphere.
- The single observed Cl profile and calculated Cl profiles agree within the measurement uncertainty. However, the measurements suggest a larger vertical gradient in Cl mixing ratio than is calculated.
- At the ClO mixing ratio maximum, most measurements are within a factor of 2 of the model prediction. One resonance fluorescence measurement gives six times more ClO than is predicted. The measurements also show a sharper than predicted decrease in ClO below the peak.
- Except for three measurements of ClO taken in summer, there does not appear to be any large discrepancy between the total amount of ClX predicted and that observed. However, the summer measurements of ClO are so large as to require much more total ClX than known sources are capable of producing.
- Model simulations of various natural and man-made perturbations to stratospheric ozone give results that are not inconsistent with the observational record.
- Although there are individual disagreements between model-calculated species profiles and measurements that still need to be examined, on balance we believe the model adequately represents the stratosphere. The disagreements point to uncertainties in the model representation of the stratosphere. The large amount of data that agree indicates that the model is doing rather well. In doing assessments, we need to understand what effect the model uncertainties have on the predictions. Consequently, sensitivity studies are an important aspect of the overall effort.

- Calculations of the effect of a reduction in total ozone (ΔO_3) on the erythema dose at the earth's surface show an amplification factor ($\Delta dose/\Delta O_3$) of 1.3-1.4 at low latitudes (where the erythema dose is greatest), 1.6-2.0 at middle latitudes, and approximately 3 at high latitudes.
- An analysis of skin cancer incidence data from several countries (Cutchis, 1978) shows that the etiology of malignant melanoma is in a chaotic state. The anatomic site behavior, age dependence, geographical location, and relative rates of incidence in males and females suggest the existence of two carcinogen agents, neither of which is solar ultraviolet radiation.
- None of the SST engine emissions (NO_x, H_2O, and SO_2) are estimated to have a major climatic effect. Water vapor has the largest individual effect on surface temperature.

1. INTRODUCTION

In 1970 and 1971, the U. S. Congress conducted a major reassessment of the U.S. supersonic transport (SST) development program. There was considerable controversy over the potential environmental effects of SST fleet operations. The concerns were related to the effects stratospheric aircraft emissions might have on stratospheric ozone, which shields the earth's surface from harmful levels of ultraviolet solar radiation, and on the climate. Initial chemical and climatic concerns were related to water vapor emissions, but these concerns shifted to emphasize oxides of nitrogen (Crutzen, 1970), which were postulated to cause substantial catalytic destruction of ozone (Johnston, 1971; Crutzen, 1972). Estimates of the ozone depletion that might arise from large SST fleet operations ranged from 3 to 50%, depending on assumptions.

Although the U. S. SST development program was canceled, the issues and the scientific problems remained. Recognizing that SSTs were being developed in other countries and that new SSTs might be developed in the U.S. in the future, the Climatic Impact Assessment Program (CIAP) was implemented by the U.S. Department of Transportation to clarify the potential environmental effects of aircraft operation in the stratosphere. The goal of this three-year program was to assess, in a series of monographs to be prepared by 1975, the potential chemical, climatic, biological, and economic effects of stratospheric aircraft emissions.

The CIAP Report of Findings (Grobecker et al., 1974) was delivered to Congress in February 1975. In addition to the CIAP studies, a concurrent and independent study was conducted by the Climatic Impact Committee of the National Academy of Sciences, and their report was distributed in April 1975 (National Research Council, 1975a). Independent studies were also carried out in Europe by the British (COMESA, 1976) and by the French (COVOS, 1976).

The conclusions of the CIAP and NRC studies were similar, although there were differences in the estimated magnitudes of the environmental effects. Large-scale aircraft operations in the stratosphere were concluded to possibly lead to unacceptable reductions in stratospheric ozone. Most of the ozone reduction was estimated to be caused by nitrogen oxide emissions with a very small effect due to water vapor emissions. The climatic effects were considered to be potentially

significant but highly uncertain. The skin cancer incidence rate was estimated to increase about 2% for each 1% reduction in the ozone column.

In 1975 the High Altitude Pollution Program (HAPP) was initiated by the Federal Aviation Administration to extend the investigations carried out during CIAP so as to ensure that stratospheric aircraft emissions will not result in unacceptable environmental effects. Lawrence Livermore Laboratory (LLL) has been an active participant in both the CIAP and HAPP programs, having undertaken an extensive effort in numerical modeling of the atmospheric response to stratospheric perturbations. In addition to addressing the issue of engine emissions, the LLL numerical models have also been applied to other proposed threats to stratospheric ozone (e.g., chlorofluoromethanes (CFMs) and increased N_2O), thereby focusing on the overall problem of stratospheric chemistry and combined effects.

The purpose of this report is to review the major changes in the aircraft emission assessments since the end of CIAP and to provide a comprehensive discussion of the current modeling assessment. A general discussion of photochemical and transport modeling techniques is included along with a description of the LLL one-dimensional transport-kinetics model that was used in the assessment. Model simulations of the natural and perturbed stratosphere are included to compare theory with observations as a means of verification of model processes. Assessments are made of the potential effects of subsonic and supersonic aircraft fleets and of a proposed hydrogen-fueled hypersonic transport fleet. Studies are made of the effects on the results of uncertainties in chemical rate coefficients, vertical transport coefficients, speculative chemical reactions, temperature feedback, hydrostatic adjustment, and various model parameters. The potential effect on ozone of aircraft emissions is compared with potential changes due to other anthropogenic perturbations. The appendices contain more detailed technical discussions of some of the material contained in the main body of the report.

2. COUPLED TRANSPORT AND CHEMICAL KINETICS MODELS

Models of stratospheric chemistry have been primarily directed toward an understanding of the behavior of stratospheric ozone. Initially this interest reflected the diagnostic role of ozone in the understanding of atmospheric transport processes. More recently, interest in stratospheric ozone has arisen from concern that human activities might affect the amount of stratospheric ozone, thereby affecting the ultraviolet radiation reaching the earth's surface and perhaps also affecting the climate (Johnston, 1971; Crutzen, 1972; National Research Council, 1975a, 1975b, 1976a, 1976b; CIAP Monograph 5, 1975; Grobecker et al., 1974; Hudson, 1977), with various potentially severe consequences for human welfare. This concern has inspired a substantial effort to develop both diagnostic and prognostic models of stratospheric ozone.

The first quantitative model of stratospheric ozone was developed by Chapman (1930). Chapman's model calculated the ozone distribution on the basis of a pure oxygen atmosphere using a simple equilibrium model. During the 1930's and 1940's, pure oxygen models of the stratosphere were further developed (Mecke, 1931; Dutsch, 1946). However, as more information about the vertical and latitudinal distribution of ozone became available and the relevant reaction coefficients and photolysis cross sections for O_2 and O_3 were more accurately measured, it became clear that pure oxygen models failed to accurately predict the atmospheric behavior of ozone (Brewer and Wilson, 1968; Hunt, 1966a). In attempts to explain this disagreement with observations, the reactions of excited states of oxygen atoms and oxygen molecules were considered and rejected as inadequate to explain the discrepancy (Brewer and Wilson, 1968), and the reactions of ozone and oxygen atoms with hydrogen-containing compounds were considered (Bates and Nicolet, 1950; Hampson, 1964; Hunt, 1966b; Dutsch, 1968; Hesstvedt, 1968; Leovy, 1969; Crutzen, 1969). When measurements of the rates of reaction of odd hydrogen species (H, OH, HO_2) with odd oxygen species (O, O_3) were made available in the late 1960's, it appeared that another loss process was needed. Crutzen (1970) and Johnston (1971, 1972) recognized the important role of the oxides of nitrogen (NO_x) in regulating stratospheric ozone, and Nicolet (1970) recognized the reaction of $O(^1D)$ with N_2O as a natural source of NO_x in the stratosphere. Stolarski and Cicerone (1974) first postulated the potential role of chlorine in influencing ozone, and

Rowland and Molina (1975) found that halogenated organic molecules (especially the chlorofluoromethanes) could act as sources of stratospheric chlorine. More recently, it has been suggested that bromine might also affect stratospheric ozone if a significant source were to exist (Wofsy et al., 1975).

2.1 CHEMISTRY OF THE STRATOSPHERE

Understanding of the chemical processes and cycles in the stratosphere has evolved rapidly over the past several years (Chang and Duewer, 1979). This section describes some of the chemical processes that are currently thought to be among the most important in determining or affecting stratospheric ozone concentrations. Chemical reactions in the following discussion will be referred to according to the numbering sequence in Table A-2 of Appendix A. The numbering sequence for photolysis reactions corresponds to Table A-4 of Appendix A.

The reaction

(J1) $O_2 + h\nu \rightarrow 2O$

is the primary process in the production of odd-oxygen species in the stratosphere. The reactions

(2) $O + O_3 \rightarrow 2O_2$,

(1) $O + O_2 + M \rightarrow O_3 + M$,

(J2) $O_3 + h\nu \rightarrow O + O_2$,

and

(J3) $O_3 + h\nu \rightarrow O(^1D) + O_2$

serve to interconvert the various odd-oxygen species ($O(^1D)$, O, O_3), and they help to limit the ozone (hence odd-oxygen) concentration. This set of reactions alone does not lead to the observed ozone concentrations, however. These reactions, first suggested by Chapman (1930), and some comparatively minor reactions involving excited oxygen species lead in a one-dimensional model to a stratospheric ozone column that is about twice the observed (see Table 1). Because

TABLE 1. Ozone columns calculated neglecting various families of chemical species. (Source: Chang and Duewer, 1979)

Families of Species Neglected*	Ozone Column (molecules/cm^2)	Altitude of O_3 Maximum (km)
None (reference model)**	8.77×10^{18}	24
ClX family neglected	9.44×10^{18}	24
HO_x family neglected	8.26×10^{18}	24
NO_x family neglected	6.25×10^{18}	28
HO_x and ClX families neglected	8.31×10^{18}	24
NO_x and ClX families neglected	9.79×10^{18}	26
NO_x and HO_x families neglected	7.53×10^{18}	25
NO_x, HO_x and ClX families	16.06×10^{18}	23

*Families were neglected by setting the concentrations of species in the family and all their source species equal to zero.

**The reference model contains 18 ppb NO_x, 1 ppb HO_x, and 1.5 ppb ClX at 35 km. (NO_x = NO + NO_2 + HNO_3 + 2 x N_2O_5 + $ClNO_3$; HO_x = OH + HO_2 + 2 x H_2O_2; ClX = Cl + ClO + HCl). The model chemistry is that described in Luther (1978).

ozone destruction via the Chapman cycle is approximately proportional to the square of the ozone concentration, this set of reactions accounts for roughly only 25% of the actual ozone sink.* In order to account for the rest of the ozone loss, it is necessary to consider several other processes that can destroy odd-oxygen.

Odd-hydrogen species (HO_x, e.g. H, OH, and HO_2) can destroy odd-oxygen while being themselves regenerated (i.e., catalytically destroy odd-oxygen) via several reaction sequences. Examples of reaction sequences leading to net odd-oxygen loss include:

*Since ozone is the overwhelming component of odd-oxygen and it is always in chemical equilibrium with $O(^1D)$ and O, for many discussions it is convenient to refer to ozone destruction rather than odd-oxygen destruction for the sake of brevity.

(13) $O + HO_2 \rightarrow OH + O_2$
(11) $O + OH \rightarrow H + O_2$
(14) $H + O_2 + M \rightarrow HO_2 + M$

net $O + O \rightarrow O_2$,

(11) $O + HO \rightarrow H + O_2$
(15) $H + O_3 \rightarrow OH + O_2$

net $O + O_3 \rightarrow 2O_2$,

(10) $OH + O_3 \rightarrow HO_2 + O_2$
(12) $HO_2 + O_3 \rightarrow OH + 2O_2$

net $O_3 + O_3 \rightarrow 3O_2$;

and

(9) $O(^1D) + H_2O \rightarrow 2OH$
(10) $OH + O_3 \rightarrow HO_2 + O_2$
(17) $OH + HO_2 \rightarrow H_2O + O_2$

net $O(^1D) + O_3 \rightarrow 2O_2$

Each of these catalytic cycles involves only hydrogen-containing chemical species. The last sequence is of interest in that the first reaction generates odd-hydrogen radicals from water and the last reaction converts them back into water. Water is not normally treated as part of odd-hydrogen. For odd-hydrogens, reaction (17) is considered to be a major termination step that limits the abundance of reactive odd-hydrogen species in the stratosphere. This reaction, therefore, decreases the overall efficiency of the HO_x in destroying odd-oxygen. In doing so, the participation of reaction (17) in this particular chain nevertheless contributes to some net odd-oxygen destruction. Analysis of chemical interactions via catalytic cycles provides a basis for understanding the physical processes leading to the final observables such as the stratospheric column density of ozone, but it does not quantify the relative strength of particular reaction pathways.

The odd-nitrogen species (NO_x, e.g. N, NO, and NO_2) can catalytically destroy odd-oxygen by a number of reaction sequences such as:

(3) $NO + O_3 \rightarrow NO_2 + O_2$
(4) $NO_2 + O \rightarrow NO + O_2$

net $O + O_3 \rightarrow 2O_2$

and

(28) $NO_2 + O_3 \rightarrow NO_3 + O_2$
(J20) $NO_3 + h\nu \rightarrow NO + O_2$
(3) $NO + O_3 \rightarrow NO_2 + O_2$

net $O_3 + O_3 \rightarrow 3O_2$.

Odd-chlorine species (ClX, e.g. Cl and ClO) can catalytically destroy odd-oxygen via reaction sequences such as:

(33) $Cl + O_3 \rightarrow ClO + O_2$
(35) $ClO + O \rightarrow Cl + O_2$

net $O + O_3 \rightarrow 2O_2$.

The above catalytic cycles are neither exhaustive nor unique. Many others may be identified from the list of reactions in Tables A-2 and A-4.

In addition to these catalytic cycles resulting in net odd-oxygen loss, there are null cycles (do-nothing cycles). Reaction (3) $NO + O_3 \rightarrow NO_2 + O_2$ followed by (J4) $NO_2 + h\nu \rightarrow NO + O$ instead of (4) will lead to no net change in odd-oxygen. Similarly, reaction (33) $Cl + O_3 \rightarrow ClO + O_2$ followed by (J12) $ClO + h\nu \rightarrow Cl + O$ instead of (35) will also lead to no net change in odd-oxygen. These null cycles compete with the catalytic destruction cycles, thereby diminishing the effectiveness of individual families of chemical species (NO_x, HO_x, and ClX) in destroying odd-oxygen. As it turns out, most of the NO_2 formed from reaction (3) or any other path returns via photolysis of NO_2. Hence, the null cycle involving

reaction (J4) is very effective in controlling the efficiency of NO_x catalytic destruction of odd-oxygen. Null cycles involving ClO photolysis are not very effective since the reaction rate for (J12) is much smaller than that of (35). Consequently, ClX catalytic cycles are affected little by the presence of null cycles within the ClX family. The case for the HO_x family is similar.

The strength of catalytic destruction cycles can be reduced by removing the catalysts. This is accomplished through the formation of relatively inactive "reservoir" species from more active species. Examples of this include formation of nitric acid, chlorine nitrate, hydrochloric acid, water, hydrogen peroxide, and pernitric acid through reactions such as (18), (37), (45), (41), (19), (17), and (56). These more stable species can regenerate the active species slowly. In fact, these "reservoir" species are often the most abundant members within individual families of species. Transport out of the stratosphere serves as a major sink for these "reservoir" species and indirectly as a loss for the active species.

There are important coupling interactions among the chemical families that affect ozone. An analysis of models with computed ambient levels of HO_x, NO_x, or ClX separately (all roughly consistent with measured stratospheric concentrations) shows that any one of the three families of species could lead to an ozone column no more than 20% larger than the observed column, and no one family is of primary importance in determining the column (Table 1). In fact, computations with either ClX or NO_x alone (plus Chapman reactions) lead to an ozone column lower than that computed when all three families are considered (Table 1). To understand this result, one must go beyond the simple concept of catalytic cycles within individual families and consider the complex interactions between the various active species among the families.

The sequence of reactions (33) $Cl + O_3 \rightarrow ClO + O_2$, (36) $ClO + NO \rightarrow NO_2 + Cl$, and (J4) $NO_2 + h\nu \rightarrow NO + O$ forms a null cycle involving two families of species that occurs at a fairly fast rate throughout the stratosphere. This null cycle not only provides an additional do-nothing path for the odd-nitrogens, but it is the only effective known null cycle for the odd-chlorine species. Consequently, it weakens the effectiveness of both ClX and NO_x in destroying odd-oxygen in the stratosphere. A similar null cycle involving HO_x and NO_x is (10) $OH + O_3 \rightarrow HO_2 + O_2$, (24) $HO_2 + NO \rightarrow OH + NO_2$, and (J4) $NO_2 + h\nu \rightarrow NO + O$. This cycle is especially effective in the lower stratosphere. With these coupled null cycles competing with the catalytic cycles, it becomes clear how interference

mechanisms can lead to slightly more total ozone when all three families are present with apparently additive odd-oxygen destruction catalytic cycles.

Of course, this is an over-simplified qualitative picture. The actual quantification of all the possible paths is considerably more complicated. For example, reactions (24) and (36) are not only critical in providing the effective but otherwise absent null cycles for the ClX and HO_x families, but they also create additional net odd-oxygen destruction catalytic cycles if the NO_2 molecule so created returns to NO via (4) $NO_2 + O \rightarrow NO + O_2$ instead of photolyzing. Another example of a mixed catalyst destruction sequence is the series of reactions: (60) $HO_2 + ClO \rightarrow HOCl + O_2$; (J24) $HOCl + h\nu \rightarrow OH + Cl$; (33) $Cl + O_3 \rightarrow ClO + O_2$; and (10) $OH + O_3 \rightarrow HO_2 + O_2$. This sequence has the net effect $2O_3 \rightarrow 3O_2$.

In addition, reactions that couple the various families can also catalyze the interconversion of active species and "reservoir" species. Reactions (56) $HO_2 + NO_2 + M \rightarrow HNO_4 + M$ and (58) $HNO_4 + OH \rightarrow H_2O + O_2 + NO_2$; reactions (41) $Cl + HO_2 \rightarrow HCl + O_2$ and (39) $OH + HCl \rightarrow H_2O + Cl$; and reactions (60) $ClO + HO_2 \rightarrow HOCl + O_2$ and (62) $HOCl + OH \rightarrow H_2O + ClO$ all have the net effect of the single reaction (17) $OH + HO_2 \rightarrow H_2O + O_2$. These examples are but a fraction of the couplings of potential importance.

In summary, NO_x, HO_x, and ClX are all of comparable importance in catalyzing ozone destruction in the natural atmosphere, but the roles of the individual species are difficult to separate because the various reactive species are strongly coupled, not only via the formation or destruction of relatively inactive "reservoir" species, but also through positive and negative interference with the basic odd-oxygen destruction processes. Because of the complexity of these coupling mechanisms (and others not discussed) and the need to consider them all in estimating the interaction of various species, numerical models have become an essential tool in the interpretation of stratospheric measurements as well as in the prediction of the effects of potential perturbations.

2.2 MODELING PHOTOCHEMICAL AND TRANSPORT PROCESSES

As shown in Fig. 1, the local concentrations of trace species in an air parcel are determined by the chemical and photochemical processes and nonchemical

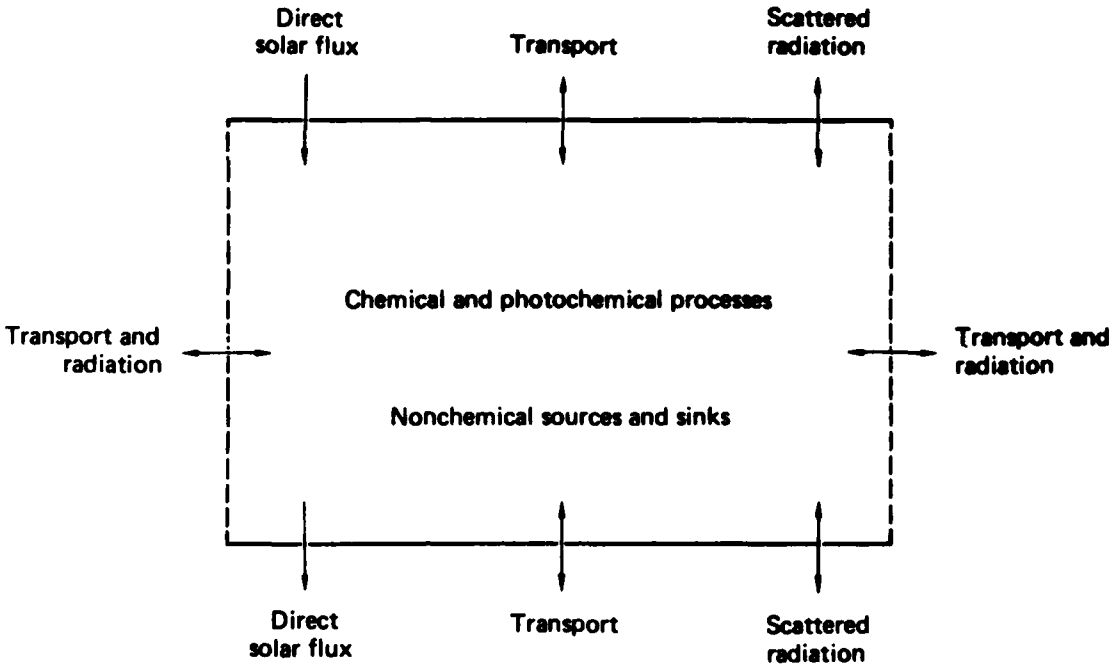

FIGURE 1. Processes affecting the concentration of species in an atmospheric volume.

sources and sinks occurring within the parcel, and by the transport and radiative fluxes into and out of the parcel. Mathematical models of the chemical processes in the stratosphere are governed by the chemical species conservation equation

$$\partial c_i/\partial t + \nabla \cdot \underline{F}_i(c_i,\underline{x},t) = P_i\,[c,J(\underline{x},t,c),\ k(T(\underline{x},t),\ \rho)\,]$$

$$- L_i[\,c,J(\underline{x},t,c),\ k(T(\underline{x},t),\rho\,)\,]c_i + S_i(\underline{x},t) \quad , \tag{1}$$

where $c_i = c_i(\underline{x},t)$ is the concentration of the i^{th} chemical constituent; c is the general representation of all constituents; P_i and $L_i c_i$ are the production and loss of c_i caused by photochemical interactions; T is the ambient air temperature; ρ is the ambient air density; $\underline{F}_i$ is the transport flux of c_i; S_i represents any other possible sinks or sources of c_i; J represents photodissociation coefficients; k represents chemical reaction rate coefficients; and all of these variables are defined at a given spatial position $\underline{x} = \underline{x}(x,y,z)$ at time t. The explicit display of the major interdependent relations of these variables in Eq. (1) illustrates the nonlinearity and general complexity of this mathematical system. Equation (1)

is defined over a spatial domain D with appropriate boundary conditions. Formally, there is one conservation equation for each chemical species in the stratosphere. In practice, about three dozen individual chemical species are known to be of potential consequence in describing the chemical balances affecting the ozone budget in the stratosphere.

It should be noted that an approximation is introduced in the use of spatially and temporally averaged concentrations to calculate the nonlinear chemical terms in Eq. (1). Most of the reactions are bimolecular with rates of reaction of the form

$$k_{ij}\, c_i\, c_j$$

where k_{ij} is the rate constant for reaction of species i with species j. The approximation arises because one does not obtain the same average rate by (a) first averaging the concentrations and then multiplying, as one would find by (b) first multiplying then averaging. The latter method (b) gives the correct result, but for all practical purposes it is not computationally achievable. The former case (a) is a simplifying approximation that can be handled. The effect of this approximation can potentially be quite large, even for physically plausible atmospheric conditions (Hilst, 1972). Work is in progress to develop methods of estimating useful bounds for the errors that may be induced under various conditions.

Classification of Models

Depending on the nature and the extent of problems to be studied, any particular model may include different levels of detail in its representation of the spatial variation of trace species distributions. The difference in resolution serves as a useful and convenient basis for model classification.

Box models have spatial homogeneity as their fundamental assumption (complete uniform mixing of individual trace species). Consequently, these models are represented by a set of ordinary differential equations describing the time evolution of individual trace species as controlled by chemical interactions only, i.e., Eq. (1) averaged over all space under consideration. Such models have been very useful in the diagnosis of experiments in laboratory kinetics and in the analysis of global budgets of long-lived trace species.

One-dimensional models have been the most widely used diagnostic and prognostic tools in stratospheric research. These models are designed to simulate the vertical distribution of atmospheric trace species. They include a detailed description of chemical interactions and of atmospheric attenuation of solar radiation, but the effect of atmospheric transport is described in a simplified way. In one-dimensional models of the stratosphere, a longitudinal and latitudinal global average of the transport flux is assumed. The resulting net vertical transport flux F_{z_i} of any minor constituent c_i is represented through a diffusion approximation in which F_{z_i} is assumed to be proportional to the gradient of the mixing ratio of that trace species:

$$F_i = F_{z_i} = - K_z \rho \frac{\partial}{\partial z} (c_i/\rho) \quad , \tag{2}$$

where z is the altitude and K_z is the one-dimensional vertical diffusion coefficient. One of the major assumptions in applying Eq. (2) to a one-dimensional representation of the atmosphere is that the globally-averaged vertical transport can be represented as a diffusive process.

The models are considered to represent either global or midlatitude averages. One-dimensional models can describe the main features of atmospheric chemistry without excessive demands on computer time.

Two-dimensional models with spatial resolution in the vertical and meridional directions and improved representation of transport (mean motion and eddy mixing) are far more realistic than the one-dimensional models. The two-dimensional fluxes in Eq. (1) are now represented by the sum of two terms, $\underline{F}_i = c_i \underline{V} - \rho \underline{\underline{K}} \nabla (c_i/\rho)$, where $\underline{V}$ is the mean meridional velocity and the 2 x 2 matrix $\underline{\underline{K}}$ is the eddy diffusion coefficient tensor. These models can simulate both seasonal and meridional variations of trace species distributions. The price for this additional information is a considerable increase in computational cost and required input data. Unfortunately, even for these complex models, the transport representations must still be empirically derived from limited data. There is no feedback from changes in composition to the transport processes. This major coupling step can only be accomplished in a realistic sense in a three-dimensional model.

Three-dimensional models give, in principle, the closest simulation of the real atmosphere. The three-dimensional transport fluxes $\underline{F}_i = c_i \underline{V}$ are obtained

through the solution, in all three dimensions, of the appropriate equations of continuity for momentum, energy, and mass (species). These models can, in principle, include most, if not all, of the important feedback mechanisms in the real world. They are, however, very demanding of computer time and memory, and so far the chemistry has had to be simplified to such a degree that important details may have been lost.

One-dimensional models are generally the most detailed and complete in terms of the treatment of photochemical processes. The one-dimensional models used by the major modeling groups now include the Chapman reactions, the NO_x, HO_x and ClX catalytic cycles, and many of the transfer reactions among these basic cycles. In addition, essentially all one-dimensional models contain reactions for the species resulting from methane oxidation, and many have included bromine and sulfur chemistry in their calculations. Some even treat aerosol formation and loss.

The number of reactions included in present one-dimensional models range from approximately 60 to 400 chemical and photochemical reactions involving approximately 24 to 60 species whose concentrations are calculated. As an example, the LLL model presently contains 134 reactions to determine the distributions of 39 species.

The more extensive reaction sets used in some models include many minor reactions, but a comparison of representative models indicates that the chemical kinetics systems in current use are in essential agreement. However, reaction rate coefficients have been changed and additional reactions have been included over the last few years as a result of new laboratory measurements and as the understanding of the chemistry of the atmosphere continues to evolve.

Transport Representation

Globally-averaged vertical transport is represented in one-dimensional models using a vertical diffusion coefficient. The diffusion coefficients are derived from atmospheric data. Chemical tracers (CH_4 and N_2O) and radionuclides from past atmospheric nuclear tests (^{14}C, ^{90}Sr, ^{95}Zr, and ^{185}W) have been used as source data for deriving and testing the coefficients.

In the derivation of the coefficients, it is assumed that the value of K_z is a function of only the transporting motion field. An example of how

globally-averaged measurements of CH_4 may be used to derive a K_z profile is shown in Eq. (3):

$$\frac{\partial}{\partial z}\left\{K_z\rho\left(\frac{\partial}{\partial z}\frac{[CH_4]}{\rho}\right)\right\} - k_{67}[O(^1D)][CH_4] - k_{64}[OH][CH_4] - k_{68}[Cl][CH_4] = 0 , \quad (3)$$

where $[CH_4]$, ρ, k_{67}, k_{64} and k_{68} are known from measurements and $[O(^1D)]$, [OH], and [Cl] are measured or derived from model calculations. Because there are only a few CH_4 measurements available, there is significant uncertainty in the K_z profile. A similar problem exists for derivations using N_2O measurements, although the calculation is simplified somewhat since N_2O loss depends only on photolysis and reaction with $O(^1D)$.

Vertical diffusion coefficient profiles that have been used by various modeling groups in the past have varied significantly, differing by as much as an order of magnitude in value in the middle stratosphere (National Research Council, 1976b). The K_z profiles currently in use tend to differ less than was the case several years ago. Two commonly used K_z profiles are shown in Fig. 2. In general the profiles are similar in their essential characteristics. They have a rather large value in the troposphere, a much lower value in the region near the tropopause, and a large value in the upper stratosphere.

The LLL K_z profile was derived using both CH_4 and N_2O measurement data. Figures 3 and 4 compare the model-derived species profiles with the measurements of CH_4 and N_2O. The small amount of data, particularly above 30 km, is apparent in these figures.

Current models reproduce the methane profile, but they do not accurately reproduce the N_2O, $CFCl_3$ and CF_2Cl_2 profiles using the same transport parameterization that yields agreement with CH_4. Consequently, a compromise transport coefficient may be used that provides a reasonable fit to the data for the various species. The methane distribution is also affected by the OH content. Thus, changing the transport coefficient would require that some mechanism be found that reduces the OH concentration in the 20-30 km region, but such mechanisms are only speculative at present.

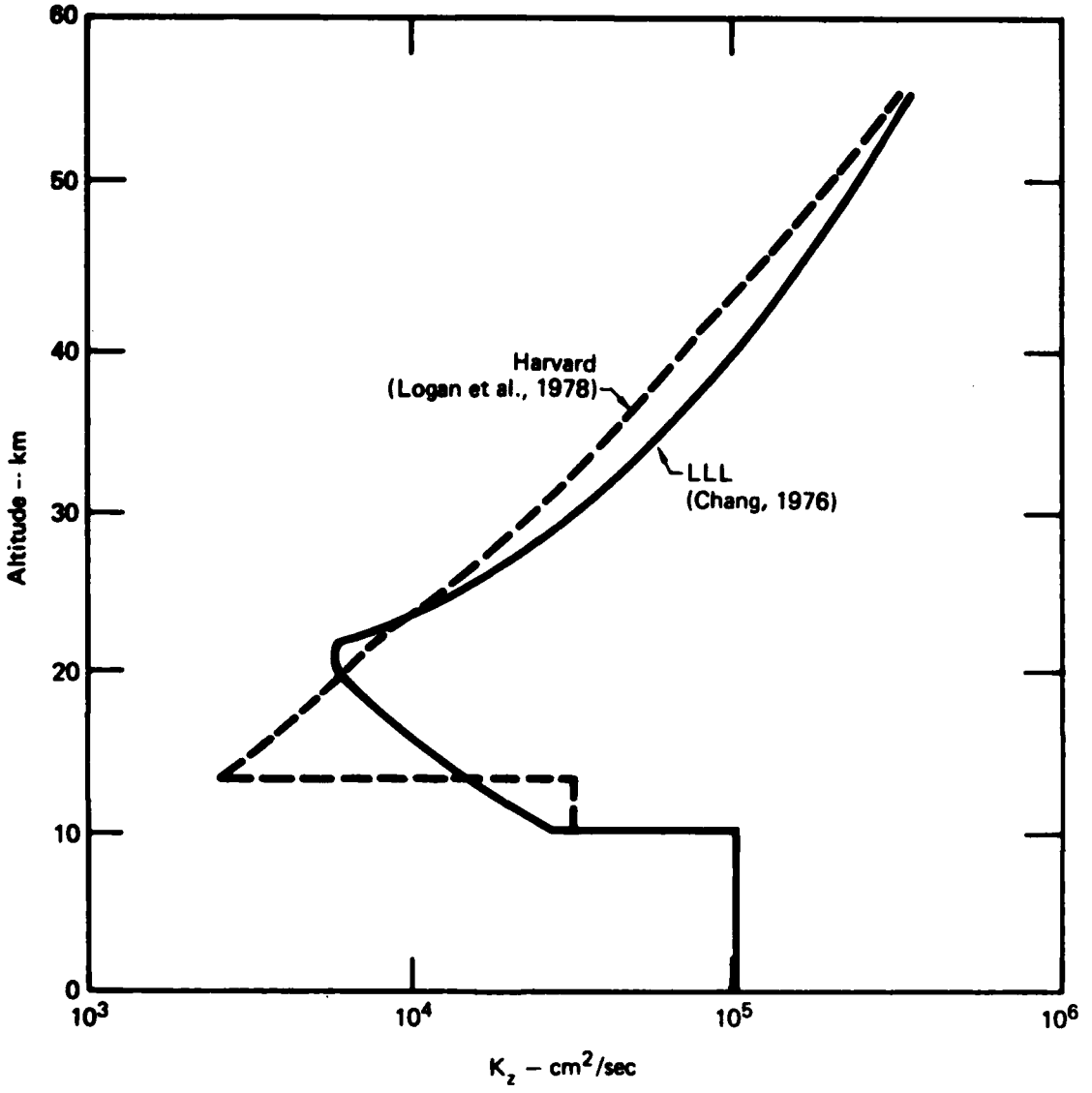

FIGURE 2 Vertical transport coefficients currently being used by two modeling groups.

Radiative Processes

Photodissociation processes in the atmosphere are often extremely important mechanisms for the production and destruction of chemical species. The photodissociation rate, J_i, for species i to give a product j is defined by

$$J_{i \to j} = \int_{\lambda} Q_{\lambda,i} \sigma_{\lambda,i} F_{\lambda}(z) \, d\lambda \quad , \tag{4}$$

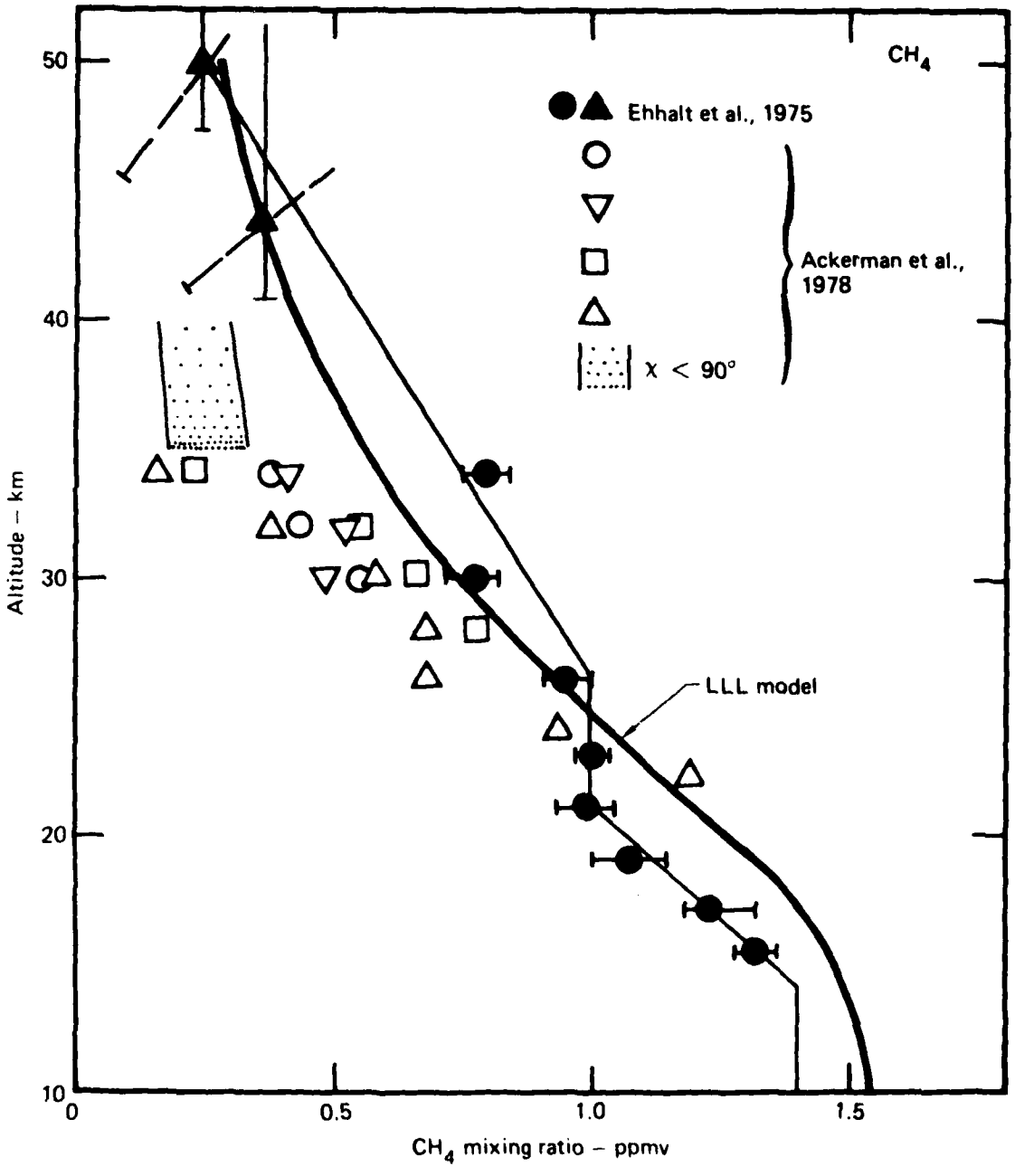

FIGURE 3 Comparison of computed and observed CH_4 mixing ratio profiles. The parameter χ refers to solar zenith angle.

where $Q_{\lambda,i} = Q_{\lambda,i(i\rightarrow j)}$ is the quantum yield for photodissociation of species i to result in production of species j; $\sigma_{\lambda,i}$ is the photoabsorption cross section; and $F_\lambda(z)$ is the flux density. The flux density is affected by changes in the

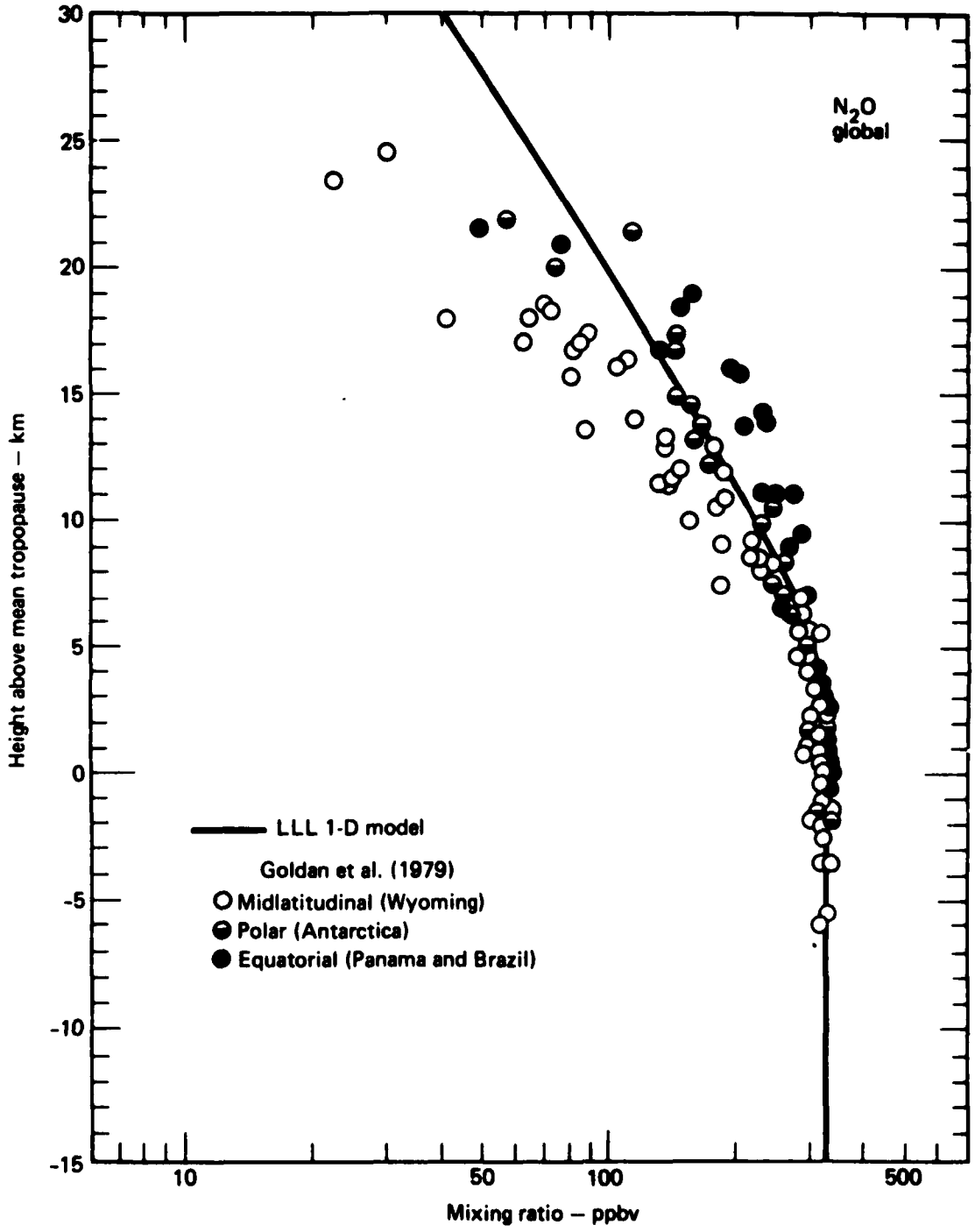

FIGURE 4. Comparison of computed and observed N_2O mixing ratio profiles.

concentration profiles of absorptive species predicted by the model and by the overburden of absorptive and scattering species. Input parameters affecting the calculated photodissociation rate are the wavelength dependence of the quantum yield and absorption cross sections (which are based on laboratory measurements), the solar flux at the top of the atmosphere, the total column of absorptive species above the top of the model (which are based on atmospheric measurements), and the solar zenith angle (which varies by the season and time of day at a given latitude).

The importance of molecular multiple scattering and the surface albedo on determining atmospheric photodissociation rates is now well recognized (Luther and Gelinas, 1976; Callis et al., 1976; Kurzeja, 1976; Luther et al., 1978). Most one-dimensional models now include the effect of multiple scattering not only because of the effect it has on the photodissociation rates, but because of the impact it has on ambient species concentration profiles and on model sensitivity to perturbations (Luther et al., 1978). When multiple scattering is treated, the flux density in Eq. (4) includes contributions from both the direct and diffuse flux components.

Changes in stratospheric composition can affect the stratospheric temperature profile via the solar and longwave radiation balance. Changes in temperature affect chemical reaction rates, which in turn feed back on composition. This temperature feedback mechanism has been included in recent one-dimensional model calculations (McElroy et al., 1974; Luther et al., 1977; Tuck, 1977; Boughner, 1978). In these calculations the stratospheric temperature profile is calculated by using a radiative transfer model that includes solar absorption and longwave interaction by the radiatively important stratospheric species.

Physical Domain and Boundary Conditions

The choice of spatial domain depends on the chemical species of interest and the level of detail desired. For each individual species either boundary concentrations or fluxes must be prescribed. Because atmospheric measurements of many chemical species are inadequate, it is difficult to construct reliable boundary conditions for some species. In practice, an iteration between estimated boundary conditions, model simulation results, and appropriate comparisons with available atmospheric data must be carried out. The need for accurate boundary conditions

can be reduced by extending the physical domain beyond the minimum required by the problem at hand. Moving the boundary beyond a buffer zone serves to reduce the model sensitivity to uncertainties in boundary conditions. In the vertical direction, many models, especially one-dimensional models, cover the region from the earth's surface to above 50 km.

Averaging Processes

In the formulation of models, certain yet unspecified averaging processes must be applied so as to provide a link with physical reality and the means for interpretation of the solutions from such models. Formally $c_i(x,t)$ for Eq. (1) is assumed to be uniform over a unit volume in a unit time interval. But in a representation with reduced dimensionality and/or coarse spatial resolution, c_i must represent certain spatial and temporal averages. Without detailed data on spatial and temporal variations, it is not possible to devise a totally consistent averaging procedure for the nonlinear photochemical reaction rates. This is likely to be the case for many years to come. Nevertheless, the considerable computational difficulty created by diurnal variations in solar flux can be removed through diurnal averaging procedures. This allows the solution of time-dependent problems over long time durations using a diurnally-averaged model with a considerable savings of computer time.

Sources and Sinks

In addition to the sources and sinks caused by the interactive chemistry, the model must include the effect of sources and sinks caused by other processes. Net sources and sinks at the earth's surface for each species must be taken into account in determining necessary flux or concentration boundary conditions. Both wet and dry removal processes for trace atmospheric constituents must be parameterized. The effects of these removal processes are generally approximated using a first-order loss rate that varies with altitude and species. Cosmic ray production of nitric oxide is also included in the models in a parametric way.

Other Physical Data

Altitude distributions of major constituents such as N_2 and O_2 are generally fixed in the calculations with concentrations based on a reference such as the U. S. Standard Atmosphere (1976). Some trace species distributions may also be fixed based on atmospheric measurements. Species such as CO and H_2 have been treated this way in the past at LLL (these species are now calculated). Because of the difficulty in treating water vapor in the troposphere, many models fix the concentration of water vapor in the troposphere, while calculating its concentration in the stratosphere. Unless temperature feedback effects are included, the temperature profile is specified based on a standard reference such as the U. S. Standard Atmosphere (1976).

Time-Dependent and Steady-State Solutions

Once the mathematical model is fixed (i.e., all parameterizations of the relevant physical variables are determined), the system of differential equations are to be solved. For simplicity and computational economy, steady-state solutions of Eq. (1) are often useful and desirable. Such solutions add additional requirements for time-averaging procedures, since local incident solar fluxes vary both diurnally and seasonally and may vary on even longer time scales. In diagnostic applications, steady-state solutions used in a snapshot manner can yield useful information.

Fully time-dependent models are more useful both diagnostically and prognostically, although their solutions are considerably more complicated and computationally more expensive. For the analysis of atmospheric data on many short-lived species, time-dependent models, in particular diurnal models, must be used.

3. MODEL SIMULATIONS OF STRATOSPHERIC OBSERVATIONS

3.1 STRATOSPHERIC COMPOSITION

Comparison with observational data on trace species concentrations is an important aspect of validating the performance of numerical models of the stratosphere. Although comparisons with observations are a necessary part of model validation, these comparisons alone are not sufficient to validate the performance of the model because we know from past experience (Duewer et al., 1977) that models with significantly different chemistry and sensitivity can predict very similar ambient species profiles.

Two somewhat different sets of chemical reaction rate coefficients and photolysis cross sections were used in the calculations presented in this report. Most of the calculations were performed prior to the NASA Workshop at Harpers Ferry, West Virginia (June 1979), and utilized chemical rates based primarily on JPL (1979). After the NASA Workshop, we repeated several of the perturbation calculations using chemical rates based on the recommendations of the chemistry panel at the NASA Workshop. These two chemistries are described in Appendix A as 1979a and 1979b chemistries.

In this section, we compare the results of our current one-dimensional model using 1979b chemistry with measured trace species concentrations. Much of the measurement data used in the comparisons were derived from information communicated at the NASA Harpers Ferry Workshop. As such, some is preliminary in nature. The evaluation of measurements is strongly influenced by that of the NASA panels as reflected at the Workshop. We have also reported a band of model-predicted concentrations based on work presented at the NASA Workshop. Our model results using 1979a chemistry (see Appendix A) were within the band of model predictions indicated. Our discussion in this section closely parallels some of that in the NASA document, reflecting, in part, our participation in writing parts of that document.

$O(^3P)$

There is good agreement between model-calculated distributions (Fig. 5) and the few available measurements. However, the $O(^3P)$ concentration is in a near photoequilibrium with O_3, and the ozone column used in the calculations is calculated for equinox conditions whereas the measurements are winter measurements. Because O_3 was not measured at the same time that O was, there is some danger that the apparent good agreement is fortuitous.

O_3

Ozone profiles vary significantly with latitude and season. Total column ozone ranges from about 200 m·atm·cm in the tropics to about 400 m·atm·cm near the

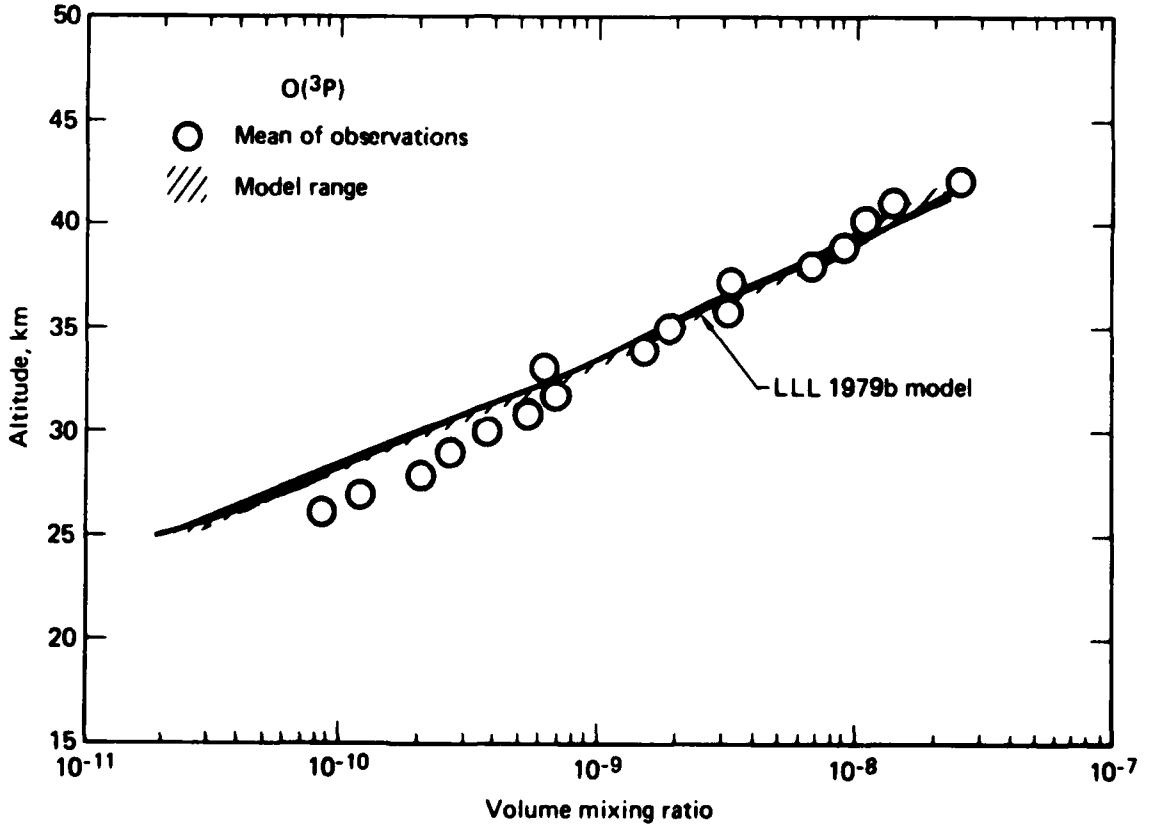

FIGURE 5. Comparison of computed and observed $O(^3P)$ volume mixing ratio. The model range applies to model calculations reported at the NASA Harpers Ferry Workshop, June 1979.

poles. The altitude of the peak concentration is lower near the poles than at the equator. The model-derived O_3 profile shown in Fig. 6 resembles observations of O_3 taken at middle latitudes. The range of rocket and balloon measurements shown in Fig. 6 is taken from the data for middle latitudes in the U.S. Standard Atmosphere (1976).

OH, HO_2

Within the plausible error in the measurements, there appears to be reasonable agreement between theoretical calculations and the few available measurements of OH and HO_2 in the stratosphere (see Figs. 7 and 8). Data are available only between 28 and 38 km for HO_2. The point-to-point variability of the measurements for both species exceeds measurement precision. This suggests that the different air masses measured may have significantly different histories. It would be desirable if, in the future, concurrent measurements of various species (OH, HO_2, O_3, H_2O, etc.) would be made. If such concurrent measurements

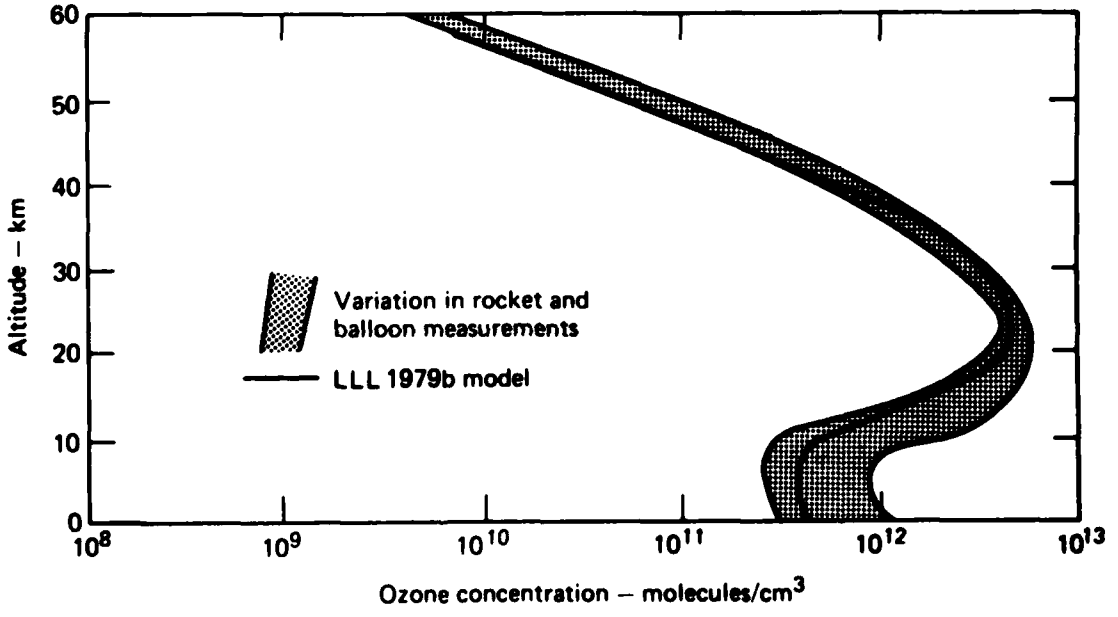

FIGURE 6. Comparison of computed and observed ozone concentration profiles. The rocket and balloon measurement data are taken from the U.S. Standard Atmosphere (1976).

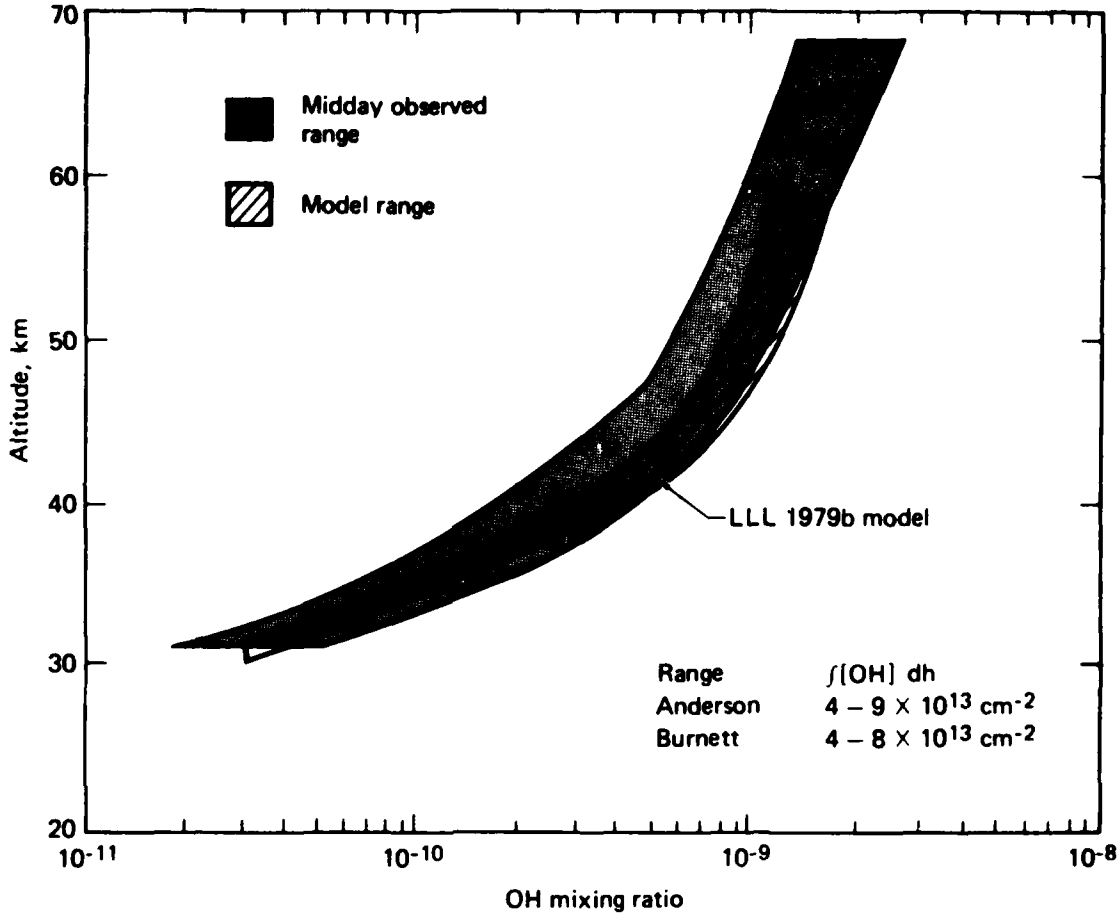

FIGURE 7. Comparison of computed and observed OH mixing ratio profiles. The model range applies to model calculations reported at the NASA Harpers Ferry Workshop, June 1979.

become available, it may be possible to explain local variability, as well as to usefully examine ratios (e.g., HO_2/HO) in relation to those expected theoretically. Comparison of the total OH column calculated by current one-dimensional models with the observations of Burnett and Burnett (1979) does not indicate significant differences in average column content.

NO

The measurements shown in Fig. 9 are from midlatitudes and near-local-noon conditions. When compared to calculated noon profiles, the calculated profiles are

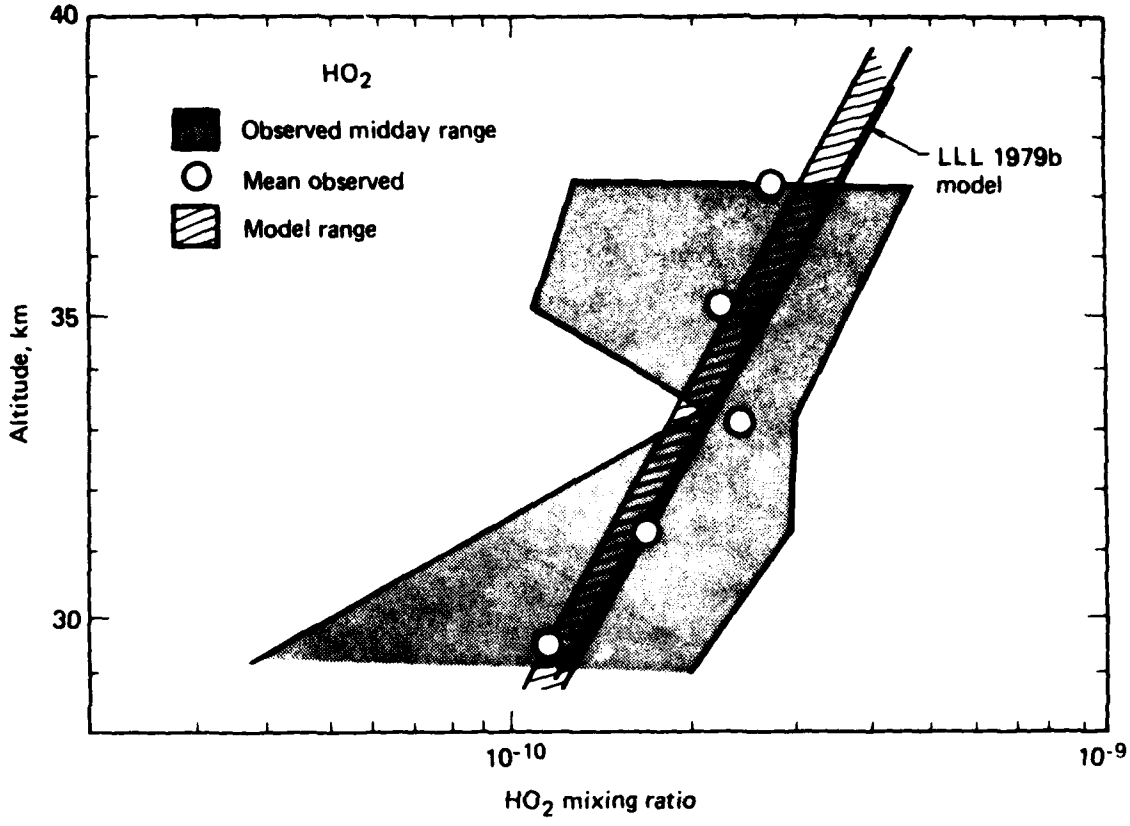

FIGURE 8. Comparison of computed and observed HO_2 mixing ratio profiles. The model range applies to model calculations reported at the NASA Harpers Ferry Workshop, June 1979.

significantly larger than the observations above 30 km. The maximum difference occurs in the upper stratosphere where NO is the dominant NO_x species. One contribution to the difference between models and observations is the overprediction of the total NO_x content by current models. The apparent NO maximum near 40 km lends some credibility to the hypothesis that the treatment of NO photolysis may underestimate the actual upper stratospheric NO sink.

Recent measurements of NO (discussed by H. Schiff and others at the N.A.T.O. Advanced Study Institute on Atmospheric Ozone held in Portugal in October 1979) find much higher concentrations in the upper stratosphere than previous measurements. These measurements agree well with model calculations. However, the reason for disagreement with previous observations (whether it is due to natural variability or measurement errors) must be resolved.

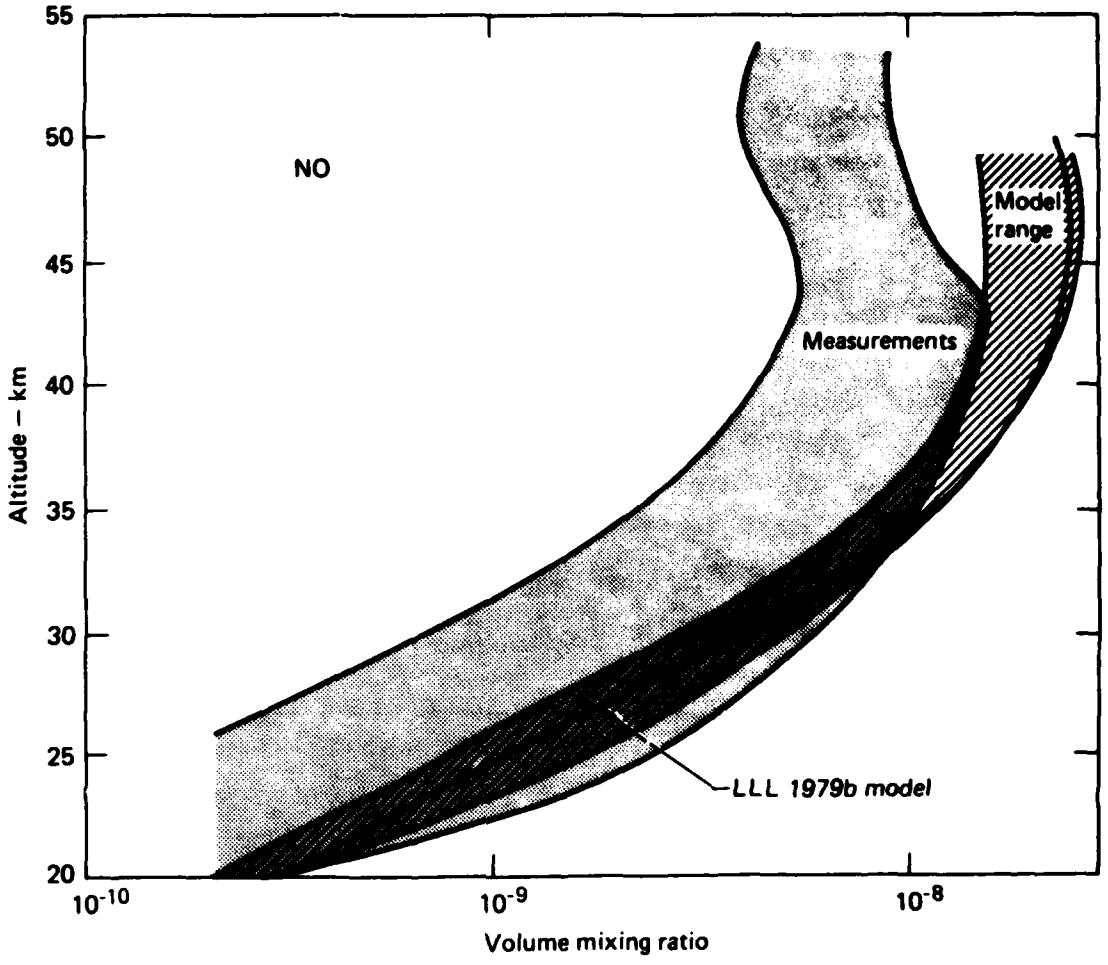

FIGURE 9. Comparison of computed and observed NO mixing ratio profiles. The model range applies to model calculations reported at the NASA Harpers Ferry Workshop, June 1979.

NO_2

Figure 10 compares the model-calculated range of distributions for NO_2 with that measured at sunset near the fall equinox at 40-50°N. The models approximate 30°N equinox conditions which leads to uncertainty regarding the differences found in the lower stratosphere.

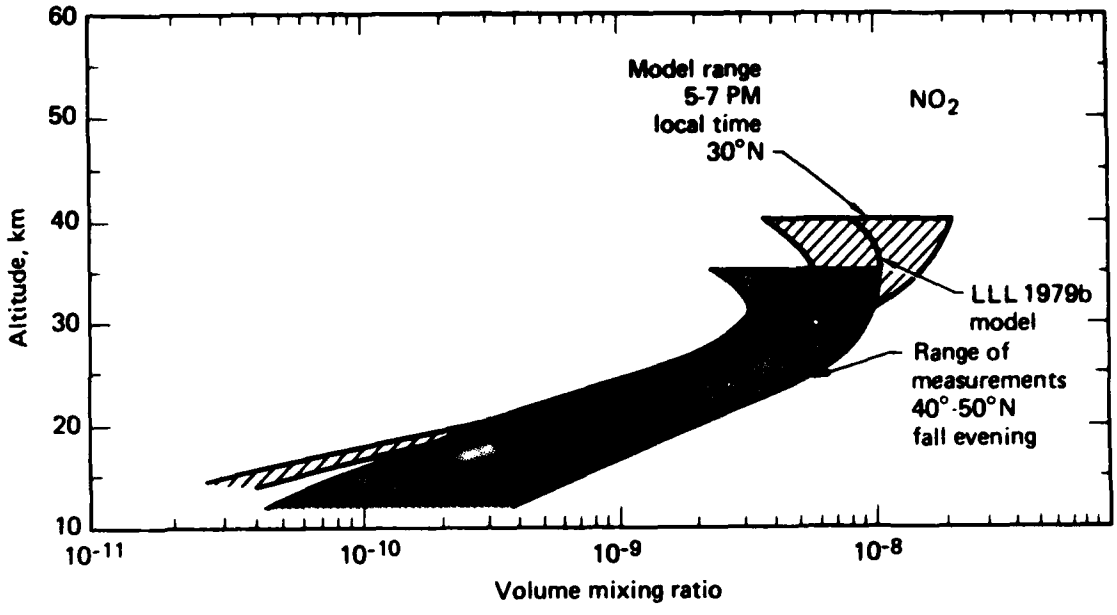

FIGURE 10. Comparison of computed and observed NO_2 mixing ratio profiles. The model range applies to model calculations reported at the NASA Harpers Ferry Workshop, June 1979.

HNO_3

Current models predict more HNO_3 than is observed above about 25 km (Fig. 11). In part this may simply reflect the higher-than-observed NO_x concentrations currently calculated. However, this does not appear to be sufficient to explain the entire difference, nor is it likely that model overprediction of OH between 25 and 35 km is responsible for the difference, since model OH and observations are in good agreement between 28-35 km.

Total NO_y

Our theoretical model presently calculates approximately a factor of 2 more NO_y ($NO + NO_2 + HNO_3$) than has been measured (Figs. 9-12). However, it should be noted that in situ measurements of all three species are not available with readily comparable techniques to permit an unambiguous comparison between theory and measurements.

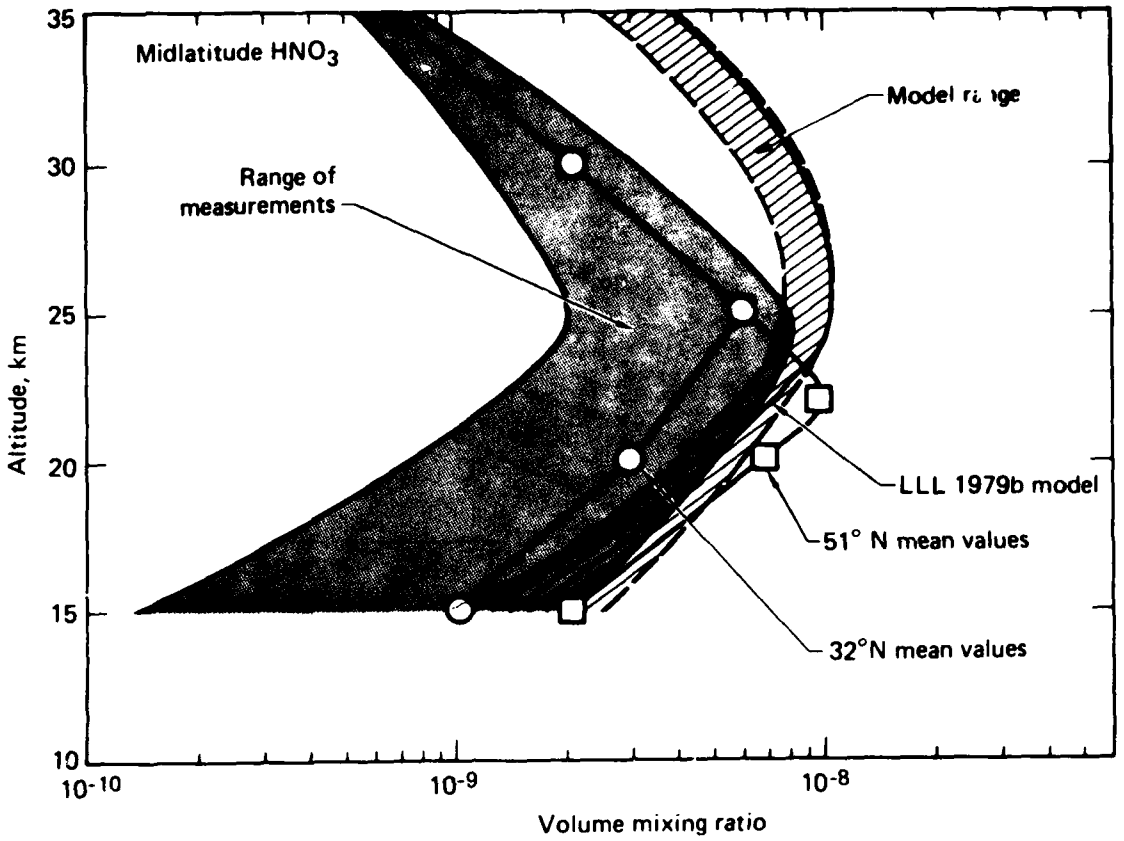

FIGURE 11. Comparison of computed and observed HNO_3 mixing ratio profiles. The model range applies to model calculations reported at the NASA Harpers Ferry Workshop, June 1979.

Part of the reason for the difference between model and observation may be that the model predicts too much N_2O in the upper stratosphere, since N_2O is the primary source for NO_x in the stratosphere by reaction with $O(^1D)$. More measurements of N_2O in the upper stratosphere would be necessary to confirm this hypothesis. The N_2O content in one-dimensional models is sensitive to the choice of vertical transport coefficient used in the calculation.

Other possible factors that might cause the models to overpredict NO_y would include: (1) A lower rate coefficient for $O(^1D) + N_2O \rightarrow 2NO$ than is currently recommended. The data for this process are not in good agreement. However, if anything, they suggest a faster rate coefficient. (2) $O(^1D)$ may be overestimated. This could happen if the quantum yield for $O(^1D)$ production from O_3 photolysis has a stronger temperature dependence than is used in the models.

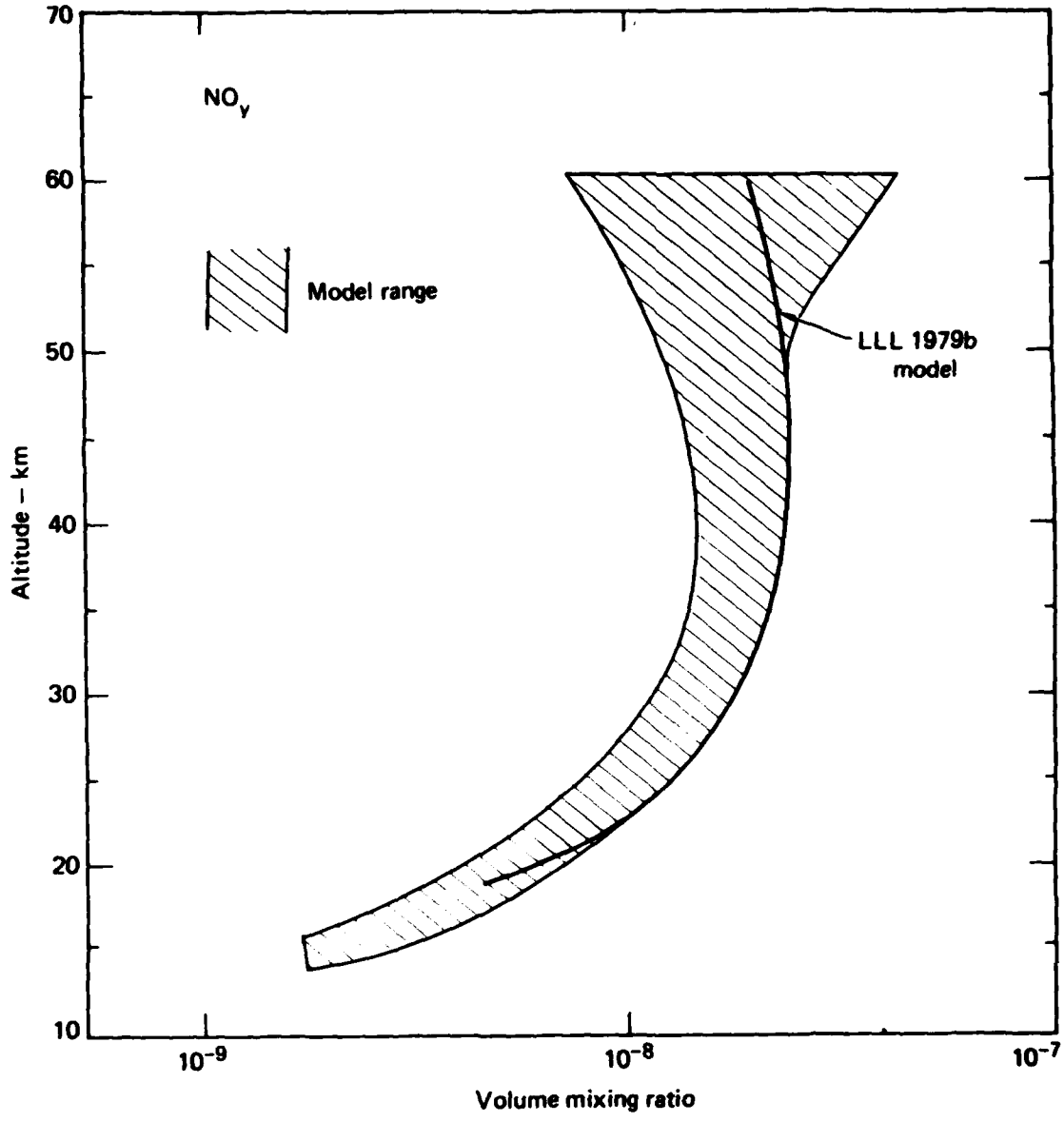

FIGURE 12. Comparison of computed total NO_y mixing ratio profiles. The model range applies to model calculations reported at the NASA Harpers Ferry Workshop, June 1979.

(3) The rate at which NO photolysis occurs may be underestimated in the models. Frederick and Hudson (1979) estimate their results to be uncertain by a factor of 3. Adoption of their treatment decreased the photolysis rate by a factor of ~ 3 from the previous value in the model which resulted in an increase of the model-calculated NO_x by about 40%.

HNO_3/NO_2

The ratio of HNO_3/NO_2 currently calculated by models (Fig. 13) is much higher than is observed by Evans et al. (1976) but is within the error bounds of other measurements. In none of these measurements were both species measured by similar techniques. Concurrent measurements taken at a given point with the same technique are needed to establish whether a discrepancy actually exists. Even then, because of the difference in chemical lifetimes, it would be difficult to determine the time history of both NO_2 and HNO_3 that led to the ratio observed. If a discrepancy does exist, one possible explanation would be that current estimates of OH in the lower stratosphere (below $\sim$30 km) are too large. Another possibility would be that the sinks for HNO_3 are underestimated.

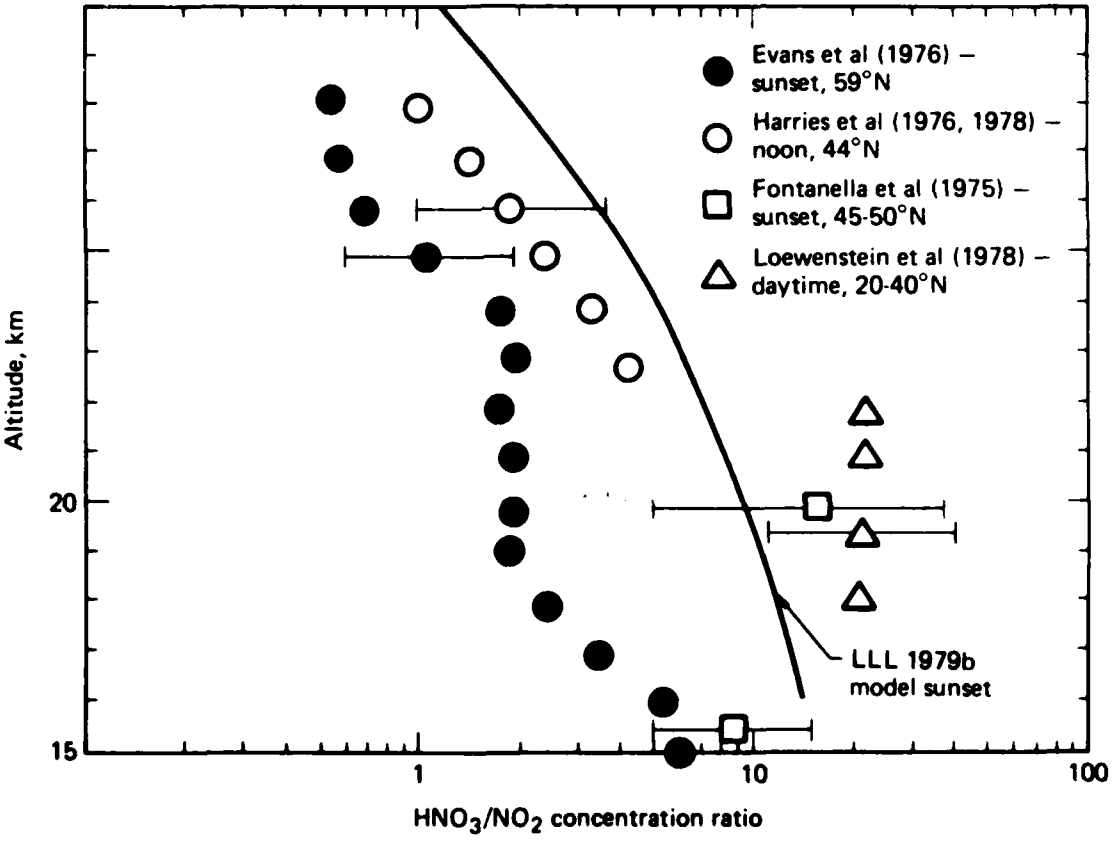

FIGURE 13. Comparison of computed and observed HNO_3/NO_2 concentration ratio profiles.

N_2O_5

We currently calculate a N_2O_5 concentration of $\sim$ 2.5 ppb near sunrise. This can be compared to the value of 2 ppb deduced for N_2O_5 by Evans et al. (1978) based upon measurements of other species a few hours after sunrise. It should be noted that the measurement was not made at the latitude and season the model most nearly approximates. Until further measurements are made, the comparison is inconclusive.

Cl, ClO

In Fig. 14 we compare model predictions and observations of Cl and ClO. The model predictions shown apply to 32^{o}N (where all reported measurements to date have been made) and mid-day solar zenith angles at equinox. The indicated range of calculated profiles encompasses the results of various groups and chemical models.

The single observed Cl profile (and one additional Cl observation at a single altitude) and calculated Cl profiles agree within the measurement uncertainty of $\pm$ 35%. However, the measurements suggest a larger vertical gradient in Cl mixing ratio than is predicted. More Cl measurements are needed to determine whether any seasonal or spatial variations exist and, if so, whether these are consistent with model predictions.

For ClO, at the mixing ratio maximum, with the exception of the 14 July 1977 measurement, the resonance fluorescence measurements are within a factor of about 2 of the predicted ClO abundances. The September through December ClO measurements show a significantly sharper than predicted gradient below the mixing ratio peak. Except for the summer of 1979, summer measurements give more ClO than the September through December measurements. The 14 July 1977 measurement gives six times more ClO than is predicted near the mixing ratio peak, and exceeds by about a factor of 3 the total chlorine mixing ratio believed to be present in the stratosphere. The laser heterodyne radiometer measurement also shows more than twice as much ClO as is predicted near the mixing ratio peak and a sharper than predicted decrease in ClO at lower altitudes. The millimeter-wavelength results imply slightly less ClO than the mid-range of model

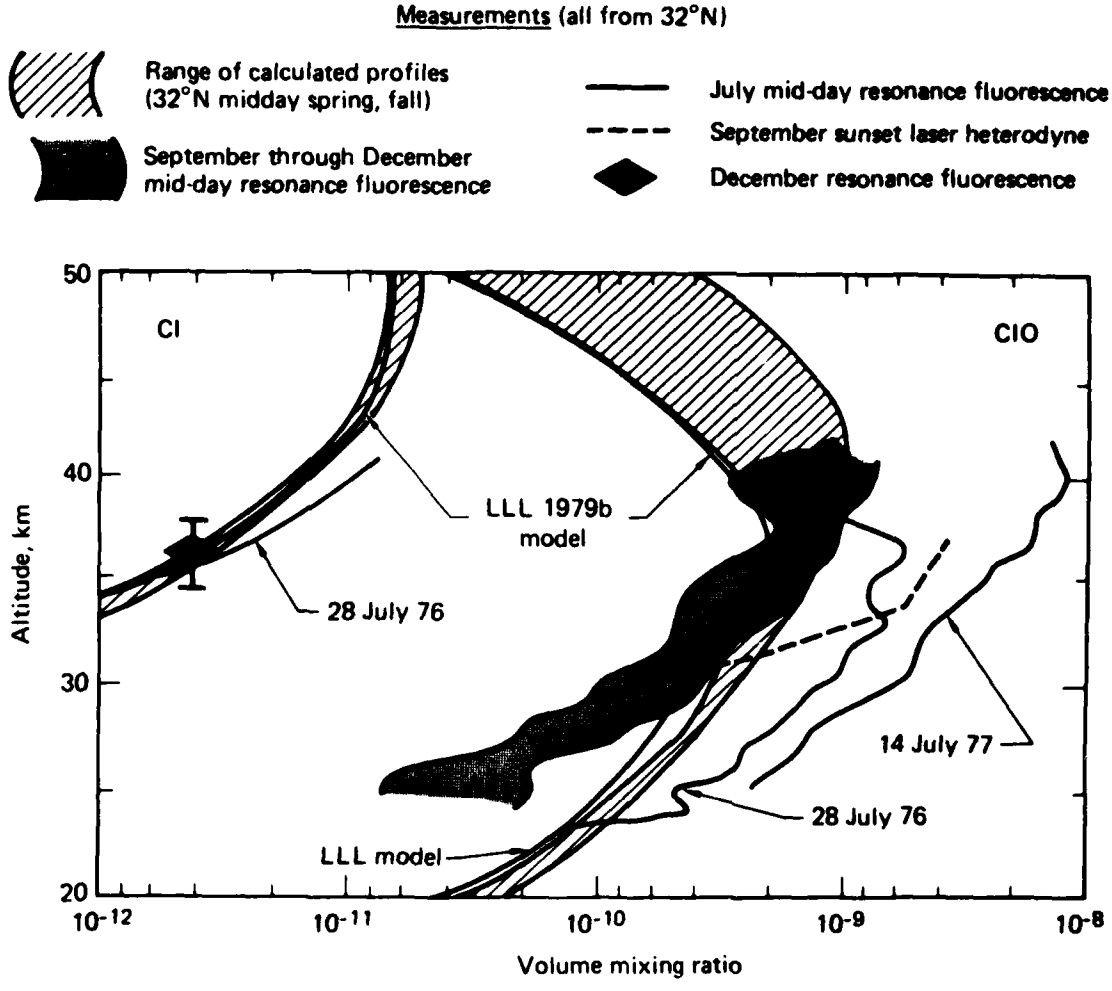

FIGURE 14. Comparison of computed and measured mixing ratio profiles for Cl and ClO. The model range applies to model calculations reported at the NASA Harpers Ferry Workshop, June 1979. LLL model results using 1979a chemistry fell within the model range.

predictions and substantially less ClO than the July 1977 resonance fluorescence and the 20 September 1978 laser heterodyne results. A broader data base is needed to explain the difference in these results as well as the large (factor of 10) variation in the ClO profiles observed but not predicted by one-dimensional models.

Because the 14 July 1977 resonance fluorescence ClO measurement cannot be explained in light of our present understanding of stratospheric chemistry, Anderson et al. (1979) have given its analysis special attention. After careful examination, they have concluded that the large ClO values are not caused by instrument

malfunctions and, using simultaneous measurements of other species, have concluded it implies either:

1. ClO was injected into the observed region prior to the measurement in a time which is comparable with the chemical response time of odd oxygen; or
2. The reaction $ClO + O \rightarrow Cl + O_2$ is not rate limiting in the closure of the chlorine catalytic cycle; or
3. There exists an odd-oxygen production term proportional to ClX and competitive with direct O_2 photolysis in the middle and upper atmosphere.

At present it is uncertain which, if any, of these explanations is correct.

The differences between theoretical calculations and observations of the ClO gradient below 34 km also require attention. At present, speculations for explaining these differences range from the possibility of a missing chemical reaction or an incorrect rate constant in present theory to the possibility of it being an artifact of the transport parameterization used in current models, or an artifact of the measurement techniques.

Cl/ClO Ratio

Measurements and model calculations of the Cl/ClO ratio are shown in Fig. 15. The Cl/ClO ratios from the 28 July 1976 resonance fluorescence measurements (Anderson et al., 1979) agree to within measurement uncertainty with most calculations. It is difficult at present to make any conclusions regarding this comparison because of the experimental uncertainties, the limited amount of data, the apparent variability of ClO, and the poor agreement between models and observations for ClO.

HCl

Although there may be significant disagreement (as large as 30-40% when compared with the IR spectra data, much larger if compared to the filter or

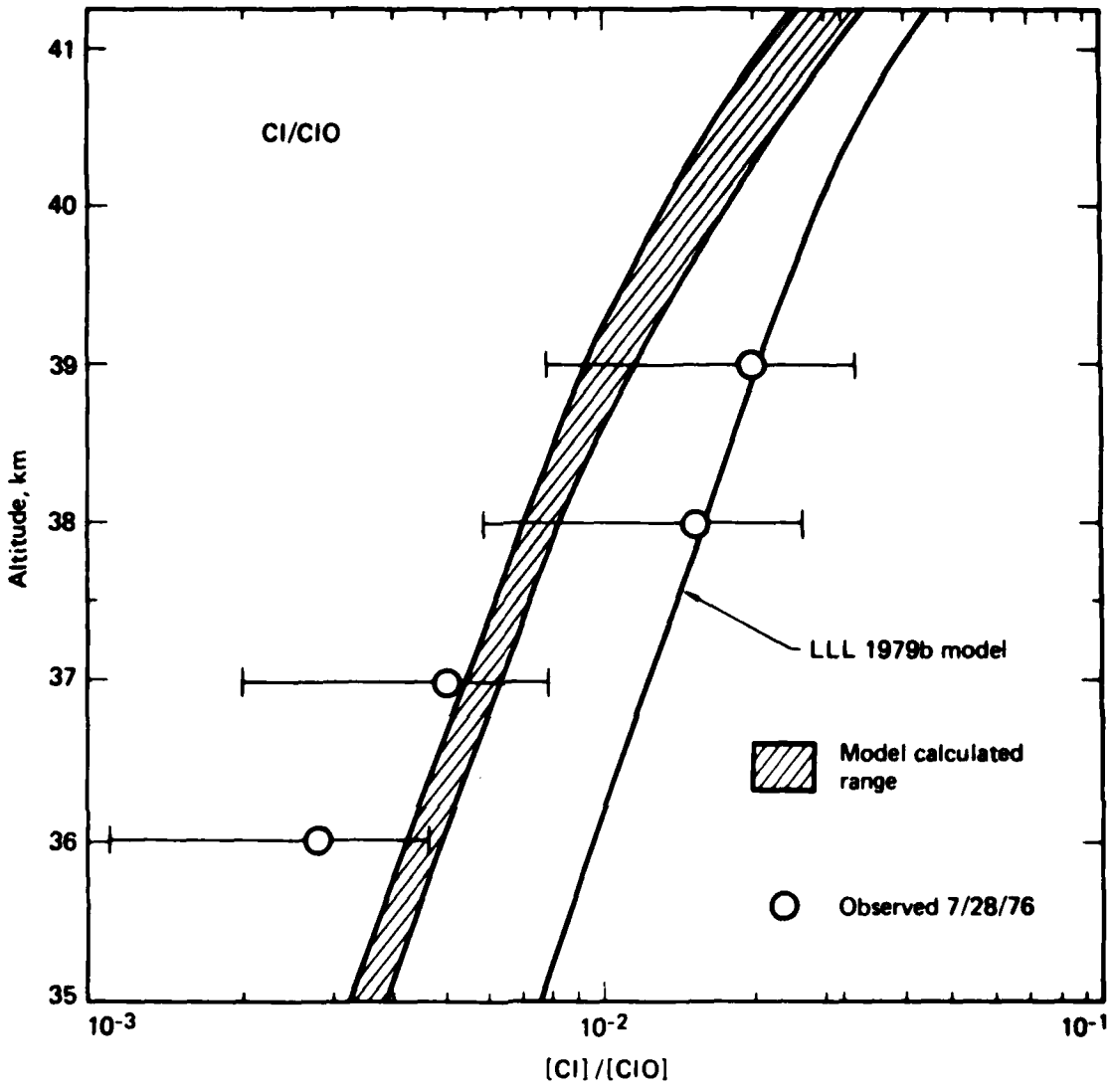

FIGURE 15. Comparison of computed and measured Cl/ClO concentration ratio. The model range applies to model calculations reported at the NASA Harpers Ferry Workshop, June 1979. LLL model results using 1979a chemistry fell within the model range.

radiometer data) above 30 km (Fig. 16), the uncertainty in the observational data in this altitude range is such as to probably encompass the areas of disagreement.

$ClONO_2$

The only observational data for $ClONO_2$ are from one flight by Murcray (1979). As shown in Fig. 17, there is excellent agreement if the fast production

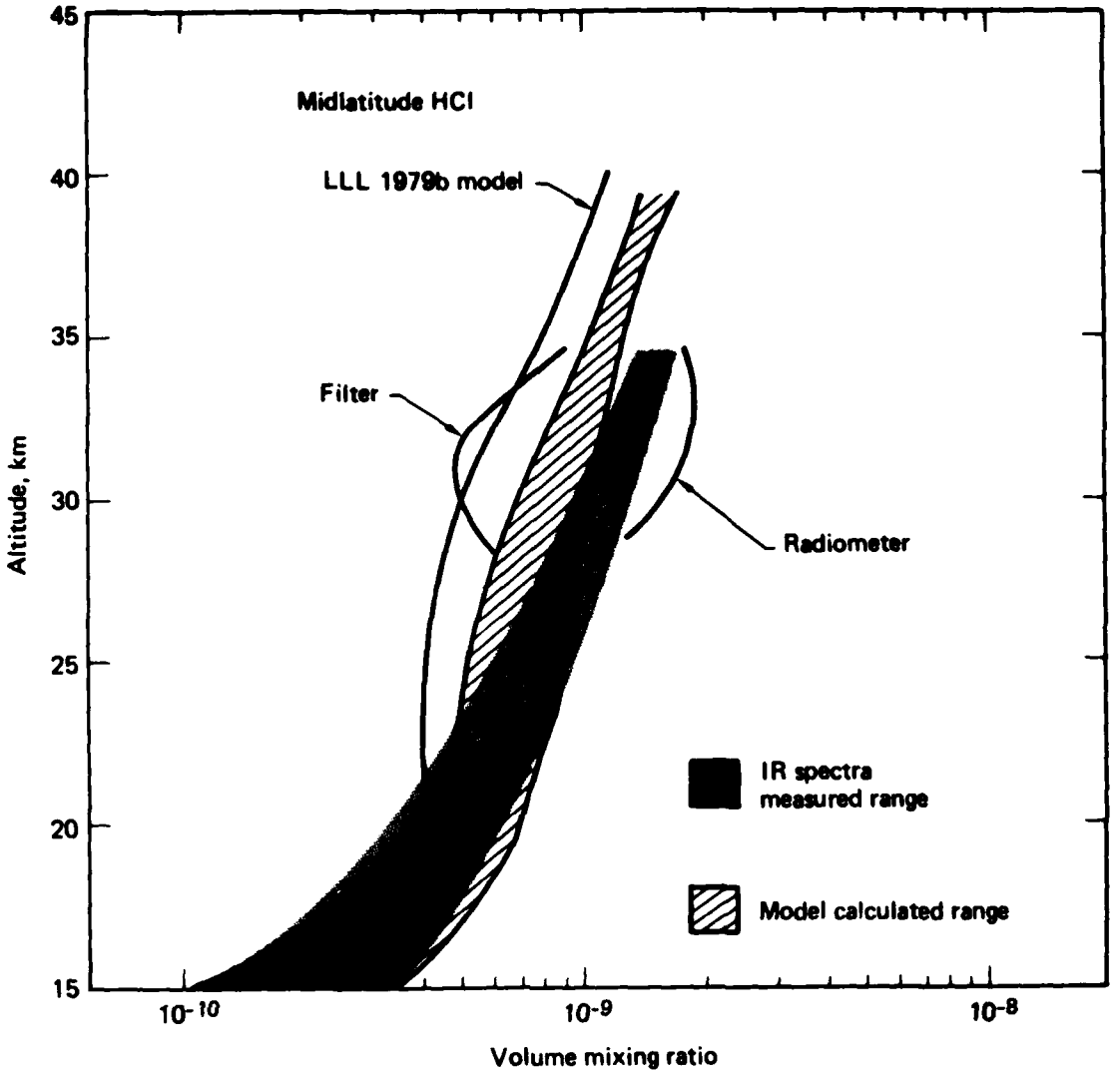

FIGURE 16. Comparison of computed and observed HCl mixing ratio profiles. The model range applies to model calculations reported at the NASA Harpers Ferry Workshop, June 1979. LLL model results using 1979a chemistry fell within the model range.

rate for $ClONO_2$ is used in the calculations, whereas there is a factor of 3 difference if the slower production rate is used (see Section 4 discussion regarding the rate of production of $ClONO_2$).

Until further data are available, it is difficult to make any conclusive statements regarding this species. However, the limited amount of data available does not indicate any gross discrepancies between theory and observations.

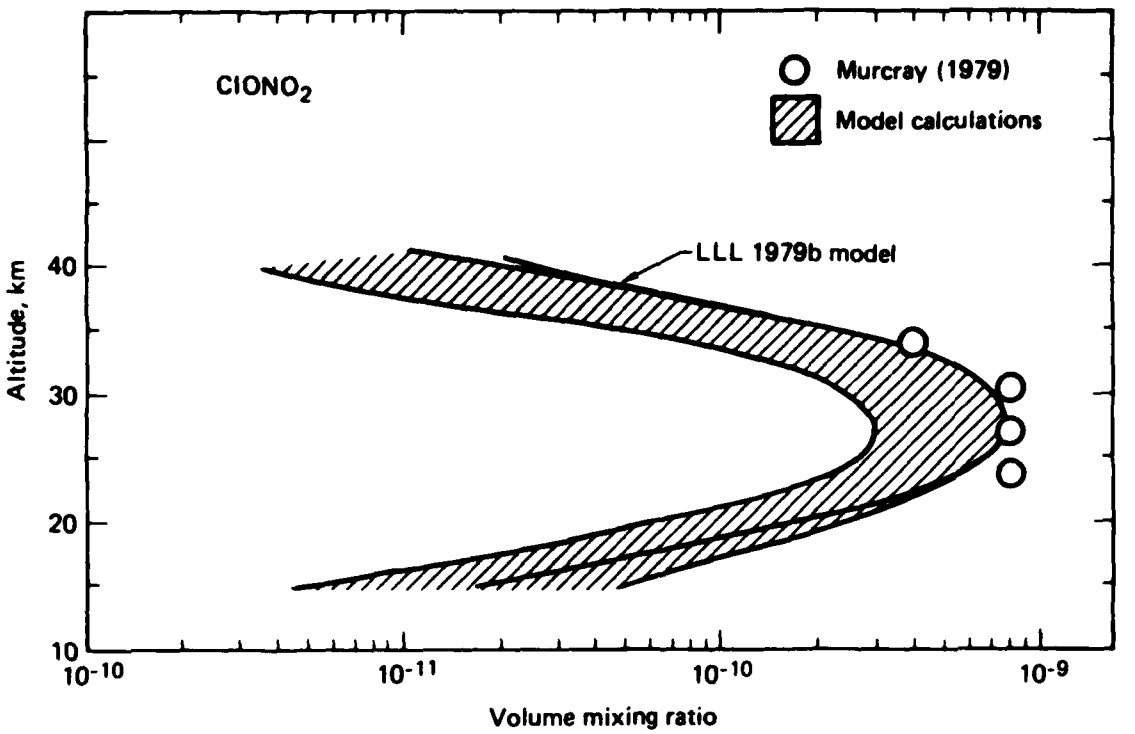

FIGURE 17. Comparison of computed and observed $ClONO_2$ mixing ratios. The model range applies to model calculations reported at the NASA Harpers Ferry Workshop, June 1979.

Total ClX

There now exists a limited number of measurements for Cl, ClO, HCl, and $ClONO_2$ in the stratosphere. Except for three measurements of ClO taken in summer (Anderson, 1979; Menzies, 1979), there does not appear to be any large discrepancy between the total amount of ClX predicted and that observed. However, the summer measurements of ClO are so large as to require much more total ClX than known sources are capable of producing. This implies the possibility of an unknown source for ClX in the atmosphere, an error in the observation, or some unusual episodic event.

3.2 MODEL SIMULATIONS OF PAST PERTURBATIONS

Possible Long-Term Solar Variations and the Effects on Temperature and Ozone*

In the study of potential anthropogenic influences on the stratospheric ozone budget it is necessary to first understand the natural variations of ozone. In order to achieve early detection of anthropogenic trends and to establish the magnitude of such effects, we must differentiate the natural stratospheric ozone variations from the man-made effects that are of comparable time scales. The suggested correlation between ozone and sunspot number is of primary interest. If this relation is real, then for the next few years the theoretically predicted effect of CFM's on ozone may not be directly detectable unless the effect of this ozone-solar cycle relation can be quantified and removed from the ozone data. At this time, the most plausible mechanism coupling the sunspot cycle and atmospheric ozone is the change in solar flux between 180 and 340 nm from solar maximum to solar minimum (Heath and Thekaekara, 1977; Callis and Nealy, 1978; Penner and Chang, 1978). Theoretically, a variation in solar flux between 180 and 340 nm of approximately 30% (maximum to minimum) can lead to local ozone changes as large as 10% near 35 km, and total ozone column changes of approximately 5% (Penner and Chang, 1978). This is comparable to the predicted CFM effect of ozone decreases of up to 5% around the year 1990. Consequently, the possible influence of periodic or aperiodic changes in solar UV flux intensities tends to obscure changes due to the present levels of CFM's, and this may continue for the next decade. The same is also true for the local ozone concentrations in the upper stratosphere.

The data that support a variation in solar UV fluxes during a solar cycle are limited (Heath and Thekaekara, 1977) and need to be confirmed with other independent measurements. Simon (1978) has pointed out the difficulty in the absolute calibration of the measuring instruments, especially those aboard a satellite.

*See Appendix D for a more detailed discussion.

Since the direct monitoring of solar UV fluxes and ozone are both of limited use in establishing the ozone-solar cycle relation, we are left with the monitoring of trace species other than ozone as a possible independent method for validating the effects of solar UV flux variations. We examined the possible variations of 31 trace species that result from hypothetical solar UV variations with the LLL time-dependent model of stratospheric chemistry, including self-consistently calculated stratospheric temperature and atmospheric adjustment to hydrostatic equilibrium (Penner and Chang, 1979). From this study we identified N_2O as a most likely candidate for monitoring to study coupling between variations in solar UV and atmospheric composition (see Appendix D). Furthermore, there remains the question of the effect of transport-related variability that can only be resolved with a set of upper stratospheric data.

The Atmospheric Nuclear Tests of the 1950's and 1960's*

Past atmospheric tests of nuclear devices larger than about one megaton (TNT) yield provide a potentially significant source of NO_x to the stratosphere. During the late 1950's and early 1960's, large numbers of such tests were carried out, and the NO_x released to the stratosphere in 1961 and 1962 should have been comparable to the amount that would be released by about 2.7 years operation of a large SST fleet (i.e., one emitting $\sim 10^8$ molecules cm^{-2} sec^{-1}). The paper by Chang, Duewer and Wuebbles (1979) gives an account of the predicted effects through early 1978. Figure 18 gives the computed ozone column change as a function of time. For computations made with 1979b chemistry (see Appendix A), the two curves give the ozone depletion calculated for injection altitudes based on a parameterization by Foley and Ruderman (1972) or on the lower altitude observations of Seitz et al. (1968). The two treatments are thought to bound the plausible range of injection altitudes.

Both treatments predict maximum ozone depletions of less than 2% for the largest annual-average change. The largest change is only about 1.25% if a 1-2-1 smoothing function is applied to annual perturbations. The computed changes are

*See Appendix F for a more detailed discussion.

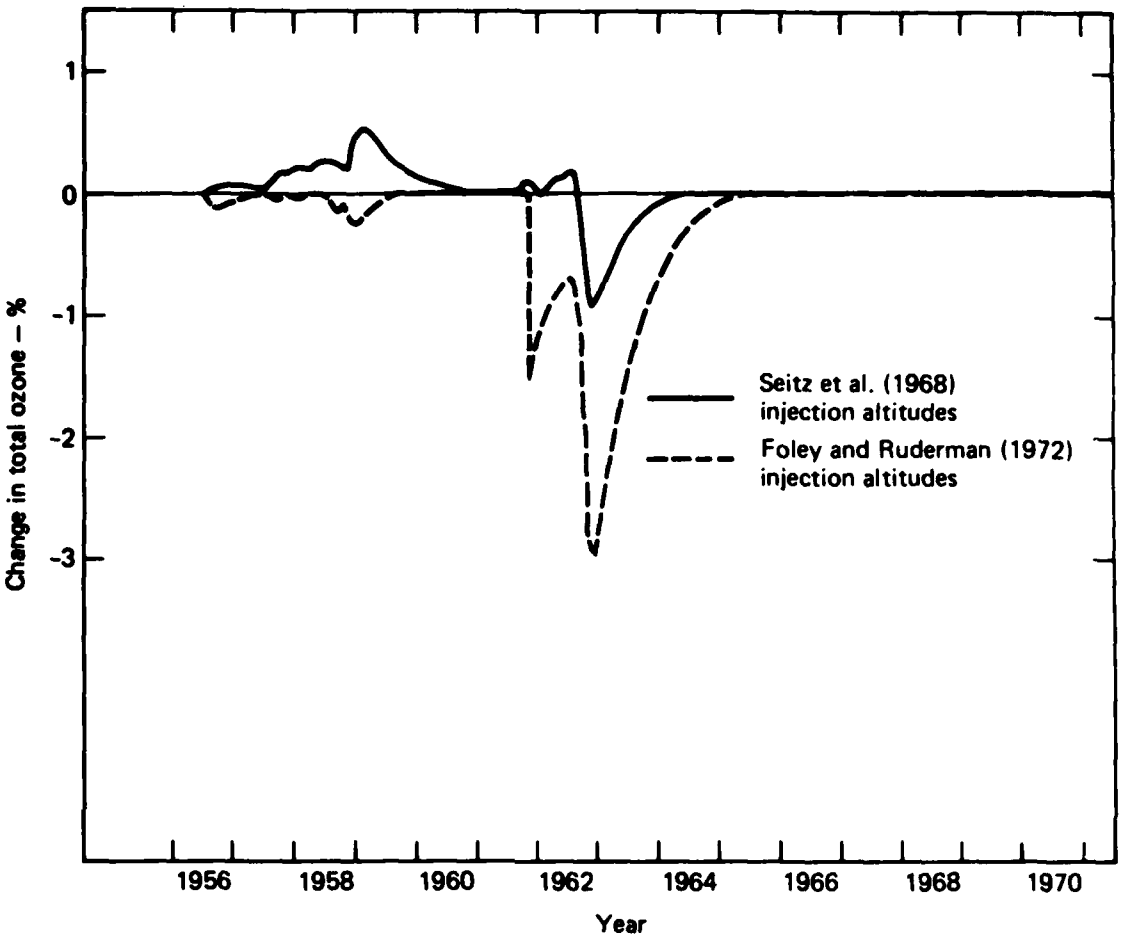

FIGURE 18. The computed change in total ozone resulting from atmospheric nuclear testing during the 1950's and 1960's.

clearly within the observed variability in the ozone record as analyzed by Angell and Korshover (1978).

Figure 19 gives the computed changes at selected altitudes. The ozone concentration decreases at all altitudes above 25 km. However, at lower altitudes the concentration of ozone was computed to increase significantly, which accounts for the net increase in total ozone prior to 1962 shown in Fig. 18. Some of these computed changes are much larger than the change in the ozone column. However, the predicted ozone variations at specific altitudes are still only about the same magnitude as the variations in Umkehr-based ozone concentrations.

Thus, the model-predicted response to the atmospheric nuclear tests does not lead to conflict with the ozone record, but it also does not seem to explain much of

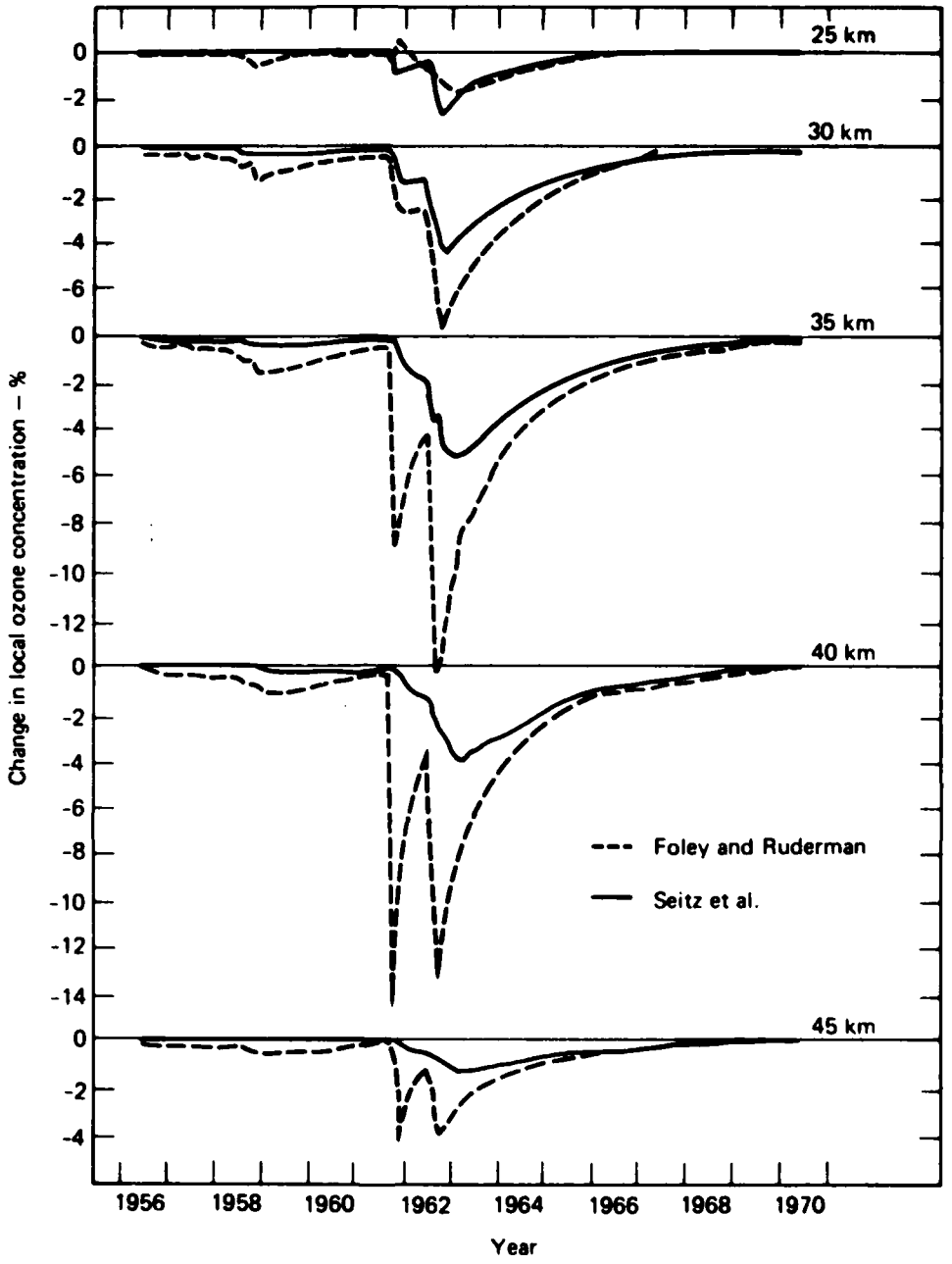

FIGURE 19. The computed change in local ozone concentration at various altitudes resulting from atmospheric nuclear testing during the 1950's and 1960's. Ozone concentrations in the lower stratosphere and upper troposphere (not shown) were computed to increase, which accounts for the net increases in total ozone prior to 1962 shown in Fig. 18.

the observed ozone variation. The predicted effect on ozone of the nuclear tests should be considered in any attempt to model ozone variations during the 1960's since the predicted changes in ozone at specific altitudes are comparable to both the observed variations and to the variations calculated for such phenomena as the hypothesized variation of ultraviolet light tied to the solar cycle, or the predicted change in ozone from CFM production through 1978.

Polar Cap Absorption Events

Crutzen et al. (1975) noted that large polar cap absorption (PCA) events should produce significant quantities of NO_x in the middle and upper stratosphere, especially at high latitudes. Indeed the PCA events of August 1972 were estimated to have produced several times as much NO_x as the ambient content of the atmosphere in the region above 40 km. In a comparison with Nimbus 4 ozone data, Heath et al. (1977) found that the agreement between predicted ozone change and observation was quite good north of 75° latitude and above 4 mb (the model under predicted the perturbation by roughly 30%). Since those calculations were made, several important changes in model chemistry have occurred. However, these changes have had only a modest effect on the sensitivity of the model to large injections of NO_x at high altitude and high latitude. There are two recent recalculations of the effect of the August 1972 PCA event in the literature. Fabian et al. (1979) found that their computed ozone change was in excellent agreement with observation if more recent estimates of the NO production per ion pair are used. However, the agreement between observation and computation at lower latitudes was less satisfactory, although still qualitatively encouraging. Borucki et al. (1978) report similar findings, and also find that their model substantially underpredicts the ozone perturbations at altitudes near 30 km.

The August 1972 PCA events seem to provide a useful test of the short-term (several days) response of stratospheric ozone to NO_x increases above about 40 km. Unfortunately, the test is not directly applicable to lower altitude, midlatitude NO_x perturbations occurring over long (several year) time periods. The nature of the NO_x injection and of the O_3 data do not permit resolution of questions about the adequacy of model simulations of transport phenomena or of the chemistry of the lower stratosphere. Thus, PCA events provide the only

phenomenon for which models forecast an observable and observed stratospheric ozone perturbation in response to an NO_x change, but the nature of the perturbation and the response differ from the problems associated with SST operations to an extent that precludes its direct use as a calibration point for SST predictions of column ozone changes. Nonetheless, the good agreement above 40 km is encouraging since it suggests at least that models are adequately representing the short-term response of ozone to NO_x injections at higher altitudes.

The Solar Eclipse on February 26, 1979*

In addition to ozone observations, measurements of other minor constituents during a solar eclipse could provide validation of the short time constant chemistry in atmospheric models. Consequently, experiments for upcoming solar eclipses, when properly supported by theoretical analysis, could contribute significantly to our understanding of atmospheric chemistry. In fact, given the proper data on trace species concentrations during an eclipse, such measurements could provide a direct demonstration that the currently proposed major reactions of NO_x, HO_x, and ClX species are indeed concurrently functioning in the stratosphere in the manner suggested by laboratory chemistry. However, the measurements yield little information about slower processes that can have large effects on model sensitivity.

We have examined theoretically (Wuebbles and Chang, 1979) the expected effect of a solar eclipse on stratospheric minor constituents. Primary emphasis was given to the total eclipse that occurred over North America on February 26, 1979. Variations similar to those computed for this particular case should be expected for other total eclipses. Totality was the longest ($\sim$ 3 minutes) at 50^{o}N latitude for the February 1979 eclipse.

While ozone, tropospheric water vapor, and temperature were held fixed in the model for most of our eclipse calculations, the model was also run with calculated ozone to examine the expected response of ozone to an eclipse. Our analysis has shown that fixing the ozone distribution does not significantly affect the temporal variations calculated for other species during the eclipse. Solar flux variations during the eclipse were based on Hunt (1965).

*See Appendix E for a more detailed discussion.

Those species having chemical lifetimes less than a few hours are expected to vary significantly from normal diurnal behavior during a solar eclipse. Local concentrations of the species could be quite variable, and therefore we should focus on relative changes rather than absolute magnitudes.

The model-calculated response of ozone during an eclipse essentially agreed with Hunt (1965). A significant increase in O_3 is to be expected in the upper stratosphere and in the mesosphere as a result of the conversion of $O(^3P)$ to ozone through the reaction $O(^3P) + O_2 + M \rightarrow O_3 + M$ accompanied by decreased photolysis of O_2 and O_3. The maximum increase in O_3, found at the end of totality, was computed to be 15% and 45% at 50 and 55 km, respectively. Larger fractional changes are expected in the mesosphere. Since most of the atmospheric ozone is at lower altitudes in the stratosphere, an insignificant change in the total ozone column is expected. Significant changes were also predicted to occur in NO, NO_2, Cl, ClO, OH and HO_2 concentrations.

The results of this study suggest that significant and detectable variations are expected for some of the important stratospheric minor constituents during a solar eclipse. Such observations, particularly simultaneous observations of trace species, would demonstrate clearly the simultaneous functioning of the various important photochemical catalytic cycles in the stratosphere.

The model calculations were completed prior to the eclipse. Measurements during the solar eclipse of February 26, 1979, were made with NASA's aircraft. This plane carried instruments to measure NO, O_3, and temperature at 20 km (instrument of Starr, Craig, and others of NASA-Ames) and to measure the NO and NO_2 columns above 20 km (by David Murcray of University of Denver). Preliminary results by Starr and Craig show no change in O_3 at 20 km during the eclipse (as was predicted), and they show excellent agreement with the theoretically expected change in NO. A detailed comparison between this measurement and model calculations is being made. In any case, the results demonstrate that the reactions $NO + O_3$ and $NO_2 + h\nu$ occur in the stratosphere at rates similar to those computed theoretically.

4. POTENTIAL CHANGES IN OZONE CAUSED BY AIRCRAFT EMISSIONS

4.1 EMISSION INDEXES AND FLEET PROJECTIONS

In this report we consider the potential effects on atmospheric ozone of several different aircraft emissions scenarios. These emission scenarios were developed for three basically different applications: (1) the projected 1990 fleet, (2) a commercially viable fleet of supersonic transports, and (3) a commercially viable fleet of hypersonic transports. In all of the perturbation calculations discussed in Sections 4 and 5, the "ambient" or "unperturbed" atmospheric conditions refer to the model-calculated initial state rather than to atmospheric measurements.

1990 Fleets

We developed emission profiles for both high and low projected 1990 aircraft fleet sizes. In the case of the projected 1990 high fleet, we adopted the emissions factors and fleet projections used by Oliver et al. (1977) in their Table 2-33. The projection used by Oliver et al. (1977) was based on A. D. Little, Inc. (1976) with corrections to the mean flight altitude of the projected SST fleet of 142 Concordes and TU 144's and an emissions factor ~ 4 times larger than used by A. D. Little, Inc. (1976) for CF6 engines (which Oliver et al., 1977, treated as having the same emissions indexes as JT9D engines). The NO_x emission index for SST's was assumed to be 20 g NO_2/kg fuel.

In converting the projected emissions in Table 2.33 of Oliver et al. (1977) to a format compatible with the one-dimensional model, we treated the model as a Northern Hemisphere model, summed emissions over all latitudes between zero and $90^{\circ}N$ at a given altitude, and converted kg/year at each altitude to molecules cm^{-3} s^{-1} over a 1-km-thick layer centered at even-kilometer altitudes. Table 2 gives the emission rates actually used in our calculation.

We also examined the effects of the projected subsonic fleet without the SST contribution using the emissions given in Table 2 for the subsonic fleet only. We generated a 1990 low estimate by multiplying the 1990 high estimate emissions by

TABLE 2. Projected 1990 aircraft emissions of NO_x (Oliver et al. (1977) high estimate). The low estimate of emission rates equals 0.633 times the high estimate.

Injection Altitude (km)	NO_x Injection Rate Total Fleet (molecules $cm^{-3}s^{-1}$)	NO_x Injection Rate Subsonic Only (molecules $cm^{-3}s^{-1}$)
6	90	90
7	179	179
8	265	265
9	665	665
10	1167	1167
11	1161	1161
12	520	520
13	75	75
14	18*	12
15	18	
16	33	
17	43	
18	29	
19	8	

*Emissions from the SST fleet are included at 14 km and above.

0.633, the ratio of the 1990 low estimate fuel usage to the 1990 high estimate fuel usage given in Table 2.25 of Oliver et al. (1977).

SST Fleets of Commercially Viable Size

In treating hypothetical SST fleets of commercially viable magnitude, we have considered a fleet emitting 1000 molecules of NO_x $cm^{-3}s^{-1}$ and 1.77×10^5 molecules of H_2O $cm^{-3}s^{-1}$ over a 1-km-thick layer in the Northern Hemisphere, which is equivalent to 6.2×10^8 kg of NO_x (as NO_2) and 4.3×10^{10} kg of H_2O per year. These emission rates correspond to a fuel usage of 3.5×10^{10} kg yr^{-1} by SST's, assuming the emission indexes are 18 g NO_2/kg fuel and 1.25 kg H_2O/kg fuel. The NO_x emissions index for currently realizable

SST engines has been estimated to be as high as 22 g NO_2/kg fuel or as low as 15.6 g NO_2/kg fuel. A still unresolved discrepancy exists between spectroscopic and probe sampling methods of determining NO_x emissions (Oliver et al., 1977). If the spectroscopic analyses are correct, the above-cited emission index should be increased by a factor of 2 to 3 for SST operations.

Future technologies may be capable of reducing the NO_x emission index by several fold. A three-fold reduction in the NO_x emission index is projected for some existing design concepts (Popoff et al., 1978). We consider NO_x emission indexes of 18 g NO_2/kg fuel for current technology and 6 g NO_2/kg fuel for future technology.

The number of SST's corresponding to a fuel usage of 3.5×10^{10} kg yr^{-1} is difficult to determine on an absolute scale. The number of SST's corresponding to a given fuel usage is inversely proportional to the expected hours/day of flight and the fuel usage per hour. Estimates of the hours per day of flight at cruise altitude have varied from 4.4 to 7.5 hrs. Estimates of fuel usage have ranged from 16,800 to 19,100 kg/hr for the Concorde, from 52,000 to 60,000 kg/hr for the B2707, and as low as 44,000 kg/hr for a hypothetical advanced design similar to the B2707 (Popoff et al., 1978). Thus, more than a two-fold variation in engine emissions from a projected SST fleet is possible based on different estimates of aircraft operation and fuel consumption rate. A fuel usage of 3.5×10^{10} kg yr^{-1}, therefore, corresponds to about 750-1000 Concordes, or 180-660 advanced SST's. Thus, our standard emissions rates are compatible with a large fleet of SST's.

Hypersonic Transport Emissions

In addition to the effects of subsonic and supersonic fleets, we projected a range of emissions and environmental impacts of a possible hypersonic transport (HST) fleet. For this purpose, we adopted the emissions indexes given in CIAP Monograph 2 (1975), Chapter 6 for a fleet of research HST's of gross takeoff weight 2.27×10^5 kg operating at Mach 8 and cruise altitude of "36.68" km. According to data in CIAP Monograph 2, the hypothesized HST operations would consist of an initial acceleration to hypersonic speeds (and cruise altitude) using rocket engines, followed by about five minutes of SCRAMjet operation, followed by a cruise mode during which most emissions would consist of liquid hydrogen boil-off for cooling.

The SCRAMjet would use 670 kg/flight of liquid H_2; the rocket engines would use 2450 kg/flight of liquid H_2, and 14,650 kg/flight of liquid oxygen (CIAP Monograph 2, p. 6-7); but it would only release a total of 1650 kg/flight of water vapor and 615 kg/flight of H_2 (CIAP Monograph 2, p. 6-8). Thus, the fuel use and emissions estimates given in CIAP Monograph 2 for rocket operations are incompatible, with not enough mass being emitted. This difficulty would be resolved by increasing the water vapor emissions by a factor of 10. Cooling at cruise altitude would consume an additional 309 kg of liquid hydrogen per flight.

The emissions consist of H_2O, H_2, H, OH, NO, and O as given in Table 3. In analyzing the effects of HST emissions, only cooling and SCRAMjet emissions

TABLE 3. HST emissions on a per-flight basis. Data are from CIAP Monograph 2, Ch. 6, assuming a cruising speed of MACH 8, a cruise altitude of 36.68 km, and H_2:O_2 ratio of 1.

	Emissions per flight		Altitude (km)	Emissions rate for 1000 flights/day (molecules $cm^{-3}s^{-1}$)**
	(kg)	(moles)		
SCRAMJet				
H_2O	5705.	317,000	36.68	8504
H_2	136.7	68,350	36.68	1820
H	13.1	13,100	36.68	350
OH	132.3	7,800	36.68	210
NO	137.4	4,500	36.68	123
O	34.4	2,150	36.68	58
Rocket (not included in calculation)				
H_2O*	16,500	917,000	0-36 mostly tropospheric	
H_2	615	307,500	0-36	
Cooling in Flight				
H_2	308.5	154,200	36	4130

*H_2O emissions from rockets have been increased by a factor of ten to permit mass balance.

**Emissions in a 1-km-thick layer.

were treated, and these were based on the data presented in Table 6-9 of CIAP Monograph 2. Rocket emissions were neglected since much of the rocket emissions would occur in the troposphere. In order to approximate a commercially viable fleet, we increased the emissions to correspond to an HST fleet with 1000 flights/day. Because even these emissions are relatively small, and the CIAP-Monograph-2-based emissions estimates may not apply to commercial-scale fleet operations (they are based on research flights), we also examined the effects of a 10-fold larger emission, perhaps interpretable as longer flights or flights of heavier aircraft. The emissions of H_2O, H_2, NO, and OH were treated simply as a source of the molecules in question. Emissions of H-atoms (the code calculates H-atoms as an equilibrium species) were treated as emissions of an equivalent number of HO_2 molecules, while the small emissions of O atoms were ignored.

Because NO_x emissions are responsible for the major portion of the predicted change in total ozone, it might be attractive to use more than the stoichiometric amount of OH in the SCRAMjets in order to reduce NO_x emissions. According to CIAP Monograph 2, operating at a stoichiometric ratio of 1.5 instead of 1 would reduce NO_x emissions by more than a factor of three while increasing H_2O and H_2 emissions by factors of about 1.1 and 3, respectively. The net effect of these changes in emissions should be a smaller ozone perturbation.

We wish to emphasize that we performed no independent calculations of HST emissions indexes, and that the fleet projections are no more than crude parametric estimates of the approximate level of activity that might be associated with a mature, commercially successful fleet of HST's. If specific aircraft designs were to be proposed, the emissions should be independently projected.

4.2 CURRENT ASSESSMENT RESULTS

The LLL one-dimensional transport-kinetics model has been used to assess the potential chemical effects of aircraft engine emissions in the troposphere and the stratosphere. Calculations were made using projected fleet sizes for subsonic and supersonic aircraft as well as for a range of emission rates at particular injection altitudes. In order to determine the effect of uncertainties in various input

parameters on the assessment calculations, several sensitivity studies were also performed and are reported in the following section.

Subsonic and Supersonic Aircraft Fleets

The altitude of injection has a significant effect on the computed change in ozone because of the increase in residence time with altitude and because of the variation with altitude of the dominant chemical reactions and cycles. Table 4 shows the effect on total ozone at steady state of the same NO_x injection rate at different injection altitudes. An injection rate of 1000 molecules $cm^{-3}s^{-1}$ over a 1-km-thick layer was used for NO_x, and there was no injection of H_2O.

Injections of NO_x over the altitude range of 7 to 20 km resulted in a net increase in total ozone in each case. The change in total ozone increased with increasing injection altitude for the troposphere and lower stratosphere. Throughout this region HO_x chemistry is the dominant chemical destruction process for ozone. When HO_x chemistry is more efficient than NO_x catalytic destruction of ozone, injections of NO_x lead to a net increase in odd oxygen production through the reaction sequences:

TABLE 4. The change in total ozone resulting from an NO_x injection of 1000 molecules $cm^{-3}s^{-1}$ distributed over a 1-km-thick layer centered at the injection altitude. The calculations were made using 1979a chemistry (Appendix A).

Injection Altitude (km)	Change in Total Ozone (%)
7	0.25
9	0.40
11	0.64
13	0.84
17	1.34
20	1.31

$$\begin{aligned} &NO + HO_2 \rightarrow NO_2 + OH \\ &NO_2 \xrightarrow{h\nu} NO + O \end{aligned} \qquad (5)$$

$$\text{net } HO_2 \rightarrow OH + O$$

and

$$\begin{aligned} &NO_2 + OH \xrightarrow{M} HNO_3 \\ &OH + HNO_3 \rightarrow H_2O + NO_3 \\ &NO_3 \xrightarrow{h\nu} NO_2 + O \end{aligned} \qquad (6)$$

$$\text{net } 2OH \rightarrow H_2O + O$$

The reaction sequence (5) acts to shift HO_x more toward OH, thereby increasing the loss rate of HO_x by the reaction $HO_2 + OH \rightarrow H_2O + O_2$. Reaction sequence (6) acts to reduce HO_x as OH and HO_2 are converted to H_2O and HNO_3. Conversion to H_2O, and to a lesser extent HNO_3, acts as a sink for HO_x, since the chemical lifetimes of these reservoir species is long compared to the time for transport into the troposphere. Injections of NO_x act to increase the rates of the above reactions. The net effect of reaction sequences (5) and (6) is a reduction of HO_x and an increase in odd oxygen production, both of which contribute to an increase in ozone. Of course, the odd-hydrogen species may have been generated through reaction of $O(^1D)$ with H_2O. If this is the case, the odd oxygen produced via (5) or (6) only regenerates that used in the initiation of a catalytic cycle. It is important, nonetheless, because these sequences compete for HO_x with odd-oxygen destroying sequences.

Increases in NO_x concentration in the upper stratosphere lead to a reduction in ozone concentration in this region due to the greater importance of the NO_x catalyzed ozone destruction at these altitudes. The 20-km injection of NO_x resulted in a smaller net increase in total ozone than did the 17-km injection case, since more NO_x reached the upper stratosphere causing a greater reduction in ozone concentration at high altitudes relative to the increase at lower altitudes. This effect was found to be sensitive to the shape of the K_z profile used, however.

The standard model uses fixed-value boundary conditions for all species (except CCl_4) at the ground. Using flux boundary conditions for the species

N_2O, CH_4, CH_3Cl, and HCl, resulted in slightly larger increases in total ozone (< 0.1% in absolute change) when compared to the fixed boundary condition case. Consequently, the choice of boundary condition has only a very small effect on the assessment results. Fixed-value boundary conditions are used in the model calculations unless otherwise noted.

The model was tested for interference effects by comparing the effect of simultaneous injections at the various injection altitudes given in Table 4 with the sum of the changes in ozone for individual injection altitudes. Table 5 shows that there is a destructive interference. That is, the simultaneous injections resulted in less change in total ozone than the sum of the changes caused by individual injections. This implies that summing the results of separate calculations for subsonic and supersonic fleets will not give the same answer as considering the effect of the two fleets simultaneously.

The effect of NO_x emissions by subsonic and supersonic fleets projected for 1990 are given in Table 6. Using the high estimate of the fleet sizes, the effect of subsonic and supersonic aircraft combined is estimated to be an increase in total ozone of 2.01%. This number represents the steady state change in ozone due to

TABLE 5. Synergism test using fixed boundary conditions and 1979a chemistry.

Case	ΔO_3(%)
Simultaneous injections	3.68
Sum of individual injections	4.78

TABLE 6. The computed change in total ozone at steady state using NO_x emission estimates for 1990 subsonic and supersonic fleets (1979b chemistry).

Case	Change in Total Ozone (%)	
	Subsonic and Supersonic	Subsonic Only
Oliver et al. (1977) high 1990 fleet estimate	2.01	1.86
Low 1990 fleet estimate	1.39	1.29

constant NO_x emission rates at the rates estimated for 1990. The subsonic fleet alone (injection altitudes up to 14 km) is estimated to cause an increase in total ozone of 1.86%. The small effect of the supersonic fleet is due primarily to the small fleet size projected for 1990. Using the lower estimate for fleet emissions, the corresponding numbers for ΔO_3 are 1.39% for the combined fleets and 1.29% for the subsonic fleet alone.

It should be noted that the effects of the existing 1979 subsonic fleet are of the order of 0.5% increase in total ozone. This effect is not negligible when compared to the estimated present-day effects of CFMs. Thus, an accurate assessment of the effects of subsonic aircraft will be important in interpreting ozone data for trends due to other anthropogenic influences.

The changes in ozone concentration for the high and low estimates of subsonic and supersonic fleet emissions are shown in percent in Fig. 20 and in absolute concentration in Fig. 21. The largest absolute increase in ozone concentration occurs near 12 km, and the region of increasing ozone extends up to about 26 km. Between 26 and 39 km there is a small decrease in ozone concentration.

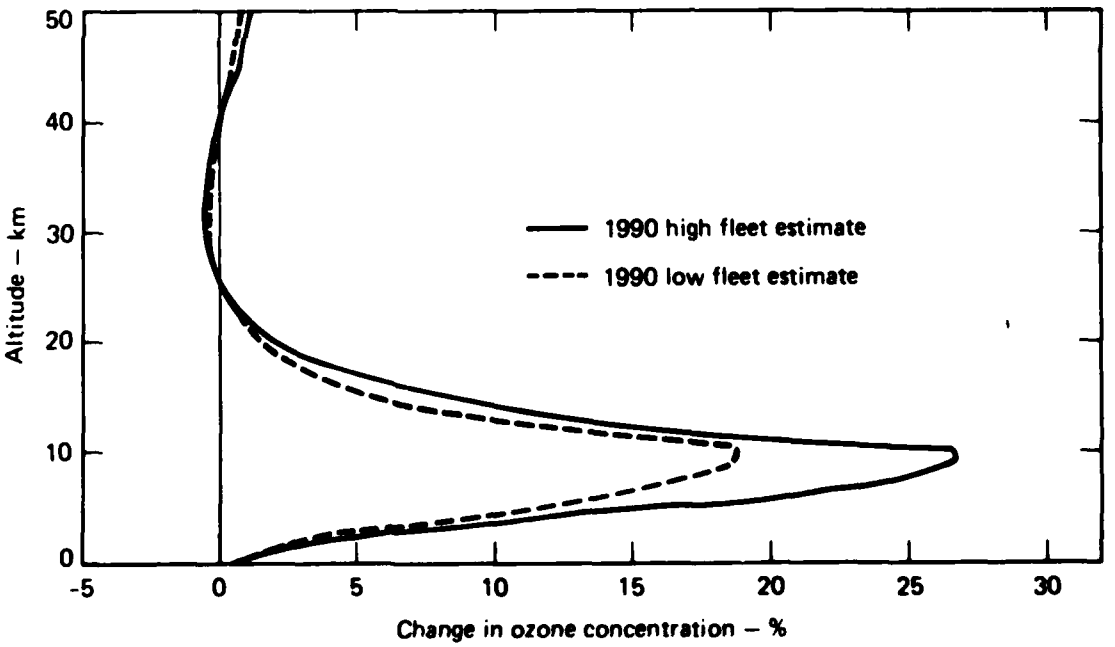

FIGURE 20. The percent change in ozone concentration due to subsonic and supersonic aircraft computed for 1990 high and low fleet estimates (1979b chemistry).

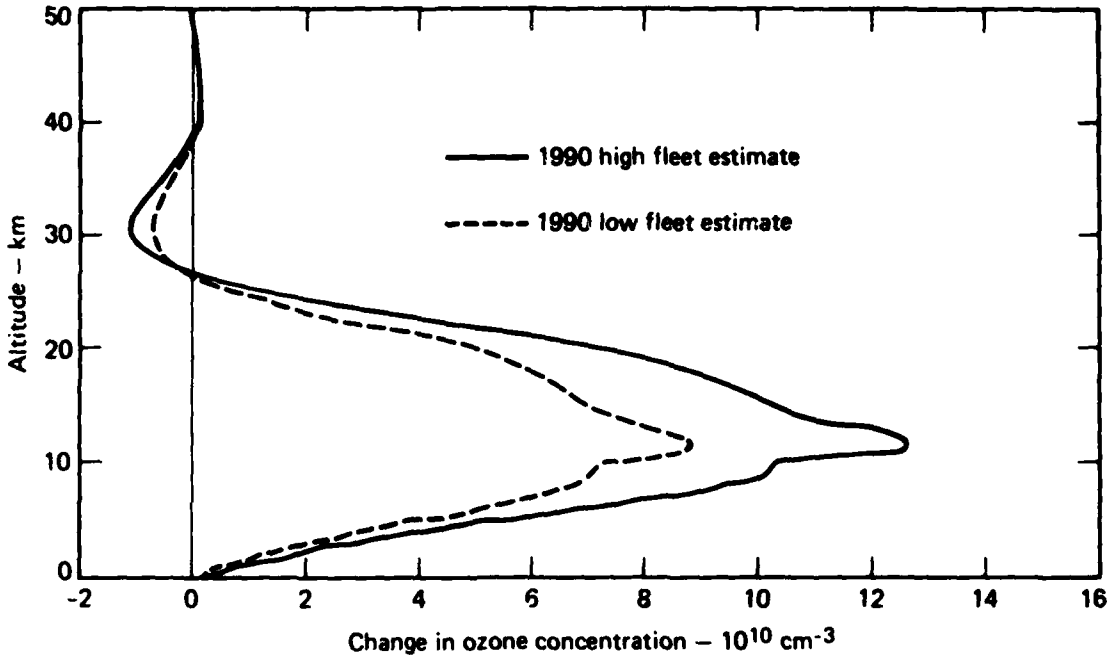

FIGURE 21. Same as Fig. 20 except the change in ozone concentration is expressed as molecules cm^{-3} (1979b chemistry).

It should be recognized that the bulk of the ozone change calculated for the subsonic fleet occurs in the upper troposphere. As a result, it is sensitive to the treatment of such poorly understood phenomena as wet and dry removal processes and surface boundary conditions for rarely measured species. The tropospheric pressures differ from the pressure conditions used in most direct measurements of chemical rate coefficients (to a greater degree than stratosphere pressures). Heterogeneous reactions, which might have a significant effect on the calculations, are not included, and the one-dimensional treatment is not as good an approximation for the troposphere as it is for the stratosphere because of the strong latitudinal and longitudinal gradients in many trace species. Thus, the results for the 1990 fleet estimates are suggestive but are by no means definitive.

Assessments of potential changes in ozone due to future large fleets of supersonic transports have focused on injection altitudes of 17 and 20 km. In updating these assessments, we have assumed an emission index of 18 kg fuel for NO_x and 1250 kg fuel for H_2O. These emission indexes are based on current engine technology. It may be possible through future advances in technology that the NO_x emission index could be reduced to 6 kg (one-third of present value).

Calculations of O_3 given a constant fuel consumption rate at cruise altitude (3.5 x 10^{10} kg/yr in a hemispheric shell) are shown in Table 7 for different emission indexes. The NO_x emission rate of 1000 molecules $cm^{-3}s^{-1}$, which roughly estimates the emissions from a commercially viable fleet, was chosen as a reference case. The equivalent annual hemispheric injection rates of NO_x and H_2O are given in Table 8.

For each of the perturbations considered, there was an increase in total ozone. When the water vapor injection is included with the NO_x injection, there is less of an increase in total ozone because of the additional ozone destruction caused by HO_x which is produced from dissociation of H_2O. For the advanced

TABLE 7. The change in total ozone due to NO_x and H_2O emissions distributed over a 1-km-thick layer centered at the injection altitude.

Injection Altitude (km)	Injection Rate (molecules $cm^{-3}s^{-1}$)		Change in Total Ozone (%)	
	NO_x	H_2O	1979a Chemistry	1979b Chemistry
17	1000	0	1.34	1.25
17	1000	177,000	1.18	
17	333	177,000	0.32	
20	1000	0	1.31	1.14
20	1000	177,000	0.91	
20	333	177,000	0.07	

TABLE 8. Equivalent annual hemispheric injection rates for various NO_x and H_2O emissions.

Species	Injection Rate	
	(molecules $cm^{-3}s^{-1}$)	(kg/yr*)
NO_x	333	2.1×10^8
NO_x	1,000	6.2×10^8
H_2O	177,000	4.3×10^{10}

*Hemispheric injection assuming uniform injection over a 1-km-thick layer.

technology case (reduced NO_x emission), the increase in total ozone due to the NO_x injection is still greater than the reduction due to the H_2O injection, the net effect being a very small increase in total ozone.

In comparing the results from different models, a method that proved useful in the past was to compare the ratio $\Delta NO_y(\%)/\Delta O_3(\%)$ rather than just comparing ΔO_3 (Chang and Johnston, 1974; Chang, 1974). Although models differed in their computed values for ΔO_3, they gave quite similar values for the ratio $\Delta NO_y/\Delta O_3$. At that time the models were predicting reductions in total ozone, and a typical value for the ratio was -5 or -6. Values of this ratio for the current model results are shown in Table 9. The ratio has a value of approximately 10 for a 17 km injection altitude with some dependence on the NO_x injection rate. ΔNO_y varies linearly with NO_x injection rate, but ΔO_3 is nonlinear, particularly for injection rates greater than 1000 molecules $cm^{-3}s^{-1}$. This is even more apparent for the 20-km injection altitude results where the ratio is 15.7 for an NO_x injection rate of 500 and increases to 24.6 for an injection rate of 2000. Because of the nonlinear characteristic of ΔO_3 for large injection rates, the ratio $\Delta NO_y/\Delta O_3$ is only useful for comparing model results for small injection rates.

TABLE 9. Changes in O_3 and NO_y column densities for various NO_x emission rates (1979a chemistry).

Injection Altitude (km)	NO_x Injection Rate (molecules $cm^{-3}s^{-1}$)	ΔO_3 (%)	ΔNO_y (%)	$\Delta NO_y/\Delta O_3$
17	500	0.72	7.0	9.7
17	1000	1.34	14.0	10.4
17	2000	2.37	28.0	11.8
20	500	0.75	11.8	15.7
20	1000	1.31	23.6	18.0
20	2000	1.91	47.0	24.6

Hypersonic Transport Fleet

The hypothesized hypersonic transport fleet making 1000 flights per day was calculated to cause a -0.218% change in column ozone. Emissions from a fleet ten times larger were calculated to cause a -2.06% change in column ozone. The NO_x emissions from the latter fleet by themselves caused an ozone change of -2.13%.

Figure 22 shows the local percentage changes in ozone vs. altitude for the 10,000 flight per day HST emissions and the NO_x emissions alone from 10,000

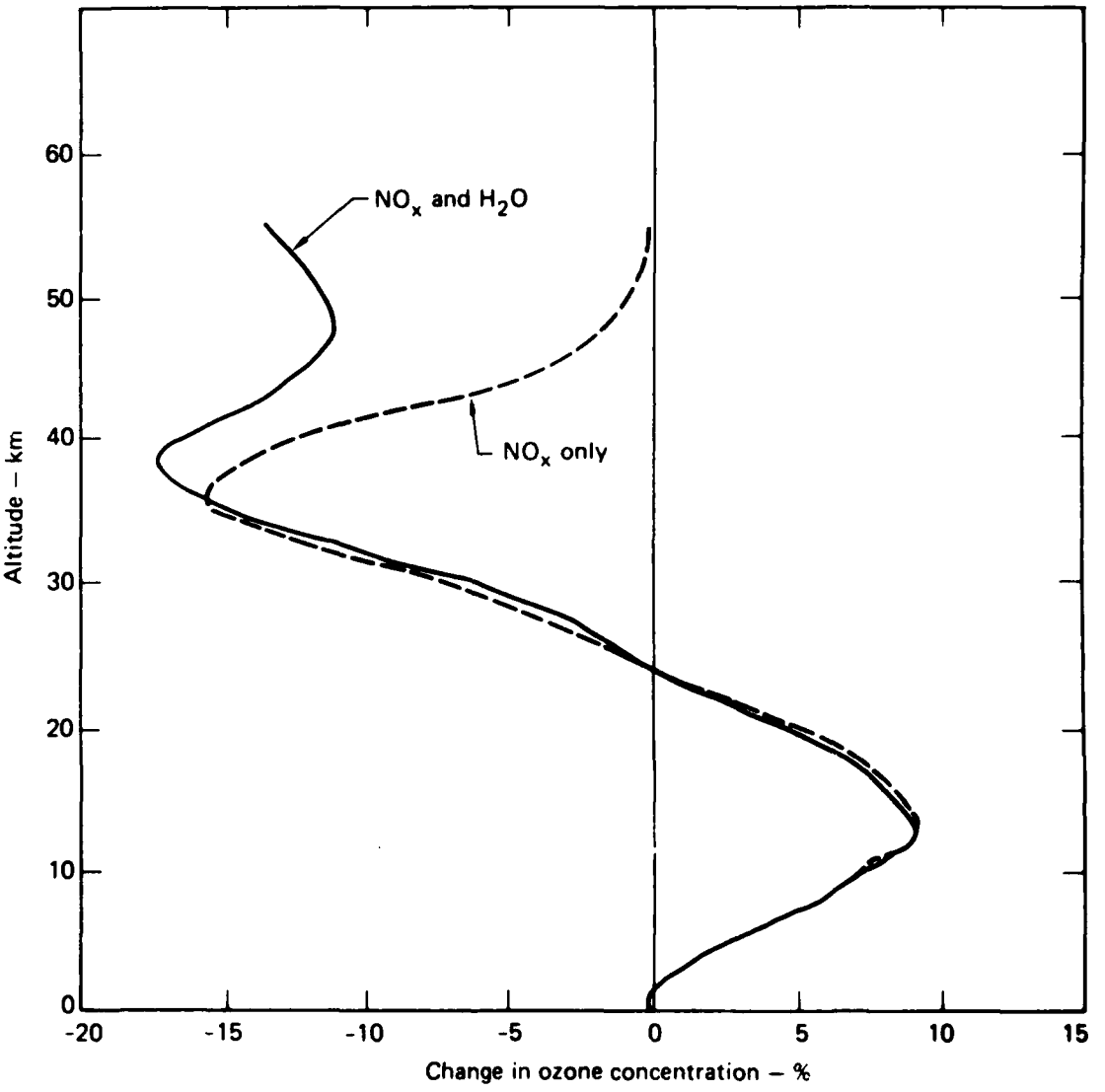

FIGURE 22. The change in ozone concentration caused by HST emissions for a fleet with 10,000 flights per day (1979b chemistry).

flights per day of HST's. (Because ΔO_3 is roughly linear in emissions rate over the range considered, large fleets were chosen to avoid comparing very small local changes that might contain significant numerical noise.) As is evident, the NO_x emissions dominate the ozone changes below $\sim$ 40 km, while H_2O and H_2 emissions are responsible for most of the ozone change at higher altitudes. Because most of the ozone column is below 40 km, the integral column change is largely a result of the NO_x emissions.

4.3 SENSITIVITY STUDIES

Effect of Variations in K_z

Use of the vertical transport parameter K_z in the one-dimensional model enables atmospheric transport to be parameterized in a mathematically simple and convenient manner resembling diffusion. Various K_z profiles have been developed for use in one-dimensional models using N_2O and CH_4 measurement data. Because of variations in the data and because neither N_2O nor CH_4 are perfect tracers, there is no unambiguously correct K_z profile.

The K_z profile currently being used in the LLL one-dimensional model is shown in Fig. 23. The K_z values averaged over the stratosphere are considerably higher than was typical of K_z profiles used during the DOT's Climatic Impact Assessment Program (CIAP), which ended in 1975. Two profiles that were used for many of the assessments included in the CIAP Report of Findings (Grobecker et al., 1974) are also shown in Fig. 23. The Chang (1974) and Hunten (1975) K_z profiles result in slower transport between the middle stratosphere and the troposphere, so there is a larger build-up of emitted species in the stratosphere for constant injection rates.

Calculations of the change in total ozone as a result of an NO_x injection rate of 1000 molecules $cm^{-3}s^{-1}$ are shown in Table 10 using the LLL, Chang (1974), and Hunten (1975) K_z profiles. The Chang (1974) and Hunten (1975) profiles are used to provide continuity with the earlier CIAP assessments; They are not representative of K_z profiles currently in use by any modeling group.

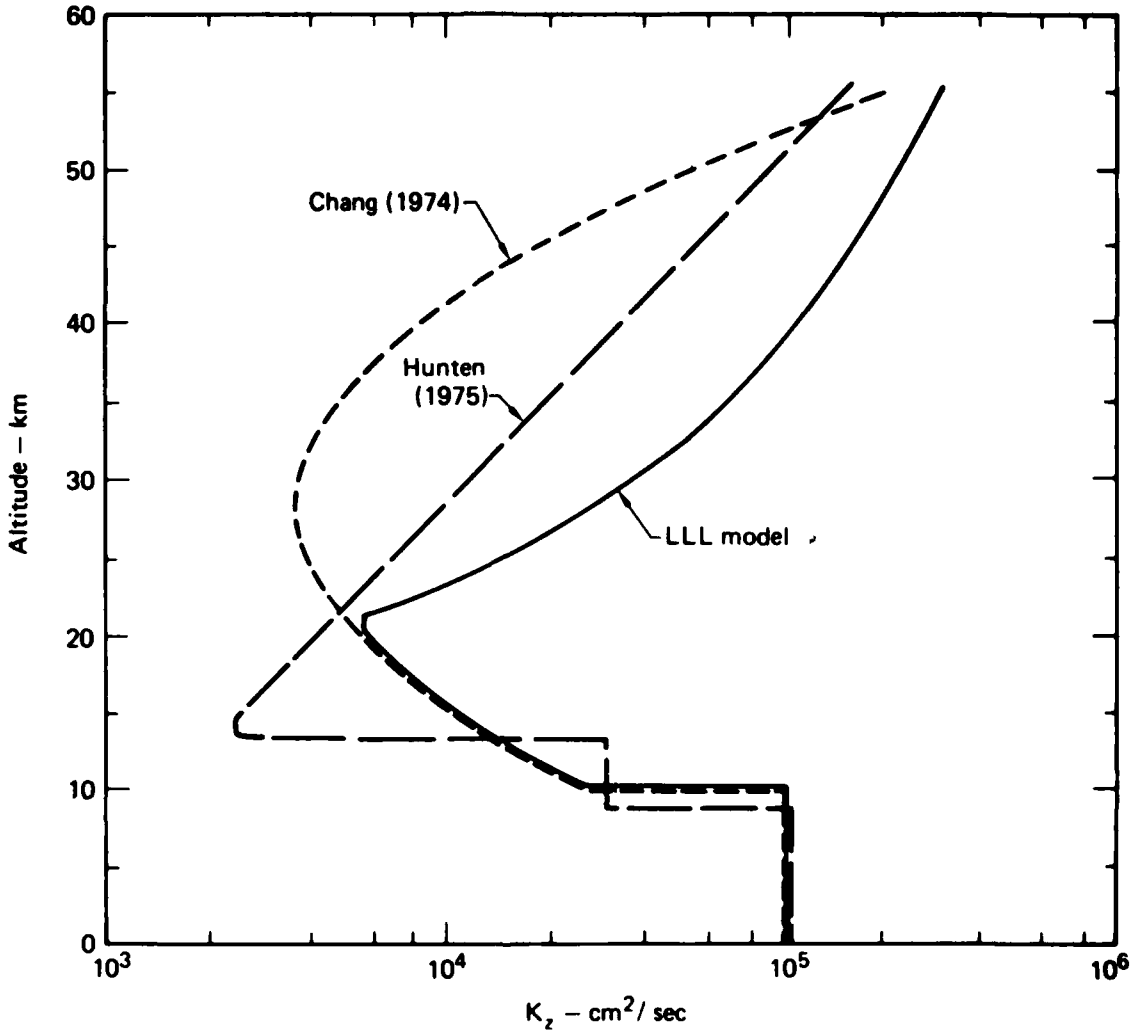

FIGURE 23. Vertical transport coefficient profiles used in the sensitivity study. The Chang (1974) and Hunten (1975) profiles are included for historical purposes.

The results in Table 10 show that changes in the K_z profile since 1975 have had a significant effect on the computed change in total ozone. Not only have changes in model chemistry caused a reduction (and reversal in sign) in the computed magnitude of ΔO_3, but the changes in K_z have been significant as well. It is still true that the choice of K_z profile is a source of uncertainty in the one-dimensional calculations, but the range of results using currently popular profiles would not be as large as that in Table 10.

TABLE 10. The effect of the choice of K_z profile on the change in total ozone computed for an NO_x emission rate of 1000 molecules $cm^{-3}s^{-1}$ (1979a chemistry).

Injection Altitude (km)	Change in Total Ozone (%)		
	LLL K_z	Chang (1974) K_z	Hunten (1975) K_z
17	1.34	1.91	2.65
20	1.31	2.49	2.07

Effect of Variations in Background ClX

The effect of aircraft engine emissions on stratospheric composition is coupled with other stratospheric perturbations. As chlorofluoromethanes (CFM's) continue to be released to the atmosphere, there will be a gradual increase in the background concentration of ClX (Cl + ClO + HCl). Model calculations indicate a present day stratospheric ClX concentration of more than 1 ppbv. Assuming CFM releases at the 1976 release rate indefinitely into the future, the background ClX concentration is projected to increase to 2 ppbv around 1990 and to 4 ppbv around 2020. To assess the effect of changes in background ClX concentration on the model sensitivity, several NO_x perturbation calculations were repeated using a range of ClX concentrations. The results are shown in Table 11. In each case the ClX concentration was held constant. So the change in total ozone is the steady state value for a constant injection rate (i.e., the ΔO_3 value does not pertain

TABLE 11. The effect of variations in background ClX on the computed change in total ozone (1979a chemistry).

Injection Altitude (km)	NO_x Injection Rate (molecules $cm^{-3}s^{-1}$)	Change in Total Ozone (%)		
		1.14 ppb ClX	1.83 ppb ClX	3.76 ppb ClX
17	500	0.65	0.72	0.89
17	1000	1.22	1.34	1.69
17	2000	2.14	2.37	3.03
20	500	0.61	0.75	1.12
20	1000	1.04	1.31	2.03
20	2000	1.42	1.91	3.28

to any particular year) relative to a natural atmosphere with the same ClX concentration.

Table 11 shows that the change (increase) in total ozone resulting from an NO_x injection increases as the ClX concentration increases. The reason for the increase in ΔO_3 is related to the mechanism by which an NO_x injection leads to an increase in total ozone. The increase in total ozone comes about because for these magnitudes of NO_x injections, NO_x interferes with the more efficient ozone destruction by HO_x and ClX. Increasing the background ClX concentration means that there is more ozone destruction by ClX in the ambient case, so there is more that can be interfered with by the injected NO_x.

The change in total ozone versus NO_x injection rate is shown in Figs. 24 and 25 for ClX concentrations of 1.14, 1.83 and 3.76 ppbv. The change in total ozone is approximately linear with NO_x injection rate for injection rates up to 500 molecules $cm^{-3}s^{-1}$ (over a 1-km-thick layer). The nonlinear relationship between ΔO_3 and NO_x injection rate begins to show up for injection rates between 500 and 1000 molecules $cm^{-3}s^{-1}$, becoming more noticeable at larger injection rates. Linearity becomes a poor approximation at a lower injection rate for a 20-km injection than for a 17-km injection.

The ClX concentration, in addition to affecting the magnitude of ΔO_3, also affects the relative magnitudes of the 17- and 20-km perturbations. For 1.83 ppbv ClX, the change in total ozone is nearly the same for both 17- and 20-km injection altitudes for injection rates up to 800 molecules $cm^{-3}s^{-1}$. For larger injection rates, ΔO_3 is larger for the 17-km injection than for the 20-km injection. On the other hand, when ClX is 3.76 ppbv ΔO_3 is larger for the 20-km injection than for the 17-km injection.

Effects of Speculative Reactions and Mechanisms

There are several reactions that have been suggested to be of possible importance in the stratosphere but have not been measured yet. Also, there are a few reactions for which anomalous pressure/temperature dependencies have been suggested but not demonstrated. We have examined the sensitivity of model predictions to a subset of such hypothetical reactions. The subset selected was based on the following criteria: (1) the hypothesized reaction or mechanism has at

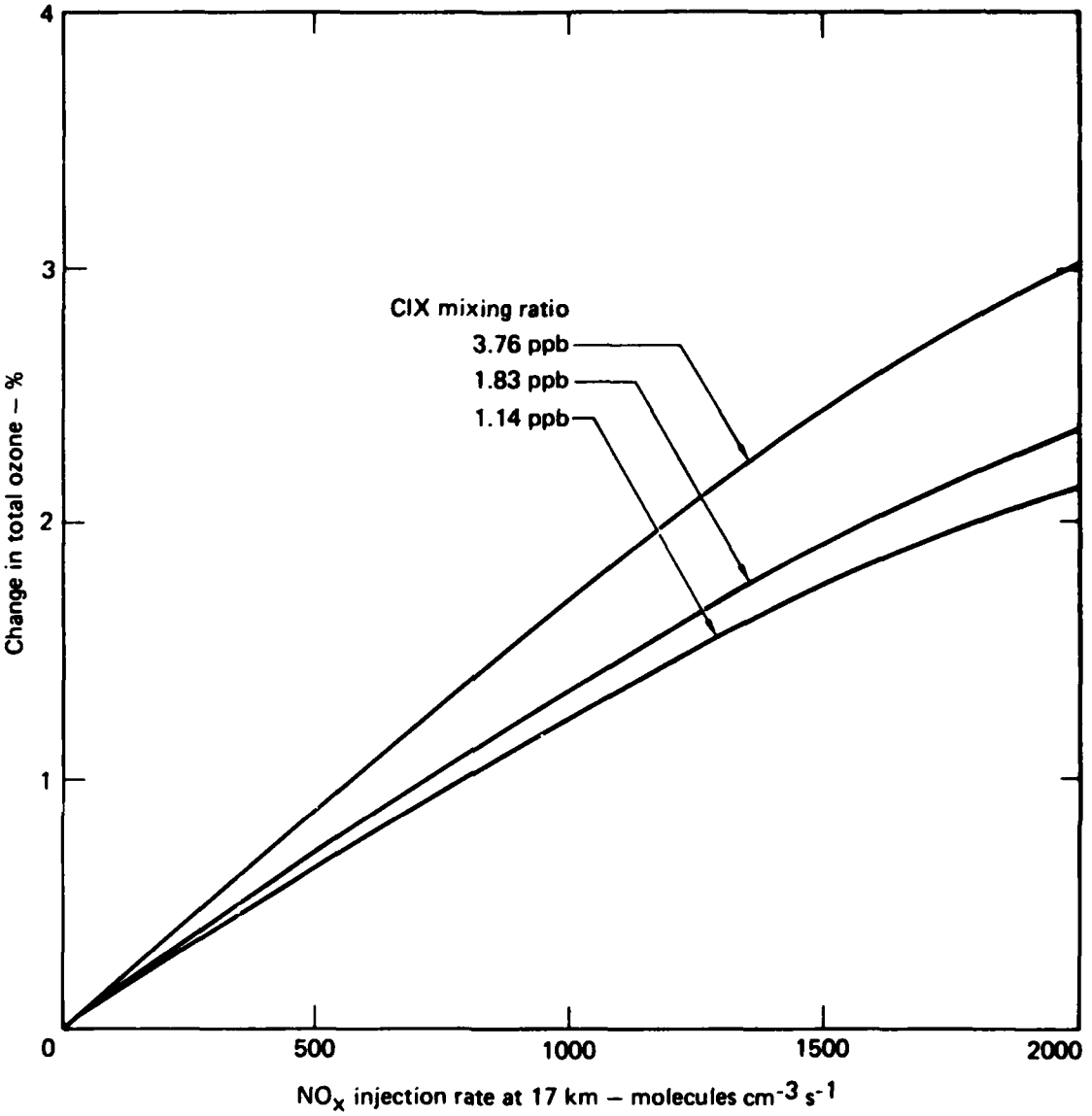

FIGURE 24. The change in total ozone as a function of NO_x injection rate at 17 km for various background ClX concentrations (1979a chemistry).

least some support from laboratory work, and (2) the hypothesized reaction appears to have the potential for causing a major change* in predicted effects of SST's or

*In this context a major change would consist of a change in the computed steady-state effect of chlorofluoromethanes at 1975 levels by at least 50% or a change in sign or 2-fold increase in computed SST effects. Not all of the cases studied actually have such large effects and some mechanisms not studied might have larger effects.

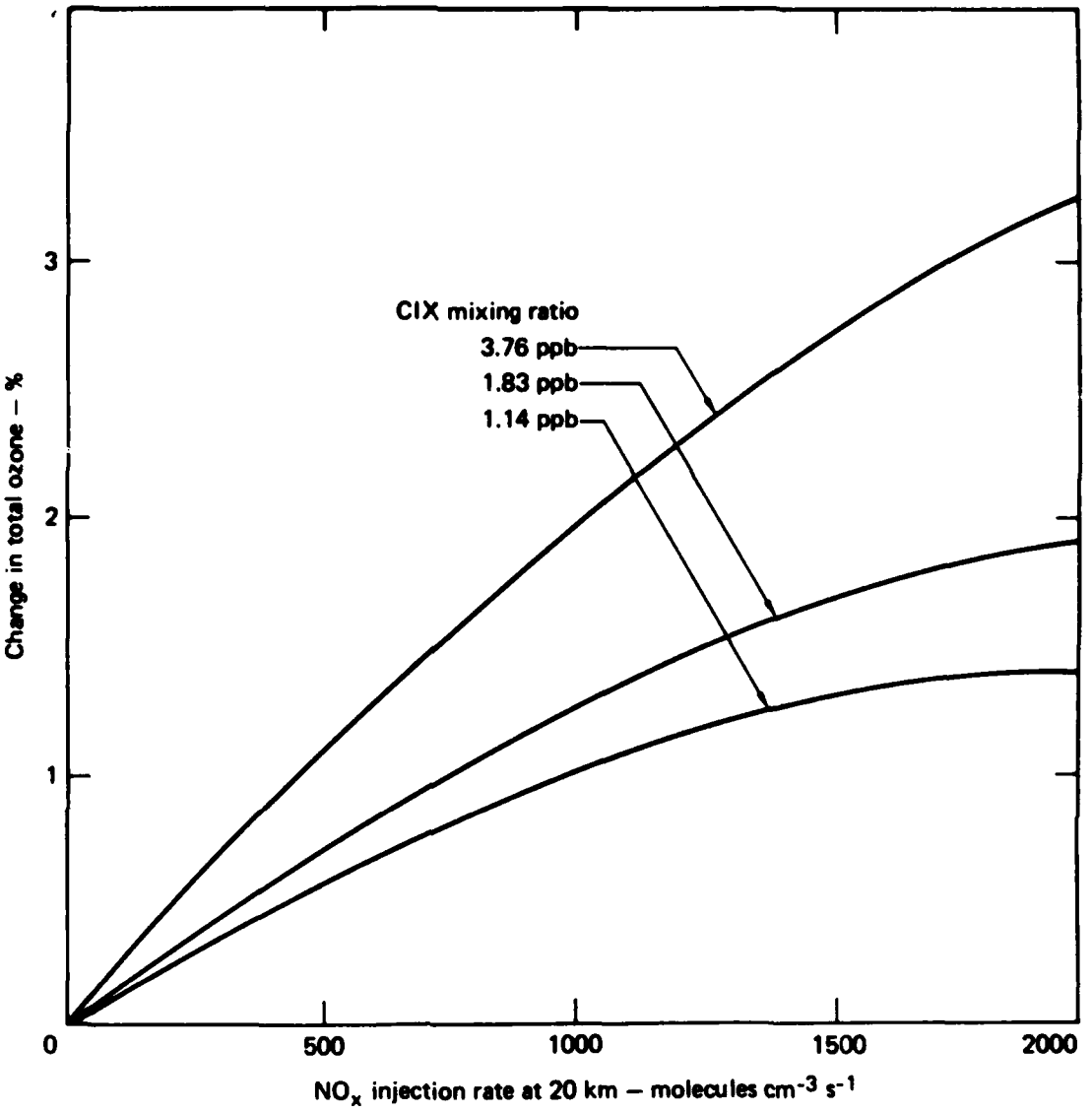

FIGURE 25. The change in total ozone as a function of NO_x injection rate at 20 km for various background ClX concentrations (1979a chemistry).

CFM's. The reasons for selecting these two criteria were to reduce the number of possible cases to be considered and to focus attention on mechanisms that appear to have a maximum potential for altering model predictions. It must be stressed that most of the mechanisms considered here have no more than a weak basis in actual measurement. The purpose of this section is to suggest experiments that might deserve some priority. It is not to suggest that the hypothesized mechanisms or their computed effects are particularly likely to be true.

In this section we will discuss the major effects on the computed ambient atmosphere and model sensitivity of the various mechanisms considered. Although the changes to the ambient species concentration profiles may tend to either improve or worsen the agreement with observations for various species, we have not established a criterion for agreement (or disagreement) upon which to evaluate the likelihood that the mechanism actually occurs or to eliminate it from consideration. By combining the description of the effects on the ambient profiles discussed in this section with the comparison with observations discussed in Section 2, the reader can form his own opinion on this matter.

1. Chlorine Nitrate Formation

In terms of published evaluations of mechanistic data, perhaps the most plausible speculation is that roughly 75% of the reaction between ClO and NO_2 forms a relatively short-lived species isomeric with chlorine nitrate, and the effective rate of chlorine nitrate formation is only about one-fourth of the observed rate of reaction between ClO and NO_2. In JPL (1979) (and NASA, 1979) no firm choice is made between the assumption that all of the reactions between ClO and NO_2 lead to chlorine nitrate and the assumption that only about 25% do, although most modelers have adopted the first assumption. The choice of treatment for this reaction is one of the major differences between the 1979a and 1979b chemistries. As can be seen from Table 12, if the slower rate of chlorine nitrate formation is assumed, the calculated effects of an SST fleet become more positive than in the base case, while the computed effects of CFM's become more negative. In each case, the fractional change is of the order of a factor of 1.3. Clearly, the correct treatment of chlorine nitrate formation is of substantial importance. It is also worth noting that if the isomeric products have greater photolytic stability than $ClONO_2$, or if, as impurities, they account for some of the observed absorption spectrum of $ClONO_2$, the effect of chlorine nitrate isomers on predictions might actually be reversed. This could happen if the mean rate of loss of some $ClNO_3$ products were to be slower than that presently assumed for $ClONO_2$ so that larger concentrations of $ClNO_3$ species would be generated.

When the low rate is assumed for chlorine nitrate formation, a significant (>10%)* change in the ambient state is computed for Cl, ClO, HCl, HOCl, and

*All percent changes reported in this section refer to fractional changes in the quantity relative to the standard (1979b model) ambient conditions or model sensitivity.

TABLE 12. Results of sensitivity calculations for speculative chemical reactions and mechanisms.

Model Content	Ambient Ozone Column (Dobson units)	Change in Total Ozone (%)		
		17-km NO_x Injection*	20-km NO_x Injection*	CFM** Production
Baseline Model (1979b) - NASA Harpers Ferry Workshop, ∿2 ppb ClX	322	1.25	1.14	-14.6
Slower rate of $ClONO_2$ formation	312	1.42	1.54	-19.3
Photolysis of $XONO_2$ to $XO + NO_2$ products	324	1.35	1.20	-12.2
Pressure and temperature dependent HO_x disproportionation reactions	339	0.47	-0.40	-8.9
HCl production from $ClO + OH$, $ClO + HO_2$	334	0.74	0.02	-4.4
ClO_3 production, $K_{equilibrium}$ as for ClO_2 from NASA 1010, no other reaction of ClO_3	322	1.24	1.11	-14.0
$OClO_2$ production $K_{equilibrium}$ as for ClO_2 from NASA 1010, subsequent chemistry described in text	337	1.51	1.40	-6.91
$OClO_2$ production $K_{equilibrium}$ as for ClO_2 from JPL (1979) subsequent chemistry described in text	323	1.27	1.16	-14.0
$OClO_2$ production $K_{equilibrium}$ as for ClO_2 from NASA 1010, subsequent chemistry described in text and P,T dependent HO_x disproportionation reactions	353	0.49	-0.51	0.73

*Rate of emission is 1000 molecules (NO) $cm^{-3}s^{-1}$ over a 1-km-thick layer.

**Constant release rate at 1976 levels.

$ClNO_2$, all of which increase by nearly a factor of 2 at 25-30 km, while $ClNO_3$ is reduced by a factor of 3 to 4 at almost all altitudes. Thus, this hypothesis exacerbates the apparent disagreement between observation and calculation for the shape of the ClO vertical profile and destroys the apparent agreement between calculation and the preliminary chlorine nitrate measurement reported by Murcray (1979).

2. Photolysis of $XONO_2$ Species

Almost equally uncertain are the products of the photolysis of species of the form $XONO_2$, where X = OH, Cl, NO_2. In the base case it has been assumed that all of these reactions lead to X + NO_3. This assumption is largely based on the experimental results of Chang et al. (1979) for chlorine nitrate.

Other products are possible, perhaps the most distinct (in terms of model predictions) would be XO + NO_2 (or for N_2O_5, $2NO_2$ + O). In a computation in which all of these photolyses were assumed to yield XO + HO_2 products (except N_2O_5 which was assumed to yield $2NO_2$ + O), the computed effects of SST emissions became more positive by 5-10% (of the change computed for the base case) while the effects of CFM's became less negative by about 17%. Thus, resolving the question of photolysis products of XOClO species is of modest importance to perturbation calculations.

In terms of species concentrations, only NO_3 and N_2O_5 displayed large changes (both were reduced by a factor of two to three at the region of their largest mixing ratios, and by up to 90% at some (lower) altitudes). Several other species displayed changes on the order of 10-15% at some altitudes.

3. Pressure-Dependent Rates for HO_x Disproportionation Reactions

A significant pressure, inverse temperature and water vapor dependence has been reported for the reaction $HO_2 + HO_2 \xrightarrow{M,H_2O} H_2O_2 + O_2$ (Cox, 1978; Hamilton and Lii, 1977; Cox and Burrows, 1979). Furthermore, while the measurements of the reaction HO_2 + OH at low pressures seem only mildly inconsistent with each other, the indirect values inferred at higher pressures (Hochanadel et al., 1972; DeMore and Tschuikov-Roux, 1974; DeMore, 1979) are substantially (2 to 4 fold) faster than the values measured at low pressures. In this context, the poorly understood pressure, temperature, and water vapor dependence of HO_2 + HO_2 suggests the possibility that HO_2 + OH may also be affected by

similar phenomena. As can be seen in Table 12, when we assumed that the expression given by Cox (1978) for $k_{HO_2+HO_2}$,

$$k_{HO_2+HO_2} = \frac{(3.25\times10^{8} + 4\times10^{-10}[M]/(1 + 3.5\times10^{-16}[M]\ e^{-2060/T}))}{8[M] + 4.08\times10^{20}}, \quad (7)$$

and an expression for k_{OH+HO_2} designed to yield a low-pressure value compatible with Chang and Kaufman (1978), and a high pressure value compatible with the larger rate constants reported at high pressure, i.e.,

$$k_{HO_2+OH} = (5 \times 10^{-30} \times M + 3 \times 10^{-11})(300/T)^{3} \quad , \quad (8)$$

there were major changes in model predictions for both SST's and CFM's. Here it should be emphasized that the expression used for the rate constant for reaction of HO_2 with OH is completely arbitrary. It was designed to approximately fit high- and low-pressure data. Had a Lindeman-Hinshelwood expression been fit to the same data, or had a constant ratio to the $HO_2 + HO_2$ rate been assumed, the effects would have been different (probably larger) but equally plausible. The form chosen reflects the postulation of a pressure independent abstraction mechanism coupled with a pressure dependent enhancement reflecting complex formation (with a limiting value well above 1×10^{-10} at room temperature).

Elucidation of the pressure and temperature dependencies of the HO_x radical disproportionation reactions should be of high priority to those concerned with SST effects and of considerable importance to those concerned with CFM production effects. The assumed change in the $HO_2 + OH$ reaction is substantially more important than the change in the $HO_2 + HO_2$ reaction within the stratosphere. However, the $HO_2 + HO_2$ reaction is of significant importance in the troposphere, and the effects of subsonic aircraft operations are expected to be sensitive to it, as would be the effects of CH_3CCl_3 emissions.

When the above assumptions were made about the HO_x disproportionation reactions, many species changed by roughly a factor of two between $\sim$10 and 20 km. Roughly two-fold reductions (between $\sim$10 and 20 km) occurred for OH, HO_2, Cl, ClO, and CH_2O while H_2O_2 was reduced by roughly the square of the fractional reduction in HO_2. Computed NO and NO_2 displayed two-fold increases over the same altitude range. Species that were only slightly changed included HNO_3 (<10% changes) and CH_4 ($\sim$10% increase at high altitudes).

Thus, changes in the HO_x disproportionation rates akin to those considered here would cause substantial changes in computed profiles of short lived species in the region from 10 to 20 km. Some of these changes tend to improve agreement with observation, others tend to reduce it. Although CH_4 increases at higher altitudes, the increase is not large enough to demand a major revision in K_z even if future experiments should suggest the pressure-dependent disproportionation rates used here to be fair approximations of reality. For CH_4 to increase substantially at higher altitudes, it would be necessary for an increase in k_{OH+HO_2} to extend to substantially lower air densities.

All of the above speculations have at least some direct basis in laboratory measurements. The speculations that follow are even more tenuous than the above.

4. HCl Formation from HO_x + ClO

The reaction between OH and ClO could yield HO_2 + Cl or HCl + O_2 at low pressures, or at higher pressures it might yield a moderately stable species of the form HOOCl (a peroxide) or HOClO (an acid). Either of these last species might be expected to be unstable with respect to disproportionation in a condensed phase, but gas phase stability seems possible. In any case, the production of HCl + O_2 from HO + ClO would seem likely to have the most drastic effect on model predictions. The overall reaction has a rate constant of 9.2×10^{-11} at room temperature, and the products HO_2 + Cl account for at least 65% of the products (Leu and Lin, 1979). These products have little effect on model sensitivity.

An investigation of the effect of this reaction producing HCl assuming a rate constant of 2×10^{-12} cm^3/sec suggested that model sensitivity to a CFM perturbation could be reduced by $\sim$40%; at 1×10^{-12} cm^3/sec the sensitivity would be reduced by roughly 20%.

A similar argument could be applied to the reaction:

$$HO_2 + ClO \rightarrow HOCl + O_2 \qquad (9)$$

$$HO_2 + ClO \rightarrow HCl + O_3 \quad . \qquad (10)$$

The only evidence suggesting a plausible role for reaction (10) is that at temperatures below room temperature, the rate of the overall reaction increases substantially as the temperature is reduced (C. Howard et al., NOAA Aeronomy Laboratory, Boulder, private communication, 1979). This suggests the possibility

that a five-centered complex might be formed and HCl + O_3 eliminated. If the rate of HCl formation via this reaction were to be as large as 1 x 10^{-12} cm^3/sec, then the effect of CFM's would be reduced by ∿ 50%, and, if the rate were to be even larger, increases might be computed from CFM releases.

Table 12 gives the sensitivities obtained when both HO + ClO → HCl + O_2 and HO_2 + ClO → HCl + O_3 were assumed to have rate constants of 1 x 10^{-12} cm^3/sec. As is evident, these reactions might have a major impact on both CFM and SST effects, and they might have a smaller but significant effect on computed CFM effects at rates as low as ∿1 x 10^{-13} cm^3/sec.

The effect on the model sensitivity to an NO_x perturbation is largely a result of there being a lessened rate of ClX and HO_x catalytic destruction of ozone with which NO_x can interfere. Also, null cycle sequences involving ClX and HO_x are not as effective in competing with ozone-destroying sequences for NO. The reduced sensitivity to CFM perturbations results from both an increase in the rate at which HCl is formed and a transfer of ClO and HO_x radicals into null cycle sequences from odd-oxygen destroying sequences.

There is the possibility that the reaction HO_2 + HO_2 → H_2O + O_3 might occur to some extent. An analysis of available data (H. Johnston, University of California at Berkeley, private communication, 1979) suggests an upper limit of about 5% of the total rate for this reaction. If the similar reaction HO_2 + ClO → HCl + O_3 had a branching ratio of less than 0.05, it would have no more than a modest effect on model sensitivity (based on calculations made in 1978, the reaction HO_2 + HO_2 → H_2O + O_3 would need to have a branching ratio of nearly 0.1 to be of even marginal significance in stratospheric perturbation studies).

The model-calculated ambient atmosphere with rates for both OH + ClO → HCl + O_2 and HO_2 + ClO → HCl + O_3 set to 10^{-12} cm^3/sec contained about half as much Cl, ClO, $ClONO_2$, $ClNO_2$ and HOCl as did the normal ambient, whereas HCl increases of about a factor of two were calculated near 30 km. No other measured species were significantly (> 10%) affected, although H_2O_2 and CH_3OOH were reduced by about 30% between 25 and 35 km.

Although model predictions are indeed sensitive to these reactions, the likelihood that they occur is probably not very great. Thus, while an effort should be made to measure them, an upper limit less than ∿10^{-13} cm^3/sec would resolve most of the issues they raise.

5. ClO_3 Chemistry

A final mechanism that was studied was the possibility that O_2 and ClO add to form a molecule with a binding strength comparable to that of ClOO, the complex formed from Cl and O_2. There is evidence for some such phenomenon from the effect of added O_2 on the quantum yield for ozone loss in systems containing Cl_2, O_3 and O_2 (Wongdontri-Stuper et al., 1978; J. Birks, University of Colorado, private communication, 1979).

If it is assumed that the formation and decomposition rate constants for the process $ClO + O_2 \rightarrow ClO_3$ are those given in NASA 1010 (1977) for $Cl + O_2 \rightarrow ClO_2$ and no subsequent chemistry occurs (only the formation and thermal decomposition of the complex occur), then model sensitivities are virtually unaffected. Approximately 2 to 5% of the inorganic chlorine in the lower stratosphere is in the form of ClO_3, and all computed changes in ambient concentrations are small. Even though the coupling between ClO and ClO_3 is very rapid, and ClO_3 is computed to be larger than ClO between $\sim$6 and 22 km, most of the ClO_3 apparantly comes from the much more abundant HCl and $ClONO_2$. However, if the structure of the ClO_3 complex were $OClO_2$, then it is possible that the following reactions would occur:

$$OClO_2 \xrightarrow{h\nu} O + OClO \qquad (11)$$

and

$$OClO_2 + NO \rightarrow OClO + NO_2 \qquad (12)$$

Because ClO and OClO have comparable heats of formation, the endoergicity of the photolysis would approximate 60 kcal plus the binding energy of the complex. This suggests an endoergicity for reaction (11) comparable to that for NO_2 photolysis. Thus, at least in principle, reaction (11) might have an effective J value as large as about 10^{-3} sec^{-1}. The reaction $OClO + NO \rightarrow NO_2 + ClO$ has a rate constant of about 3×10^{-13} cm^3/sec at room temperature (JPL, 1979). Given the similarities in the reactions, a similar sort of rate constant might be estimated for $OClO_2 + NO$. If one assumes that the J value for $OClO_2$ photolysis is 10^{-4} sec^{-1}, that the rate of reaction with NO is 1×10^{-12} cm^3/sec, and that the formation and decomposition rates are those given for ClO_2 in NASA 1010 (1977), then one estimates a moderate (20%) increase in the (small) ozone increase computed from SST operations and more than a 50%

reduction in the effect of CFMs. If on the other hand one assumes the same subsequent chemistry but a lower stability for the complex, say that given for ClO_2 in JPL (1979), then no significant effect on model sensitivity is predicted.

Thus, for the formation of a complex between O_2 and ClO to significantly affect model sensitivity, the complex must have a binding energy approaching 6 kcal, and either photolysis or reaction with NO must be reasonably fast. However, if the complex were to be stable (bound by more than 8 kcal) and the subsequent chemistry were reasonably fast, one might even compute a decrease in ozone for NO_x injections and an increase in column ozone from CFM increases. Similarly, if the HO_x reactions were pressure dependent and $OClO_2$ were to have the chemistry discussed above, one would calculate a decrease in column ozone for the 20-km NO_x injection and an increase in column ozone from the CFM scenario (see Table 12). There is, of course, a lengthy chain of speculative assumptions required to achieve such results.

Even though the $OClO_2$ chemistry discussed above is completely speculative, its potential for large effects may justify the attempt to study it by those chiefly interested in CFM effects.

Finally, it should be noted that the simplest (but probably not the most likely) route back to computed effects of SST operations (like those obtained in CIAP Monograph 3 (1975) and NRC (1975a) would be for the HO_x disproportionation reactions to have fast rates (either via the pressure/temperature effects hypothesized above, or through an error in the post 1976 measurements) and for the reaction of HO_2 + NO to be slower than is now thought to be the case. Although it seems unlikely that the growing body of experimental results involving HO_2 chemistry would all be wrong (at least at low pressures where many of the measurements have been direct and the data analysis reasonably straightforward), it cannot be denied that the new measurements have produced a startling number of unexpected negative temperature dependencies for apparently bimolecular reactions involving HO_2 (and ClO as well). While theories of reaction rates can no doubt be created to fit such data, the pre-existing theories do not easily lead to the observed rate constants. Although it seems very likely that the resolution of such problems will indeed come via a modification of theory, additional confirmatory measurements of some of the anomalous temperature dependences using independent, if perhaps less direct, techniques would still be welcomed.

Effects of Uncertainties in Chemical Rate Coefficients

Probably the best method for assessing the sensitivity of model predictions to errors in the inputs that describe fairly well understood quantities (e.g., rate constants for which experimental precision is the dominant source of error) is a Monte Carlo calculation (e.g., Stolarski et al., 1978). As yet, no such calculation has been carried out for a perturbation resulting from aircraft operations. In part this reflects the hypothesis that prediction error is dominated by error in poorly known reactions with unquantifiable error.

Even a full sensitivity analysis (like that of Butler, 1979) has not yet been performed. The most recent sensitivity study on the NO_x system was a partial sensitivity analysis carried out in 1975 by Duewer et al. (1975, 1977). The major conclusions of that study were that large prediction errors were possible, and that a few reactions dominated the error. Subsequent events have shown the first conclusion to be valid. The large changes in model sensitivity to NO_x injection that have occurred have been dominated by changes in the rate coefficients for the five reactions that were identified as plausible sources of error in the 1975 and 1977 reports. In the intervening years, many rate coefficients have been determined or redetermined with substantially improved accuracy. For the majority of the reactions in the model, experimental precision is probably a reasonably good estimate (as well as a lower bound) to the actual error in the measured rate, and model predictions are only weakly sensitive to modest errors in most rate coefficients. Nonetheless, the composite error in prediction caused by such errors could be significant, although, since it is unlikely that random errors will reinforce each other, this is not too likely to be realized.

Several reactions that still seem plausible candidates for serious errors and that seem to have the potential to change the qualitative conclusions that might be drawn from model predictions are discussed in the preceeding section. Here we will explore a historical method of assessing overall model uncertainty. Table 13 gives the change in O_3 calculated for several perturbations using the structure of our current model but using the rate coefficients recommended in NBS 866 (1975) and NBS 513 (1978) as well as the current results. In calculating the response for 1975 and 1977 chemistries, we excluded species (such as HOCl or HNO_4) that the LLL model contemporary with the rate compendium in question did not include. In

TABLE 13. The effect of the choice of rate coefficients on model sensitivity using the structure of the current LLL model.

Chemistry	1950 Ambient O_3 (DU)	Change in Total Ozone (%)				
		1990 High Subsonic	17 km SST*	20 km SST*	CFM 1978	CFM Steady-State
1975 (NBS 866)	288	-0.31	-3.94	-9.12	-0.76	-7.5
1977 (NBS 513)	366	1.43	1.20	-0.52	-0.98	-12.7
1979a** (JPL, 1979)	324	2.01	2.57	2.18	-1.92	-19.4
1979b (NASA, 1979)	327	1.86	2.00	1.06	-1.30	-14.6

*NO_x injection rate of 2000 molecules $cm^{-3}s^{-1}$ over a 1-km-thick layer. The contribution to ClX due to CFMs is not included in these calculations.

**The rate of $OH + ClO \rightarrow HCl + O_2$ is set to zero.

addition, we include the results of calculations made using the 1979a chemistry with the rate coefficient for the reaction $OH + ClO \rightarrow HCl + O_2$ set to zero.

The conclusion to be drawn from Table 13 is that over the last five years, changes in evaluated recommendations for chemical rate coefficients have resulted in substantial changes in the model predicted response to perturbation, and that even recent recommendations appearing a few months apart carry a significant amount of uncertainty. (However, the differences between model predictions are not such as to change any qualitative conclusions if one restricts ones self to post-1976 models with consistent physics.)

A comparison of the results in Table 13 with the results of LLL calculations in earlier years given in Table 14 for some of the perturbations demonstrates that other changes in model structure have had quantitatively significant effects, but would have had little effect on the qualitative conclusions drawn from model predictions of aircraft effects.

The uncertainty limits for reactions in the various evaluations (NBS 513 (1975), NBS 866 (1978), NASA 1010 (1977), JPL (1979), NASA Harpers Ferry) have generally become smaller when individual reactions are considered. However, over the same

TABLE 14 Ozone perturbation calculations for an NO_x injection rate of 2000 molecules $cm^{-3}s^{-1}$ reported in previous LLL annual reports.*

Report Date	Change in Total Ozone - %	
	17 km Injection	20 km Injection
2/73	—	-33.
7/74	-4.80	-10.15
5/75	-5.30	-11.23
6/76 early work	-5.30	-11.23
6/76 late work	-1.75	-5.21
9/77 early work	-1.31	-4.79
9/77 late work	1.96	0.55
9/78	3.21	3.59
9/79	2.00	1.06

*1979 results do not include the contribution to chlorine from CFMs. 1976-1978 results include varying levels of chlorine.

period, new and often highly uncertain reactions have been recognized, and it is far from obvious that the error that might be associated with rate coefficients actually included in models has gotten smaller over the last decade. Moreover, "new" reactions have been introduced to the modeling community at a fluctuating but not obviously decreasing rate.

Effect of Temperature Feedback and Hydrostatic Adjustment

In the calculations up to this point, the U. S. Standard Atmosphere (1976) temperature profile was used, and temperature was not allowed to change. Changes in the concentrations of species that are radiatively important (either solar or longwave) will affect the temperature profile by changing radiative fluxes and heating or cooling rates. At a given pressure level, as the temperature changes, the air density will also change as defined by the equation of state. Since chemical reaction rates are affected by changes in temperature and air density, it is important to assess the magnitude of these effects on the assessment calculation.

Air density can be computed in a one-dimensional model by assuming hydrostatic equilibrium (i.e., the pressure at any height is determined by the weight of the column of air above that point, and the air density is determined by the equation of state given the temperature). Expressed mathematically,

$$dP = -\rho g\, dz \tag{13}$$

and

$$P = \rho RT \tag{14}$$

where P is pressure, ρ is density, g is the acceleration of gravity, z is altitude, R is the gas constant and T is temperature. The temperature is computed using a radiative transfer model assuming radiative equilibrium in the stratosphere (see Appendix A). In our calculations, the temperature profile is computed above 13 km, and is specified below this altitude. Changes in surface temperature may be imposed, but they are not calculated in this version of the model. The model includes solar absorption and longwave exchange by O_3, H_2O and CO_2 along with solar absorption by NO_2 (Luther et al., 1977).

We assume that the change in surface temperature is negligible. Ozone reductions of up to 30% due to NO_x injections were computed to cause less than a 0.1 K change in surface temperature by Ramanathan et al. (1976). An increase in the stratospheric water vapor mixing ratio of 2 ppmv is estimated to cause an increase in surface temperature of < 0.2 K (Grobecker et al., 1974, p. F125). Increasing the surface temperature in our model by 0.2 K causes a change in total ozone of -0.06%. Neglecting changes in surface temperature of this magnitude has no significant effect on the results.

In studying the effect of temperature feedback and hydrostatic adjustment on model sensitivity, we considered four calculation alternatives: (1) temperature feedback with hydrostatic adjustment, (2) temperature feedback without hydrostatic adjustment, (3) constant temperature using the ambient computed temperature and pressure profiles,* and (4) constant temperature using the U.S. Standard Atmosphere temperature and pressure profiles. The results are presented in Table 15.

*The temperatures and pressures were computed at equilibrium using temperature feedback and hydrostatic adjustment, then they were kept fixed for the perturbation calculation.

The constant temperature calculation using the ambient computed temperature profile (consistent with hydrostatic adjustment) is the reference case with which to compare the effects of temperature feedback and hydrostatic adjustment. Table 15 shows that inclusion of temperature feedback leads to a larger increase in total ozone compared to the constant temperature calculation (ambient profile). When hydrostatic adjustment is included, the increase in total ozone is even larger. To understand these effects, we need to look at the change in temperature versus height.

For analysis purposes, we consider the results for an NO_x injection rate of 1000 molecules $cm^{-3}s^{-1}$ and an H_2O injection rate of 177,000 molecules $cm^{-3}s^{-1}$ at 20 km. The change in local ozone concentration is shown in Fig. 26 and the change in the temperature profile is shown in Fig. 27. The temperature increases below 20 km causing an increase in the chemical destruction rate of ozone. Thus, there is less of an increase in ozone concentration in this region when temperature feedback is included. Conversely, above 20 km the temperature decreases, thereby slowing the rates of reaction and leading to less ozone reduction in this region.

The change in absolute ozone concentration is shown in Fig. 28. Most of the difference between the three calculations occurs in the 20-40 km region. The reactions that are most important in terms of ozone destruction are more strongly dependent upon temperature in the 20-40 km region than at other altitudes.

In the case with hydrostatic adjustment, the air in the 14-20 km region expands due to the rise in temperature. As the air expands it lifts the atmosphere above so that a given pressure level is raised in altitude relative to the ambient profile. Conversely, where the temperature decreases, there is contraction. The combination of expansion below and contraction above results in a raising of the altitude of the pressure levels at altitudes below 43 km. At this altitude the combined effects of expansion and contraction cancel each other, and the pressure remains unchanged at this altitude. Thus, the pressure is increased at altitudes between 14 and 43 km.

Since density is determined by the equation of state [Eq. (14)], the change in density at any altitude can be expressed in terms of the fractional changes in temperature and pressure at this altitude

$$\frac{\Delta\rho}{\rho} = \frac{\Delta P}{P} - \frac{\Delta T}{T} \qquad (15)$$

TABLE 15. The effect of temperature feedback and hydrostatic adjustment on model sensitivity (1979a chemistry).

Injection Altitude (km)	Injection Rate (molecules $cm^{-3}s^{-1}$)		Change in Total Ozone (%)			
	NO_x	H_2O	Temperature Feedback with Hydrostatic Adjustment	Temperature Feedback without Hydrostatic Adjustment	Constant* Ambient Temperature	U.S. Standard Atmosphere Temperature
17	1000	0	1.45	1.30	1.20	1.34
17	1000	177,000	1.37	1.24	1.04	1.18
17	333	177,000	0.43	0.40	0.26	0.32
20	1000	0	1.36	1.17	1.10	1.31
20	1000	177,000	1.29	1.03	0.70	0.91
20	333	177,000	0.33	0.27	-0.02	0.07

*See footnote on page 74.

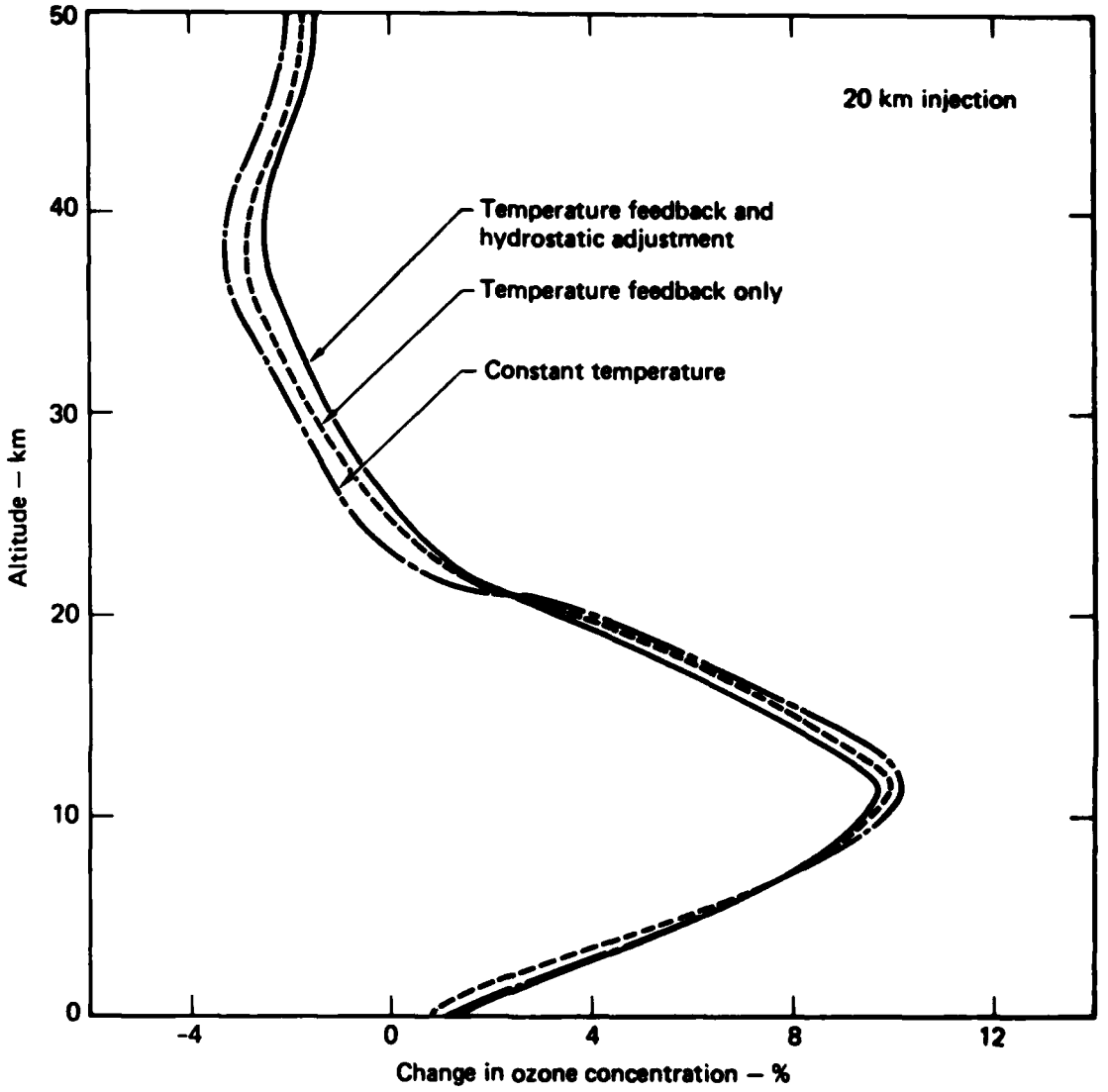

FIGURE 26. The change in ozone concentration caused by an NO_x injection of 1000 molecules $cm^{-3}s^{-1}$ and an H_2O injection of 177,000 molecules $cm^{-3}s^{-1}$ at 20 km (1979a chemistry).

ΔP and ΔT have the same sign in the region 14-20 km, and they have opposite signs between 20 and 43 km. Consequently, the effects of ΔP and ΔT on $\Delta\rho$ are additive above 20 km, and they tend to cancel each other below 20 km. The combined effect is a small decrease in density between 14 and 18 km and an increase in density at all higher altitudes. The largest fractional increase (0.74%) in ρ occurred at 22 km. An increase in air density tends to increase ozone by increasing the rate of reaction of

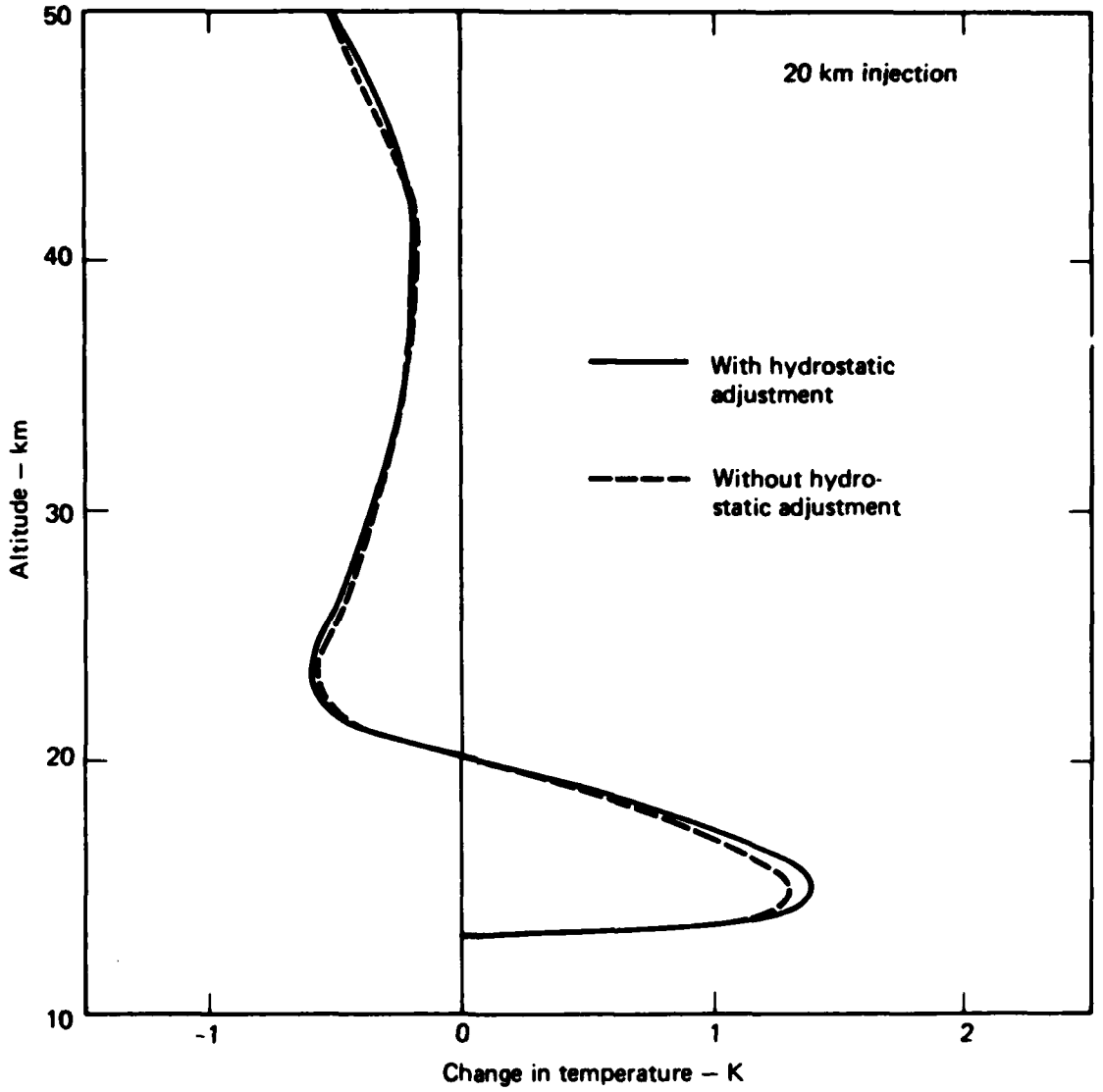

FIGURE 27. The change in temperature versus altitude for the 20 km injection perturbation described in Fig. 26 (1979a chemistry).

$O + O_2 + M \rightarrow O_3 + M$ and other three-body reactions. Most three-body reactions tend to convert more-active species into less-active species.

The results with temperature feedback and hydrostatic adjustment represent the most complete model calculations in terms of physical processes and feedback mechanisms. The changes in ozone concentration computed with these processes included are shown in Figs. 29 and 30 for various injection rates of NO_x and H_2O at an injection altitude of 17 km. The results for an NO_x injection rate of

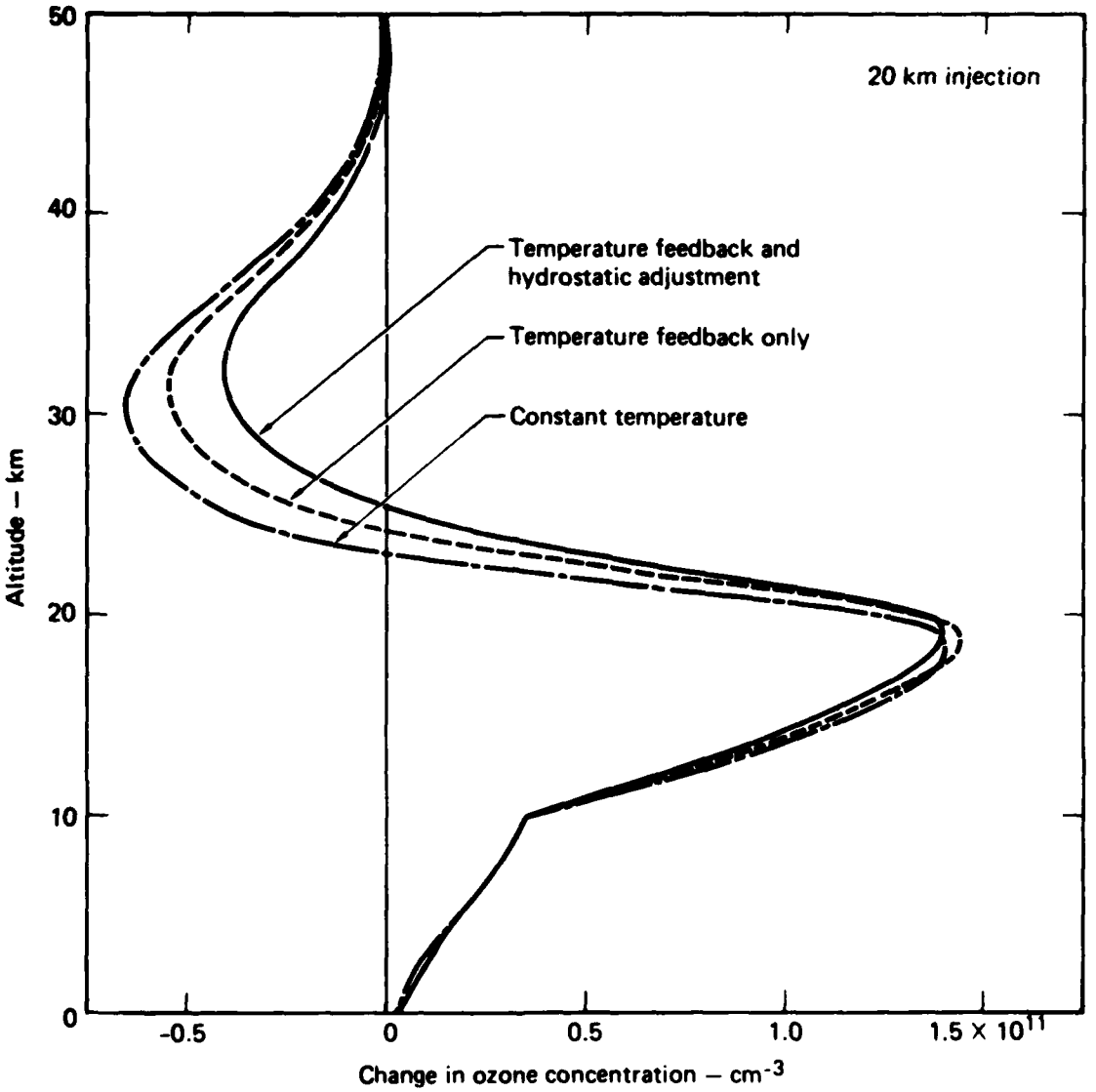

FIGURE 28. Same as Fig. 26 except the change in ozone concentration is expressed in molecules cm^{-3} (1979a chemistry).

1000 molecules $cm^{-3}s^{-1}$ with and without a simultaneous H_2O injection are nearly identical below 26 km. The injection of H_2O only leads to noticeable differences in the computed change in ozone concentration above 26 km.

Given the same H_2O injection rate, the results for NO_x injection rates of 1000 or 333 molecules $cm^{-3}s^{-1}$ are quite different. The lower NO_x injection rate causes much less change in ozone concentration in the middle and lower stratosphere; the relative magnitudes of the change in ozone concentration being roughly proportional to the NO_x injection rate. This result indicates that the

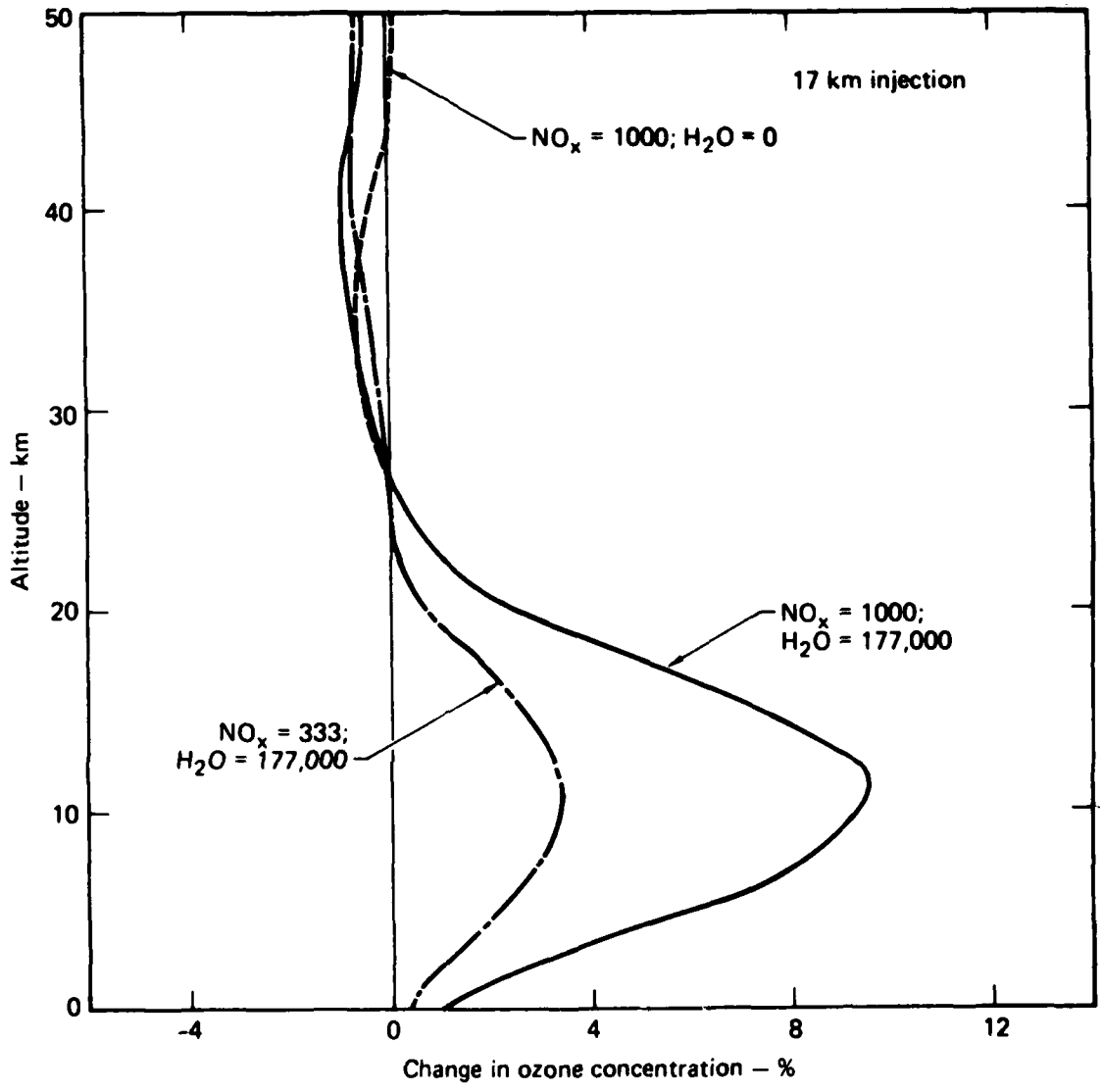

FIGURE 29. The change in ozone concentration due to various NO_x and H_2O injection rates at 17 km. The injection rates have units of molecules $cm^{-3}s^{-1}$ over a 1-km thick layer. The calculations include temperature feedback and hydrostatic adjustment (1979a chemistry).

NO_x injection rate is a much more important (and sensitive) parameter than the H_2O injection rate in estimating the effects of projected aircraft fleets.

Another important conclusion from Table 15 is that the choice of temperature profile in a constant temperature calculation can have a significant effect on model sensitivity. The difference between the ΔO_3 values using the ambient or the U.S. Standard Atmosphere temperature profile is the same magnitude as the difference between including and not including temperature feedback.

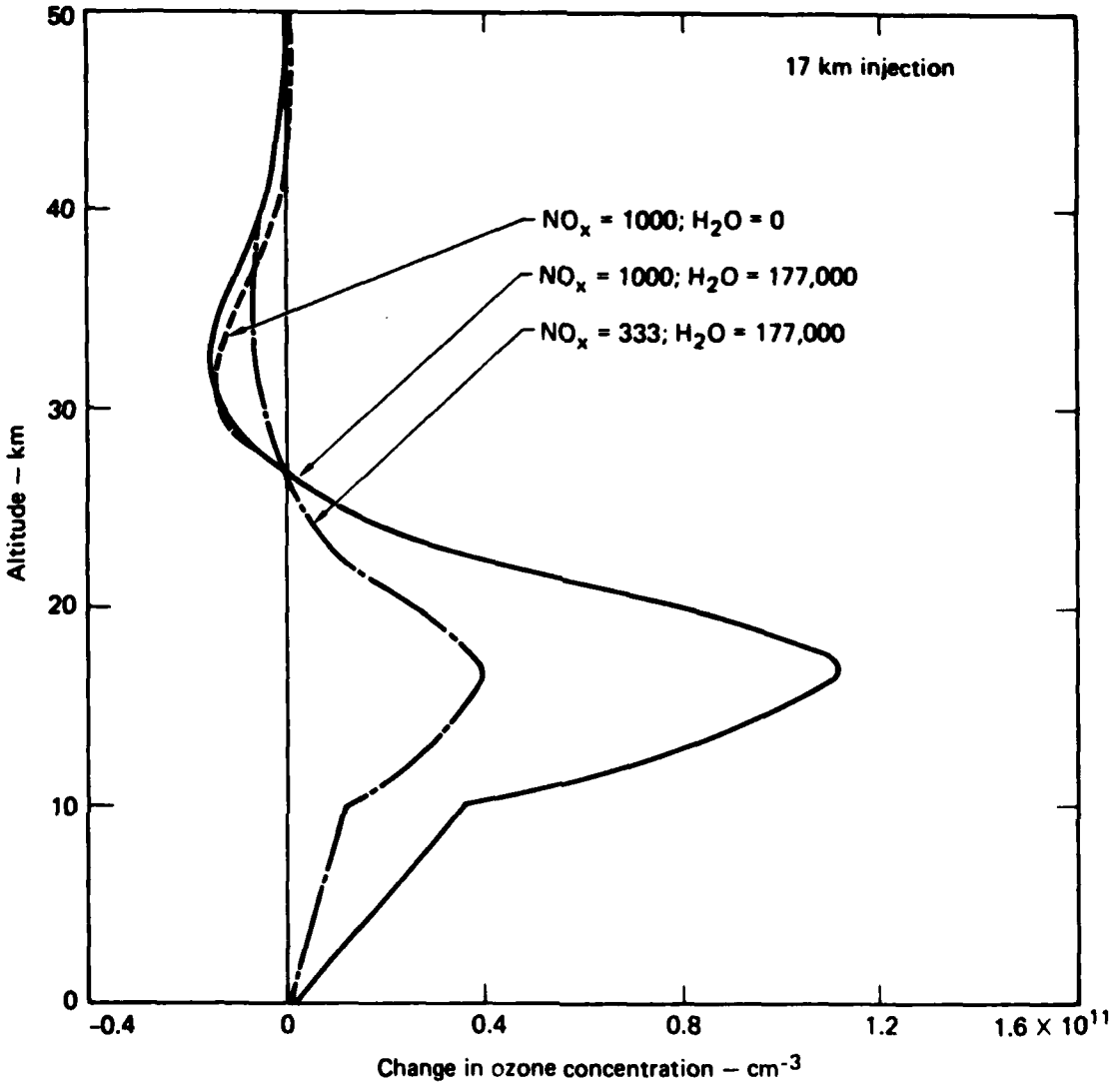

FIGURE 30. Same as Fig. 29 except the change in ozone concentration is expressed in molecules cm^{-3} (1979a chemistry).

4.4 COMPARISON WITH OTHER RESULTS

In terms of model predicted effects of a given perturbation, there are two types of comparisons that might be made: (1) a comparison with earlier results and (2) an intercomparison of the predictions of various models at a given time. Comparison with earlier results offers a guide to the stability of the values of

widely accepted inputs (e.g., chemical rate coefficients and solar flux calculations) and the effects of changes in "state-of-the-art" treatments of various physical parameters. A comparison with contemporary results offers a guide to the effects of differing values for input parameters that do not have widely accepted values (e.g., rainout parameterizations and thermal feedback effects).

There have been several previous assessments of the effects of high altitude aviation on the environment. The CIAP reports (CIAP Monographs, 1975; Report of Findings, 1974) summarize the results of many investigators who worked on the problem during the early 1970's. The Report of Findings (Grobecker et al., 1974) stresses the effects of fleets expected before 1990. The National Academy of Sciences report (NRC, 1975a) presents another summary of almost the same body of work with an emphasis on the larger fleets to be expected at some future time if supersonic transports were to be a commercial success.

The COMESA (1975) and COVOS (1976) reports cover English and French studies made at about the same time. These reports stress effects from moderate numbers of Concordes. Many of these results as well as the results of some later studies by Crutzen and ourselves are summarized by Oliver et al. (1977).

More recent assessment results were reported by Luther (1978) and Popoff et al. (1978). Oliver et al. (1978) reviewed the assessments made between December 1976 and June 1978.

Figure 31 provides a summary of previous LLL assessments of the effects of SST operations based on an injection of 2000 molecules (NO) $cm^{-3}s^{-1}$ distributed over a 1-km-thick layer centered at 17 or 20 km. This injection rate was a standard for assessment and comparison purposes and did not pertain to any particular fleet estimate. The results in Fig. 31 demonstrate the combined effects of the evolution of our understanding of stratospheric chemistry and evolution of the treatment of physical phenomena such as multiple scattering of light, the averaging of reaction rates over diurnal cycles, the treatment of boundary conditions, and the transport parameterization. Although many different factors have contributed to the variation described in Fig. 31, the evolution of model chemistry has been the most important single factor.

Figure 32 demonstrates the influence of changes in the evaluations of various rate coefficients. The results were obtained using our 1979 model, but the rate coefficients used in the model were modified to agree with those recommended in NBS 866 (1975), NBS 513 (1978), and JPL (1979). This provides three assessments at

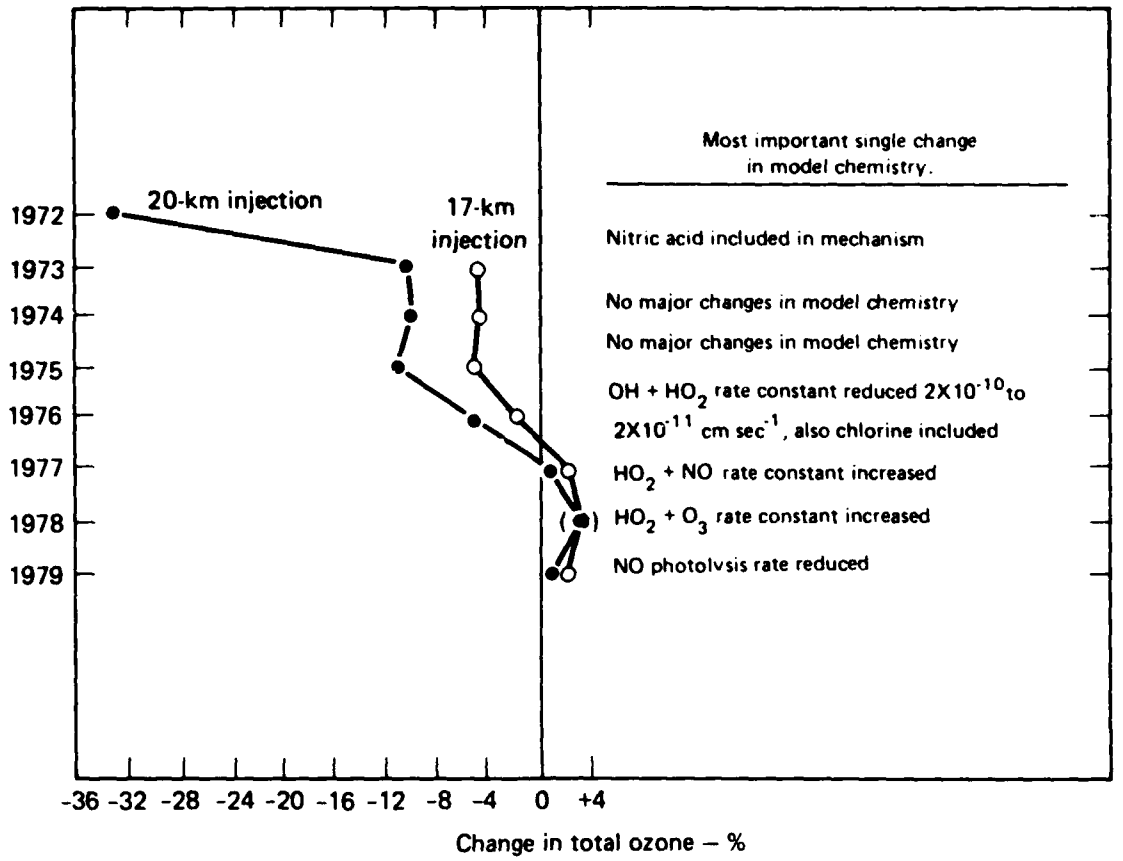

FIGURE 31. The historical evolution of LLL model calculations of the change in total ozone due to an NO_x injection of 2,000 molecules $cm^{-3}s^{-1}$ over a 1-km thick layer centered at either 17 km (open circles) or 200 km (solid circles). The values for 1978 are approximate because they are extrapolated from model calculations in 1978 that used half this NO_x injection rate.

two-year intervals and a fourth (current) value six months more recent than the last. The chemistries so generated do not correspond precisely to any in previous use at LLL. Moreover, only the O_3, NO and NO_3 photolysis rates were adjusted to reflect earlier treatments of photolysis. All other photolysis rates were left at 1979 values. The 1975 chemistry corresponds more nearly to that used in our 1976 calculations than our 1975 calculations.

Figures 31 and 32 demonstrate that the model predicted response to NO_x injections has varied substantially over the past eight years, and that much of that variation has come via differences in the recommended values for rate constants (combined with newly recognized chemical reactions). While it is encouraging to

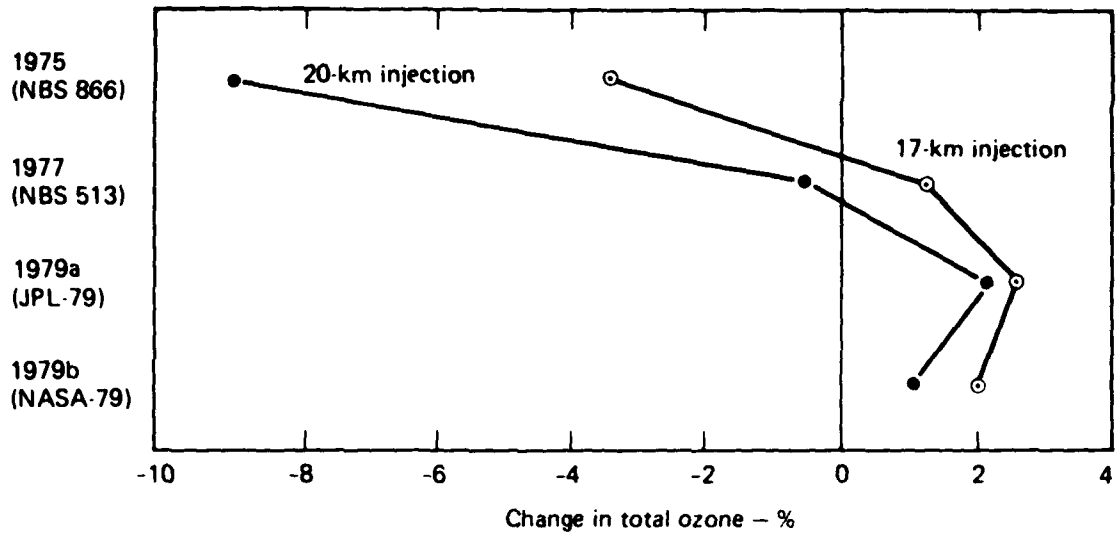

FIGURE 32. The change in total ozone due to an NO_x injection of 2,000 molecules $cm^{-3}s^{-1}$ computed using the structure of the current one-dimensional model with variations in model chemistry corresponding to various sets of photochemical rate recommendations. The reaction $OH + ClO \rightarrow HCl + O_2$ was not included in this 1979a calculation.

note that the post-1977 assessments have not varied as widely as the earlier assessments did, it is discouraging to note that the most pronounced variations came several years apart (in 1972 and 1976-1977) and that during the intervening years (1973-1975) the assessments were nearly as stable as those of the last three years.

In the CIAP era, intercomparison of different models revealed that for those using similar chemistries a very considerable range of predicted perturbations could be explained on the basis of differences in the fractional change in NO_x caused largely by differences in the parameterizations of vertical transport (Chang and Johnston, 1974).

Partly because the range of one-dimensional transport parameterizations in current use is much smaller than it was before 1975, there is much more of a consensus among modelers than there was in 1975. At the NASA sponsored Harpers Ferry workshop (June 1979) nine different modeling groups computed the effects of an injection of 10^8 molecules NO $cm^{-2}sec^{-1}$ distributed over roughly 1-km altitude centered at roughly 17 or 20 km. For a 17-km injection the range of values for the change in total ozone was +1.3 to +3.4% (only one was greater than 2.6%), and for the 20-km injection the range was +1.1 to +4.6% (only one was greater than

AD-A085 128 CALIFORNIA UNIV LIVERMORE LAWRENCE LIVERMORE LAB F/G 21/5
POTENTIAL ENVIRONMENTAL EFFECTS OF AIRCRAFT EMISSIONS,(U)
OCT 79 F W LUTHER, J S CHANG, W H DUEWER W-7405-ENG-48
UNCLASSIFIED UCRL-52861 FAA/EE-79-23 NL

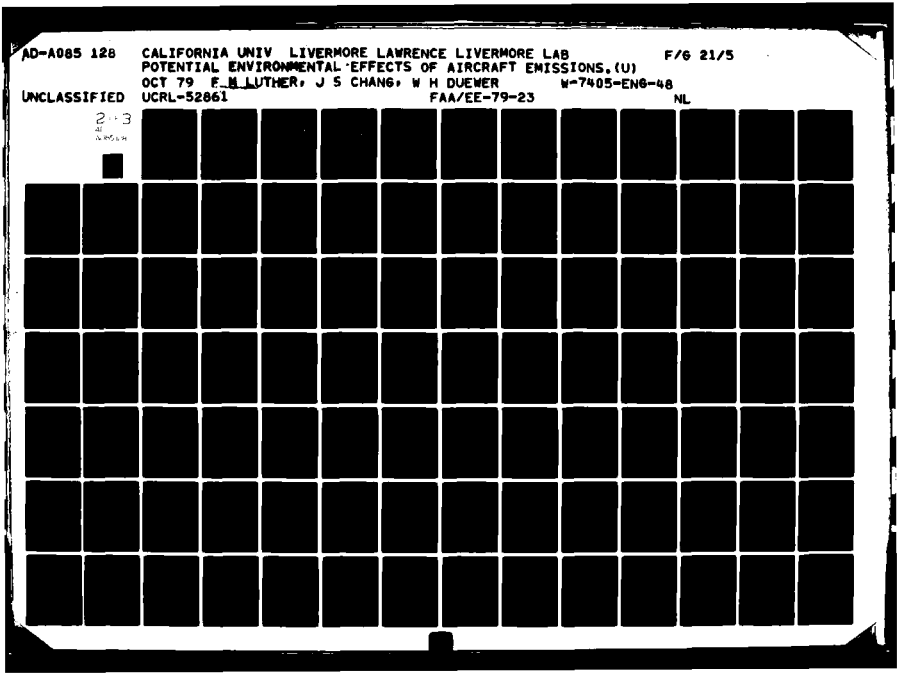

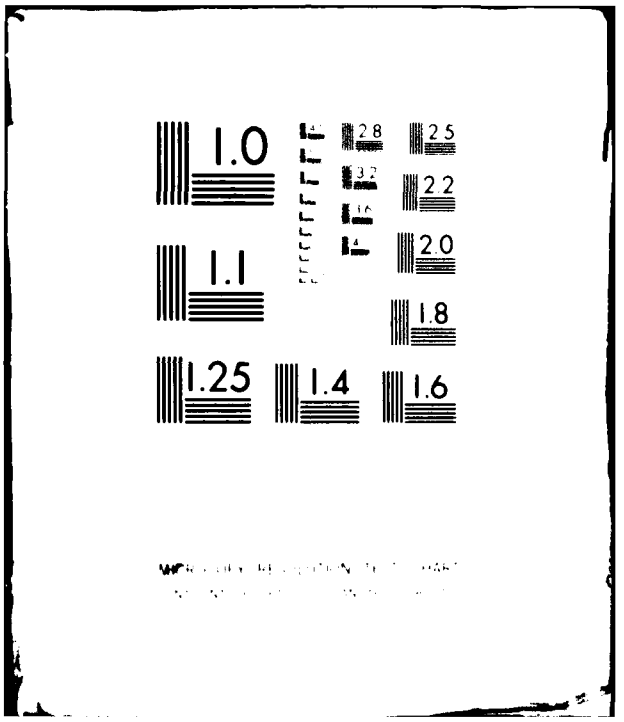
1.0
1.1
1.25
1.4
1.6
1.8
2.0
2.2
2.5
2.8
3.2

3%). In both cases, the LLL predictions were slightly smaller than the majority of the other models, although in neither case were the LLL predictions the extreme predictions. Because the models were independently formulated, the small range of predicted effects suggests that none of the predictions is seriously affected by errors in coding or through unique treatments of some processes. Much of the present difference in model predictions still appears to be explainable on the basis of differences in the vertical transport coefficients used.

A final comparison would be between models of differing dimensionality. Unfortunately, only a few direct comparisons can be made since the chemistries used in multidimensional models have usually been simpler than those used in one-dimensional models. Recent two-dimensional results (Hidalgo, 1978; R. C. Whitten, private communication, 1979) have been at least qualitatively similar to one-dimensional results with similar chemistry. That is, recent two-dimensional calculations, like recent one-dimensional calculations, predict that a large supersonic transport fleet would cause small (1-3%) ozone column increases over most of the globe with an increase in the lower stratosphere (and upper troposphere) and a decrease at higher altitudes. Published three-dimensional calculations have not included a complete model chemistry (Cunnold et al., 1977) but have been qualitatively similar to those obtained with models of lower dimensionality in the past.

In summary, independent one-dimensional model predictions of the effects of NO_x injections are presently in good agreement with each other. They also seem to be in semiquantitative agreement with models of higher dimensionality and similar chemistry. However, model predictions have changed substantially over the last eight years, and there is little that suggests similar changes in model sensitivity might not occur in the future.

5. POTENTIAL CHANGES IN OZONE RESULTING FROM OTHER PERTURBATIONS

Many potentially significant perturbations to stratospheric ozone have been proposed. In order to put the effects of aircraft engine emissions presented in Section 4 in perspective, we present assessments for other anthropogenic perturbations. Just as the effects of aircraft emissions were shown to depend on the effects of other perturbing influences, such as the concentration of ClX and the atmospheric temperature structure, the changes in O_3 resulting from the other perturbations considered here also depend on the interference effects of multiple perturbations.

Our effort has been primarily directed toward the assessment of predicted changes for individual perturbations since future perturbation scenarios are often quite uncertain. Of the perturbation scenarios considered here, only the increases in the concentrations of chlorofluoromethanes and CO_2 are well established. Changes in stratospheric H_2O, increases in N_2O and increases in stratospheric CH_3CCl_3 are predicted on uncertain knowledge of budgets and, in the case of CH_3CCl_3, uncertain tropospheric chemistry. Where possible, we include comparisons to observations as well as a review of previous assessments with a history of the effects of various model changes and improvements in chemistry.

5.1 CHLOROFLUOROMETHANES

It has been firmly established that the chlorofluoromethanes, $CFCl_3$ and CF_2Cl_2, have been increasing in the troposphere and stratosphere, and the observed increase is consistent with model estimates based on the historical production rates. The CFM's are photolyzed in the stratosphere to yield free chlorine which may catalytically destroy ozone.

Computed concentration profiles of $CFCl_3$ and CF_2Cl_2 are compared with measurements in Figs. 33 and 34, respectively. Tropospheric concentrations of $CFCl_3$ and CF_2Cl_2 computed in our model are about 10% and 14% smaller, respectively, than those measured by R. Rasmussen (private communication, 1979). The differences could be caused by too-fast model transport into the upper

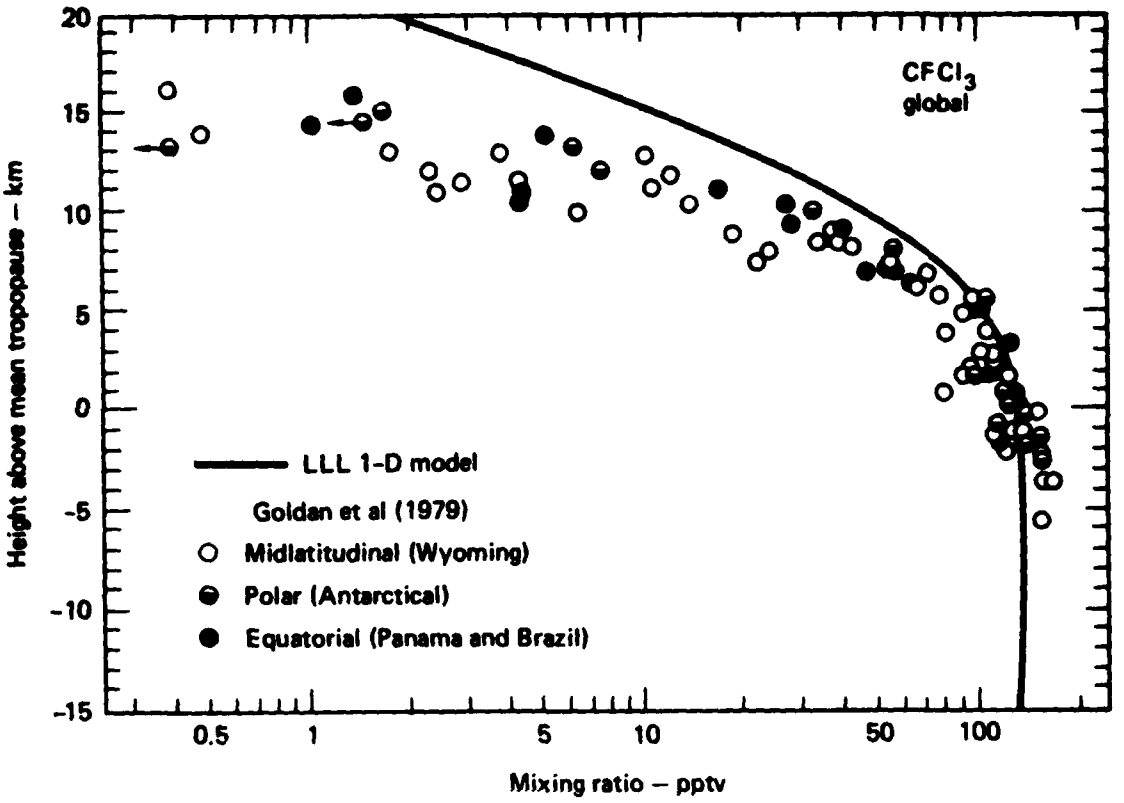

FIGURE 33. Comparison of computed and observed $CFCl_3$ mixing ratio profiles.

stratosphere since transport parameters are derived by model fitting to upper atmospheric CH_4 and N_2O.

Quantitative estimates of the depletion of ozone have changed as models, physics, and chemistry have improved. In 1976 the predicted change in total O_3 due to steady-state production of CFM's at 1973 rates was estimated to be -7.5% (National Research Council, 1976b). In 1977 a major change in the model chemistry occurred when the rate for

$$HO_2 + NO \rightarrow OH + NO_2 \qquad (16)$$

was measured to be almost 40 times faster than previously thought (Howard and Evenson, 1977). In addition, some models at that time included diurnally averaged reaction rates and multiple scattering effects. The depletion estimates in 1977 ranged from -10.8 to -16.5% for the various modeling groups (Hudson, 1977); the LLL estimate was -15.0%. With our current model, we predict a change of -14.2%

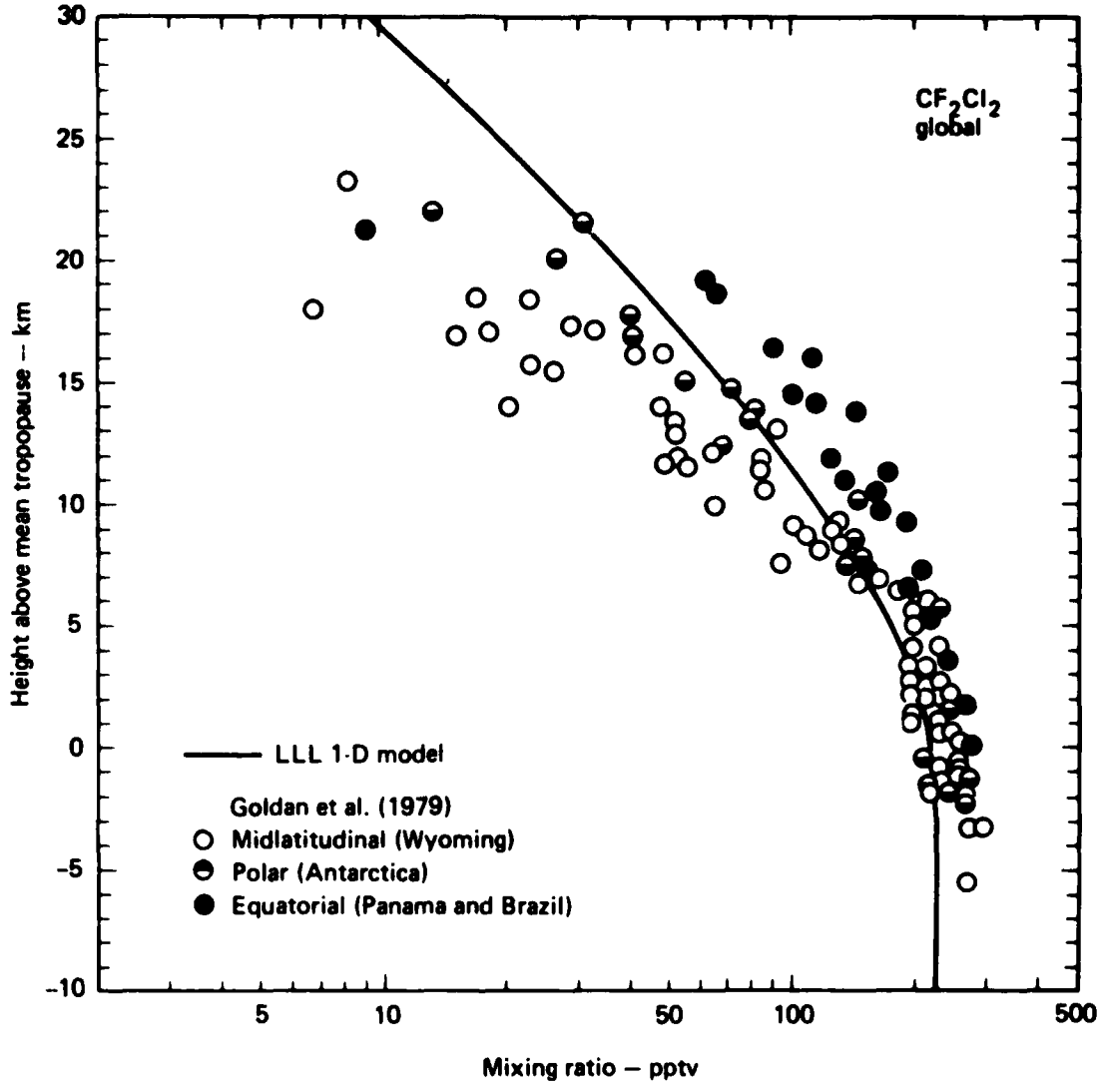

FIGURE 34. Comparison of computed and observed CF_2Cl_2 mixing ratio profiles.

in total O_3 at steady-state assuming constant CFM production at the 1976 rates. (The 1976 production rates are 3.2% smaller for $CFCl_3$ and 2.9% larger for CF_2Cl_2 than those for 1973.) In order to evaluate the effect on model sensitivity of changes to the model, we have calculated the change in ozone at steady state for 1976 CFM release rates using a number of different chemistries. The results labeled 1976 Chang et al. (1979) and 1977 Chang et al. (1979) given in Table 17 and Fig. 35 were obtained by changing only the two- and three-body chemical reaction rates in our current model to the values used in 1976 and 1977

TABLE 16. Recent LLL one-dimensional model calculations of the effect of continued release of CFM's at the 1976 rate.

Model Chemistry	Unperturbed Total O_3 c. 1950 (molecules cm^{-2})	ΔO_3(%)	
		In 1978	At Steady State
1975 NBS 866 with 1979 model	7.73×10^{18}	-0.8	-7.5
1976 Chang et al. (1979) (Appendix F)	7.49	-0.4	-4.2
1976 Old NO Photolysis	7.67	-0.6	-5.8
1976 Non-Diurnal	8.50	-0.0	-1.3
1977 NBS 513 with 1979 model	9.80	-1.0	-12.7
1977 Chang et al. (1979) (Appendix F)	9.18	-1.1	-11.2
1977 Non-Diurnal	10.1	-0.5	-4.7
1979a chemistry	8.81	-1.5	-14.0
1979a less OH + ClO	8.68	-2.0	-19.4
1979b chemistry	8.81	-1.3	-14.2

(see list of reactions and rates in Appendix F). Rates for the CH_4 oxidation reactions were left at their current values, although in 1976 and 1977 the full CH_4 oxidation scheme was not in our model. We also studied the effect of not including diurnal averaging for these two chemistries, and we studied the effect of using the old NO photolysis parameterization (which results in $\sim$ 50% less NO_x in the ambient stratosphere) for the 1976 chemistry.

For the model calculations labeled 1975 NBS 866 and 1977 NBS 513, the reaction rates and photolysis rates were made consistent with those publications. The O_3 quantum yield for $O(^1D)$ was set to zero at wavelengths higher than 310 nm, and the old NO photolysis parameterization (based on Cieslik and Nicolet, 1973) was used.

Using our standard model (with diurnal averaging and the NO photolysis rates of Frederick and Hudson (1979)), we calculate changes in total ozone of -4.2%, -11.2%, -14.0%, and -14.2% for the 1976, 1977, 1979a and 1979b chemistry models, respectively. Ambient column ozone increased from 7.49×10^{18} cm^{-2} for the 1976 chemistry to 9.18×10^{18} cm^{-2} for the 1977 chemistry. This is primarily a

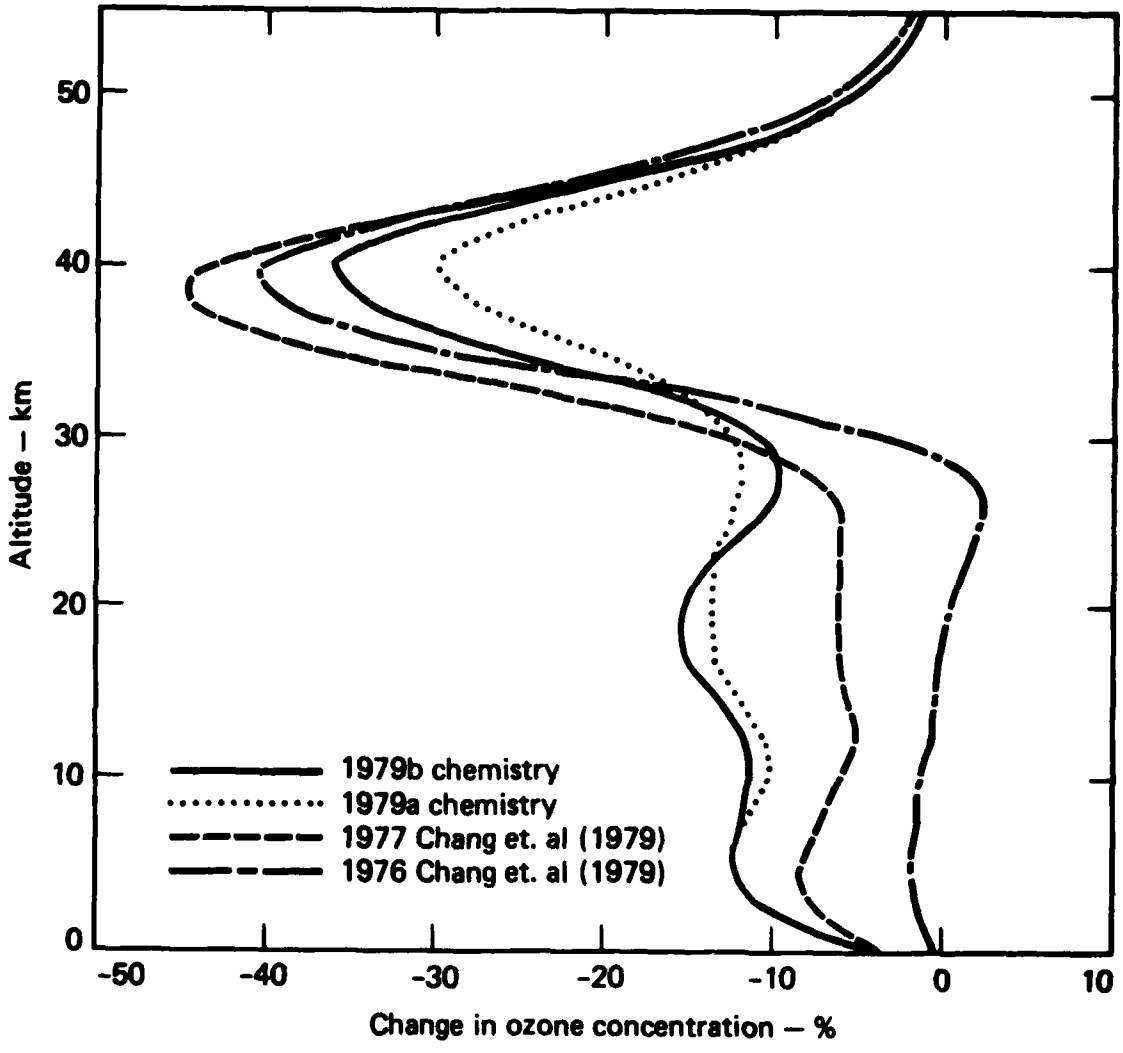

FIGURE 35. The change in ozone concentration at steady state resulting from CFM's released at the 1976 rate. Various photochemical rate data were used in the calculations.

result of the rate change for reaction $HO_2 + NO \rightarrow HO + NO_2$. With the faster rate the efficiency of the NO_x and HO_x catalytic ozone destruction cycles are reduced, resulting in higher ambient ozone levels. ClX then plays a relatively larger role in regulating the ozone concentration. These changes result in a larger ozone reduction for a given CFM perturbation (ΔO_3 = -11.2% for the 1977 chemistry for constant CFM production at the 1976 rates compared to only -4.2% for the 1976 chemistry).

Many changes to chemical rate constants on the order of 30% or more occurred between our 1977 chemistry and our 1979b chemistry. One major change affecting the CFM perturbation calculation was the inclusion of HOCl. HOCl is formed by the reaction,

$$ClO + HO_2 \rightarrow HOCl + O_2 \quad , \tag{17}$$

and is destroyed by photolysis,

$$HOCl \xrightarrow{h\nu} OH + Cl \quad . \tag{18}$$

Destruction of O_3 is more efficient at lower altitudes if HOCl is included in the model (compare current chemistry with that for 1977 and 1976 in Fig. 35). When HOCl is included, ClX shifts to more Cl and less ClO. Also, a new catalytic ozone destruction cycle is created that does not depend on the limited amount of O atom,

$$\begin{aligned} &OH + O_3 \rightarrow HO_2 + O_2 \\ &Cl + O_3 \rightarrow ClO + O_2 \\ &ClO + HO_2 \rightarrow HOCl + O_2 \\ &HOCl \xrightarrow{h\nu} Cl + OH \\ &\text{net} \qquad 2O_3 \rightarrow 3O_2 \end{aligned} \tag{19}$$

The major differences between O_3 sensitivity to CFM perturbation with the 1979a rates and the 1979b rates occur at high altitude (see Fig. 35). Differences in the rate of OH + HO_2 and of NO photolysis account for most of the difference in sensitivity at higher altitude. Results for the two chemistries are similar at lower altitudes because of a cancellation of effects. Differences and similarities in model sensitivity to the CFM perturbations as a function of altitude are mainly the result of changes in the relative roles of HCl and $ClONO_2$ as inactive chlorine reservoirs in the two chemistries.

In our 1979b model chemistry, $ClONO_2$ is relatively more important since the three-body rate of formation is almost four times faster than that used with the 1979a chemistry. In our 1979a chemistry, HCl is a more important chlorine reservoir since it is efficiently produced by the reaction

$$OH + ClO \rightarrow HCl + O_2 \qquad (20)$$

[Reaction (20) is not included in the 1979b chemistry.]

Figure 36 shows a number of calculated time histories for ozone under various assumptions regarding the future release rates for CFM's. For curve A it was assumed that CFM production continued at the 1976 rate until 1982, then it was lowered by 25%. In 1987, it was lowered again by 25%. The eventual steady-state ozone depletion for this case was 7.5%. For curve B, the 1976 production rate continued until 1982 and was then cut by 25%. The ozone depletion at steady state was 10.8% for this case. For curve C the 1976 production rate was used for the entire time, and the steady-state ozone depletion was 14.0%. For curve D the 1976 production rate was assumed to continue through 1980, then the CFM production was increased by 7%/year up to the year 2000. The steady-state depletion for this

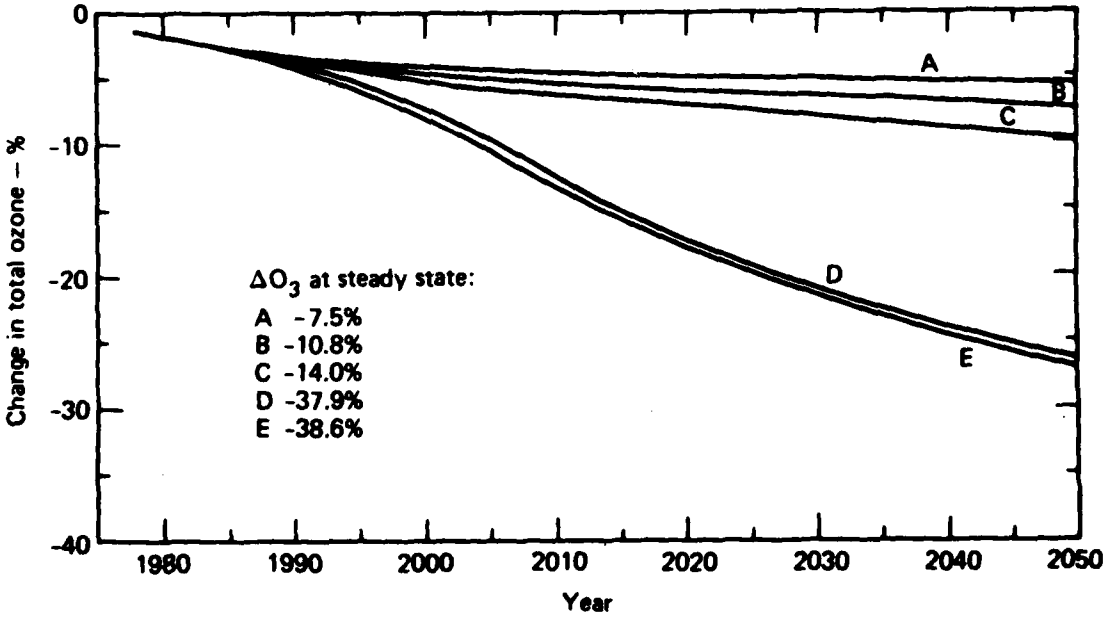

FIGURE 36. The change in total ozone as a function of time for various CFM release rate scenarios. Curve A: 1976 CFM release rate until 1982, then it is reduced by 25% and in 1987 it is reduced again by 25%. Curve B: 1976 release rate until 1982, then it is reduced by 25%. Curve C: 1976 release rate constant throughout the period. Curve D: 1976 release rate through 1980, then the release rate increased 7%/yr up to the year 2000, constant thereafter. Curve E: same as D except the increase in release rate begins in 1978. All calculations were with 1979a chemical rates.

case is 37.9%. Case E is almost the same as case D except that the increased CFM production begins in 1978. The rate of increase is such that the production rate doubles by 1990 and doubles again by 2000. The steady-state ozone depletion is 38.6%. (The 1979a chemical rates were used in all of these model calculations.)

An enlargement of the period from 1980 to 2000 is shown in Fig. 37. Also shown is a model using 1979b chemistry with CH_3CCl_3 added to the model for the case of constant 1976 production rates (case C'). For all scenarios the predicted additional reduction in total O_3 over the next 10 years is less than 2.5%. This is less than the estimated level of detectability (NASA Stratospheric Panel on Long-Term Trends, 1979).

The predicted time histories for the ozone concentration at 40 km are shown in Fig. 38. For the largest perturbation case, the ozone concentration is predicted to be reduced by an additional 4.5% by the year 1990, which is smaller than the detection limits estimated by the NASA panel for observation by balloon, rocket, or Umkehr. A trend in ozone concentration might be observed by satellite at the 1 level, but the result would be below the 95% confidence limit. Thus, a relatively long time period (>10 years) may be needed in order to confirm or refute the model predictions of CFM effects by comparison with observed ozone changes.

5.2 CHANGE IN STRATOSPHERIC H_2O

Changes in stratospheric water vapor may be caused by a variety of mechanisms. Changes due to direct injection of water vapor by aircraft and the resulting effects on the atmosphere are discussed in Section 4. Perturbations to the atmospheric composition (e.g., CO_2 or NO_2) may also cause changes in stratospheric H_2O indirectly by changing the temperature of the tropical tropopause. A temperature increase of 4 K at the tropical tropopause would increase the saturation vapor pressure by a factor of 2 (Liu et al., 1976). H_2O may also increase as a result of increases in CH_4 which is oxidized to yield H_2O in the stratosphere. Stratospheric H_2O apparently increased by approximately 30% during the period from 1964 to 1973 (Mastenbrook, 1971, 1974), but it is not obvious that these changes apply to the upper stratosphere or even that the water vapor measurements are reliable.

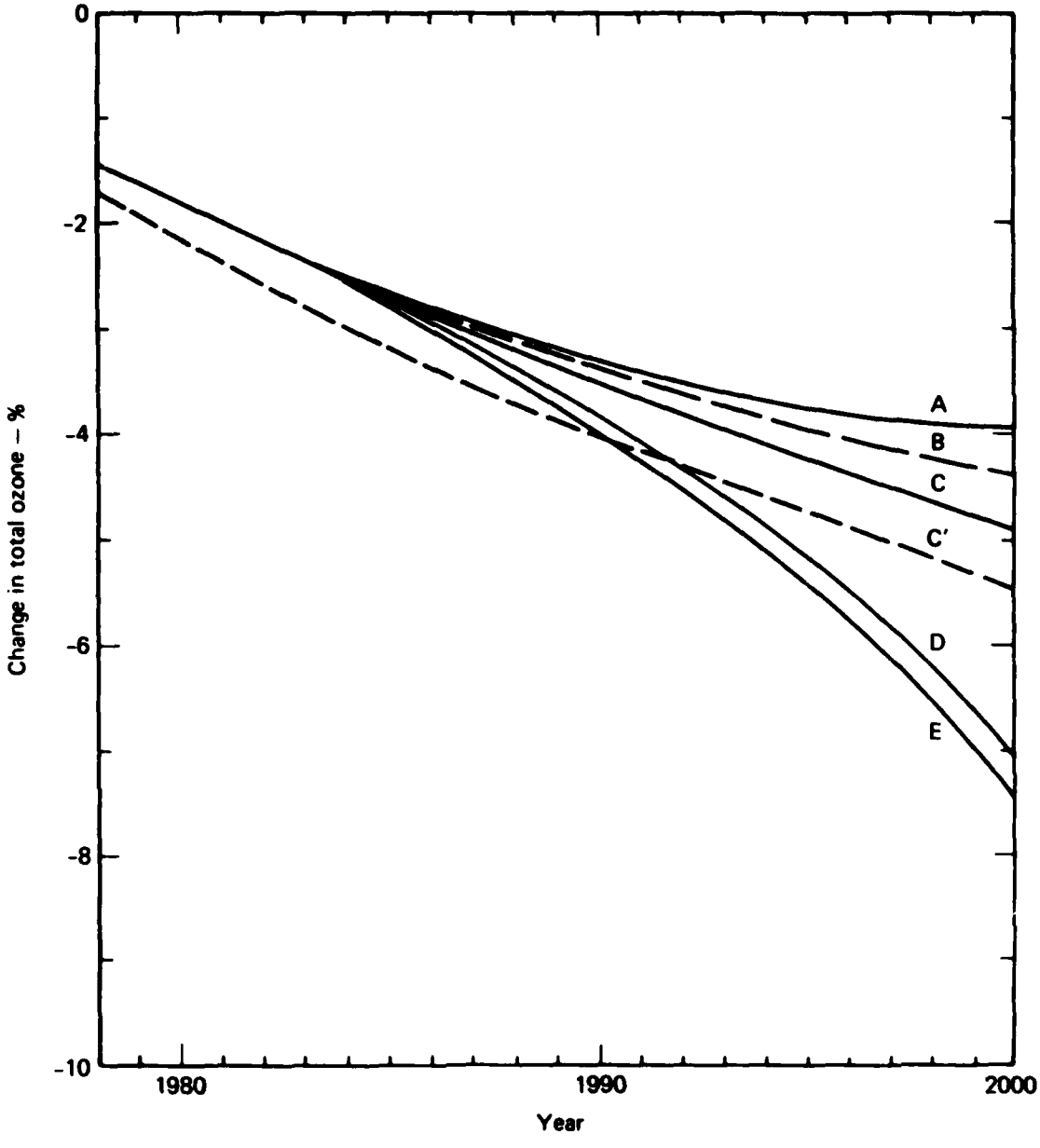

FIGURE 37. An enlargement of the period from 1980 to 2000 for the calculations presented in Fig. 36. Curve C' is the same scenario as Curve C except the 1979b model chemistry is used and CH_3CCl_3 is added.

We consider here changes in our calculated O_3 and temperature due to changes in H_2O alone. In general, these changes must be considered along with perturbations in other atmospheric species, the coupled perturbations possibly having a nonlinear effect on ozone. Our separate calculations for increases in H_2O, however, provide a background for understanding coupled perturbations.

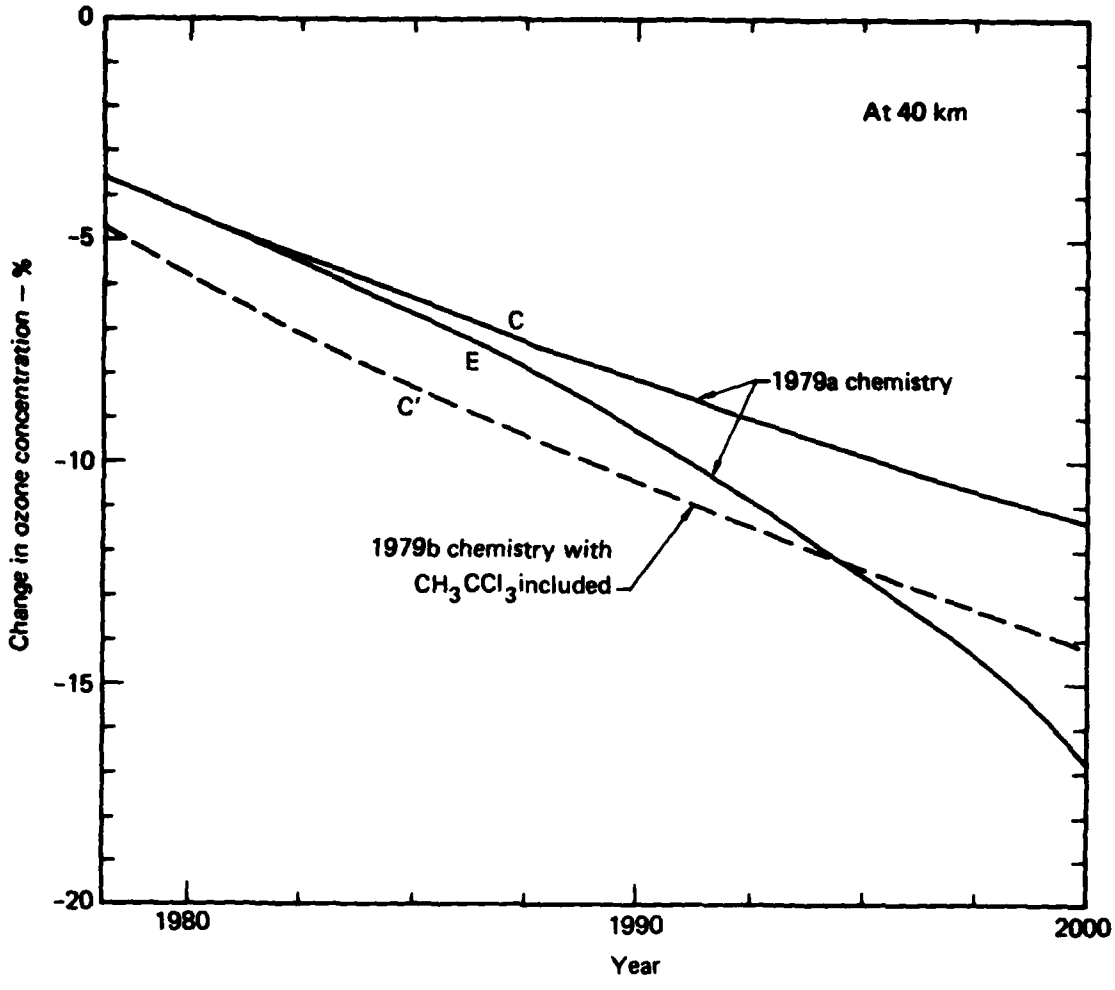

FIGURE 38. The change in ozone concentration at 40 km as a function of time for scenarios described in Fig. 36. Curve C' is the same scenario as curve C except the 1979b model chemistry is used and CH_3CCl_3 is included.

Changes in stratospheric H_2O affect ozone directly by increasing HO_x and indirectly by changing the temperature. In our model, H_2O is computed throughout the stratosphere given a boundary value at 13 km. Figure 39 shows the calculated change in temperature due to increasing H_2O by a factor of 2 at 13 km. The full line shows the case when hydrostatic equilibrium is included; the dashed line the case when it is not. Also shown is the percentage change in stratospheric H_2O as a function of altitude. The change in H_2O was the same for both cases. In both the hydrostatic and non-hydrostatic cases, the temperature is decreased because of increased cooling by H_2O and due to decreased solar

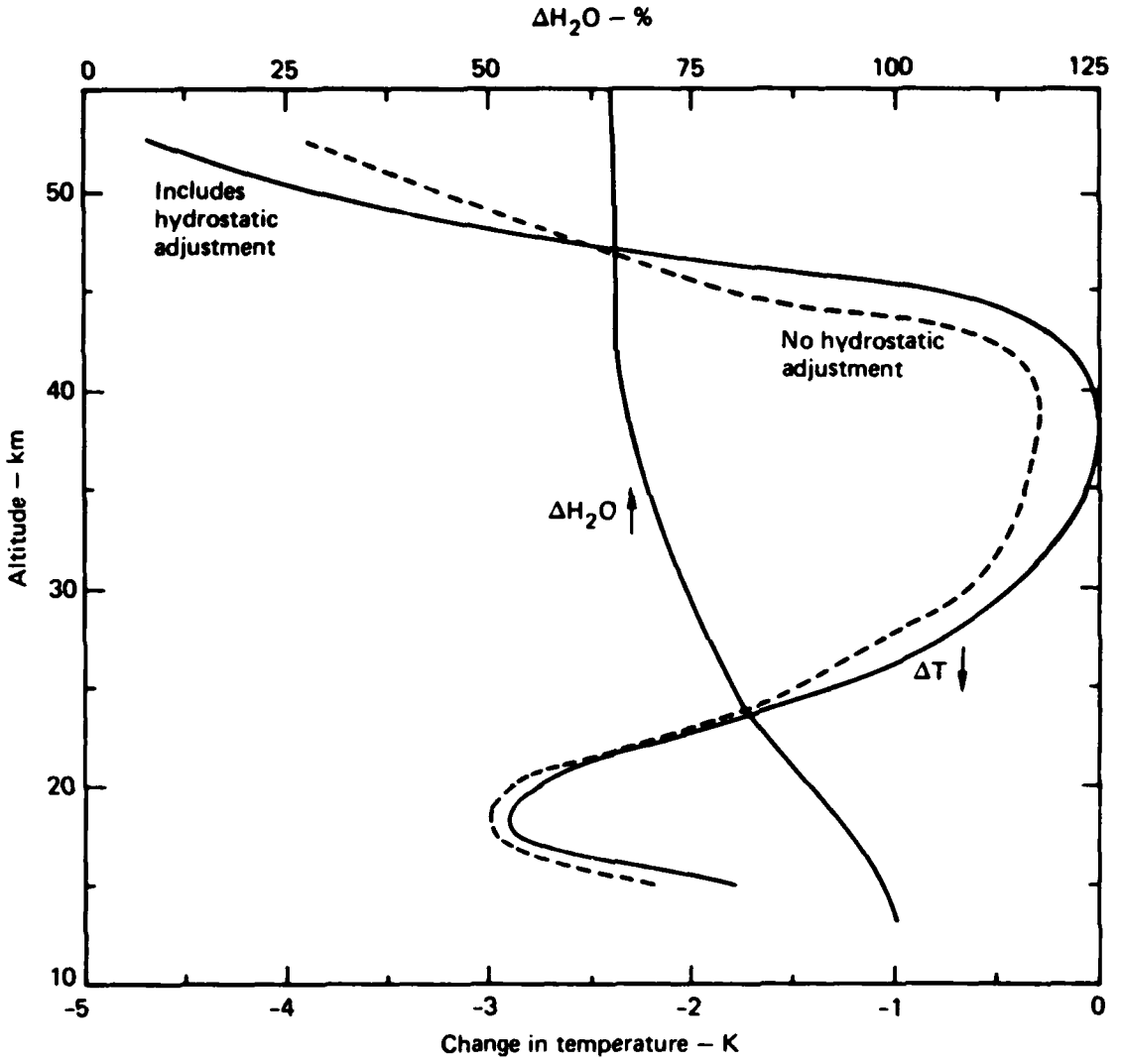

FIGURE 39. The change in temperature and the change in H_2O concentration in the stratosphere resulting from a doubling of the H_2O concentration at 13 km (below which H_2O is fixed). The change in H_2O concentrations was the same for calculations with or without hydrostatic adjustment (1979a chemistry).

absorption by O_3. Near the tropopause our calculated temperature decreases by almost 2 K, thus providing a negative feedback to any supposed increase in H_2O as a result of increases in the tropopause temperature.* The detailed changes in

*In these calculations the temperature structure below 14 km was held constant at its observed value. If the tropospheric temperature is perturbed by 2 K when H_2O is doubled, the calculated change in ozone concentration changes from -11% to -4% at 40 km, due to increases in the background ozone concentration at high altitude resulting from hydrostatic adjustment. Increasing the surface temperature 2 K caused the total ozone column to decrease by 0.6%.

temperature with altitude are related to changes in H_2O, O_3 and, in the case of hydrostatic adjustment, changes in density. As shown in Fig. 40, O_3 is decreased at most altitudes (except near 30-35 km) providing decreased solar absorption. The change in total ozone was -3.45% without temperature feedback. When temperature feedback was included, the change in total ozone was -2.15% without hydrostatic adjustment and -3.03% with hydrostatic adjustment.

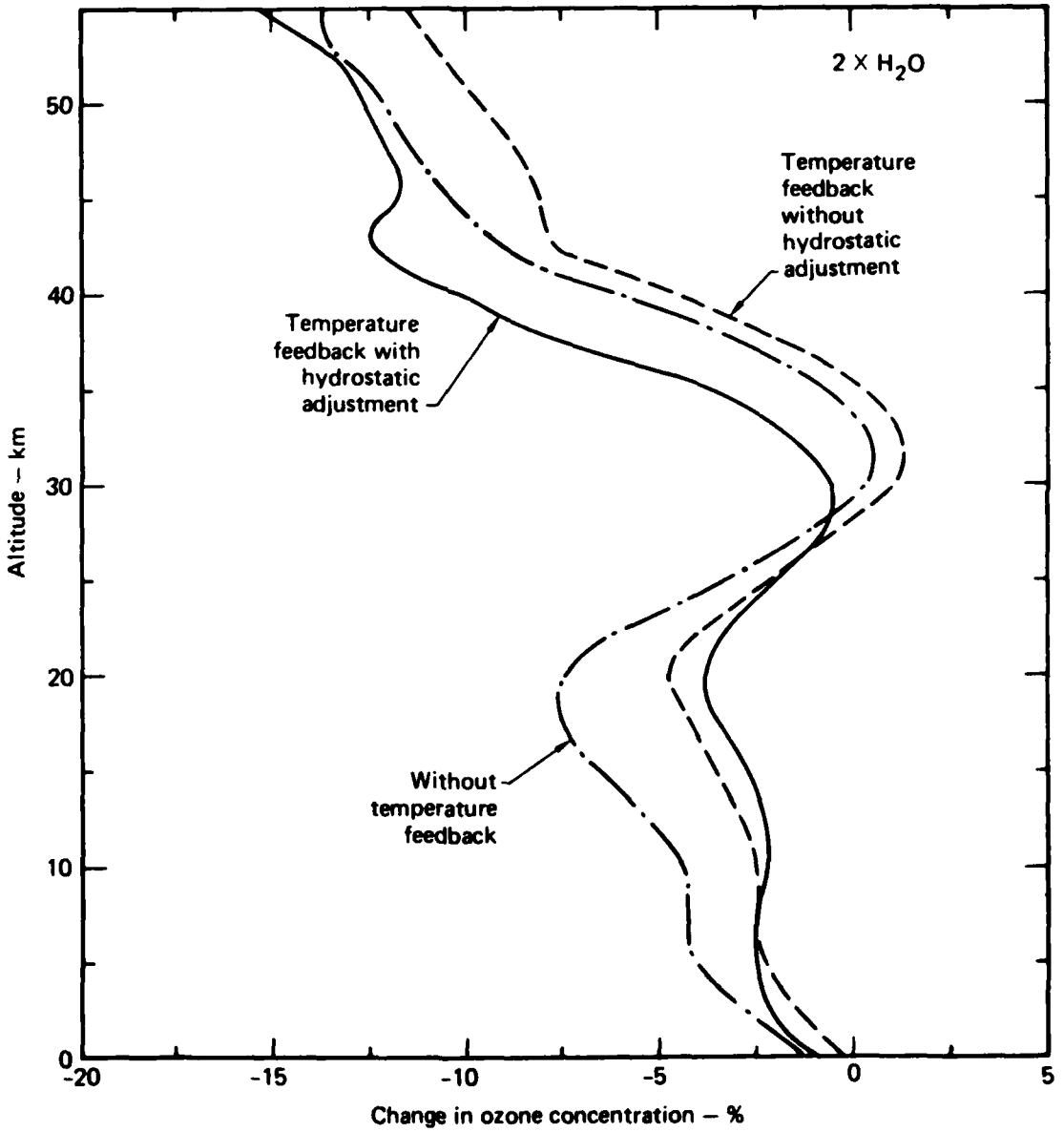

FIGURE 40. The change in ozone concentration versus altitude resulting from doubling the H_2O concentration at 13 km (1979a chemistry).

Changes in O_3 result from several competing mechanisms. Increases in H_2O cause increased HO_x which in general causes increased destruction of O_3. In the 30-35 km region, however, the increased OH causes NO_x (NO + NO_2) to decrease since a larger fraction is tied up in the reservoir species HNO_3. Thus, O_3 is actually increased between 30 and 35 km for both the case of temperature feedback without hydrostatic adjustment and the case of no temperature feedback (Fig. 40).

Comparing the case of temperature feedback without hydrostatic adjustment to the case with no temperature feedback (Fig. 40), temperature feedback acts to lessen the ozone perturbation in the atmosphere. Figure 39 shows that temperature decreases at all altitudes in the stratosphere. A decrease in temperature increases k_1 and decreases k_2 for the reactions

$$O + O_2 + M \rightarrow O_3 + M \qquad k_1 \qquad (21)$$

and

$$O + O_3 \rightarrow 2O_2 \quad . \qquad k_2 \qquad (22)$$

The reduction in temperature, therefore, tends to increase the ozone production rate and decrease the odd-oxygen destruction rate.

When hydrostatic adjustment is included along with temperature feedback, the reduction in ozone concentration is larger at altitudes above 27 km and smaller at lower altitudes. Hydrostatic adjustment affects the quantities $[O_2]$ and [M] in reaction (21). A general decrease in temperature, as occurs in this case, causes the atmosphere to contract, thereby lowering the altitude of a given pressure level. In the upper stratosphere, [M] and $[O_2]$ decrease as the atmosphere contracts. [M] may either increase or decrease at lower altitudes depending upon the combined effect of the change in temperature and the change in scale height, H, where H = kT/mg. Expression (23) relates [M] to temperature and scale height

$$[M]T = [M]_o T_o e^{\left[-\int_{z_o}^{z} \frac{1}{H}\,dz\right]} \quad , \qquad (23)$$

where the subscript o refers to values at $z_o = 0$. Changes in temperature dominate at low altitudes, resulting in an increase in [M] when T decreases. At higher altitudes changes in the exponential expression dominate and [M] decreases.

Since $[O_2] = 0.21[M]$, changes in [M] significantly affect the ozone production rate via reaction (24).

The equilibrium ozone concentration is given approximately by the expression

$$[O_3]^2 = \frac{k_1 J_1 [O_2]^2 [M]}{k_2 J_2 (1 + A)} \quad , \tag{24}$$

where J_2 refers to the photolysis rate for O_3, J_1 is the photolysis rate for O_2, and A is a term associated with destruction of odd oxygen by ClX, HO_x and NO_x (Nicolet, 1975). For any given altitude level, J_1 and J_2 also may change as a result of changes in the overburden of O_3. In the case shown, the combination of changes in O_2, M, J_1 and J_2 lead to larger O_3 depletion above about 27 km with hydrostatic adjustment when H_2O is doubled than when hydrostatic adjustment is not included. The details in the profile of $O_3(z)$ near 45 km for the case with temperature feedback and hydrostatic adjustment are due to changes in the relative roles of cycles for catalytic destruction of ozone together with changes in the temperature dependent rates, k_1/k_2.

5.3 INCREASE IN N_2O

Concern that human perturbations to the nitrogen cycle might lead to enhanced concentrations for atmospheric N_2O has stimulated interest in the budget for this gas. Tropospheric N_2O is the major source for stratospheric NO_x so perturbations in N_2O are expected to alter stratospheric chemistry.

The fertilizer source of fixed nitrogen is currently estimated to be about 4.2×10^7 tN/yr, which converts to a source of 1.5×10^6 tN/yr as N_2O (estimate of Logan et al., 1978). Combustion provides about 1.5×10^6 tN/yr as N_2O directly (Weiss and Craig, 1976; Pierotti and Rasmussen, 1976). These anthropogenic sources are thus currently significant relative to the natural sources and could grow in the future and lead to a doubling of N_2O perhaps by the early part of the next century (Logan et al., 1978). This doubling time is very uncertain due to the lack of detailed understanding of the cycle for N_2O.

The level of atmospheric N_2O determines the atmospheric response to chlorine changes, and vice versa, mainly because of the coupling of chemistry by

$ClONO_2$. Figure 41 illustrates how the percentage change in total O_3 with increased N_2O depends on the level of background ClX and on the chemical rate constants in the model. The dashed curves were produced using chemical rate constants that were used in 1978 (see Luther, 1978). The solid line refers to results using the 1979a rate constants. The major differences between the 1978 and 1979 chemistries as they affect this perturbation are: (1) the NO photolysis rate is slower in the 1979 chemistries so that the background level of NO_x is $\sim$ 50% higher, and (2) the $ClONO_2$ formation rate via $ClO + NO_2 \xrightarrow{M} ClONO_2$ is almost four

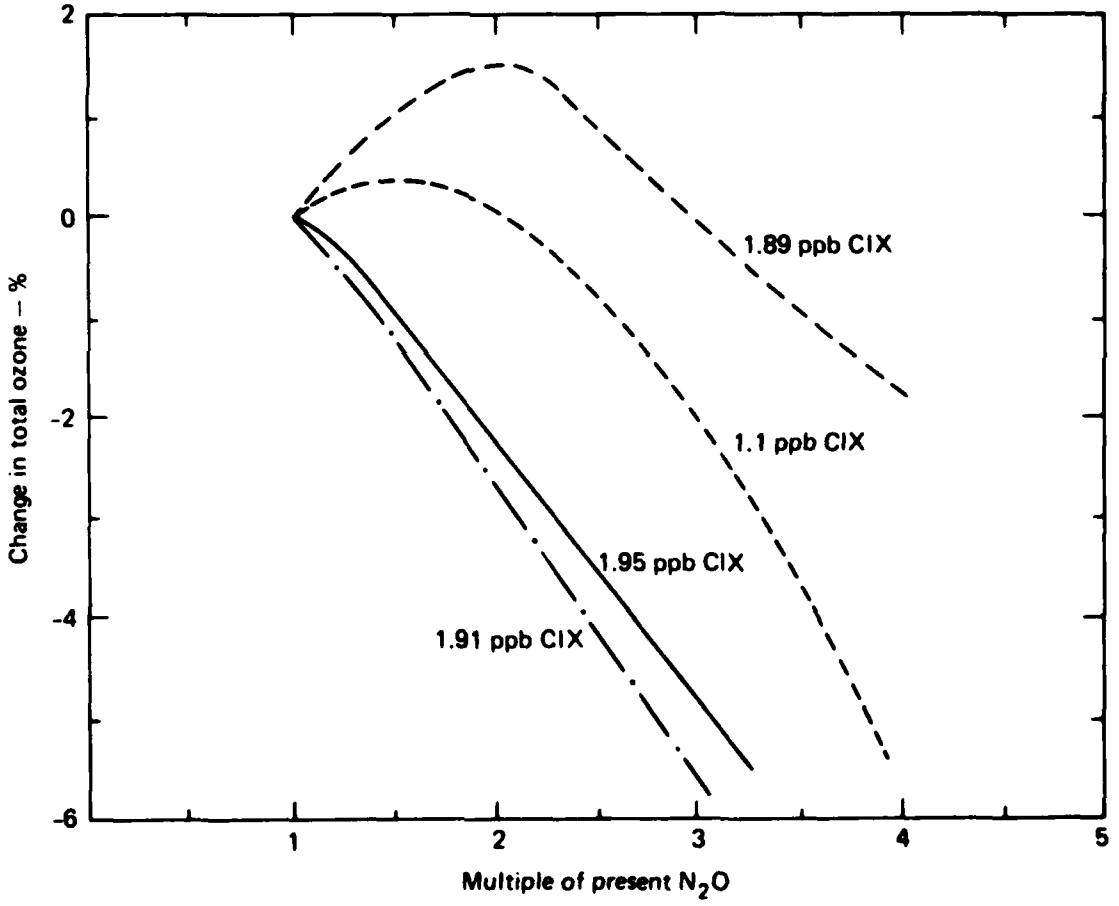

FIGURE 41. The change in total ozone resulting from an increase in N_2O expressed in multiples of the present ground level concentration, which is 325 ppbv. The results produced using the 1979a chemistry are indicated by the solid line. The results using chemical rate data that were used in 1978 (Luther, 1978) are shown by the dashed curves. The dash-dot line refers to results using the fast $ClONO_2$ formation rate (see text).

times slower in the 1979a chemistry. Both changes tend to diminish the predicted O_3 increase as N_2O is increased. Even for 1.95 ppbv ClX, ozone decreases for all N_2O perturbations with the 1979a chemistry. This remains true even for the fast rate of $ClONO_2$ formation as indicated by the dot-dash line in Fig. 41, so most of the qualitative change in results is due to the change in NO photolysis.

Figure 42 shows the percent change in O_3 as a function of altitude for the 1979a chemistry for 2 perturbations of N_2O: 1.5 times and 3.0 times the present ground level concentration which is 325 ppbv. The predicted change in total O_3 depends on the net effect of increases in O_3 below about 23 km and decreases above that level. Changes in chemistry can shift the balance of these two regions and cause effects of different magnitude and sign for various N_2O perturbations.

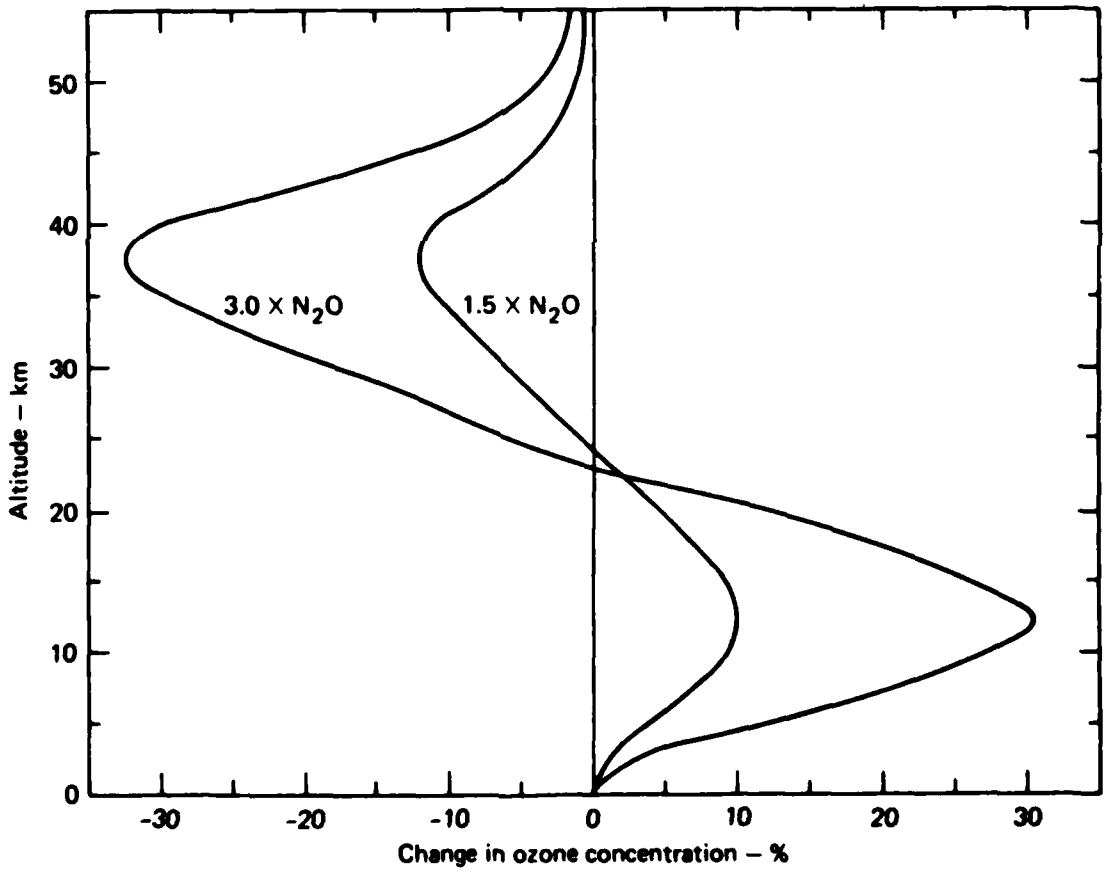

FIGURE 42. The change in ozone concentration versus altitude resulting from N_2O increases of 1.5 and 3.0 times the present ground level concentration (1979a chemistry).

Thus, the assessment of the effects of future perturbations in N_2O depends on both uncertain chemistry and uncertain knowledge of the N_2O budget.

5.4 DOUBLING OF CO_2

Systematic measurements of CO_2 since 1958 (Keeling et al., 1976a and b) have shown a rise in atmospheric CO_2 concentrations that has been attributed primarily to the use of fossil fuels. The CO_2 levels were 315 ppm in 1958, 320 ppm in 1965, and 334 ppm in 1978. By the year 2000 atmospheric CO_2 is expected to be between 365 and 400 ppm. Detailed prediction of the doubling time depends on uncertain knowledge of the budget for CO_2. Assuming that fossil fuel usage continues to increase at 4.3%/yr and that about half of the CO_2 released resides in the atmosphere, the atmospheric CO_2 concentration would double by about 2030, but estimates using other assumptions vary from 2015 to 2070. It is possible that the concentration could be limited to less than 500 ppm by shifting away from fossil fuels and relying more on solar and nuclear energy.

An increase in CO_2 is expected to lead to changes in the thermal structure of the atmosphere. In particular, a doubling of CO_2 has been estimated to increase the global mean surface temperature by 1.5 to 3 K due to the greenhouse effect (Schneider, 1975; Augustsson and Ramanathan, 1977). The temperature should decrease in the stratosphere, where the infrared opacity is smaller than in the troposphere.

The calculated change in temperature as a function of altitude for doubled CO_2 (320 to 640 ppm) is shown in Fig. 43. These calculations assumed normal summer temperatures in the troposphere (U.S. Standard Atmosphere, 1976). We tested the effect of tropospheric temperature changes by increasing the specified temperature below 14 km by 2 K when CO_2 was doubled (Fig. 44). The calculated ozone profile for this case was nearly the same as for the case when the tropospheric temperature remained unchanged and CO_2 was doubled (local ozone concentrations were within 2.6% at all altitudes). The calculated temperatures above 14 km were also similar, differing by less than 0.7 K. In this test the background atmosphere remained fixed (no hydrostatic adjustment). When hydrostatic adjustment was included, the local ozone increase near 40 km was about 15%, which was larger than the perturbation for no tropospheric temperature change

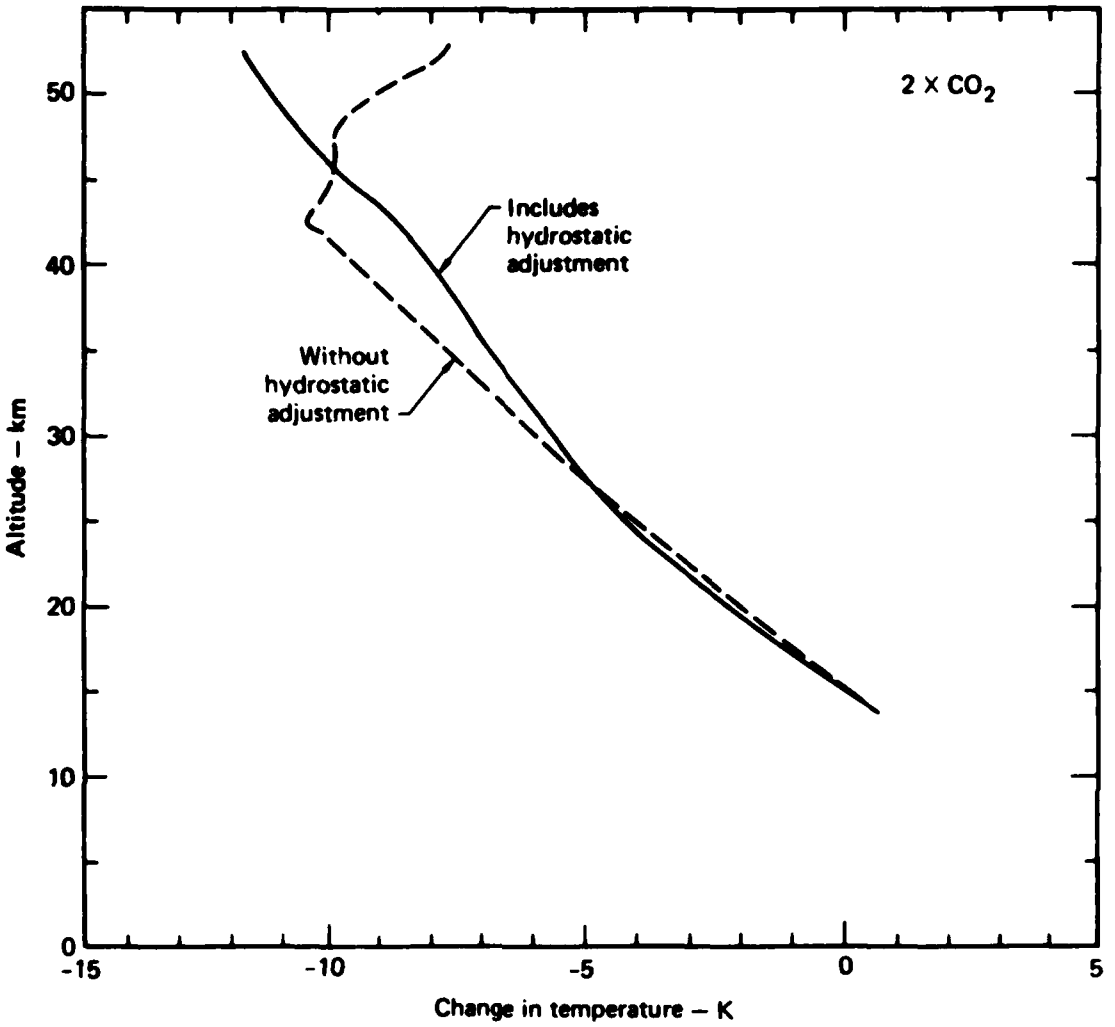

FIGURE 43. The change in stratospheric temperature for a doubling of the CO_2 concentration (320 to 640 ppm). Changes in the ozone concentration also affect the change in temperature in this calculation (1979a chemistry).

but smaller than the calculated change when hydrostatic adjustment was neglected entirely. The detailed structure of the temperature change for the cases with and without hydrostatic adjustment may be understood by examining the calculated changes in ozone shown in Fig. 44. Without hydrostatic adjustment, the stratospheric temperature decrease leads to an increase in O_3 at all altitudes. The O_3 increase tends to offset the calculated temperature decrease due to CO_2 above 40 km by increasing solar absorption by O_3. The calculated temperature decrease is a maximum near 42 km.

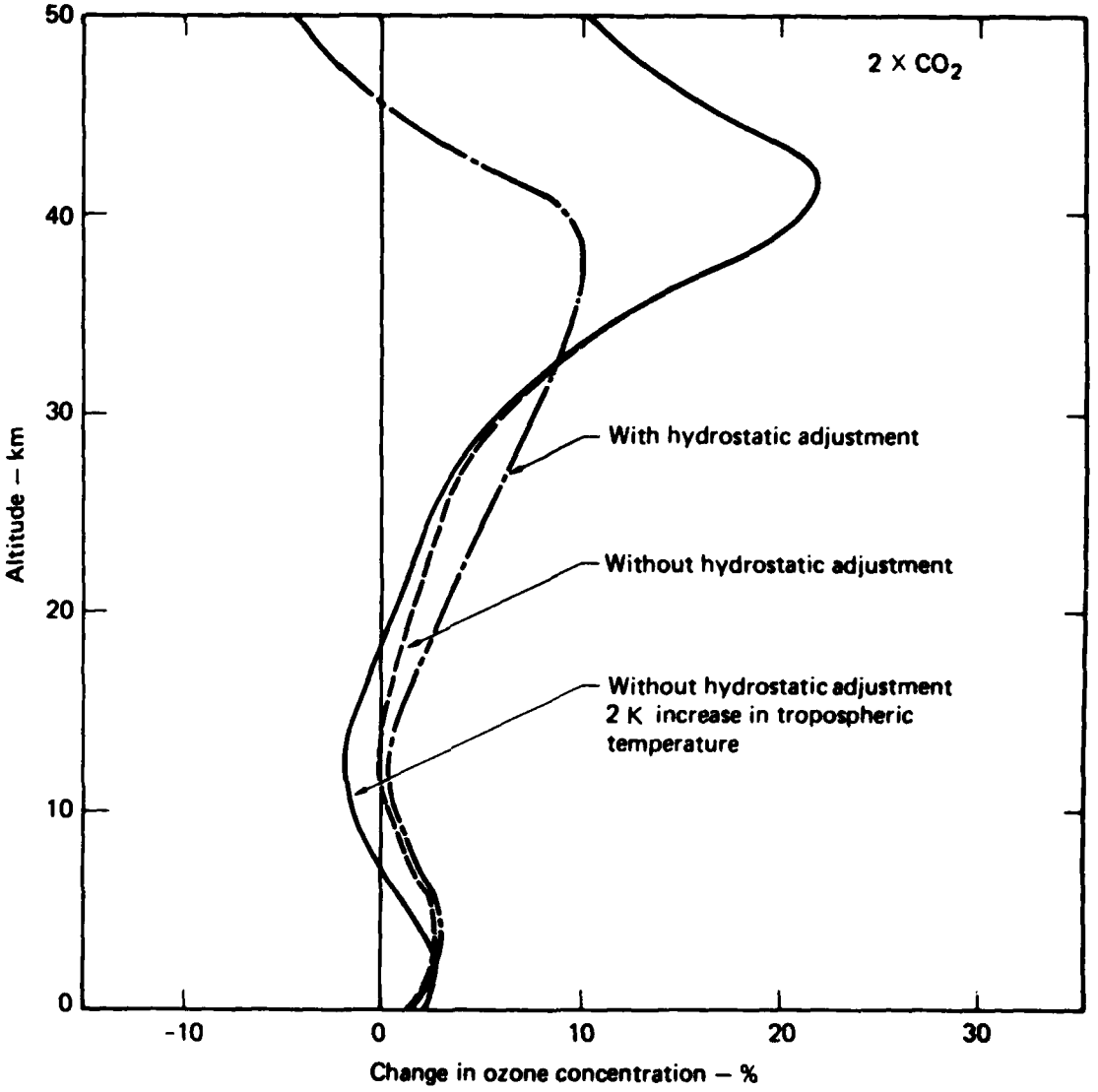

FIGURE 44. The change in ozone concentration resulting from a doubling of the CO_2 concentration (1979a chemistry).

With hydrostatic adjustment, however, ozone decreased above 45 km even though the temperature decreased. This is due to the decrease in background air density in agreement with expressions (23) and (24). As a result of the ozone decrease, the temperature (Fig. 43) decreased further above 45 km.

The change in total O_3 for a doubling of CO_2 was +5.06% with hydrostatic adjustment and +4.74% without. The larger change for the hydrostatic case reflects the behavior of O_3 near 25 km, as shown in Fig. 45. At this level, the photolysis

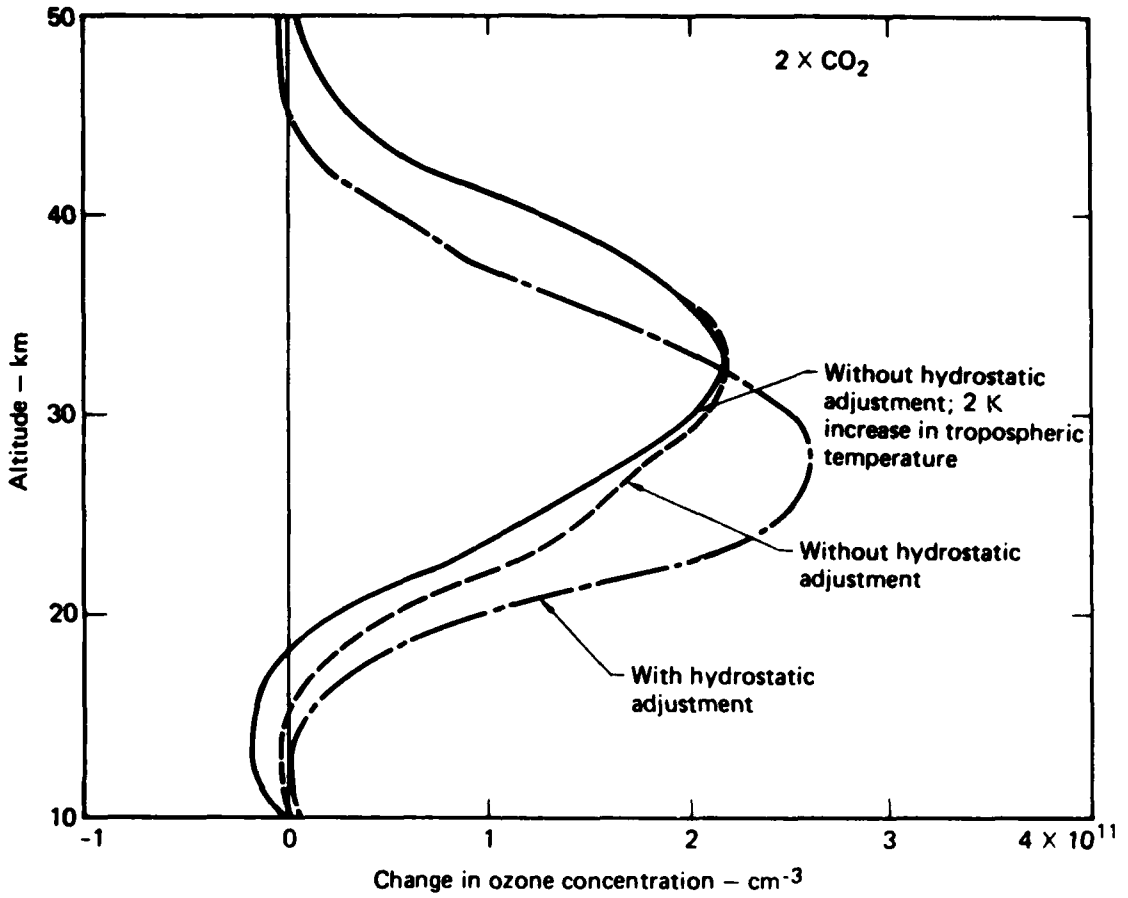

FIGURE 45. Same as Fig. 44 except the change in ozone concentration is expressed in molecules cm^{-3}.

rates for O_2 and O_3 both decreased for doubled CO_2 as a result of the larger optical depth (more O_3 above 25 km). The change in optical depth is larger for the case without hydrostatic adjustment, so J_1, particularly, decreases more for this case, causing a smaller increase in O_3. When the surface temperature was increased 2 K, the change in total ozone was 4.17% without hydrostatic adjustment.

5.5 INCREASE IN CH_3CCl_3

The use and release of methylchloroform, CH_3CCl_3, which is used as a cleaning agent, has been increasing at a steady rate. Its presence in the atmosphere has been observed since 1974 (Cox et al., 1976), and it has been suggested that its

continued use will lead to a reduction of ozone (McConnell and Schiff, 1978). The sinks for CH_3CCl_3 are photolysis and reaction with OH in the stratosphere,

$$CH_3CCl_3 + h\nu \rightarrow \text{products} \qquad (25)$$

$$CH_3CCl_3 + OH \rightarrow CH_2CCl_3 + H_2O \quad . \qquad (26)$$

Stratospheric destruction of CH_3CCl_3 leads to release of Cl atoms which are able to destroy ozone. Reaction (26) is also effective in the troposphere, so the growth of stratospheric CH_3CCl_3 is limited. The effectiveness of reaction (26) for removing tropospheric CH_3CCl_3, however, is fairly uncertain. The major uncertainties result from inadequate knowledge of the tropospheric OH distribution and the rate of reaction. The rate for reaction (26) is uncertain since there are several conflicting measurements of its rate at room temperature and of its temperature dependence (JPL, 1979). Comparison of the budget for CH_3CCl_3 with available measurements leads to an estimate for the tropospheric lifetime of between 8 and 11 years (Chang and Penner, 1978). Model calculated lifetimes are considerably shorter, implying larger tropospheric destruction rates, on average, than conform to the measurements. For example, using the historical release rate data from Neely and Plonka (1978) in our one-dimensional model, we calculate an average abundance near the surface for January 1978 of 47.3 pptv using the 1979a chemistry. The rate coefficient for reaction (26) was 2.5×10^{-12} exp(-1450/T) (see JPL, 1979). We calculate 66.1 pptv using the 1979b chemistry and a rate coefficient of 5.4×10^{-12} exp(-1820/T) for (26). These rates differ by about a factor of 2 at temperatures characteristic of the upper troposphere and by about 50% near the surface. Measurements taken by R. Rasmussen (private communication, 1979) give an average concentration of 101 pptv for CH_3CCl_3. Our values would be higher if we had included solar absorption by clouds in the troposphere which decreases the photon flux density affecting $O(^1D)$ production via $O_3 \xrightarrow{h\nu} O_2 + O(^1D)$. $O(^1D)$ production is the main source for OH in the troposphere since $O(^1D) + H_2O \rightarrow 2OH$. Absorption by clouds is expected to decrease $O(^1D)$ in the lower troposphere, on average, by perhaps as much as a factor of 2. Our calculated surface OH concentration should then decrease between 30 and 50%, and some of the current discrepancy in CH_3CCl_3 concentration would be removed. The OH concentration, however, needs considerable clarification

since model calculations are less than in situ observations (Philen et al., 1978). Thus, our calculated ozone depletion estimates by CH_3CCl_3 must be considered preliminary.

With CH_3CCl_3, $CFCl_3$, and CF_2Cl_2 releases included in our model, the calculated reduction in total ozone in 1978 was 1.7% (relative to 1950) using 1979b chemistry, whereas without CH_3CCl_3, O_3 decreased by 1.3%. The total stratospheric chlorine burden increased by 7%. Figs. 37 and 38 show the time history for O_3 depletion at constant 1976 production rates for $CFCl_3$, CF_2Cl_2. The CH_3CCl_3 release rate at the earth's surface is constant at 1.23×10^7 molecules cm^{-2} s^{-1} beyond 1978. At steady state ozone decreased 15.2%, whereas without CH_3CCl_3 it decreased 14.2%. Of course, the effects of CH_3CCl_3 could be much greater if its use were to continue to increase.

REFERENCES

Ackerman, M., D. Frimout, C. Muller, and D. J. Wuebbles, "Stratospheric Methane Measurements and Predictions," Pageoph, 117, 367-380, 1978.

Agustsson, T. and V. Ramanathan, "A Radiative-Convective Model Study of the CO_2 Climate Problem," J. Atmos. Sci., 34, 448-451, 1977.

Anderson, J., "In Situ Measurements of Cl, ClO, HO, HO_2, O_3, and O," paper presented at the Workshop on Upper Atmospheric Measurements, Seattle, Washington, September 5-7, 1979.

Anderson, J. G., H. J. Grassl, R. E. Shetter, and J. J. Margitan, "Stratospheric Free Chlorine Measured by Balloon Borne in situ Resonance Fluorescence," manuscript dated February, 1979.

Angell, J. K. and J. Korshover, "Global Ozone Variations: An Update into 1976," Mon. Wea. Rev., 106, 725, 1978.

Arthur D. Little, Inc., "Stratospheric Emissions Due to Current and Projected Aircraft Operations," C77327-10, 1976.

Bates, D. R. and M. Nicolet, "The Photochemistry of Atmospheric Water Vapor", J. Geophys. Res., 55, 301-327, 1950.

Borucki, W. J., D. S. Colburn, R. C. Whitten, L. A. Capone, M. Covert, "Model Analysis of the Ozone Depletion Due to the August 1972 Solar Proton Event," EOS, 59, 284, 1978.

Boughner, R. E., "The Effect of Increased Carbon Dioxide Concentrations on Stratospheric Ozone," J. Geophys. Res., 83, 1326, 1978.

Brewer, A. W. and A. W. Wilson, "The Regions of Formation of Atmospheric Ozone", Quart. J. Roy. Met. Soc., 94, 249-265, 1968.

Burnett, C. R. and E. B. Burnett, "Spectroscopic Measurements of the Vertical Abundance of Hydroxyl (OH) in the Earth's Atmosphere," EOS, 60, 336, 1979.

Butler, D., NASA Goddard Space Flight Center, private communication, 1979.

Callis, L. B., Jr., R. E. Boughner, V. Ramanathan, and J. E. Nealy, "Ozone: Effect of UV Variability and Stratospheric Coupling Mechanisms," presented at the Internation Joint Symposium on Atmospheric Ozone, Int. Comm. on Atmos. Ozone and Int. Comm. on Atmos. Chem. and Global Pollut., Dresden, East Germany, August 9-17, 1976.

Callis, L. B., Jr. and J. E. Nealy, "Solar UV Variability and Its Effect on Stratospheric Thermal Structure and Trace Constituents," Geophys. Res. Letters, 5, 249, 1978.

Chang, J. S., "Simulations, Perturbations, and Interpretations," in Proceedings of the 3rd CIAP Conference, U.S. Department of Transportation, Cambridge, MA, Report DOT-TSC-OST-74-15, 330-341, 1974.

Chang, J. S., Eddy diffusion profile described in "First Annual Report of Lawrence Livermore Laboratory to the High Altitude Pollution Program," edited by F. M. Luther, Rep. UCRL-50042-76, Lawrence Livermore Laboratory, Livermore, CA 1976.

Chang, J. S., J. R. Barker, J. E. Davenport, and D. M. Golden, "Chlorine Nitrate Photolysis by a New Technique: Very Low Pressure Photolysis," Chem. Phys. Lett., 60, 385-390, 1979.

Chang, J. S. and W. H. Duewer, "Modeling Chemical Processes in the Stratosphere," Ann. Rev. Phys. Chem., 30, 443-469, 1979.

Chang, J. S., W. H. Duewer and D. J. Wuebbles, "The Atmospheric Nuclear Test of the 50's and 60's: A Possible Test of Ozone Depletion Theories," J. Geophys. Res., 84, 1755-1765, 1979.

Chang, J. S. and H. S. Johnston, "The Effect of NO_x Effluents on Ozone," in Proceedings of the 3rd CIAP Conference, Cambridge, MA, U.S. Department of Transportation Report DOT-TSC-OST-74-15, pp. 323-329, 1974.

Chang, J. S. and F. Kaufman, "Upper Bound and Probable Value of the Rate Constant of the Reaction $OH + HO_2 \rightarrow H_2O + O_2$," J. Phys. Chem., 82, 1683-1687, 1978.

Chang, J. S. and J. E. Penner, "Analysis of Global Budgets of Halocarbons," Atmos. Env., 12, 1867-1873, 1978.

Chapman, S., "A Theory of Upper Atmospheric Ozone", Memoirs. Roy. Met. Soc., 3, 103-125, 1930.

CIAP Monograph 2, "Propulsion Effluents in the Stratosphere," U.S. Department of Transportation, Washington, D. C., 1975.

CIAP Monograph 3, "The Stratosphere Perturbed by Propulsion Effluents," DOT-TST-75-53, U.S. Department of Transportation, Washington, D. C., 1975.

CIAP Monograph 5, "Impacts of Climatic Change on the Biosphere," Report DOT-TST-75-55 (NTIS), 1975.

Cieslik, S. and M. Nicolet, "The Aeronomic Dissociation of Nitric Oxide," Planet. Space Sci., 21, 925-938, 1973.

COMESA, "The Report of the Committee on Meteorological Effects of Stratospheric Aircraft," Parts 1 and 2, United Kingdom Meteorological Office, Bracknell, 1976.

COVOS, Bertin, M., R. Borshi, G. Brasseur, R. Joattor, and M. Maignan, "Models Mathematiques de la Stratosphere Comite' d'Etudes Sur Les Consequences des Vols Stratospheriques," Rapport No. 6A, 1976.

Cox, R. A., "Kinetics of HO_2 Radical Reactions of Atmospheric Interest," Papers Presented at the WMO Symposium on the Geophysical Aspects and Consequences of Change in the Composition of the Stratosphere, Toronto, 26-30 June, 1978, WMO No. 511, 1978.

Cox, R. A. and J. P. Burrows, "Kinetics and Mechanism of the Disproportionation of HO_2 in the Gas Phase," J. Phys. Chem., 83, 2560-2568, 1979.

Cox, R. A., R. G. Derwent and A. E. J. Eggleton, "Photochemical Oxidation of Halocarbons in the Troposphere," Atmos. Env., 10, 305-308, 1976.

Crutzen, P. J., "Determination of Parameters Appearing in the 'Dry' and the 'Wet' Photochemical Theories for Ozone in the Stratosphere," Tellus, 21, 368-388, 1969.

Crutzen, P. J., "The Influence of Nitrogen Oxides on the Atmospheric Ozone Content," Quart. J. Roy. Met. Soc., 96, 320-325, 1970.

Crutzen, P. J., "SST's — A Threat to the Earth's Ozone Shield," Ambio, 1, 41-51, 1972.

Crutzen, P. J., I. S. Isaksen, and G. C. Reid, "Solar Proton Events: Stratospheric Sources of Nitric Oxide," Science, 189, 457-459, 1975.

Cunnold, D. K., F. N. Alyea, and R. G. Prinn, "Relative Effects on Atmospheric Ozone of Latitude and Altitude of Supersonic Flight," AIAA Journal, 15, 337-345, 1977.

DeMore, W. B., "Reaction of HO_2 with O_3 and the Effect of Water Vapor on HO_2 Kinetics," J. Phys. Chem., 83, 1113-1118, 1979.

DeMore, W. B. and E. Tschuikow-Roux, "Temperature Dependence of the Reaction of OH and HO_2 with O_3," J. Phys. Chem., 78, 1447-1451, 1974.

Duewer, W. H., D. J. Wuebbles, H. W. Ellsaesser, and J. S. Chang, "NO_x Catalytic Ozone Destruction: Sensitivity to Rate Coefficients, Lawrence Livermore Laboratory Report UCRL-77917, 1975; J. Geophys. Res., 82, 935-942, 1977.

Dutsch, H. U., "Photochemische Theorie des Atmospharischen Ozons unter Berucksichtigung von Nichtgleichgewichtszustanden und Luftbewegungen, Dissertation University of Zurich, 1946.

Dutsch, H. U., "The Photochemistry of Stratospheric Ozone," Quart. J. Roy. Meteoro. Soc., 94, 483-497, 1968.

Ehhalt, D. H., L. E. Heidt, R. H. Lueb, and W. Pollock, "The Vertical Distribution of Trace Gases in the Stratosphere," Pageoph, 113, 389-402, 1975.

Evans, W. F. J., H. Fast, J. B. Kerr, C. T. McElroy, R. S. O'Brien, D. I. Wardle, J. S. McConnell and B. A. Ridley, "Stratospheric Constituent Measurements from Project Stratoprobe," Papers Presented at the WMO Symposium on the Geophysical Aspects and Consequences of Changes in the Composition of the Stratosphere, Toronto, 26-30 June 1978, WMO-No. 511, 1978.

Evans, W. F. J., J. B. Kerr, D. I. Wardle, J. C. McConnell, B. A. Ridley, and H. I. Schiff, "Intercomparison of NO, NO_2, and HNO_3 Measurements with Photochemical Theory," Atmosphere, 14, 189, 1976.

Fabian, P., J. A. Pyle, and R. J. Wells, "The August 1972 Solar Proton Event and the Atmospheric Ozone Layer," Nature, 277, 458-460, 1979.

Foley, H. M. and M. A. Ruderman, "Stratospheric Nitric Oxide Production from Past Nuclear Explosions and Its Relevance to Projected SST Pollution," Paper P-894, Institute for Defense Analysis, Jason, Arlington, VA, 1972.

Fontanella, J. C., A. Girard, L. Gramount, and N. Louisnard, "Vertical Distribution of NO, NO_2 and HNO_3 as Derived from Stratospheric Absorption Infrared Spectra," Applied Optics, 14, 825, 1975.

Frederick, J. D. and R. D. Hudson, "Predissociation of Nitric Oxide in the Mesosphere and Stratosphere," J. Atmos. Sci., 36, 737-745, 1979.

Goldan, P. D., W. C. Kuster, D. L. Albritton, and A. L. Schmeltekopf, "Stratospheric $CFCl_3$, CF_2Cl_2, and N_2O Height-Profile Measurements at Several Latitudes," preprint, NOAA Aeronomy Laboratory, Boulder, CO, 1979.

Grobecker, A. J., S. C. Coroniti, and R. H. Cannon, Jr., "CIAP Report of Findings, The Effects of Stratospheric Pollution by Aircraft," Report DOT-TST-75-50, U. S. Department of Transportation, Washington, D. C., 1974.

Hamilton, E. J., Jr. and R. R. Lii, "The Dependence of H_2O and on NH_3 of the Kinetics of the Self Reaction of HO_2 in the Gas Phase Formation of $HO_2 \cdot H_2O$ and $HO_2 \cdot NH_3$ Complexes," Int. J. Chem. Kinet., 9, 875-885, 1977.

Hampson, J., "Photochemical Behavior of the Ozone Layer", Tech. Note 1627, Canadian Arm. Res. and Dev. Establishment, 1964.

Harries, J. E., "Ratio of HNO_3 to NO_2 Concentration in the Daytime Stratosphere," Nature, 274, 235, 1978.

Harries, J. E., D. G. Moss, N. R. W. Swann, and G. F. Neill, "Simultaneous Measurements of H_2O, NO_2, and HNO_3 in the Daytime Stratosphere from 15 to 35 km," Nature, 259, 300-302, 1976.

Heath, D. F., A. J. Krueger, and P. J. Crutzen, "Influence of a Solar Proton Event on Stratospheric Ozone," Science, 197, 886-889, 1977.

Heath, D. F. and M. P. Thekaekara, "The Solar Spectrum Between 1200 and 3000 A," in The Solar Output and Its Variation, O. R. White (ed.), Colorado Assoc. Univ. Press, Boulder, CO, p. 193, 1977.

Hesstvedt, E., "On the Effect of Vertical Eddy Transport on Atmospheric Composition in the Mesosphere and Lower Stratosphere", Geofys. Publ. Norske Vidensk. Akad. Olso, 27(4), 1968.

Hidalgo, H., "Status of Representative Two-Dimensional Models of the Stratosphere and Troposphere as of Mid-1978," report no. FAA-AEE-78-23, U.S. Department of Transportation, Federal Aviation Administration, Washington, D.C., 1978.

Hilst, G. R., "Solutions of the Chemical Kinetic Equations for Initially Inhomogeneous Mixtures," in Proceedings of the Second Conference on the Climatic Impact Assessment Program, November 14-17, 1972, U.S. Department of Transportation Report DOT-TSC-OST-73-4, 1973.

Hochanadel, C. J., J. A. Ghormley, and P. J. Ogren, "Absorption Spectrum and Reaction Kinetics of HO_2 Radical in the Gas Phase," J. Chem. Phys., 56, 4426-4432, 1972.

Howard, C. J. and D. M. Evenson, "Kinetics of the Reaction HO_2 with NO," Geophys. Res. Letters, 4, 437, 1977.

Hudson, R. D., (ed.), "Chlorofluoromethanes and the Stratosphere," NASA Reference Publication No. 1010, Goddard Space Flight Center, Greenbelt, Maryland, 1977.

Hunt, G. G., "A Theoretical Study of the Changes Occurring in the Ozonosphere During a Total Eclipse of the Sun," Tellus, 18, 516-523, 1965.

Hunt, B. G., "The Need for a Modified Photochemical Theory of the Ozonosphere", J. Atmos. Sci., 23, 88-94, 1966a.

Hunt, B. G., "Photochemistry of Ozone in a Moist Atmosphere", J. Geophys. Res., 71, 1385-1498, 1966b.

Hunten, D. M., "Vertical Transport in Atmospheres," in Atmosphere of Earth and Planets, edited by B. M. McCormac, pp. 59-72, D. Reidel, Hingham, MA, 1975.

Johnston, H. S., "Reduction of Stratospheric Ozone by Nitrogen Oxide Catalysts from Supersonic Transport Exhaust", Science, 173, 517-522, 1971.

Johnston, H. S., "Newly Recognized Vital Nitrogen Cycle", Proceedings of the National Academy of Sciences, 69, 2369-2372, 1972.

JPL Publication 79-27, "Chemical Kinetic and Photochemical Data for Use in Stratospheric Modeling," NASA Panel for Data Evaluation, 1979.

Keeling, C. D., J. A. Adams, Jr., C. A. Ekdale, Jr., and P. R. Guenther, "Atmospheric CO_2 Varitions at the South Pole, Tellus, 28, 552-564, 1976a.

Keeling, C. D., R. B. Bacaston, A. E. Bainbridge, C. A. Ekdahl, Jr., P. R. Guenther, L. S. Waterman, and J. F. S. Chin, "Atmospheric CO_2 Variations at Mauna Loa Observatory, Hawaii," Tellus, 28, 538-551, 1976b.

Kurzeja, R. J., "The Production of Transport of Ozone and Other Minor Constituents in the Stratosphere," Ph.D. Thesis, Microfilm 76-28636, Florida State University, Tallahassee, 1976.

Leovy, C. B., "Atmospheric Ozone: An Analytic Model for Photochemistry in the Presence of Water Vapor," J. Geophys. Res., 74, 417-426, 1969.

Leu, M. T. and C. L. Lin, "Rate Constants for the Reactions of OH with ClO, Cl_2, and Cl_2O at 298 K," Geophys. Res. Lett., 6, 425-428, 1979.

Liu, S. C., T. M. Donahue, R. J. Cicerone, and W. L. Chameides, "Effect of Water Vapor on the Destruction of Ozone in the Stratosphere Perturbed by ClX or NO_x Pollutants," J. Geophys. Res., 81, 3111-3118, 1976.

Logan, J. A., M. J. Prather, S. C. Wofsy, and M. B. McElroy, "Atmospheric Chemistry: Response to Human Influence," Phil. Trans. Roy. Soc. London, 290, 187-234, 1978.

Lowenstein, M., W. L. Starr, and D. G. Murcray, "Stratospheric NO and HNO_3 Observations in the Northern Hemisphere for Three Seasons," Geophys. Res. Lett., 5, 531, 1978.

Luther, F. M., ed., "Annual Report of Lawrence Livermore Laboratory to the FAA on the High Altitude Pollution Program — 1978," Lawrence Livermore Laboratory Report UCRL-50042-78, September 30, 1978.

Luther, F. M. and R. J. Gelinas, "Effect of Molecular Multiple Scattering and Surface Albedo on Atmospheric Photodissociation Rates," J. Geophys. Res., 81, 1125-1132, 1976.

Luther, F. M., D. J. Wuebbles, and J. S. Chang, "Temperature Feedback in a Stratospheric Model," J. Geophys. Res., 82, 4935-4942, 1977.

Luther, F. M., D. J. Wuebbles, W. H. Duewer and J. S. Chang, "Effect of Multiple Scattering on Species Concentrations and Model Sensitivity," J. Geophys. Res., 83, 3563-3570, 1978.

Mastenbrook, H. J., "The Variability of Water Vapor in the Stratosphere," J. Atmos. Sci., 28, 1495-1501, 1971.

Mastenbrook, H. J., "Water-Vapor Measurements in the Lower Stratosphere," Can. J. Chem., 52, 1527-1531, 1974.

McConnell, J. C. and H. I. Schiff, "Methyl Chloroform: Impact on Stratospheric Ozone," Science, 199, 174-177, 1978.

McElroy, M. B., S. C. Wofsy, J. E. Penner, and J. C. McConnell, "Atmospheric Ozone: Possible Impact of Stratospheric Aviation," J. Atmos. Sci., 31, 287-303, 1974.

Mecke, R., "The Photochemical Ozone Equilibrium in the Atmosphere", Trans. Faraday Soc., 27, 375-378, 1931.

Menzies, R. T., "Remote Measurement of ClO in the Stratosphere," Geophys. Res. Letters, 6, 151, 1979.

Murcray, D., "Infrared Techniques for Remote Sensing," paper presented at the Workshop on Upper Atmospheric Measurements, Seattle, Washington, September 5-7, 1979.

NASA Reference Publication 1010, "Chlorofluoromethanes and the Stratosphere," R. D. Hudson (ed.), 1977.

NASA Reference Publication (draft), "The Stratosphere: Present and Future," R. D. Hudson (ed.), prepared at the NASA Workshop, Harpers Ferry, Pennsylvania, June 1979.

National Research Council, Climatic Impact Committee, Environmental Impact of Stratospheric Flight: Biological and Climatic Effects of Aircraft Emissions in the Stratosphere, National Academy of Sciences, Washington, D. C., 1975a.

National Research Council, Long-Term Worldwide Effects of Multiple Nuclear Weapons, National Academy of Sciences, Washington, D. C., 1975b.

National Research Council, Halocarbons: Environmental Effects of Chlorofluoromethane Release, National Academy of Sciences, Washington D. C., 1976a.

National Research Council, Halocarbons: Effects on Stratospheric Ozone, see Appendix D, National Academy of Sciences, 1976b.

NBS Special Publication 513, "Reaction Rate and Photochemical Data for Atmospheric Chemistry — 1977," R. F. Hampson, Jr., and D. Garvin (eds.), National Bureau of Standards, Washington, D. C., 1978.

NBS Technical Note 866, "Chemical Kinetics and Photochemical Data for Modeling Atmospheric Chemistry," R. F. Hampson, Jr. and D. Garvin (eds.), National Bureau of Standards, Washington, D. C., 1975.

Neely, W. P. and J. M. Plonka, "Estimation of Time Averaged Hydroxyl Radical Concentrations in the Troposphere," Environ. Sci. and Tech., 12, 317, 1978.

Nicolet, M., "Aeronomic Reactions of Hydrogen and Ozone," in Mesospheric Models and Related Experiments, G. Fiocco (ed.), Reidel Publication Co., Dordrecht, Holland, 1-51, 1970.

Nicolet, M., "Stratospheric Ozone: An Introduction to Its Study," Rev. Geophys. Space Phys., 13, 593-636, 1975.

Noxon, J. F., "Stratospheric NO_2, II. Global Behavior," to be published in J. Geophys. Res., 1979.

Oliver, R. C., E. Bauer, H. Hidalgo, K. A. Gardner, and W. Wasylkiwskyj, "Aircraft Emissions: Potential Effects on Ozone and Climate: A Review and Progress Report," Federal Aviation Administration Report FAA-EQ-77-3, 1977.

Oliver, R. C., E. Bauer, and W. Wasylkiwskyj, "Recent Developments in the Estimation of Potential Effects of High Altitude Aircraft Emissions on Ozone and Climate," Report No. FAA-AEE-78-24, U.S. Department of Transportation, Federal Aviation Administration, Washington, D. C., 1978.

Penner, J. E. and J. S. Chang, "Possible Variations in Atmospheric Ozone Related to the Eleven Year Solar Cycle," Geophys. Res. Letters, 5, 817-820, 1978.

Penner, J. E. and J. S. Chang, "The Relation Between Atmospheric Trace Species Variabilities and Solar UV Variability," Lawrence Livermore Laboratory Report UCRL-83029, submitted for publication, 1979.

Philen, D., W. Heaps, and D. D. Davis, "Boundary Layer and Free Tropospheric OH Measurements at Tropical and Sub-tropical Latitudes in the Northern and Southern Hemispheres," presented at AGU Fall Meeting, San Francisco, CA, December 1978.

Pierotti, D. and R. A. Rasmussen, "Combustion as a Source of Nitrous Oxide in the Atmosphere," Geophys. Res. Letters. 3, 265, 1976.

Poppoff, I. G., R. C. Whitten, R. P. Turco, and L. A. Capone," An Assessment of the Effect of Supersonic Aircraft Operations on the Stratospheric Ozone Content," NASA RP-1026, 1978.

Ramanathan, V., L. B. Callis, and R. E. Boughner, "Sensitivity of Surface Temperature and Atmospheric Temperature to Perturbations in the Stratospheric Concentration of Ozone and Nitrogen Dioxide," J. Atmos. Sci., 33, 1092-1112, 1976.

Rowland, F. S. and M. J. Molina, "Chlorofluoromethanes in the Environment," Rev. Geophys. Space Phys., 13, 1-35, 1975.

Schneider, S. H., "On the Carbon Dioxide Climate Confusion," J. Atmos. Sci., 32, 2060, 1975.

Seitz, H., B. Davidson, J. P. Friend, and H. W. Feely, Numerical Models of Transport Diffusion and Fallout of Stratospheric Radioactive Material (Final Report on Project STREAK), USAEC Report NYO-3654-4, 1968.

Simon, P. C., "Irradiation Solar Flux Measurements Between 120 and 400 nm Current Position and Future Needs," Planet. Space Sci., 26, 355-365, 1978.

Stolarski, R. S. and R. J. Cicerone, "Stratospheric Chlorine: A Possible Sink for Ozone," Can. J. Chem., 52, 1610-1615, 1974.

Stolarski, R. S., D. M. Butler, and R. D. Rundel, "Uncertainty Propagation in a Stratospheric Model: II. Monte Carlo Analysis of Imprecisions Due to Reaction Rates," J. Geophys. Res., 83, 3074, 1978.

Thompson, B. A., P. Harteck and R. R. Reeves, Jr., "Ultraviolet Absorption Coefficients of CO_2, CO, O_2, H_2O, N_2O, NH_3, NO, SO_2, and CH_4 between 1850 and 4000A," J. Geophys. Res., 68, 6431-6436, 1963.

Tuck, A. F., "Numerical Model Studies of the Effect of Injected Nitrogen Oxides on Stratospheric Ozone," Proc. R. Soc. London, 355, 267-299, 1977.

U. S. Standard Atmosphere, 1976, NOAA-S/T 76-1562, U. S. Government Printing Office, Washington, D. C., 1976.

Weiss, R. F. and H. Craig, "Production of Atmospheric Nitrous Oxide by Combustion," Geophys. Res. Letters, 3, 751, 1976.

Wofsy, S. C., M. B. McElroy, and Y. L. Yung, "The Chemistry of Atmospheric Bromine," Geophys. Res. Letters, 2, 215-218, 1975.

Wongdontri-Stuper, W., R. K. M. Jayanty, R. Simonaitis, and J. Heicklen, "The Cl_2 Photosensitized Decomposition of O_3: The Reactions of ClO and OClO with O_3," preprint, 1978.

Wuebbles, D. J. and J. S. Chang, "A Theoretical Study of Stratospheric Trace Species Variations During a Solar Eclipse," Geophys. Res. Letters, 6, 179-182, 1979.

APPENDIX A. DESCRIPTION OF THE LLL ONE-DIMENSIONAL TRANSPORT-KINETICS MODEL

In Section 2, we gave a general description of the theoretical models used to study the stratosphere with particular emphasis placed on one-dimensional transport-kinetics models. In this appendix, we will describe particular aspects of the LLL one-dimensional transport-kinetics model in relation to the previous discussion.

PHYSICAL DOMAIN

The LLL one-dimensional model extends from the ground to 56.25 km. The model currently calculates the vertical concentration distributions of 39 (2 of which are used only in sensitivity studies) atmospheric trace constituents. The model contains 134 (14 of which are used only in sensitivity studies) chemical or photochemical reactions. Table A-1 lists the species solved for in the model. Of these species, $O(^1D)$, H, and N are assumed to be in instantaneous equilibrium. The vertical grid structure is variable, but for the calculations reported here, we have a 0.5-km-thick layer at the surface, 1-km thick layers extending from 0.5 to 34.5 km, a 1.75-km thick layer between 34.5 and 36.25 km and 2.5-km thick layers extending to 56.25 km.

TRANSPORT REPRESENTATION

As discussed previously, the vertical transport in the one-dimensional model is parameterized through a diffusion coefficient, K_z. The K_z profile used primarily in the calculations for this report was originally based on an analysis of N_2O and CH_4 measurements (NAS, 1976) with considerations also given to measurements of radionuclide debris transport in the lower stratosphere.

TABLE A-1. Species calculated in the LLL one-dimensional model.

$O(^3P)$	Cl	CH_4
O_3	ClO	HCO
NO	$ClONO_2$	CH_2O
NO_2	$ClNO_2$	CH_3
N_2O	HCl	CH_3OOH
HNO_3	OClO*	CH_3O
OH	HOCl	CH_3O_2
HO_2	CH_3Cl	CO
H_2O_2	CF_2Cl_2	H_2
NO_3	$CFCl_3$	$O(^1D)$
N_2O_5	CH_3CCl_3	N
H_2O	ClO_3*	H
HONO	CCl_4	
HNO_4		

*Used only in sensitivity studies.

The LLL one-dimensional model has been designed such that profiles of K_z utilized by other groups (or at previous times) can be easily incorporated. Such profiles have been utilized to test the sensitivity of the results to transport parameterization uncertainties (see Section 4).

CHEMISTRY

We have used two 1979 versions of model chemistry in this report (see Tables A-2 through A-4). 1979a chemistry was based primarily on the rate recommendations in JPL (1979). However, several reactions discussed in JPL (1979) are omitted in the model, and several reactions not discussed in JPL (1979) are included. This chemistry was used for many sensitivity calculations carried out in the spring of 1979. 1979b chemistry was based almost exclusively on the draft chapter on chemical reaction rates prepared at the NASA Harpers Ferry Workshop

TABLE A-2. Chemical reactions and rate coefficients where $k = A\ e^{B/T}$ used in the 1979 model chemistry.

	Reaction	A*	B	Note
1.	$O + O_2 \xrightarrow{M} O_3$	See Table A-3		3
2.	$O + O_3 \rightarrow 2O_2$	1.5×10^{-11}	-2218	1
3.	$O_3 + NO \rightarrow NO_2 + O_2$	2.3×10^{-12}	-1450	1
4.	$O + NO_2 \rightarrow NO + O_2$	9.3×10^{-12}	0	1
5.	$N_2O + O(^1D) \rightarrow N_2 + O_2$	4.8×10^{-11} 5.1×10^{-11}	0 0	1 2
6.	$N_2O + O(^1D) \rightarrow 2NO$	6.2×10^{-11} 5.9×10^{-11}	0 0	1 2
7.	$N + O_2 \rightarrow NO + O$	4.4×10^{-12}	-3220	1
8.	$N + NO \rightarrow N_2 + O$	3.4×10^{-11}	0	1
9.	$O(^1D) + H_2O \rightarrow 2OH$	2.3×10^{-10}	0	1
10.	$O_3 + OH \rightarrow HO_2 + O_2$	1.6×10^{-12}	-940	1
11.	$O + OH \rightarrow O_2 + H$	4.0×10^{-11}	0	1
12.	$O_3 + HO_2 \rightarrow OH + 2O_2$	1.1×10^{-14}	-580	1
13.	$O + HO_2 \rightarrow OH + O_2$	3.5×10^{-11}	0	1
14.	$H + O_2 \xrightarrow{M} HO_2$	See Table A-3		3
15.	$O_3 + H \rightarrow OH + O_2$	1.4×10^{-10}	-470	1
16.	$HO_2 + HO_2 \rightarrow H_2O_2 + O_2$	2.5×10^{-12}	0	1
17.	$HO_2 + OH \rightarrow H_2O + O_2$	4.0×10^{-11}	0	1
18.	$OH + NO_2 \xrightarrow{M} HNO_3$	See Table A-3		1
19.	$OH + HNO_3 \rightarrow H_2O + NO_3$	8.5×10^{-14}	0	1,10
20.	$H_2O_2 + OH \rightarrow H_2O + HO_2$	1.0×10^{-11}	-750	1
21.	$N_2 + O(^1D) \xrightarrow{M} N_2O$	See Table A-3		3

*When two entries are given, the lower one corresponds to 1979a chemistry and the upper one corresponds to 1979b chemistry.

TABLE A-2. (Continued)

Reaction	A*	B	Note
22. $N + NO_2 \rightarrow N_2O + O$	2.1×10^{-11}	-800	1
23. $NO + O \overset{M}{\rightarrow} NO_2$	See Table A-3		3
24. $NO + HO_2 \rightarrow NO_2 + OH$	4.3×10^{-12} 3.4×10^{-12}	200 250	1 2
25. $H_2 + O(^1D) \rightarrow OH + H$	9.9×10^{-11}	0	1
26. $OH + OH \rightarrow H_2O + O$	1.0×10^{-11}	-500	1
27. $N + O_3 \rightarrow NO + O_2$	2.0×10^{-11}	-3000	4
28. $NO_2 + O_3 \rightarrow NO_3 + O_2$	1.2×10^{-13}	-2450	1
29. $OH + OH \overset{M}{\rightarrow} H_2O_2$	See Table A-3		3
30. $H_2O_2 + O \rightarrow OH + HO_2$	2.8×10^{-12}	-2125	1
31. $CO + OH \overset{M}{\rightarrow} H + CO_2$	See Table 3		3
32. $O(^1D) + M \rightarrow O + M$	2.2×10^{-11}	99	5
33. $Cl + O_3 \rightarrow ClO + O_2$	2.8×10^{-11}	-257	1
34. $Cl + NO_2 \overset{M}{\rightarrow} ClNO_2$	See Table A-3		3
35. $ClO + O \rightarrow Cl + O_2$	7.7×10^{-11}	-130	1
36. $NO + ClO \rightarrow NO_2 + Cl$	7.8×10^{-12}	250	1
37. $ClO + NO_2 \overset{M}{\rightarrow} ClONO_2$	See Table A-3		3
38. $HCl + O(^1D) \rightarrow Cl + OH$	1.4×10^{-10}	0	1
39. $OH + HCl \rightarrow H_2O + Cl$	2.8×10^{-12}	-425	1
40. $O + HCl \rightarrow OH + Cl$	1.14×10^{-11}	-3370	1
41. $Cl + HO_2 \rightarrow HCl + O_2$	4.5×10^{-11}	0	1
42. $CFCl_3 + O(^1D) \rightarrow 3Cl$	2.2×10^{-10}	0	1,6
43. $CF_2Cl_2 + O(^1D) \rightarrow 2Cl$	1.4×10^{-10}	0	1,6
44. $Cl + H_2 \rightarrow HCl + H$	3.5×10^{-11}	-2290	1

TABLE A-2. (Continued)

Reaction	A*	B	Note
45. $Cl + H_2O_2 \rightarrow HCl + HO_2$	8.9×10^{-12} 1.7×10^{-12}	-925 -384	11 2
46. $ClONO_2 + O \rightarrow ClO + NO_3$	3.0×10^{-12}	-808	1,10
47. $CH_3Cl + OH \rightarrow Cl + H_2O + HO_2$	2.2×10^{-12}	-1142	1
48. $NO + NO_3 \rightarrow 2NO_2$	2.0×10^{-11} 8.7×10^{-12}	0 0	1 3
49. $NO_2 + O \overset{M}{\rightleftharpoons} NO_3$	See Table A-3		3
50. $NO_2 + NO_3 \overset{M}{\rightleftharpoons} N_2O_5$	See Table A-3		3
51. $N_2O_5 \overset{M}{\rightleftharpoons} NO_2 + NO_3$	See Table A-3		3
52. $N_2O_5 + H_2O \rightarrow 2HNO_3$	1.0×10^{-20}	0	7
53. $O(^1D) + O_3 \rightarrow 2O_2$	1.2×10^{-10}	0	1
54. $HO_2 + HO_2 + H_2O \rightarrow H_2O_2 + O_2 + H_2O$	See Table A-3		3
55. $O + NO_3 \rightarrow O_2 + NO_2$	1.0×10^{-11}	0	1
56. $HO_2 + NO_2 \overset{M}{\rightleftharpoons} HNO_4$	See Table A-3		3
57. $HNO_4 \overset{M}{\rightleftharpoons} HO_2 + NO_2$	See Table A-3		3
58. $OH + HNO_4 \rightarrow H_2O + NO_2 + O_2$	6.0×10^{-12}	-750	1,8
59. $Cl + HNO_4 \rightarrow HCl + NO_2 + O_2$	3.0×10^{-12}	-300	8
60. $HO_2 + ClO \rightarrow O_2 + HOCl$	7.0×10^{-13}	500	1
61. $Cl + HOCl \rightarrow HCl + ClO$	3.0×10^{-12}	-300	8
62. $OH + HOCl \rightarrow H_2O + ClO$	3.0×10^{-12}	-800	1
63. $O + HOCl \rightarrow OH + ClO$	1.0×10^{-11}	-2200	1
64. $OH + CH_4 \rightarrow CH_3 + H_2O$	2.4×10^{-12}	-1710	1
65. $O + CH_4 \rightarrow CH_3 + OH$	3.5×10^{-11}	-4550	1
66. $O(^1D) + CH_4 \rightarrow CH_2O + H_2$	1.0×10^{-11}	0	1
67. $O(^1D) + CH_4 \rightarrow CH_3 + OH$	1.3×10^{-10}	0	1

TABLE A-2. (Continued)

Reaction	A*	B	Note
68. $CH_4 + Cl \rightarrow HCl + CH_3$	9.9×10^{-12}	-1359	1
69. $Cl + CH_3Cl \rightarrow HO_2 + CO + 2HCl$	3.4×10^{-11}	-1256	1,6
70. $CH_3O_2 + NO \rightarrow NO_2 + CH_3O$	7.0×10^{-12} 8.0×10^{-12}	0 0	1 2
71. $Cl + CH_2O \rightarrow HCl + HCO$	9.2×10^{-11}	-68	1
72. $CH_3O_2 + HO_2 \rightarrow CH_3OOH + O_2$	6.0×10^{-12} 1.0×10^{-12}	0 0	1 2
73. $CH_3O + O_2 \rightarrow CH_2O + HO_2$	5.0×10^{-13}	-2000	1
74. $OH + CH_2O \rightarrow H_2O + HCO$	1.0×10^{-11} 1.7×10^{-11}	0 -100	1 2
75. $O + CH_2O \rightarrow HCO + OH$	3.2×10^{-11} 2.8×10^{-11}	-1550 -1540	1,10 2
76. $HCO + O_2 \rightarrow CO + HO_2$	5.0×10^{-12}	0	1
77. $OH + CH_3OOH \rightarrow CH_3O_2 + H_2O$	5.0×10^{-12} 6.2×10^{-12}	-750 -750	1,10 2
78. $CH_3 + O \rightarrow CH_2O + H$	1.0×10^{-10}	0	1
79. $CH_3O_2 + O_3 \rightarrow CH_3O + 2O_2$	1.0×10^{-14}	-600	9
80. $CH_3O_2 + O \rightarrow CH_3O + O_2$	3.0×10^{-11}	0	9
81. $ClO + OH \rightarrow HO_2 + Cl$	9.2×10^{-12} 2.0×10^{-11}	0 0	1 12
82. $CH_3 + O_2 \overset{M}{\Leftrightarrow} CH_3O_2$	See Table A-3		3
83. $ClO + OH \rightarrow HCl + O_2$	Not Used ($\sim10^{-22}$) 2.0×10^{-12}		12
84. $H_2 + OH \rightarrow H_2O + H$	1.2×10^{-11} Not Used	-2200	1
85. $H + HO_2 \rightarrow H_2 + O_2$	4.2×10^{-11} Not Used	-350	1
86. $OH + CH_3OOH \rightarrow CH_2O + H_2O + OH$	5.0×10^{-12} Not Used	-750	1,10

TABLE A-2. (Continued)

Reaction	A*	B	Note
87. $O + HNO_4 \rightarrow OH + NO_2 + O_2$	1.0×10^{12} Not Used	-2200	1,10
88. $OH + ClONO_2 \rightarrow HOCl + NO_3$	1.2×10^{-12} Not Used	-333	1,10
89. $Cl + ClONO_2 \rightarrow 2Cl + NO_3$	1.7×10^{-12} Not Used	-607	1,10
90. $HONO + OH \rightarrow H_2O + NO_2$	6.6×10^{-12} Not Used	0	1
91. $OH + NO \overset{M}{\rightleftharpoons} HONO$	See Table A-3 Not Used		3
92-97. (Not used. Reactions used only in sensitivity studies)			
98. $O + OClO \rightarrow ClO + O_2$	2.5×10^{-11}	-1166	1
99. $NO + OClO \rightarrow NO_2 + ClO$	2.5×10^{-12}	-600	1

NOTES TO TABLE A-2

1. Draft report of NASA Harpers Ferry Workshop.

2. JPL (1979). Where only one entry is given for the rate coefficient 1979a and 1979b are the same. Usually this means references 1 and 2 give the same recommendation.

3. The reaction is pressure dependent. See Table A-3 for discussion.

4. Estimate designed to be compatible with upper limit given in reference 1, and low enough to have no significant effect on model performance. Reaction is retained only to facilitate reintroduction if the evaluated upper limit should prove to be in error.

5. Weighted average of the rates of $O(^1D) + N_2$ and $O(^1D) + O_2$ from references 1 and 2.

6. Product chemistry has been simplified.

7. Estimated reaction rate. This estimate is designed to include a possible heterogeneous contribution to the overall reaction. Important only in the lower troposphere.

NOTES TO TABLE A-2 (Continued)

8. Estimated reaction rate. This rate is estimated based on the assumption that HNO_4 and HOCl resemble H_2O_2 (as treated in JPL, 1979) in reactions with Cl and OH.

9. Estimated reaction rate. Rate is estimated based on the assumption that CH_3O_2 closely resembles HO_2 in reaction with O or O_3.

10. Products are not given in references 1 or 2. The assumed products are based on the products that seem most plausible based on chemical considerations.

11. Rate based on a draft of reference 1 that trivially differs from the final draft.

12. 1979a chemistry treated the reactions of HO and ClO based on privately communicated qualitative preliminary results. The treatment is nearly an upper limit to the plausible rate coefficients based on the recent results of Leu and Lin (1979).

(June, 1979). It has a few comparatively minor differences from the final draft of that report, and it includes a few reactions not assessed at the NASA Workshop.

Two reactions treated in the 1979a chemistry are controversial and are of some importance to our sensitivity studies. These are

$$ClO + NO_2 \overset{M}{\rightarrow} ClONO_2$$

and

$$ClO + OH \rightarrow HCl + O_2$$

In the 1979a chemistry, we used the slower of the two JPL-recommended rate constants for chlorine nitrate formation, and we adopted an expression for HCl formation from OH + ClO that is about half the upper limit for that reaction path. In the 1979b chemistry, we used the faster of the two recommendations for the chlorine nitrate formation rate coefficient. Three considerations inspired this choice: (1) the majority of the chemistry panel seemed to favor the faster expression, (2) even if the bulk of the reaction between ClO and NO_2 leads to other products (as suggested by those favoring the slower rate coefficient), the other products might easily have an effect on stratospheric chemistry similar to that of $ClONO_2$, and (3) it improved the comparison between calculation and observation for both ClO and $ClONO_2$.

TABLE A-3. Rate coefficients used for pressure-dependent reactions.

Expression 1

$$k = \frac{A_o[M](300/T)^{n_o}}{1 + A_o[M](300/T)^{n_o}/A_i(300/T)^{n_i}} \; .06^{\left\{1 + \left[\log_{10}\left(\frac{A_o[M](300/T)^{n_o}}{A_i(300/T)^{n_i}}\right)\right]^2\right\}^{-1}}$$

Reaction	A_o *	n_o	A_i	n_i	Note
$HO_2 + NO_2 \xrightarrow{M} HNO_4$	2.1×10^{-31}	5.0	6.5×10^{-12}	5.0	1
$OH + NO_2 \xrightarrow{M} HNO_3$	2.6×10^{-30}	2.9	2.4×10^{-11}	1.3	1
$ClO + NO_2 \xrightarrow{M} ClONO_2$	1.6×10^{-31}	3.4	1.5×10^{-11}	1.9	1,2
	3.5×10^{-32}	3.8	1.5×10^{-11}	1.9	1,2
$O + O_2 \xrightarrow{M} O_3$	6.2×10^{-34}	2.1		0	1
$CH_3 + O_2 \xrightarrow{M} CH_3O_2$	2.2×10^{-31}	2.2	2.0×10^{-12}	1.7	1
$O(^1D) + N_2 \xrightarrow{M} N_2O$	3.5×10^{-37}	0.45		0	1
$Cl + NO_2 \xrightarrow{M} ClNO_2$	1.6×10^{-30}	1.9	3.0×10^{-11}	1.0	1
$H + O_2 \xrightarrow{M} HO_2$	5.5×10^{-32}	1.4		0	1
$OH + NO \xrightarrow{M} HNO_2$	6.7×10^{-31}	3.3	3.0×10^{-11}	1.0	1
$OH + OH \xrightarrow{M} H_2O_2$	2.5×10^{-31}	0.8	3.0×10^{-11}	1.0	1
$NO_2 + NO_3 \xrightarrow{M} N_2O_5$	1.4×10^{-30}	2.8	9.0×10^{-13}	-0.7	1
	$1.8\times10^{-32}e^{+1316/T}$	0	$9.5\times10^{-13}e^{+58/T}$	0	3

*When two entries are given, the lower one corresponds to 1979a chemistry and the upper one corresponds to 1979b chemistry.

TABLE A-3. Continued

Reaction	A_o *	n_o	A_i	n_i	Notes
$O + NO \overset{M}{\rightarrow} NO_2$	1.2×10^{-31}	1.8	3.0×10^{-11}	-0.3	1
	$1.6 \times 10^{-32} e^{+584/T}$	0			4
$O + NO_2 \overset{M}{\rightarrow} NO_3$	9.0×10^{-32}	2.0	2.2×10^{-11}	0	1
	1.0×10^{-31}	0		0	4
$N_2O_5 \overset{M}{\rightarrow} NO_2 + NO_3$	$1.18 \times 10^{-3} e^{-11180/T}$	2.8	$7.52 \times 10^{+14} e^{-11180/T}$	-0.7	5
	$1.6 \times 10^{-5} e^{-9864/T}$	0	$7.94 \times 10^{14} e^{-11122}$	0	4
$HNO_4 \overset{M}{\rightarrow} HO_2 + NO_2$	$k = \dfrac{5.2 \times 10^{-6} e^{-10015/T}}{1 + 4.86 \times 10^{-12} M^{0.61}}$				7
$OH + CO \overset{M}{\rightarrow} H + CO_2$	$k = 1.35 \times 10^{-13} \left(1 + \dfrac{M}{2.46 \times 10^{+19}}\right)$				1
$HO_2 + HO_2 + H_2O \rightarrow H_2O_2 + H_2O + O_2$	$k = \dfrac{1.1 \times 10^{-34} e^{+3730/T}}{1 + M * 3.5 \times 10^{-16} e^{-2060/T}}$				6

NOTES TO TABLE A-3

1. Expression given in NASA (1979). 1979a chemistry differed from 1979b chemistry in that the parameter 0.6 in expression 1 was set equal to 0.8 in the expression used for 1979a chemistry

2. Both expressions are recommended with no clear preference. The lower value is used in the 1979a chemistry and the upper one is used in the 1979b chemistry.

3. Private communication, D. Golden, SRI International, Inc. (1979).

4. Based on data in NBS 513 (1978).

5. Based on data in reference 1 and the equilibrium constant from NBS 513 (1978).

6. Based on Cox (1978).

7. Based on Graham et al. (1978).

In our 1979b chemistry we omitted the reaction forming HCl from OH + ClO. The decision to include this reaction in the 1979a chemistry was based on privately communicated preliminary results that seemed to suggest that the reaction probably occurred, but they have since been interpreted as providing only an upper limit. Both of these controversial choices of rate coefficient have a significant impact on model sensitivities (especially for ClX) but they oppose each other. As a result, 1979a and 1979b chemistries yield qualitatively similar perturbational sensitivities for both NO_x and ClX perturbations. The 1979b chemistry is less controversial than the 1979a chemistry and is to be preferred for purposes of comparison with other workers. All primary assessments have been repeated using 1979b chemistry. However, several sensitivity studies were not repeated, since it seemed unlikely that the qualitative results of those sensitivity studies would differ if they were repeated, and because the 1979a chemistry is well within the limits of reasonable uncertainty in our present knowledge of the atmosphere. The two chemistries are also useful in emphasizing the existance of processes for which no clear recommendation is available.

Our treatment of photolysis reactions has also been modified. There is evidence for a moderate temperature dependence in many photoabsorption cross sections. With the exception of ozone, NO, and O_2 photolysis, we have not treated this temperature dependence explicitly, but have used cross sections

TABLE A-4. Photolysis reactions. Alternative products of reaction are shown in parentheses, but they were not used in either the 1979a or 1979b chemistry.

	Reaction	Note
1.	$O_2 \rightarrow 2O$	1,2
2.	$O_3 \rightarrow O + O_2$	1,3
3.	$O_3 \rightarrow O(^1D) + O_2$	1,3
4.	$NO_2 \rightarrow NO + O$	1,4
5.	$N_2O \rightarrow N_2 + O(^1D)$	4
6.	$NO \rightarrow N + O$	5
7.	$HNO_3 \rightarrow OH + NO_2$	4
8.	$H_2O_2 \rightarrow 2OH$	4
9.	$HO_2 \rightarrow OH + O$	4
10.	$ClONO_2 \rightarrow Cl + NO_3$ ($ClO + NO_2$)	4,6
11.	$HCl \rightarrow H + Cl$	4
12.	$ClO \rightarrow Cl + O$	7
13.	$ClO \rightarrow Cl + O(^1D)$	Not used
14.	$ClNO_2 \rightarrow Cl + NO_2$	4
15.	$OClO \rightarrow ClO + O$	7
16.	$CF_2Cl_2 \rightarrow 2Cl$	4,8
17.	$CFCl_3 \rightarrow 3Cl$	4,8
18.	$CCl_4 \rightarrow 4Cl$	4,8
19.	$N_2O_5 \rightarrow NO_3 + NO_2$ ($2NO_2 + O$)	4,6
20.	$NO_3 \rightarrow NO + O_2$	4
21.	$NO_3 \rightarrow NO_2 + O$	4
22.	$H_2O \rightarrow H + OH$	9
23.	$HNO_4 \rightarrow HO + NO_3$ ($HO_2 + NO_2$)	10,6
24.	$HOCl \rightarrow OH + Cl$	4
25.	$CH_3OOH \rightarrow CH_3O + OH$	4
26.	$CH_2O \rightarrow HCO + H$	11
27.	$CH_2O \rightarrow CO + H_2$	11
28.	$CH_3Cl \rightarrow CH_3 + Cl$	4
29.	$HONO \rightarrow OH + NO$	4

NOTES FOR TABLE A-4.

1. Contributes to the optical depth of the model atmosphere.

2. The Schumann-Runge bands are given a special treatment based on Hudson and Mahle (1972).

3. The quantum yields of reactions 2 and 3 are given a special treatment based on the temperature dependent treatment of JPL (1979).

4. Based on the data of JPL (1979). Where data for several temperatures is given, we have used the data at $\sim$230 K.

5. Nitric oxide photolysis is based on the treatment of Frederick and Hudson (1979). We have used the photolysis rates averaged over the sunlit hemisphere for day time photolysis rates. 1979a chemistry used the treatment of Cieslik and Nicolet (1973).

6. The products used for XNO_3 (X = Cl, OH, NO_2) changed between our 1979a and 1979b chemistries. For 1979a they were based on the path of lowest endoergicity (except for N_2O_5 which was based on a recommendation of Johnston). For 1979b they are all based on analogy with $ClONO_2$ data of Chang et al. (1979). This treatment is highly uncertain.

7. Based on data in Watson (1974).

8. Product chemistry has been simplified.

9. Treatment based on Thompson et al. (1963).

10. Treatment based on Graham et al. (1978).

11. Treatment based on quantum yields of Moortgat and Warneck (1979) and cross sections of McQuigg and Calvert (1969).

---

measured at roughly 230 K for all temperatures. As a result our calculated trace species photodissociation rates should be more accurate for the stratosphere than for the lower troposphere.

For ozone photolysis we use quantum yields based on the recommendations of NASA (1979). Our treatment of O_2 photolysis is based on Hudson and Mahle (1972) while our treatment of NO photolysis is based on Frederick and Hudson (1979).

BOUNDARY CONDITIONS

The model now allows for either fixed concentrations or a flux condition at the surface as a lower boundary condition. For most of the calculations in this study, six species were assumed to have fixed concentrations (See Table A-5), while a surface flux was assigned to the other species. Zero flux was assumed except for those species shown in Table A-5. When those species with fixed boundary conditions in Table A-5 were given flux boundaries, a flux was determined to give an ambient concentration the same as those in Table A-5.

Zero flux was assumed for all species except NO and NO_2 at the upper boundary. NO and NO_2 are assumed to have a very small flux from the mesosphere into the stratosphere.

Water vapor concentrations are fixed in the troposphere and calculated in the stratosphere. All runs are made with fixed boundary conditions unless otherwise noted.

TABLE A-5. Boundary conditions.

Fixed Concentrations (molecules cm^{-3})	
N_2O	8.25×10^{12}
CH_4	4.03×10^{13}
H_2	1.42×10^{13}
CH_3Cl	1.56×10^{10}
H_2O	4.30×10^{17}
CO	3.04×20^{12}
Surface Flux (molecules cm^{-2} s^{-1})	
NO	3.41×10^{9}
NO_2	6.59×10^{9}
HNO_3	1.67×10^{9}
HCl	3.67×10^{10}
CCl_4	1.40×10^{6}
CF_2Cl_2	function of time
$CFCl_3$	and scenario
CH_3CCl_3	(see Section 5)

SOURCES AND SINKS

In addition to sources and sinks from the chemistry and boundary conditions described above, there are additional sinks due to dry and/or wet removal for many species in the model. A source for nitric oxide from cosmic ray dissociation of N_2 is also included based on the results of Nicolet (1974).

Wet removal processes are parameterized by a first-order loss rate. The wet removal of the trace species HNO_3, H_2O_2, HCl, ClO, $ClONO_2$, $ClNO_2$, HNO_4, HOCl, CH_2O and CH_3OOH is assumed to vary with altitude as shown in Table A-6. NO_2 is assumed to have a loss rate half the above rate.

Dry deposition rates at the surface are also parameterized by a first-order loss rate as shown in Table A-7.

TABLE A-6. Wet removal parameterization

Altitude, km	Loss Rate, sec^{-1}
0	3.86×10^{-6}
1	3.86×10^{-6}
2	3.86×10^{-6}
3	3.86×10^{-6}
4	3.86×10^{-6}
5	3.86×10^{-6}
6	1.93×10^{-6}
7	1.93×10^{-7}
8	9.58×10^{-7}
9	4.78×10^{-7}
10	0

TABLE A-7. Deposition rates in the lowest layer (z = 0).

Species	Loss Rate (sec^{-1})	Species	Loss Rate (sec^{-1})
$O(^3P)$	2.0×10^{-5}	NO_3	2.0×10^{-5}
O_3	1.0×10^{-5}	N_2O_5	2.0×10^{-5}
NO	1.0×10^{-6}	H_2O	0
NO_2	3.0×10^{-6}	HNO_4	2.0×10^{-5}
N_2O	0	HOCl	2.0×10^{-5}
HNO_3	2.0×10^{-5}	HCO	2.0×10^{-5}
OH	2.0×10^{-5}	CH_2O	1.0×10^{-5}
HO_2	2.0×10^{-5}	CH_3	2.0×10^{-5}
H_2O_2	2.0×10^{-5}	CH_3OOH	2.0×10^{-5}
Cl	2.0×10^{-5}	CH_3O	2.0×10^{-5}
$ClONO_2$	2.0×10^{-5}	CH_3O_2	2.0×10^{-5}
ClO	2.0×10^{-5}	CO	5.0×10^{-7}
CH_4	0	ClO_3	2.0×10^{-5}
H_2	1.0×10^{-7}	OClO	2.0×10^{-5}
CH_3Cl	0	HONO	2.0×10^{-5}
$ClNO_2$	2.0×10^{-5}	$CFCl_3$	0
HCl	2.0×10^{-5}	CF_2Cl_2	0
CCl_4	0	CH_3CCl_3	0

MULTIPLE SCATTERING

In order to accurately compute photodissociation rates, it is important to describe radiative processes, such as multiple scattering, in addition to attenuation by gases such as O_2, O_3 and NO_2. The importance of molecular scattering varies significantly with wavelength over the spectral range 200-750 nm. At shorter wavelengths gaseous absorption dominates and very little solar flux reaches the lower atmosphere. The region 290-330 nm is a transition region where molecular scattering is very important, especially at the longer wavelengths in this interval.

Beyond 330 nm, surface reflection is very important since the atmosphere is nearly transparent in this spectral region.

Multiple scattering is included in the model using a simplified method that is computationally fast so that it can be used for diurnal calculations. The method is similar to that of Isaksen et al. (1977) in terms of the numerical method but quite different in terms of the physical assumptions. The atmosphere is divided into optically thin layers and each layer can absorb and scatter radiation. The layer is assumed to scatter radiation isotropically with half of the scattered flux going upward and the other half downward at an average zenith angle of $\pm\overline{\theta}$. The earth's surface is also assumed to scatter isotropically, and a surface albedo of 0.25 is used to approximate the effect of clouds on the upward scattered radiation. Using a high surface albedo and no clouds gives results that are nearly identical to those from dividing the atmosphere into clear and cloudy regimes and averaging the results (the exception being the region below the cloud layer, which is not important for the model applications considered here). For each atmospheric layer there is a contribution to the solar flux density from the direct flux and by the diffuse fluxes incident on the layer from above and from below. The flux density due to the various fluxes together can be much greater (depending on the wavelength and altitude) than the flux density computed considering only gaseous absorption (Luther and Gelinas, 1976; Luther and Wuebbles, 1976).

TEMPERATURE FEEDBACK

The temperature profile above 13 km is calculated using a stratospheric radiative transfer model, and the temperature profile is specified at lower altitudes. The model includes solar absorption and long-wave interaction by O_3, H_2O, and CO_2, along with solar absorption by NO_2. The techniques adopted for treating long-wave radiative transfer are the same as those described by Ramanathan (1974). This formulation was chosen because it is computationally efficient, and its accuracy has been demonstrated (Ramanathan, 1974, 1976) by comparison with much more complex models. The effects of and justification for the simplifying assumptions used in the model are discussed by Ramanathan (1976).

A band absorptance formulation is used to treat the 9.6-μm band of O_3 and the fundamental and several hot and isotopic bands of CO_2 in the 15-μm region. An emissivity formulation is used to treat long-wave radiative transfer by H_2O. Solar absorption by O_3 is treated by using the empirical formulation given by Lindzen and Will (1973). The band absorptance formulation by Houghton (1963) is adopted for solar absorption by H_2O, and the band absorptance formulation by Ramanathan and Cess (1974) is adopted for solar absorption by CO_2. The empirical formulation of Luther (1976) is used for solar absorption by NO_2. Solar absorption by O_3 and NO_2 are treated independently because absorption by these species is weak in the region where their absorption bands overlap. Solar radiation scattered from the troposphere is included by assuming an albedo of 0.3. Doppler broadening effects are included for CO_2 and O_3 as described in Appendix B of Ramanathan (1976). The temperature dependences of the band absorptance and band intensity are included in the longwave calculations of CO_2 and O_3.

A single cloud layer is included at 6.5 km with 42% cloud cover as was suggested by Cess (1974). The lapse rate within the troposphere is assumed to be -6.5 K/km, and the temperature at the earth's surface is specified to be 288 K.

NUMERICAL METHOD

Each of the 39 species in the model has its concentration calculated at each of 44 vertical levels extending from the surface to 55 km. The numerical technique used to solve the set of over 2000 differential equations (resulting from a continuity equation for each species at each grid level) is the method described by Chang et al. (1974). The main advantage of this method, which is a variable order, multistep, implicit method, is its ability to solve sets of mathematically stiff differential equations for almost any set of input parameters, initial and boundary conditions, in particular those resulting from the chemical kinetics system described in Table A-2.

THE DIURNAL AND DIURNAL-AVERAGED MODELS

We have developed a fully diurnal-averaged model that is consistent with our diurnal model. The diurnal model is used to generate species profiles for comparison with measurements and for perturbation studies involving short time integrations (e.g., solar eclipse effects). The diurnal-averaged model is used for perturbation and sensitivity studies involving longer time integrations.

The procedure that is used in developing the fully diurnal-averaged model is also applicable to two-dimensional models. If the continuity equation is averaged over a time period (24 hours in our case) that is very small compared to the time scale of the problem of interest, then one obtains averaged terms of the form $\overline{k_{ij}c_ic_j}$ and $\overline{J_ic_i}$ where c_i is the concentration of species i at time t and altitude z, k_{ij} is the two-body chemical rate coefficient, and J_i is the photodissociation rate coefficient for species i.

We define the diurnal weighting factors $\alpha_{ij}(z)$ and $\beta_i(z)$ by

$$\overline{k_{ij}\, c_i\, c_j} = \alpha_{ij}\, \overline{k_{ij}}\, \overline{c_i}\, \overline{c_j}$$

and

$$\overline{J_i\, c_i} = \beta_i\, \overline{J_i}\, \overline{c_i} \quad .$$

Since k_{ij} is defined and is independent of time, we have

$$\alpha_{ij} = \overline{c_i\, c_j} \;/\; \overline{c_i}\, \overline{c_j}$$

and

$$\beta_i = \overline{J_i\, c_i} \;/\; \overline{J_i}\, \overline{c_i} \quad .$$

The computation of photodissociation rates can be an expensive part of stratospheric model calculations, hence evaluation of $\overline{J_i}$'s in the diurnal-averaged model can be expensive. If we define β_i by

$$\beta_i = \overline{J_i c_i} \; / \; (J_i^{noon} \overline{c_i}) \quad ,$$

then the computation in the diurnal-averaged model is greatly simplified. The diurnal model is used to determine $\overline{c_i c_j}$, $\overline{J_i c_i}$, $\overline{c_i}$, $\overline{c_j}$, and J_i^{noon} so that α_{ij} and β_i can be obtained for every chemical and photochemical reaction in the model.

REFERENCES

Cess, R. D., "Radiative Transfer Due to Atmospheric Water Vapor: Global Considerations of the Earth's Energy Balance," J. Quant. Spectrosc. Radiat. Transfer, 14, 861-871, 1974.

Chang, J. S., J. R. Barker, J. E. Davenport, and D. M. Golden, "Chlorine Nitrate Photolysis by a New Technique: Very Low Pressure Photolysis," Chem. Phys. Lett., 60, 385-390, 1979.

Chang, J. S., A. C. Hindmarsh, and N. K. Madsen, "Simulation of Chemical Kinetics Transport in the Stratosphere in Stiff Differential Systems," edited by R. A. Willoughby, Plenum Publishing Corp., New York, p. 51 ff, 1974.

Cieslik, S. and M. Nicolet, "The Aeronomic Dissociation of Nitric Oxide," Planet. Space Sci., 21, 925-938, 1973.

Cox, R. A., "Kinetics of HO_2 Radical Reactions of Atmospheric Interest," Papers Presented at the WMO Symposium on the Geophysical Aspects and Consequences of Change in the Composition of the Stratosphere, Toronto, 26-30 June 1978, WMO No. 511, 1978.

Frederick, J. E. and R. D. Hudson, "Predissociation of Nitric Oxide in the Mesosphere and Stratosphere," J. Atmos. Sci., 36, 737-745, 1979.

Graham, R. A., A. M. Winer and J. N. Pitts, Jr., "Pressure and Temperature Dependance of the Unimolecular Decomposition of NO_2NO_2," J. Chem. Phys., 68, 4505-4510, 1978.

Houghton, J. T., "The Absorption of Solar Infrared Radiation by the Lower Stratosphere," Quart. J. Roy. Meteorol. Soc., 89, 319-331, 1963.

Hudson, R. D. and S. H. Mahle, "Photodissociation Rates of Molecular Oxygen in the Mesosphere and Lower Thermosphere," J. Geophys. Res., 77, 2902-2914, 1972.

Isaksen, I. S. A., K. M. Midtbo, J. Sunde, and P. J. Crutzen, "A Simplified Method to Include Molecular Multiple Scattering and Reflection in Calculations of Photon Fluxes and Photodissociation Rates," Geophysica Norwegica, 31, 11-26, 1977.

JPL Publication 79-27, "Chemical Kinetic and Photochemical Data for Use in Stratospheric Modeling," NASA Panel for Data Evaluation, 1979.

Leu, M. T. and C. L. Lin, "Rate Constants for the Reactions of OH with ClO, Cl_2, and Cl_2O at 298 K," Geophys. Res. Letters, 6, 425-428, 1979.

Lindzen, R. S. and D. I. Will, "An Analytical Formula for Heating Due to Ozone Absorption," J. Atmos. Sci., 30, 513-515, 1973.

Luther, F. M., "A Parameterization of Solar Absorption by Nitrogen Dioxide," J. Appl. Meteorol., 15, 479-481, 1976.

Luther, F. M. and R. J. Gelinas, "Effect of Molecular Multiple Scattering and Surface Albedo on Atmospheric Photodissociation Rates," J. Geophys. Res., 81, 1125-1132, 1976.

Luther, F. M. and D. J. Wuebbles, "Photodissociation Rate Calculations," Report UCRL-78911, Lawrence Livermore Laboratory, Livermore, CA, 1976.

McQuigg, R. D. and J. G. Calvert, "The Photodecomposition of CH_2O, CD_2O, CHDO, and CH_2O-CD_2O Mixtures at Xenon Flash Lamp Intensities," J. Am. Chem. Soc., 91, 1590-1599, 1969.

Moortgat, G. K. and P. Warneck, "CO_2 and H_2 Quantum Yields in the Photodecomposition of Formaldehyde in Air," J. Chem. Phys., 70, 3639-3651, 1979.

NAS, "Halocarbons: Effects on Stratospheric Ozone," U. S. National Academy of Sciences, Washington, D. C., 1976.

NASA Reference Publication (draft), "The Stratosphere: Present and Future," R. D. Hudson (ed.), prepared at the NASA Workshop, Harpers Ferry, Pennsylvania, June 1979.

NBS Special Publication 513, "Reaction Rate and Photochemical Data for Atmospheric Chemistry — 1977," R. F. Hampson, Jr. and D. Garvin (eds.), National Bureau of Standards, Washington, D. C., 1978.

Nicolet, M., "On the Production of Nitric Oxide by Cosmic Rays in the Mesosphere and Stratosphere," Aeronomica Acta-A, No. 134, Institut D'Aeronomie Spatiale de Belgique, Brussels, 1974.

Ramanathan, V., "A Simplified Stratospheric Radiative Transfer Model: Theoretical Estimates of the Thermal Sctructure of the Basic and Perturbed Stratosphere," paper presented at the Second International Conference on the Environmental Impact of Aerospace Operations in the High Atmosphere, American Meteorological Society/American Institute of Aeronautics and Astronautics, San Diego, Calif., July 8-10, 1974.

Ramanathan, V., "Radiative Transfer Within the Earth's Troposphere and Stratosphere: A Simplified Radiative-Convective Model," J. Atmos. Sci., 33, 1330-1346, 1976.

Ramanathan, V. and R. D. Cess, "Radiative Transfer Within the Mesospheres of Venus and Mars," Astrophys. J., 188, 407-416, 1974.

Thompson, B. A., P. Harteck and R. R. Reeves, Jr., "Ultraviolet Absorption Coefficients of CO_2, CO, O_2, H_2O, N_2O, NH_3, NO, SO_2, and CH_4 between 1850 and 4000 A," J. Geophys. Res., 68, 6431-6436, 1963.

Watson, R. T., "Chemical Kinetics Data Survey VIII. Rate Constants of ClO_x of Atmospheric Interest," NBSIR 74-516, National Bureau of Standards, 1974.

APPENDIX B. EFFECT OF CHANGES IN OZONE ON UV DOSE AND SKIN CANCER INCIDENCE

Because reductions in total ozone would permit greater amounts of UV radiation to reach the surface of the earth (Cutchis, 1974, 1978; Halpern et al., 1974), a number of studies have been performed with the goal of assessing biological sensitivity to ozone-induced changes in UV radiation (National Research Council, 1973). one approach has been to correlate skin cancer incidence data directly with ozone layer thickness. The possible influence of such factors as duration of sunlight, clothing and exposure habits, and optical path length have been considered (McDonald, 1971; van der Leun and Daniels, 1975). Another approach has been to explicitly consider the dose of UV radiation received as a function of ozone amount and other climatic variables (Green and Mo, 1975). The radiation dose is then related to cancer incidence after weighting by a wavelength-dependent function accounting for variation in radiation efficacy. Both of these approaches are discussed in this section.

OZONE REDUCTIONS AND UV DOSE*

Green and coworkers developed a semi-empirical model for calculating UV radiation at the surface of the earth in the spectral region 280-340 nm (Green et al., 1974a,b; Mo and Green, 1974). They have calculated erythema (sunburn) dose as a function of total ozone, solar zenith angle, latitude, season, and cloud amount. Their model was also used in the Climatic Impact Assessment Program's analysis of ozone depletion (Green et al., 1975).

One feature of this model, and UV dosimetry in general, is that the receiver is assumed to be horizontal. The geometry of humans, however, is such that the majority of exposed skin would normally be in a nonhorizontal position. In fact, the horizontal projection of an upright person amounts to only a few percent of total surface area (Fanger, 1970).

*See Burt and Luther (1979).

The report of the National Research Council (1976a) summarizes the specific sites of origin of primary melanoma skin cancer. The data show the predominant localization of sites of origin to areas of the skin that are constantly exposed, such as the trunk and legs of males. These are, in general non-horizontal surfaces, which suggests that receiver orientation should be considered in the study of UV dose. We have extended earlier studies of erythema dose to include the effect of receiver orientation (Burt and Luther, 1979).

Using a modification of the Green model, we calculated the instantaneous erythema dose for different times of day, date, latitude, ozone amount and receiver position. In analyzing the effects of receiver orientation, we numerically integrated over wavelength and time to produce daily erythema doses for Northern Hemisphere latitudes assuming the receiver is stationary. Integrations were performed for the 15th day of each month using a time step of approximately 20 minutes. The total ozone was specified as a function of latitude based on data from the Nimbus III satellite reported by Lovill (1972).

The azimuth of the receiver was specified in two ways. First, to obtain a measure of the upper bound on erythema dose at middle latitudes in the Northern Hemisphere, the receiver was held fixed in a south-facing position. Second, to estimate the average dose for a population where there is random orientation (i.e., no preferred orientation), calculations were made while averaging over azimuth angle (a rotated receiver). Doses were computed at 20° intervals in the azimuth angle, and the average of these was used for integration. The inclination angle was held fixed at values of 0, 45, and 90 degrees. α is the angle of the receiver relative to horizontal. For a horizontal receiver, $\alpha = 0$.

Figure B-1 shows the daily erythema dose averaged over a year for a south-facing surface assuming cloudless conditions. In middle latitudes the daily average erythema dose on a surface with $\alpha = 45^{\circ}$ ranges from 90 to 96% of the dose on a horizontal surface. The dose is significantly less for inclination angles greater than 45°.

Figure B-2 shows the daily erythema dose averaged over a year for a rotated surface. In this case the daily average erythema dose in middle latitudes on a surface with $\alpha = 45^{\circ}$ is approximately 83% of the dose on a horizontal surface. At higher latitudes the dose on the rotated surface is significantly less than that on the south-facing surface.

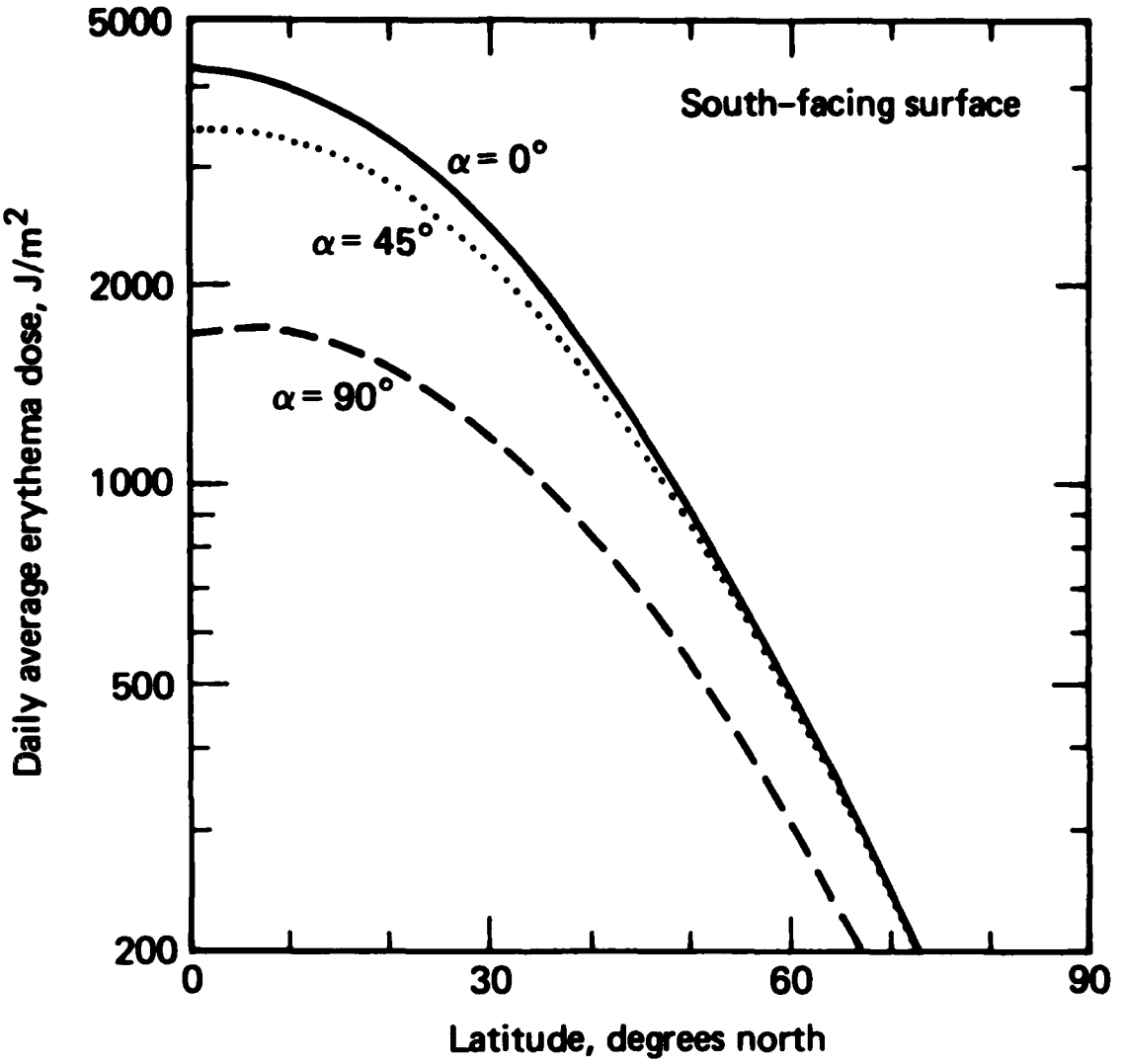

FIGURE B-1. Daily erythema dose averaged over a year for a southfacing surface.

A semilog scale is used in Figs. B-1 and B-2 to demonstrate the effect of inclination angle on the doubling distance for erythema dose. In middle latitudes the computed erythema dose on a horizontal surface doubles over 16° of latitude moving toward the equator. The angle of inclination has very little effect on the doubling distance as evidenced by the similar slopes of the curves in Figs. B-1 and B-2.

The computed doubling distance is consistent with measurements of annual-average erythema dose (Urbach and Davies, 1975), but it differs from the doubling distance for the incidence of skin cancer. Data on the incidences of skin

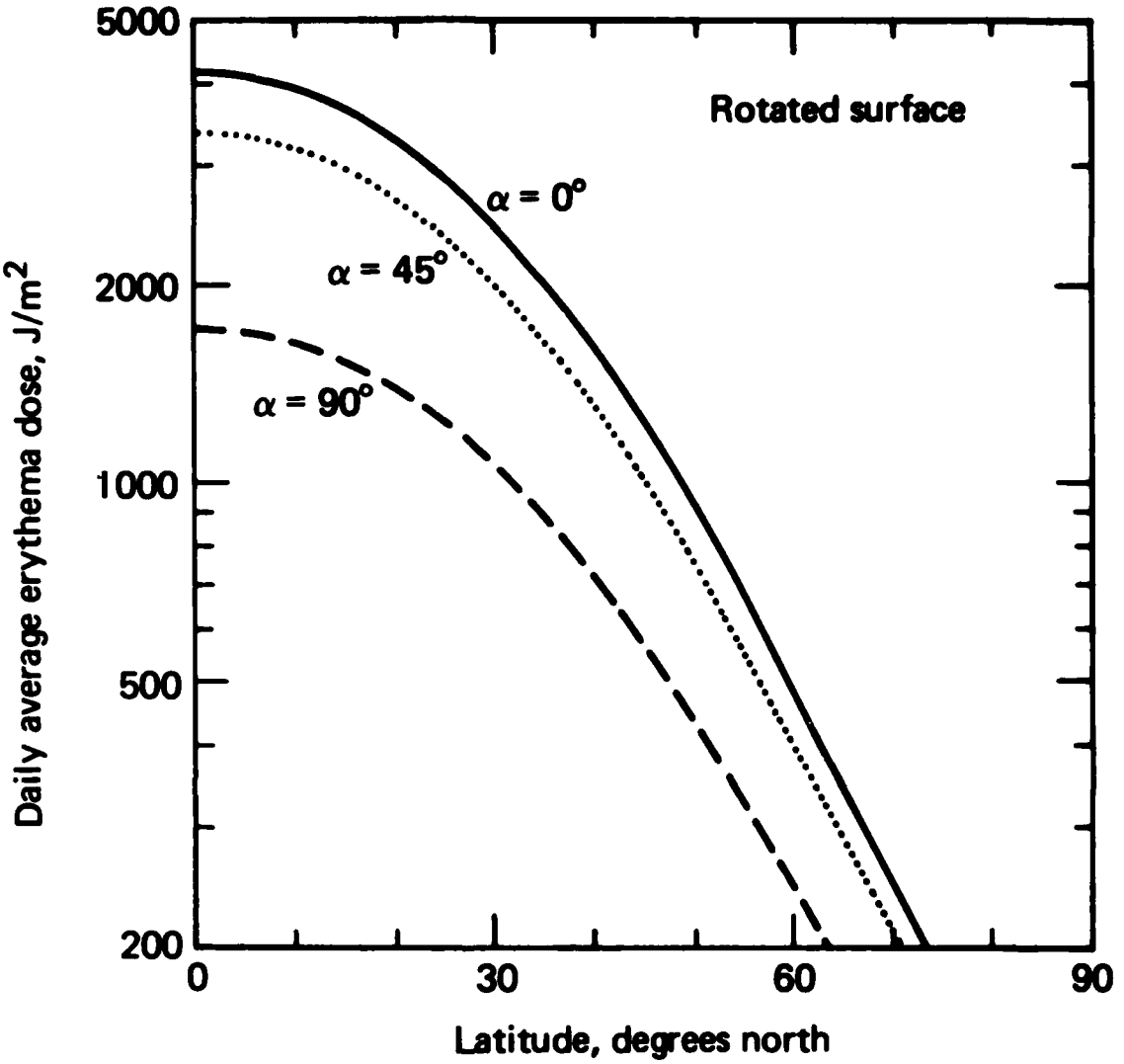

FIGURE B-2. Daily erythema dose averaged over a year for a rotated surface.

cancer in middle latitudes show a doubling over 8 to 12° of latitude (National Research Council, 1976b). Consequently, predicting the effect of a reduction in total ozone on the skin cancer incidence rate is more complex than just assessing the change in erythema dose and scaling proportionately.

The effect of a reduction in total ozone of 10% on the annual-average daily erythema dose for a rotated surface is shown in Fig. B-3. The results were almost identical for the south-facing surface. The amplification factor on erythema dose (Δ dose/ΔO_3) varies from 1.3 to 1.4 at low latitudes, from 1.6 to 2.0 at middle latitudes, and is approximately 3 at high latitudes. It is a property of atmospheric

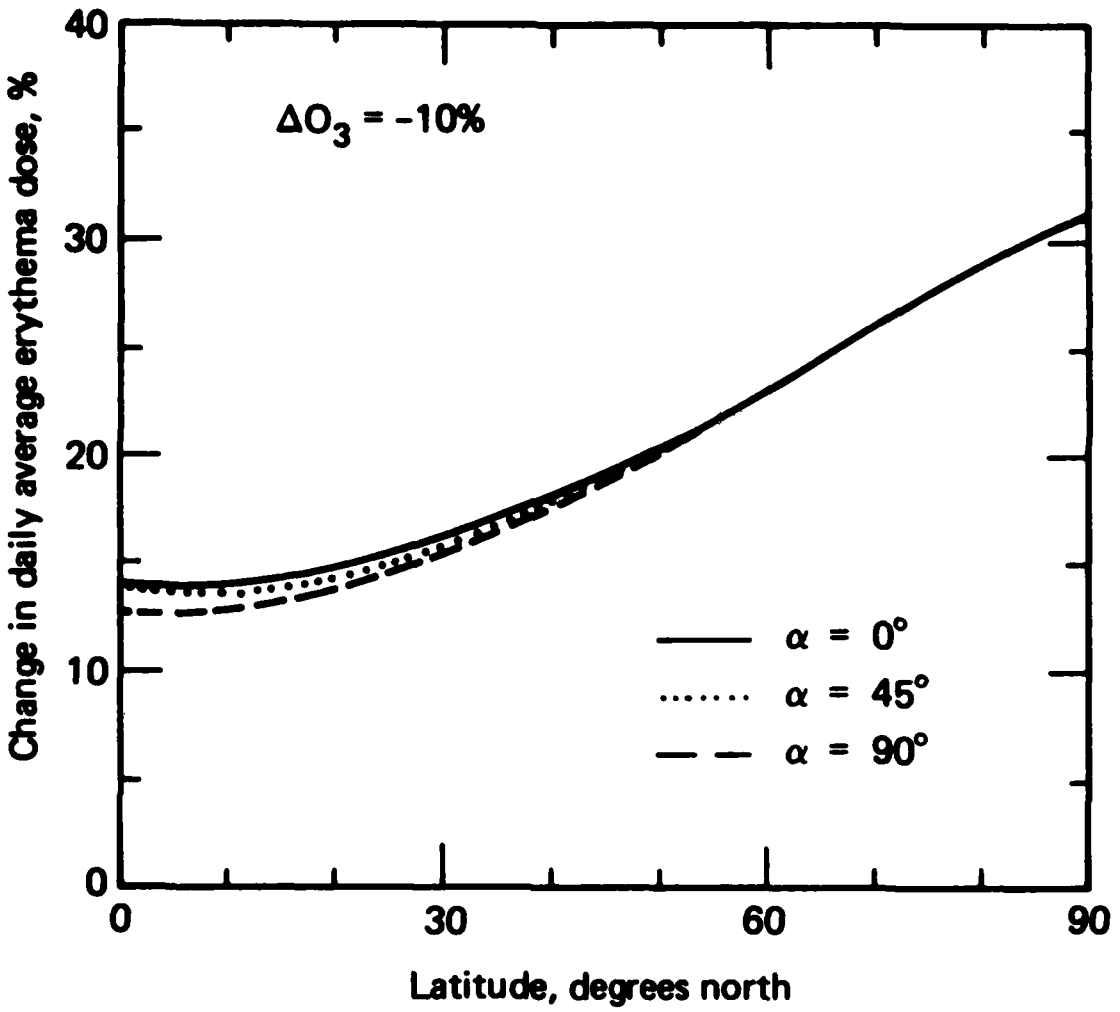

FIGURE B-3. The percent change in daily erythema dose for a rotated surface averaged over a year as a result of a 10% reduction in ozone.

transmission that a 10% reduction in the ozone column causes the greatest percent change in transmission for the largest optical depth. Because the ozone column and solar zenith angle both increase with latitude, the amplification factor is largest at high latitudes. While the percent increase in daily erythema dose at high latitudes is much greater, the total amount of radiation is very small compared to lower latitudes. Since the majority of the world's population lives south of 55°N, amplification factors in the range 1.3 to 2.0 are most realistic.

Reducing the ozone column increases both the direct and diffuse flux components, but by different factors. Since the relative contribution of the direct

and diffuse flux components to erythema dose depends upon α, the amplification factor also depends upon α. This dependence is lessened at high latitudes where the flux is almost entirely diffuse.

Figure B-4 shows the distance moved south that is equivalent to a 10% reduction in ozone based on the annual average data for a rotated surface shown in Fig. B-2. The shaded area indicates the range of values as α is varied from 0 to 90^{o}. In middle latitudes the increase in daily average erythema dose due to a 10% ozone reduction is roughly equivalent to moving south a distance of 350 to 450 km with no ozone perturbation. The equivalent distance is much greater at latitudes

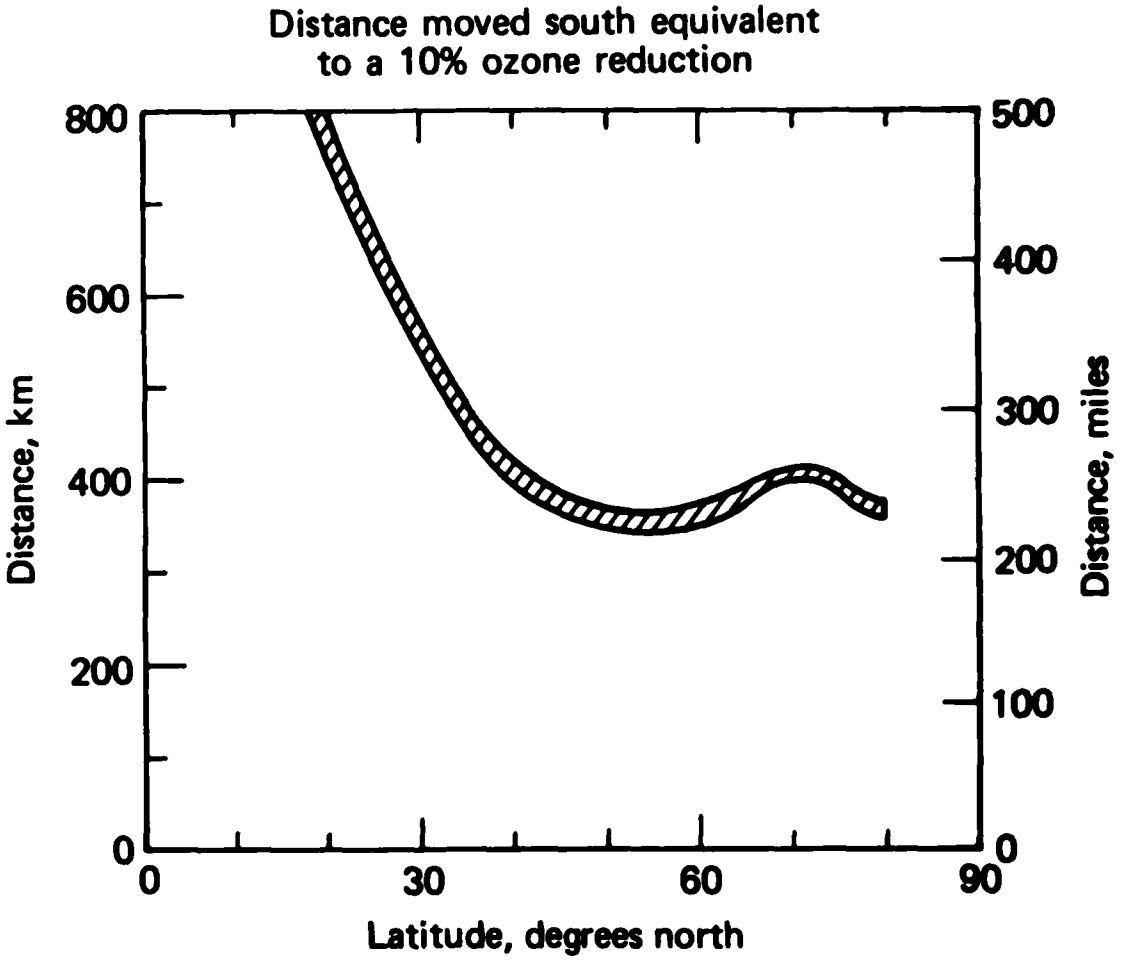

FIGURE B-4. The distance moved south equivalent to a 10% ozone reduction computed for a rotated surface. The shaded area indicates the range of values as the inclination angle is varied from 0 to 90^{o}.

toward the equator from 30°N. There is no equivalent distance for latitudes less than 15°N because the erythema dose at these latitudes with a 10% ozone reduction is greater than the unperturbed erythema dose at the equator.

UV RADIATION AND SKIN CANCER

A comprehensive study of the linkage between UV radiation and skin cancer was recently completed by Cutchis (1978). Skin cancer incidence data in countries having a predominantly white population were compared with respect to geographic, time, age, and anatomic site variations. The hypothesis that an increase in UV radiation dose is associated with an increase in the incidence of squamous cell carcinoma, basal cell carcinoma, and malignant melanoma was tested by investigating recent epidemiological data over a wide latitude band. Squamous cell and basal cell carcinomas are the most common forms of skin cancer, and they are rarely fatal. Malignant melanoma, although less common, is often fatal. Some of the principal findings of Cutchis' investigation are:

"1. The hypothesis that solar ultraviolet radiation is a dominant factor in the introduction of squamous and basal cell carcinomas in predominantly white populations is strongly supported by an examination of available worldwide incidence data.

"2. A very large number of inexplicable anomalies of various kinds are found in the worldwide incidence data which are inconsistent with the hypothesis that solar ultraviolet radiation is a significant factor in the induction of malignant melanoma, leading to the conclusion that the primary cause(s) for this class of tumors must be sought elsewhere.

"3. There is clear evidence of a latitude gradient for squamous cell and basal cell carcinoma (hereafter refered to as "other skin cancer") incidence on a worldwide basis; there is no similarly clear evidence of a latitude gradient for the incidence of malignant melanoma.

"4. The ratio of the incidence of other skin cancer for males to that for females exceeds unity for all countries, and has a strong latitude gradient, increasing toward the equator; for malignant melanoma incidence this sex ratio may be slightly greater or smaller than unity with an average value of about 0.9, and has no apparent latitude gradient. For most geographic regions, the malignant melanoma sex ratio is less than unity, a finding which is inconsistent with the solar ultraviolet radiation hypothesis for malignant melanoma.

"5. The incidence of malignant melanoma for males in Norway is 20 times higher than in Zaragoza, Spain. Since Norway is much farther from the equator than Spain, this finding contradicts the lifetime solar UV dose hypothesis. There is no evidence in the literature that such a large discrepancy (greater than 20) can be rationally attributed to ethnic differences in Caucasian populations. Neither Norway nor Zaragoza are singularities. Residents in all Mediterranean countries of Europe enjoy very low malignant melanoma mortality rates, while residents of all Scandinavian countries and Finland suffer high mortality rates.

"6. Age-specific incidence curves for malignant melanoma differ fundamentally from those for other skin cancer. In recent years the risk for other skin cancer increases almost exponentially with age, while for malignant melanoma the risk is essentially the same for adults between approximately 40 and 65 years of age. The recent age-specific incidence curves for Connecticut and New Mexico are almost idential. From these data it can be deduced that malignant melanoma incidence is not a significant function of lifetime dose or, in all likelihood, the number of acute UV doses received.

"7. There has been a worldwide increase in the incidence of both other skin cancer and malignant melanoma in almost all countries with a predominantly white population. However, exceptions can be found. Squamous cell carcinoma incidence decreased in Finland from approximately 6 per 100,000 in 1960 to 3.5 in 1973, whereas malignant melanoma during this same period increased from 2 to 3.5. In Australia, mortality from malignant melanoma doubled from 1950 to 1964 but mortality from other skin cancer decreased by 50 percent during the same period. These and other similar cases in which the time variations of incidence over a long period of time run in opposite directions constitute anomalies for the solar radiation hypothesis linking solar radiation to malignant melanoma.

"8. Malignant melanoma mortality exceeds other skin cancer mortality for both males and females and has increased with time, whereas other skin cancer mortality has decreased with time. There is evidence in some countries of a latitude gradient for malignant melanoma mortality. Since malignant melanoma also occurs in younger age groups, it poses a far more serious problem to public health. Its causative factors are clearly in urgent need of being established.

"9. Other skin cancer favors the most exposed anatomic sites (head and neck, and hands), whereas malignant melanoma favors the relatively unexposed anatomic sites (trunk and lower limb). The lower limb is more favored in the legs of females, however, and this finding is consistent with the solar radiation hypothesis.

"10. Anatomic site frequency distribution changes with latitude for squamous cell carcinoma, but anomalously appears to be independent of latitude for malignant melanoma, e.g., malignant

melanoma cases for the head and neck constitute approximately 18 percent of all melanoma cases in Finland, southern Texas, and Australia.

"11. Two dichotomies exist in anatomic site behavior for malignant melanoma which suggest the existence of two carcinogenic agents, neither of which is solar ultraviolet radiation. These are:

"A. The age-specific incidence rates for malignant melanoma in the face and foot were similar to those for other sin cancer, i.e., almost exponential with age, whereas those for the trunk and lower limb were approximately independent of age for adults older than 35 years.

"B. The incidence of malignant melanoma in the face and foot was invariant with time, whereas in the trunk and lower limb the incidence has been rising very rapidly with time. The beginning of the latter increase can be traced back to the 1880's.

"The dating back of the increase in the postulated carcinogen associated with the trunk and lower limb to the 1880's rules out the frequently expressed hypothesis that the changes in clothing and life styles since World War II and the resulting increased UV doses received were responsible for the increase in malignant melanoma in those sites. Malignant melanoma incidence in the face was independent of sex which rules out identification of the other postulated carcinogen as solar radiation.

"12. Malignant melanomas were typically found in members of the professional and managerial classes, whereas other skin cancers were typically found in semi-skilled and skilled workers. This particular finding is inconsistent with the hypothesis that lifetime UV dose is associated with malignant melanoma but may be consistent with an acute UV dose hypothesis.

"13. Many carcinogenic agents other than solar radiation have been identified or suspected in the etiology of squamous and basal cell carcinomas. However, the great majority of cases appear to be sun-related, particularly for squamous cell carcinomas.

"14. Analysis of the data indicates that urbanization is an important factor in the etiology of basal cell carcinoma. It appears to be about as significant a factor as solar radiation in northern U.S. cities.

"15. There is recent evidence in Finland, Norway, Denmark, and Warsaw that urbanization is a factor in the etiology of malignant melanoma.

"16. The three categories of malignant melanoma, i.e., lentigo-maligna, superficial spreading, and nodular, appear to have characteristics (anatomic site distrubiton, tumor development time, median age) which can be made compatible with a two- or three-carcinogen theory for the etiology of malignant melanoma.

"17. The etiology of malignant melanoma is in a chaotic state. Recently published articles suggest the possibility that virus-like particles and diet (polyunsaturated foods) may be implicated in the etiology of malignant melanoma.

"18. The data for malignant melanoma incidence in Geneva, Switzerland and Zaragoza, Spain should be further examined for possible etiological clues: Geneva has had an anomalously high male/female sex ratio (2.2) and Zaragoza has had extremely low incidence values for both males and females.

"19. The biological amplification factor for other skin cancer is equal to or greater than unity but it is unlikely that it exceeds a value of 2. Determination of this factor is a complex multi-dimensional problem and the development of a dose-response model free of uncertainty and controversy is an almost hopeless proposition at the present time."

Another recent study by Martell and Poet (1979) suggests that ultraviolet radiation contributes to restitution rather than to induction of single breaks in the chromosomes of the cells of higher organisms. This argument is contrary to the view that ultraviolet radiation causes chromosome aberrations characteristics of malignancy. They claim that tumors which have been induced in mice and rats by repeated, large doses of UV radiation are unlike human skin tumors in type and tissue site, making the results of questionable applicability to man.

Martell and Poet (1979) suggest that alpha radiation may be a primary agent of human skin cancer. Alpha radiation is an effective mutagenic agent capable of producing a wide variety of structural changes observed in human tumors. Radon daughters that concentrate on exposed skin merit special consideration as agents of skin cancer. They conclude that if structural changes in chromosomes prove to be essential to malignancy, then the case for ultraviolet radiation as an etiological agent will be difficult to defend.

REFERENCES

Burt, J. E. and F. M. Luther, "Effect of Receiver Orientation on Erythema Dose," Photochemistry and Photobiology, 29, 85-91, 1979.

Cutchis, P., "Stratospheric Ozone Depletion and Solar Ultraviolet Radiation on Earth," Science, 184, 12-19, 1974.

Cutchis, P., "On the Linkage of Solar Ultraviolet Radiation to Skin Cancer," Report No. FAA-EQ-78-19, U.S. Department of Transportation, Washington, D.C., 1978.

Fanger, P. O., Thermal Comfort, Danish Technical Press, Copenhagen, 1976.

Green, A. E. S. and J. Mo, Chapter 2, Impact of Climatic Change on the Biosphere (CIAP Monograph 5), U.S. Department of Transportation, Washington, D.C., 1975.

Green, A. E. S., T. Swada, and E. P. Settle, "The Middle Ultraviolet Reaching the Ground," Photochem. Photobiol., 19, 251-259, 1974a.

Green, A. E. S., J. Mo and J. H. Miller, "A Study of Solar Erythema Radiation Doses," Photochem. Photobiol., 20, 473-482, 1974b.

Green, A. E. S, T. Swada, and E. P. Shettle, Chapter 2, Impact of Climatic Change on the Biosphere, CIAP Monograph 5, U.S. Department of Transportation, Washington, D.C., 1975.

Halpern, P., J. V. Dave, and N. Braslau, "Sea-Level Solar Radiation in the Biologically Active Spectrum," Science, 186, 1204-1208, 1974.

Lovill, J. E., "Characteristics of the General Circulation of the Atmosphere and the Global Distribution of Total Ozone as Determined by the Nimbus III Satellite Infrared Interferometer Spectrometer," Colorado State University, Atmospheric Science Department Paper No. 180, 1972.

Martell, E. A. and S. E. Poet, "Ultraviolet Radiation Versus Alpha Radiation as Agents of Human Skin Cancer," paper presented at the CACGP Symposium on the Budget and Cycles of Trace Gases and Aerosols in the Atmosphere, Boulder, CO, August 12-18, 1979.

McDonald, J. E., "Relationship of Skin Cancer Incidence to Thickness of Ozone Layer," Congressional Record, 117, 3493, March 19, 1971.

Mo, J. and A. E. S. Green, "A Climatology of Solar Erythema Dose," Photochem. Photobiol., 20, 483-496, 1974.

National Research Council, Biological Impacts of Increased Intensities of Solar Ultraviolet Radiation, NRC Environmental Studies Board, National Academy of Sciences, Washington, D.C., 1973.

National Research Council, Halocarbons: Effects on Stratospheric Ozone, National Academy of Sciences, Washington, D.C., 1976a.

National Research Council, Halocarbons: Environmental Effects of Chlorofluoromethane Release, National Academy of Sciences, Washington, D.C., 1976b.

Urbach, F. and R. E. Davies, "Estimate of the Effect of Ozone Reduction in the Stratosphere on the Incidence of Skin Cancer in Man," in Proceedings of the Conference on the Climatic Impact Assessment Program, 4th, T. M. Hard and A. J. Broderick (eds.), DOT-TSC-OST-75-38, U.S. Department of Transportation, Washington, D. C., 1975.

van der Leun, C. J. and F. Daniels, Jr., "Biological Effects of Stratospheric Ozone Decrease: A Critical Review of Assessments," Appendix B, Chapter 7 of Impacts of Climatic Change in the Biosphere, U.S. Department of Transportation, Washington, D. C., CIAP Monograph 5, 1975.

APPENDIX C. POTENTIAL CLIMATIC EFFECTS OF STRATOSPHERIC PERTURBATIONS*

Perhaps the most widely discussed effect of a reduction in ozone is the biological effect due to increased uv radiation at the earth's surface. A change in the total amount or redistribution of radiatively important atmospheric species might also be significant in terms of the climatic effects. Calculations of the change in global mean surface temperature caused by stratospheric perturbations generally show changes of much less than 1 K, but there could be much larger changes regionally, especially at high latitudes. Calculations with two- and three-dimensional models suggest that an increase in surface temperature would increase the intensity of the hydrologic cycle, thus increasing global mean precipitation. Uncertainties regarding cloud feedback processes and how climatic changes will affect cloudiness make it difficult at this time to accurately quantify such climatic changes. The sections that follow are intended to provide only rough estimates of the potential climatic effects of large SST fleets. Any effects that appear to be significant would, therefore, be candidates for more detailed study in the future.

COMPARISON OF CHANGES IN SOLAR ABSORPTION BY O_3 AND NO_2

In the case of a stratosphere perturbed by an NO_x injection, Luther (1976) showed that the increase in solar absorption by NO_2 at steady state was a significant fraction (35 to 50%) of the decrease in solar absorption by O_3. Since that time, the sensitivity of O_3 to an NO_x injection has decreased in the transport-kinetics models. Consequently, the change in solar absorption by NO_2 is now expected to be a much larger fraction of the change in solar absorption by O_3.

Solar absorption by O_3 is shown in Fig. C-1 as a function of O_3 column density. The absorption rate given is the instantaneous value for a solar zenith angle of 60°. The radiative transfer model used to compute the solar absorption rate includes Rayleigh scattering and assumes a cloudless, plane-parallel atmosphere

*See Luther (1978).

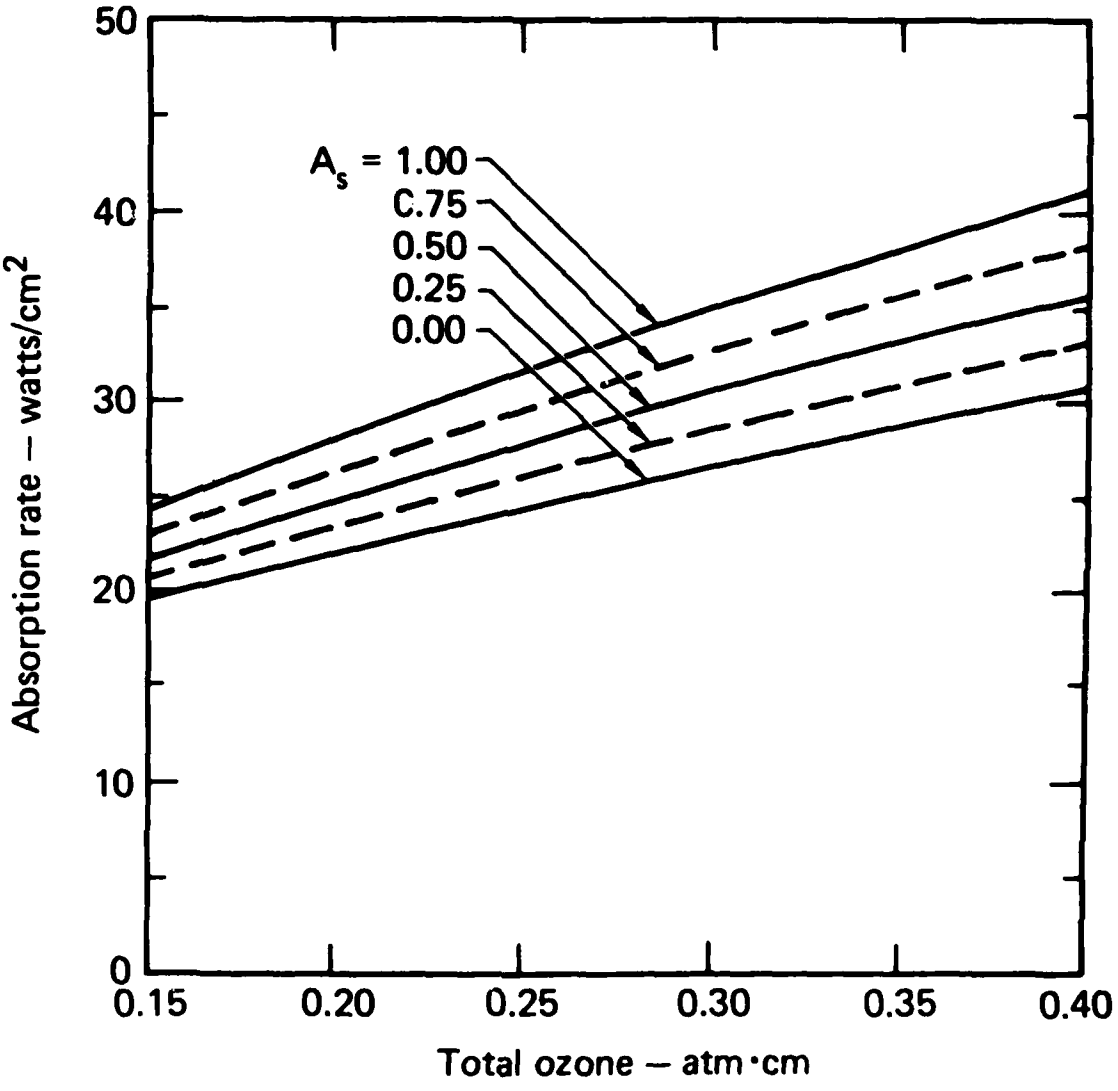

FIGURE C-1. Solar absorption by ozone for a solar zenith angle of 60°. A_S is the surface albedo.

above an isotropically scattered ground (Luther, 1978). The solar absorption by NO_2 is shown in Fig. C-2 also for a solar zenith angle of 60°.

Ambient and perturbed species concentration profiles were computed using the LLL one-dimensional transport-kinetics model. Two perturbation cases were considered: injections at 17 or 20 km of NO_x and H_2O. The injection rate for NO_x was 1000 molecules $cm^{-3}s^{-1}$, and the injection rate for H_2O was 177,000 molecules $cm^{-3}s^{-1}$ uniformly distributed over a 1-km-thick layer.

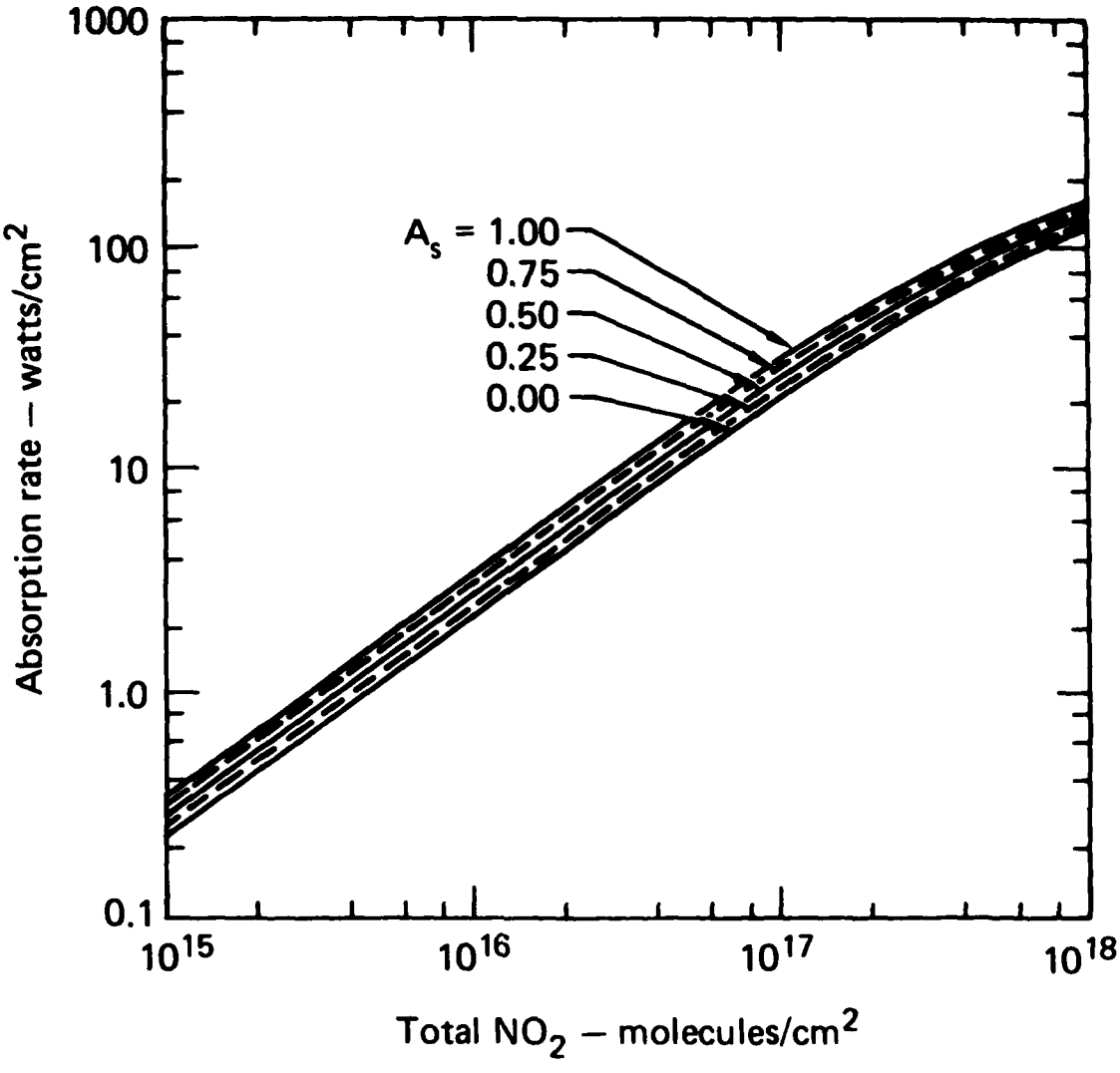

FIGURE C-2. Solar absorption by NO_2 for a solar zenith angle of 60°.

Temperature feedback and hydrostatic adjustment were included in these calculations. Changes in the O_3 and NO_2 column densities and solar absorption rates for a solar zenith angle of 60° and a surface albedo of 0.25 are summarized in Table C-1. The unperturbed column densities are 8.196 x 10^{18} molecules/cm^2 (0.305 atm.cm) for O_3 and 4.702 x 10^{15} molecules/cm^2 for NO_2.

In both cases, the injection of NO_x resulted in a small increase in total O_3. Although the changes in the O_3 column density are small, the changes in the O_3 column density are small, the change in the local O_3 concentration may

TABLE C-1. Increases in total atmospheric solar absorption by O_3 and NO_2 due to NO_x injections at the rate of 1000 $cm^{-3}s^{-1}$ and H_2O injections at the rate of 177,000 $cm^{-3}s^{-1}$. Calculations are for a solar zenith angle of 60° and a surface albedo of 0.25.

Quantity	Injection Altitude	
	17 km	20 km
ΔO_3	1.37%	1.29%
ΔNO_2	5.04%	10.51%
$\Delta Abs(O_3)$	0.20 W/m^2	0.19 W/m^2
$\Delta Abs(NO_2)$	0.06 W/m^2	0.12 W/m^2

be several percent. The change in column density reflects the net difference between regions of O_3 increase (below 26 km) and O_3 decrease (above 26 km). Consequently, although the change in the net heating may be small, the redistribution in altitude of where this heating occurs may be significant. The change in the local concentration of NO_2 is shown in Fig. C-3.

Changes in O_3 and NO_2 concentrations due to an NO_x injection lead to increases in the total solar absorption of both species. These increases are small, however, when compared to the total energy absorbed by the stratosphere.

POTENTIAL CLIMATIC IMPACT

The climatic impact of changes in stratospheric composition depends upon both the solar and longwave effects of the perturbation. Changes in temperature, in addition to affecting the transfer of longwave radiation, also affect atmospheric stability and transport. Here we will consider only the global impact of the solar and longwave effects and neglect any potential feedback on transport.

When evaluating the computed change in global mean surface temperature, changes on the order of several tenths of a degree Kelvin may be a significant climatic perturbation since regional changes in temperature might be several times greater than the global mean. Pollack et al. (1976) suggest that 0.1 K is a threshold

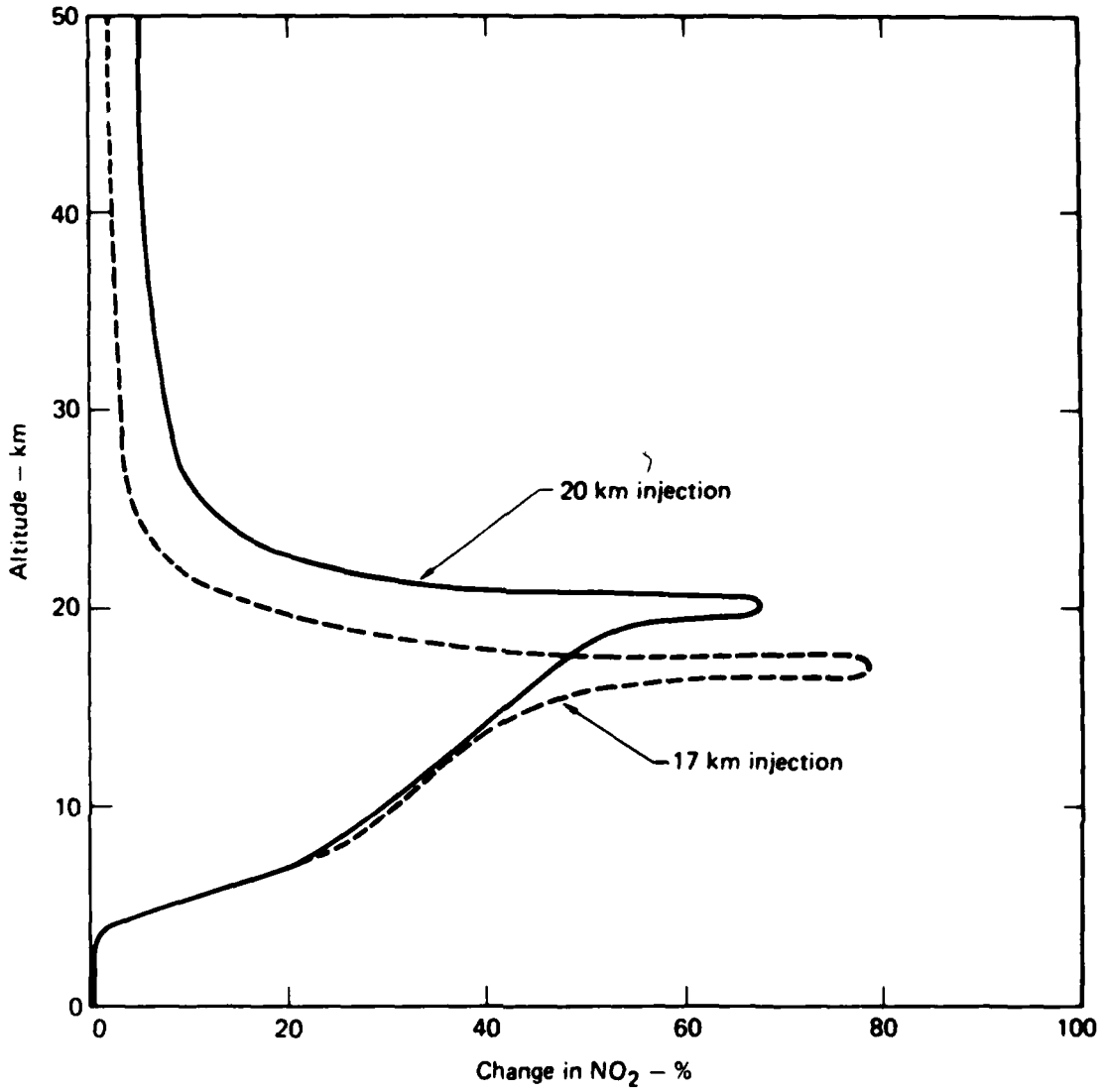

FIGURE C-3. The change in NO_2 concentration due to an NO_x injection of 1000 molecules $cm^{-3}s^{-1}$ and H_2O injection of 177,000 molecules $cm^{-3}s^{-1}$ over a 1-km thick layer at 17 or 20 km.

value for considering the change in global mean surface temperature to be significant. Computing the change in global mean surface temperature associated with past major changes in climate, they infer that values below 0.1 K would not have major consequences.

A previous assessment of the effect of changes in O_3 and NO_2 on surface temperature by Ramanathan et al. (1976) showed a cooling at the surface associated with a reduction in O_3 due to an NO_x injection. Only reductions in O_3 were

considered (not increases), and it was assumed that the changes in O_3 and NO_2 were uniform (percentagewise) between 12 and 40 km. Our present results differ from these modeling assumptions in that the changes in O_3 and NO_2 concentrations are not uniform with altitude, and there is a net increase in O_3 column density rather than a decrease. Nevertheless, the work of Ramanathan et al. (1976) is useful because it demonstrates the importance of the longwave effect of the perturbation. The reduction in total O_3 tended to warm the troposphere by increasing the transmissivity of the stratosphere for solar radiation. The reduction in stratospheric temperature due to reduced O_3, however, had a greater effect on the longwave radiation emitted downward from the stratosphere. The net result was a slight reduction in surface temperature.

A similar calculation using our current modeling results would predict an increase in temperature in the lower stratosphere (Luther and Duewer, 1978). It is possible that the longwave effect would also dominate in this case. Although the net change in temperature is uncertain, it is clear that the longwave effect would tend to warm the troposphere, whereas the solar effect would tend to cool.

In attempting to assess the effect of changes in stratospheric composition on the global mean surface temperature, it is desirable that the same model be used throughout the study. Since we do not have a climate model that may be applied to this study, we will rely on the results of other researchers.

According to Ramanathan's model (Ramanathan et al., 1976), the change in surface temperature is related to the change in ozone by

$$\Delta T_s = (0.009 \text{ to } 0.014 \text{ K})\, \Delta O_3 \quad , \tag{C.1}$$

where ΔO_3 is the percent change in ozone concentration applied uniformly over the altitude region 12-40 km. The first coefficient applies to the assumption of constant cloud top altitude whereas the second coefficient applies to the assumption of constant cloud top temperature. A similar expression relates the change in surface temperature to the percent change in NO_2 concentration between 12 and 40 km:

$$\Delta T_s = (3 \times 10^{-4} \text{ to } 6 \times 10^{-4} \text{ K})\, \Delta NO_2 \quad . \tag{C.2}$$

The expressions are not applicable directly to our results, but they may be used to

estimate an approximate value for ΔT_s. Using the method described in Luther (1978), the change in surface temperature is estimated to be less than 0.1 K for both the 17- and 20-km injection altitudes.

A recent analysis of the effect of changes in ozone on the earth's radiation balance by Ramanathan and Dickinson (1979) indicates that a vertical redistribution of ozone can produce larger perturbations to the tropospheric energy balance than do uniform changes in ozone. The change in the net radiative flux possibly can be of the opposite sign as well. Changes in the tropospheric lapse rates, which were not included in the calculations, could also affect the magnitude of ΔT_s.

We now consider the potential climatic effect of the water vapor injected into the stratosphere along with the NO_x from engine emissions. According to our model calculations in which the stratospheric water vapor profile is computed, the increase in the stratospheric water vapor mixing ratio would be 0.10 ppmm for a 17-km injection and 0.31 ppmm for a 20-km injection. Ramanathan's model was also used in the CIAP study to estimate the change in surface temperature resulting from a change in stratospheric water vapor mixing ratio (Grobecker et al., 1974):

$$\Delta T_s = (0.2 \text{ to } 0.3 \text{ K})\, \Delta H_2O \text{ (ppmm)} \qquad \text{(C.3)}$$

The estimated change in surface temperature as a result of these changes in stratospheric water vapor are given in Table C-2. These changes in temperature are also estimated to be less than 0.1 K.

In addition to NO_x and water vapor, aircraft engines also emit SO_2, which is converted to sulfate aerosols. Assuming an emission index of 1.0 g/kg fuel, the SO_2 injection rate would be 3.4×10^7 kg/yr when the NO_x injection rate is

TABLE C-2. Change in surface temperature due to an increase in stratospheric water vapor.

Altitude of Injection (km)	ΔH_2O in Stratosphere (ppmm)	ΔT_s (K)
17	0.10	0.02-0.03
20	0.31	0.06-0.09

6.2×10^8 kg/yr. The change in surface temperature due to increased stratospheric aerosols (75% H_2SO_4) has been computed by Pollack et al. (1976). Using a radiative-convective model, they find

$$\Delta T_s = (-6.3 \text{ to } -10 \text{ K})\,\Delta\tau \quad , \tag{C.4}$$

where $\Delta\tau$ is the increase in the stratospheric optical depth. Pollack et al. find that $\Delta\tau$ is related to the mass density (m) of sulfate aerosols in $\mu g/m^3$ averaged over a 10-km thick layer by the expression $\Delta\tau = 0.031$ m. The expression $\Delta\tau = 0.038$ m was used in the CIAP Report of Findings (Grobecker et al., 1974). The aerosol mass density is obtained from the expression

$$m = \frac{HFtc(M_a/M_c)}{A\ell} \quad ,$$

where H is the fraction of the aerosols deposited in a given hemisphere, F is the SO_2 emission rate, t is the residence time, c is the conversion efficiency, M_a is the molecular weight of the aerosol, M_c is the molecular weight of SO_2, A is the aera of a hemisphere of the earth, and ℓ is the depth of the layer (10 km). For a sulfuric acid solution that is 75% H_2SO_4 by weight, $M_a/M_c = 1.6$. Values for the various quantities used by Pollack et al. (1976) and used in the CIAP Report of Findings are shown in Table C-3. The resulting values for $\Delta\tau$ are considerably smaller (by approximately a factor of 2) using Pollack et al.'s values. In both cases the values for ΔT_s are estimated to be less than -0.01 K for a 17-km injection altitude and less than -0.02 for a 20-km injection altitude. Using the criterion that changes a surface temperature less than 0.1 K would not have major consequences, none of the SST engine emissions (NO_x, H_2O, and SO_2) are estimated to have a major climatic effect. The largest individual effect on surface temperature is that of water vapor, which is estimated to cause a temperature increase of 0.06-0.09 K for a 20-km injection at 4.3×10^{10} kg/yr. The combined effect of all engine emissions on climate is likely to be an increase in global mean temperature of less than 0.1 K for these injection rates.

TABLE C-3. Factors used in calculating the change in surface temperature due to an SO_2 emission rate of 3.44×10^7 kg/yr in the Northern Hemisphere.

Source	Altitude of injection (km)	Residence time, years	Conversion efficiency	Fraction in hemisphere	$\Delta\tau$	ΔT_s,[a] (K)
Pollack et al., 1976	17	0.978	0.869	0.7	3.9×10^{-4}	-0.002 to -0.004
$\Delta\tau$ =0.031 m[b]	20	1.715	0.945	0.7	7.6×10^{-4}	-0.005 to -0.008
CIAP Report of Findings, 1974	17	1.70	0.83	1.0	1.1×10^{-3}	-0.07 to -0.011
$\Delta\tau$=0.038 m	20	3.00	0.93	1.0	2.3×10^{-3}	-0.014 to -0.023

[a] T_S = (-6.3 to -10 K) $\Delta\tau$.

[b] m is the mass density of sulfate aerosols in $\mu g/m^3$ averaged over a 10-km-thick shell.

REFERENCES

Grobecker, A. J., S. C. Coroniti, and R. H. Cannon, Jr., "CIAP Report of Findings, The Effects of Stratospheric Pollution by Aircraft," Report DOT-TST-75-50, U. S. Department of Transportation, Washington, D. C., 1974.

Luther, F. M., "Solar Absorption in a Stratosphere Perturbed by NO_x Injection," Science, 192, 49-51, 1976.

Luther, F. M., "Effects of Stratospheric Perturbations on the Solar Radiation Budget," Lawrence Livermore Laboratory Report UCRL-80429, 1978, also in Papers Presented at the WMO Symposium on the Geophysical Aspects and Consequences of Changes in the Composition of the Stratosphere, WMO-No. 511, Toronto, June 26-30, 1978.

Luther, F. M. and W. H. Duewer, "Effect of Changes in Stratospheric Water Vapor on Ozone Reduction Estimates," J. Geophys. Res., 93, 2395-2402, 1978.

Pollack, J. B., O. B. Toon, A. Summers, W. Van Camp, and B. Baldwin, "Estimates of the Climatic Impact of Aerosols Produced by Space Shuttles, SST's and Other High Flying Aircraft," J. Atmos. Sci., 15, 247-258, 1976.

Ramanathan, V. and R. E. Dickinson, "The Role of Stratospheric Ozone in the Zonal and Seasonal Radiative Energy Balance of the Earth-Troposphere System," J. Atmos. Sci., 36, 1084-1104, 1979.

Ramanathan, V., L. B. Callis, and R. E. Boughner, "Sensitivity of Surface Temperature and Atmospheric Temperature to Perturbations in the Stratospheric Concentration of Ozone and Nitrogen Dioxide," J. Atmos. Sci., 33, 1092-1112, 1976.

APPENDIX D.
THE RELATION BETWEEN ATMOSPHERIC TRACE SPECIES VARIABILITIES AND SOLAR UV VARIABILITY*

We provide here a discussion of calculated trace species variations due to solar UV variability. Our purpose is to examine those species whose variations may be observable and thus help confirm the supposed solar variations.

LONG-TERM VARIATIONS IN ODD-OXYGEN AND TEMPERATURE

Figure D-1 shows the percent changes in O_3, $O(^3P)$, $O(^1D)$ and temperature from maximum to minimum in solar UV flux variations. The percent changes are computed by dividing the differences of species concentrations corresponding to the solar UV flux maximum and minimum by the concentration at the minimum. The change in the solar flux was specified as described in Penner and Chang (1978). The changes in species concentrations are due primarily to changes in the photolysis rates for odd-oxygen production and O_3 destruction according to

$$O_2 + h\nu \rightarrow O + O \quad , \qquad J_1 \qquad \text{(D.1)}$$

and

$$O_3 + h\nu \rightarrow O_2 + O \quad . \qquad J_2 \qquad \text{(D.2)}$$

The changes in ozone concentration are sensitive to the calculated temperature increase in the stratosphere because of the temperature dependence of the reactions

$$O + O_2 + M \rightarrow O_3 + M \quad , \qquad k_1 \qquad \text{(D.3)}$$

and

$$O + O_3 \rightarrow O_2 + O_2 \quad , \qquad k_2 \qquad \text{(D.4)}$$

both of which tend to change in the direction of reducing ozone concentrations as temperature is raised. The increase in UV flux at solar maximum causes increased

*See Penner and Chang (1978, 1979).

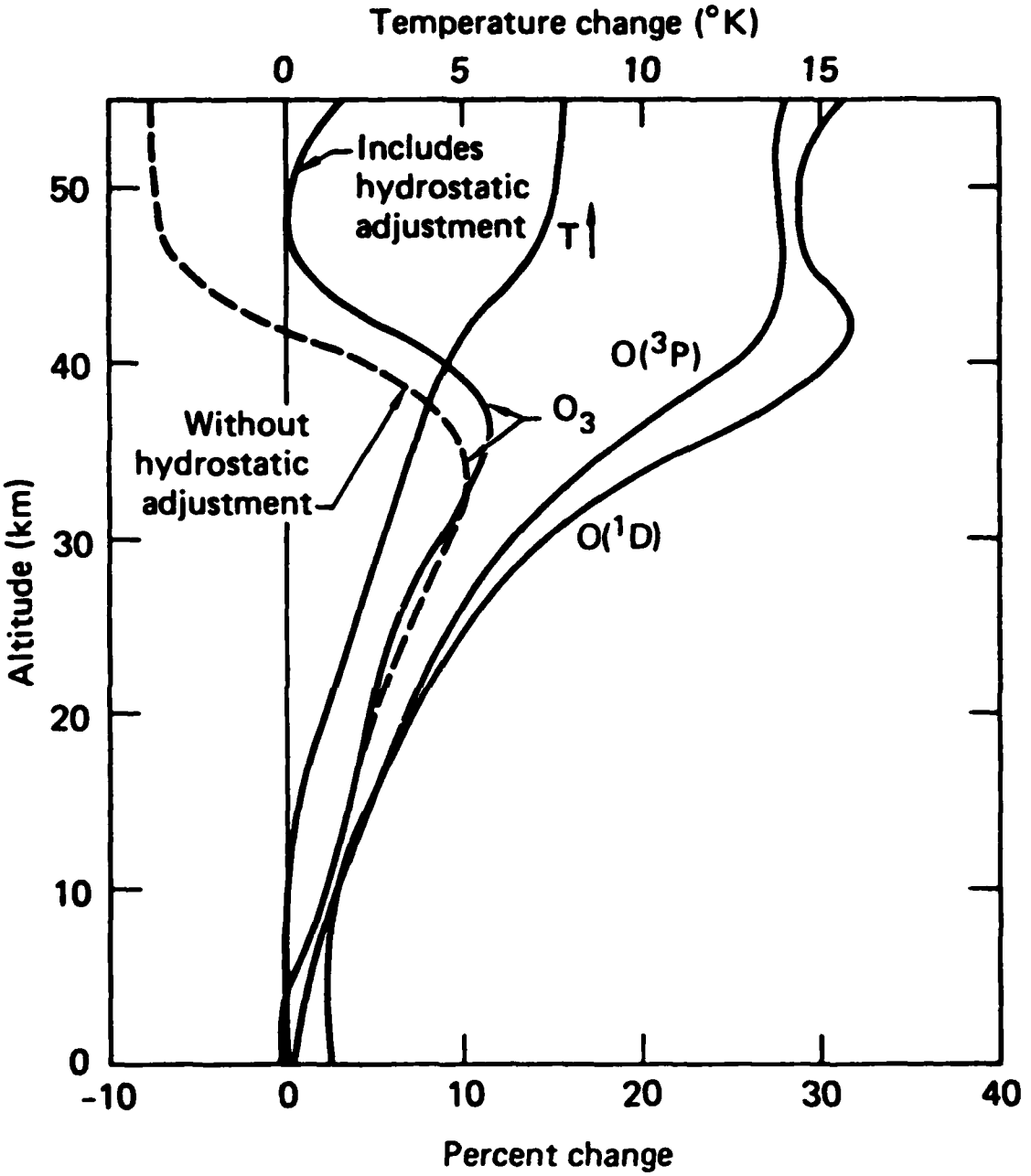

FIGURE D-1. Change in temperature (top scale) and percent change in O_3, $O(^3P)$, and $O(^1D)$ from solar minimum to solar maximum [(max-min)/min x 100] (bottom scale. The dashed line shows the calculated change in O_3 when hydrostatic equilibrium is not included.

solar absorption in the Hartley and Huggins bands of O_3, resulting in an increase in temperature. The temperature increase is further enhanced by the increases in local ozone concentrations. The present model also includes the changes in cooling rates associated with changes in stratospheric water distribution. Local H_2O remains almost constant throughout the solar cycle and the feedback on the temperature is quite small.

Changes in the temperature profile are expected to lead to changes in the background atmosphere as it adjusts to hydrostatic equilibrium (Chandra et al., 1978). Only minor differences in the variation for most species is observed when hydrostatic adjustment is included. Larger changes, however, occur in the variation of O_3, NO_2, and $O(^1D)$. Without hydrostatic adjustment, O_3 is decreased at solar maximum at high altitude due to the combined effects of increases in the rate of photolysis of O_3 and increases in the temperature (dashed line in Fig. D-1). O_3 is approximately given by

$$[O_3]^2 = \frac{J_1 k_1 [O_2]^2 [M]}{J_2 k_2 (1 + A)} \quad , \tag{D.5}$$

where A represents changes introduced by minor species in the NO_x, HO_x and ClO_x families (Nicolet, 1975). With hydrostatic adjustment, increases in $[O_2]$ and $[M]$ at high altitude tend to increase O_3. Eventually, the increase in O_3 due to hydrostatic adjustment will offset decreases in O_3 caused by an increase in J_1 and a decrease in k_1/k_2. As shown in Fig. D-1 for the present case, O_3 increased by approximately 4% at 55 km, whereas without hydrostatic adjustment, it decreased 7%.

NO_2 variations also become positive at high altitude with hydrostatic adjustment. These changes are introduced mainly because O_3 has increased, leading to a larger role for the reaction

$$O_3 + NO \rightarrow NO_2 + O_2 \quad . \tag{D.6}$$

Changes in the variations of other species due to the inclusion of hydrostatic adjustment are rather minor. The results of Penner and Chang (1978) which compare calculated ozone and temperature variations to observations are shown in

Figs. D-2 to D-4. The comparisons of variations in O_3 and temperature with observations are not significantly affected by including hydrostatic adjustment since the comparisons are for an O_3 change averaged over the altitudes 32-46 km, and the changes are dominated by the higher O_3 concentrations at the lower altitudes within this range. As shown here, however, it is necessary to include hydrostatic adjustment when discussing local ozone variations above about 37 km.

The concentration of $O(^3P)$ is determined by the balance

$$[O(^3P)] = \frac{J_2[O_3]}{k_1[O_2]\ [M]} \qquad (D.7)$$

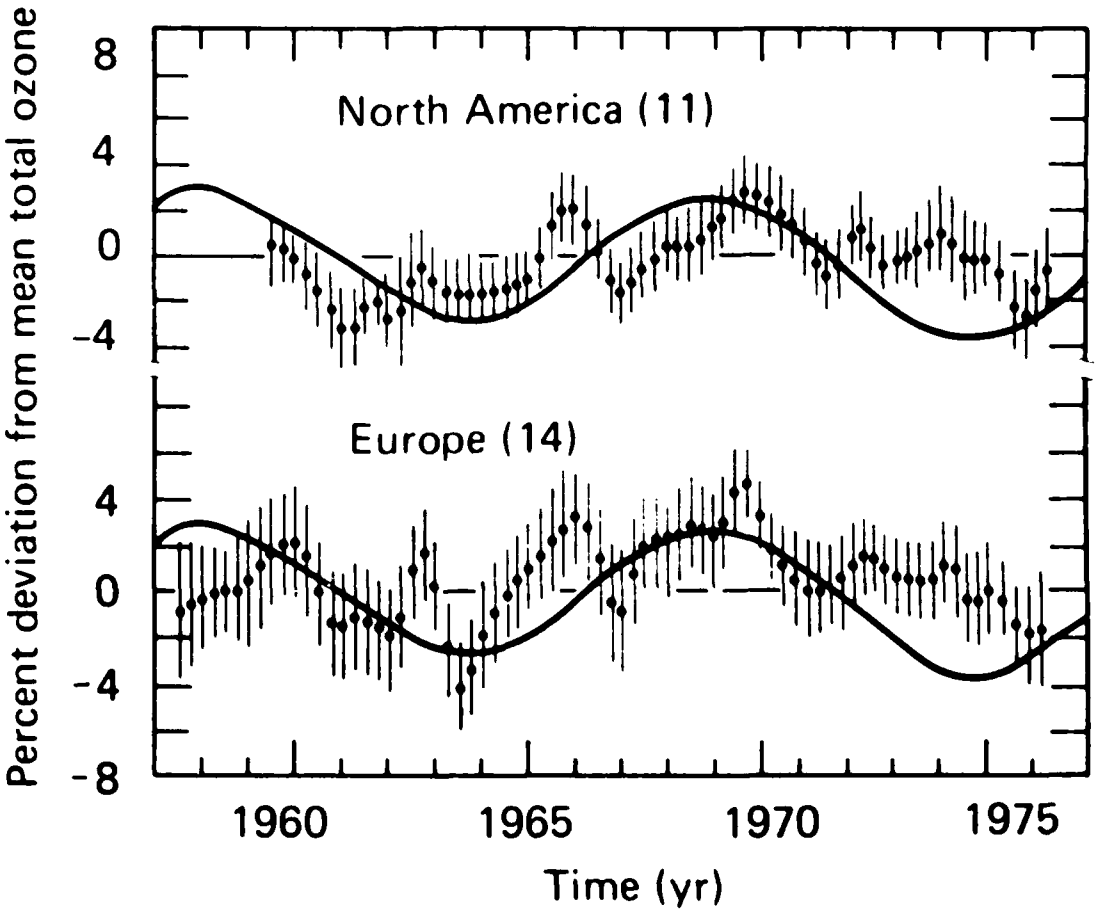

FIGURE D-2. Comparison of calculated total ozone deviations to the analysis of data by Angell and Korshover (1978a).

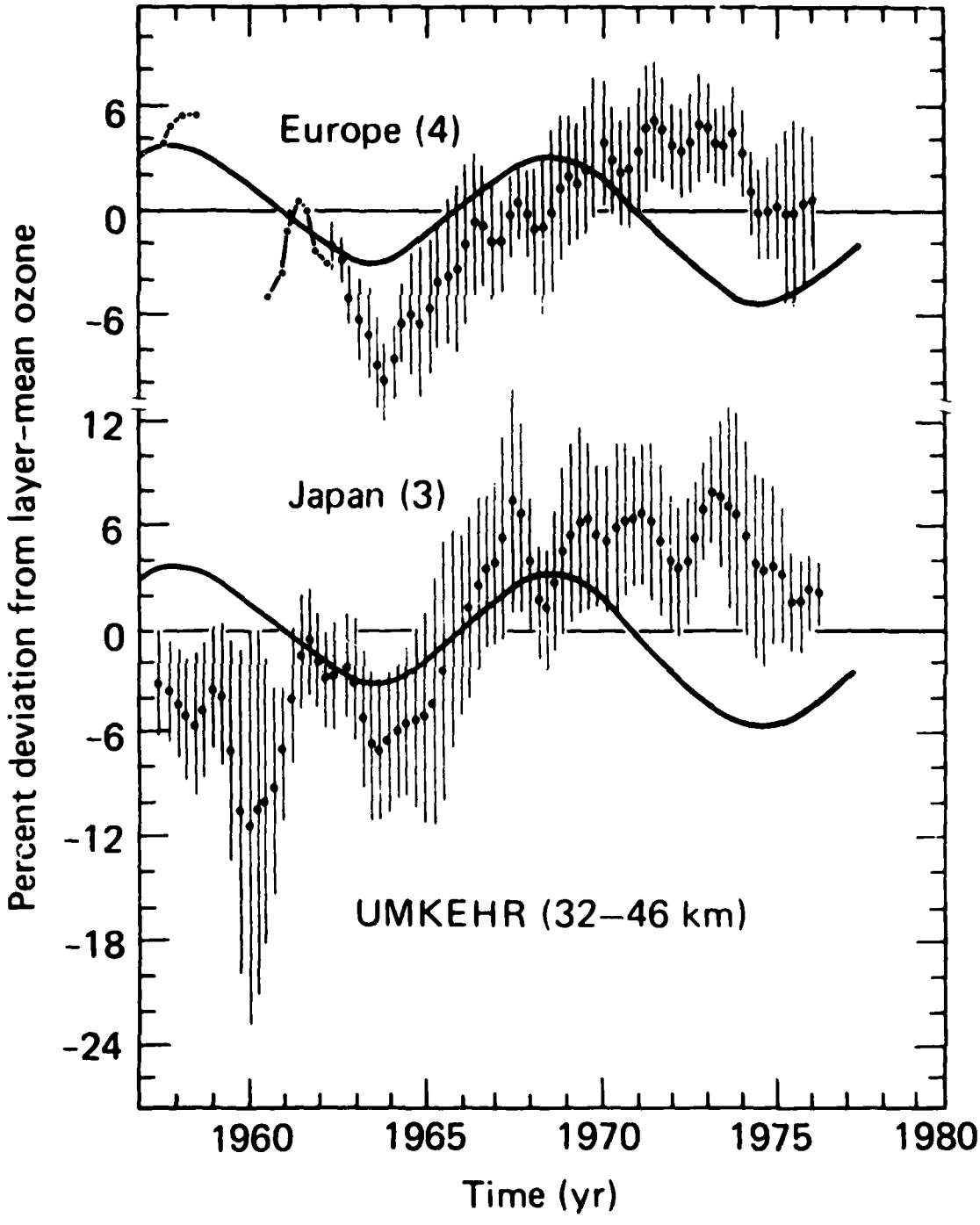

FIGURE D-3. Comparison of calculated layer-mean ozone variations to the analysis of ozone data by Angell and Korshover (1978b).

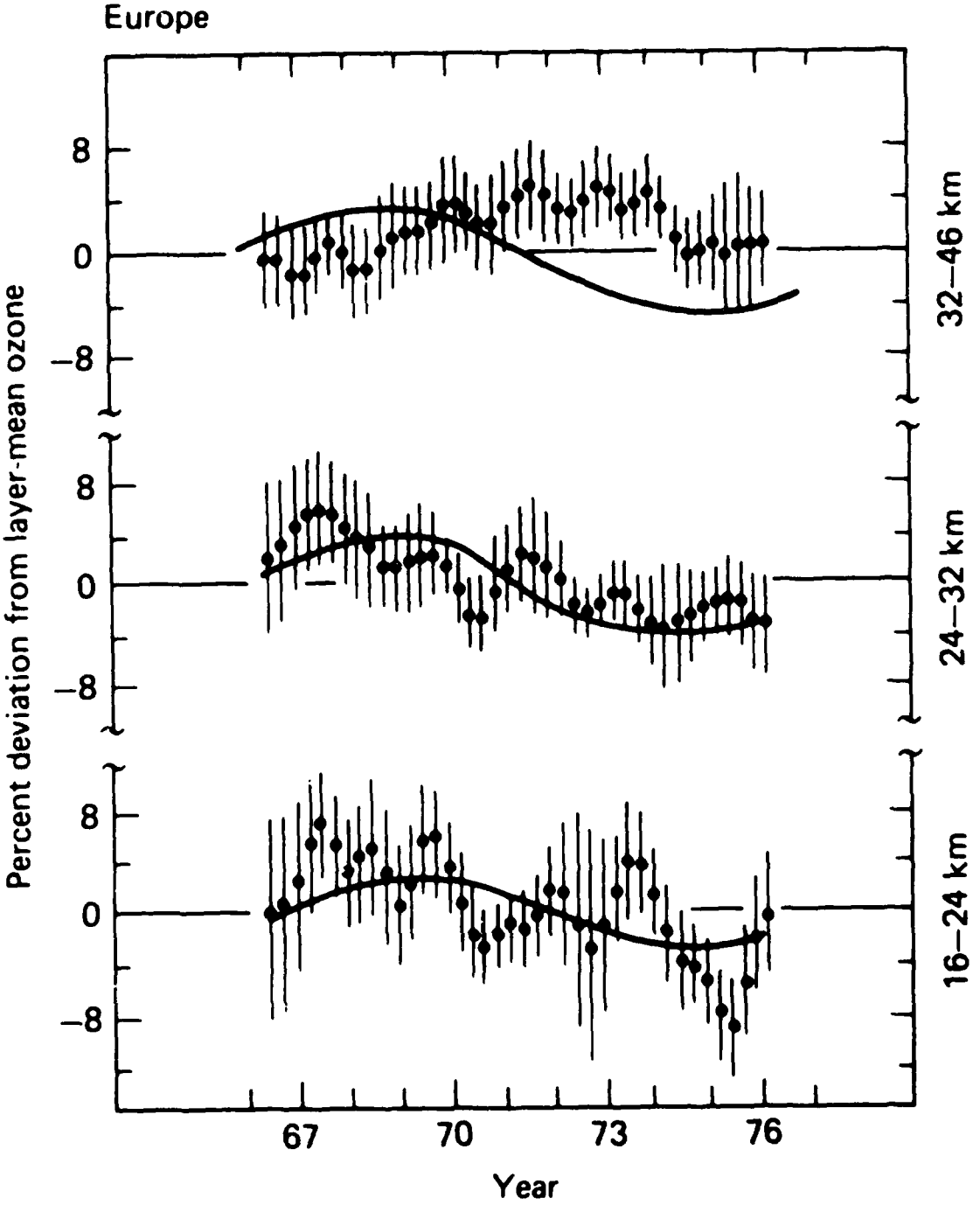

FIGURE D-4. Comparison of calculated layer-mean ozone variations to the analysis of ozone data by Angell and Korshover (1978c).

Combining Eq. (D.5) with (D.7) shows that $O(^3P)$ is only proportional to $M^{-1/2}$ so its concentration is not very sensitive to changes in M resulting from hydrostatic adjustment. $O(^3P)$ increases more than 25% above 40 km (Fig. D-1) at solar maximum due to the increase in J_2. The $O(^1D)$ concentration, also shown in Fig. D-1, is directly proportional to $J_3[O_3]$, where J_3 refers specifically to photolysis of O_3 leading to $O(^1D)$ production,

$$O_3 \xrightarrow{h\nu} O_2 + O(^1D) \qquad J_3 \quad . \tag{D.8}$$

The increases in O_3 and J_3 both drive increases in $O(^1D)$. At the highest altitudes this is offset somewhat by increased deactivation of $O(^1D)$ by collision with O_2 and N_2. It should be noted that the maximum changes of $O(^1D)$ are in the altitude range of 30 to 40 km, i.e., the principal production region of odd-nitrogen and odd-hydrogen from reactions of $O(^1D)$ with N_2O, CH_4 and H_2O. Therefore, one might expect similar variations in the trace species families NO_x and HO_x at this altitude. However, for N_2O and CH_4 the local concentrations are decreased at solar maximum so that the local rate of production of radicals is almost unchanged in the present model.

The time variations of $O(^3P)$ and $O(^1D)$ follow that of the driving function without significant time lag in the altitude range above 20 km. Below 20 km a noticeable time lag in $O(^3P)$ of a few months develops following the time lag of ozone (Fig. D-5). The response time of the total ozone column to variations in solar UV flux is less than two months, reflecting the behavior near the ozone peak around 25 km. These time lags are a function of the 1-D model transport parameterization and should be used with caution since they are sensitive to K_z.

The temperature trend is shown to be in reasonable agreement with radiosonde and rocketsonde temperature data in Fig. D-6, although there remain unexplained details (Penner and Chang, 1978; Angell and Korshover, 1978b). As a test of our understanding of ozone and temperature variations, it is of interest to examine whether the observed temperature variations might drive ozone variations, independent of changes in the solar flux. In order to study this question, we specified the temperature profile in our model and perturbed the calculated ambient temperature profile by $\pm 2.5^{\circ}K$ and $\pm 5.0^{\circ}K$ about the average value above 30 km with a linear variation in the perturbed temperature between 20 and 30 km. We calculated trace species concentrations consistent with each temperature profile.

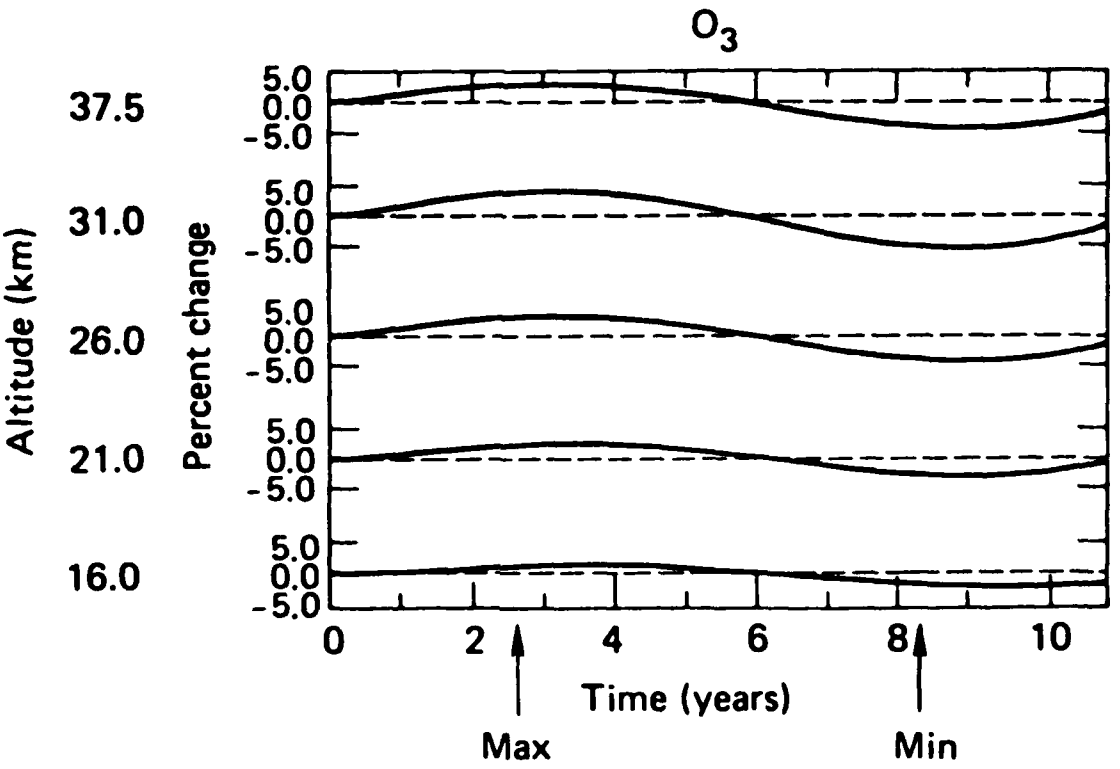

FIGURE D-5. Time variation of O_3 at selected altitudes. Solar maximum and minimum were at 2.75 and 8.25 years, respectively.

This choice of temperature perturbation provides a reasonable fit to the observed temperature variations (Quiroz, 1979; Angell and Korshover, 1978). The background atmosphere was adjusted to hydrostatic equilibrium in each case.

The results of this calculation are shown in Fig. D-7. The calculated ozone decreased below 40 km, consistent with Eq. (D.5) and the temperature dependence of reactions k_1 and k_2. Above 40 km, hydrostatic adjustment increases $[O_2]$ and [M] so that the O_3 variation becomes positive when the temperature is increased. Observations of ozone and temperature variations below 32 km show an in-phase relationship, which is contrary to the model calculations. Given the present evidence we believe that temperature changes in the stratosphere are insufficient to account for the variations in ozone. We caution, however, that these conclusions are based on a comparison of ozonesonde-derived ozone trends in Europe with radiosonde-derived temperature trends in the Western Hemisphere. These regions were chosen for comparison because they had the largest number of stations and thus provided the most precise trend estimates. Angell and Korshover's (1978a)

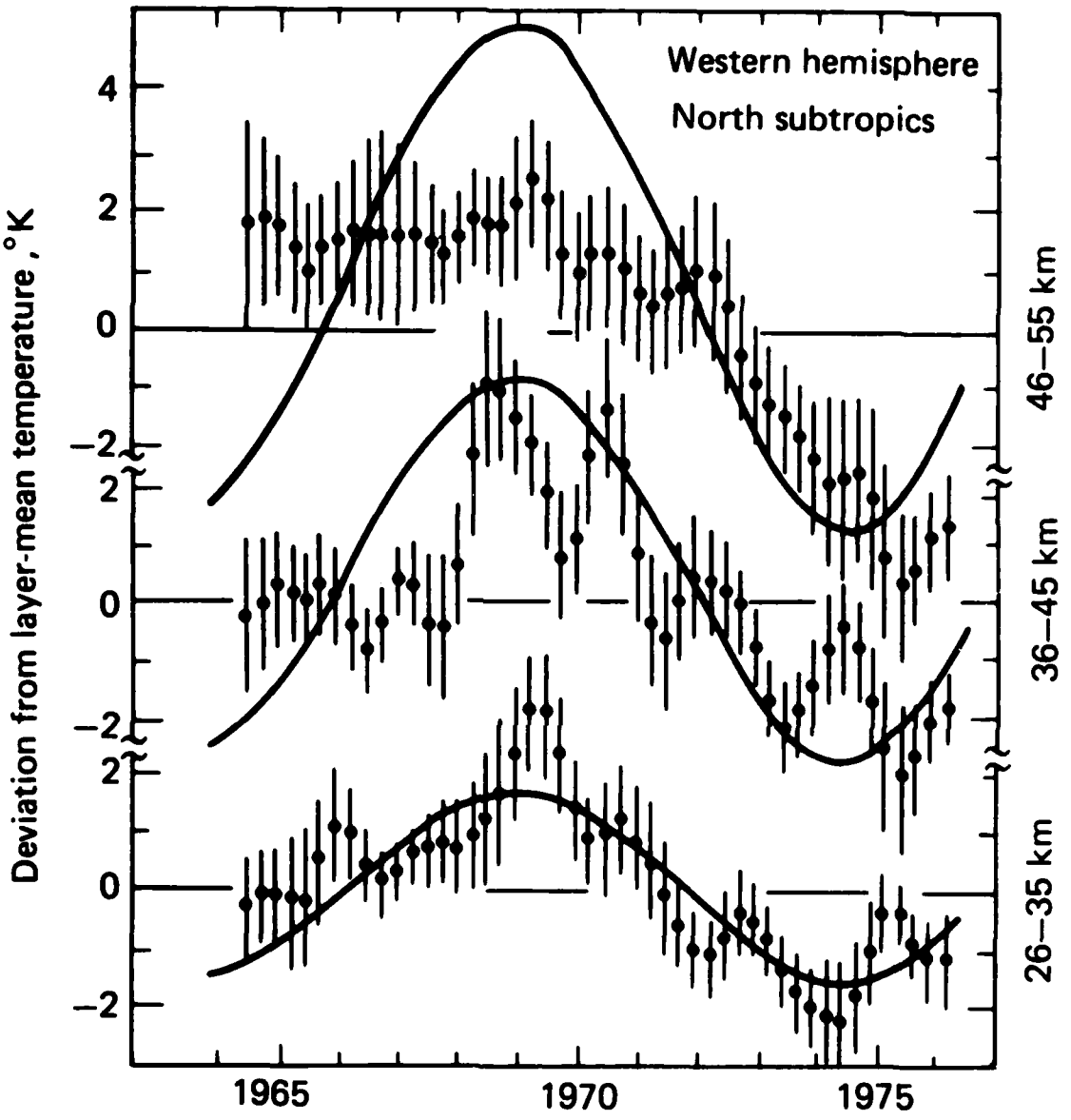

FIGURE D-6. Comparison of calculated layer-mean temperature changes to the analysis of rocketsonde measured temperature changes for the Western Hemisphere north subtropics by Angell and Korshover (1978b).

analysis of ozonesonde trends in North America indicated an increase in ozone in the layer from 24-32 km at the same time the temperature was decreasing. The North American trend was based on only 2 stations reporting for the entire time period which may not be sufficient to properly delineate a small long-term regional trend.

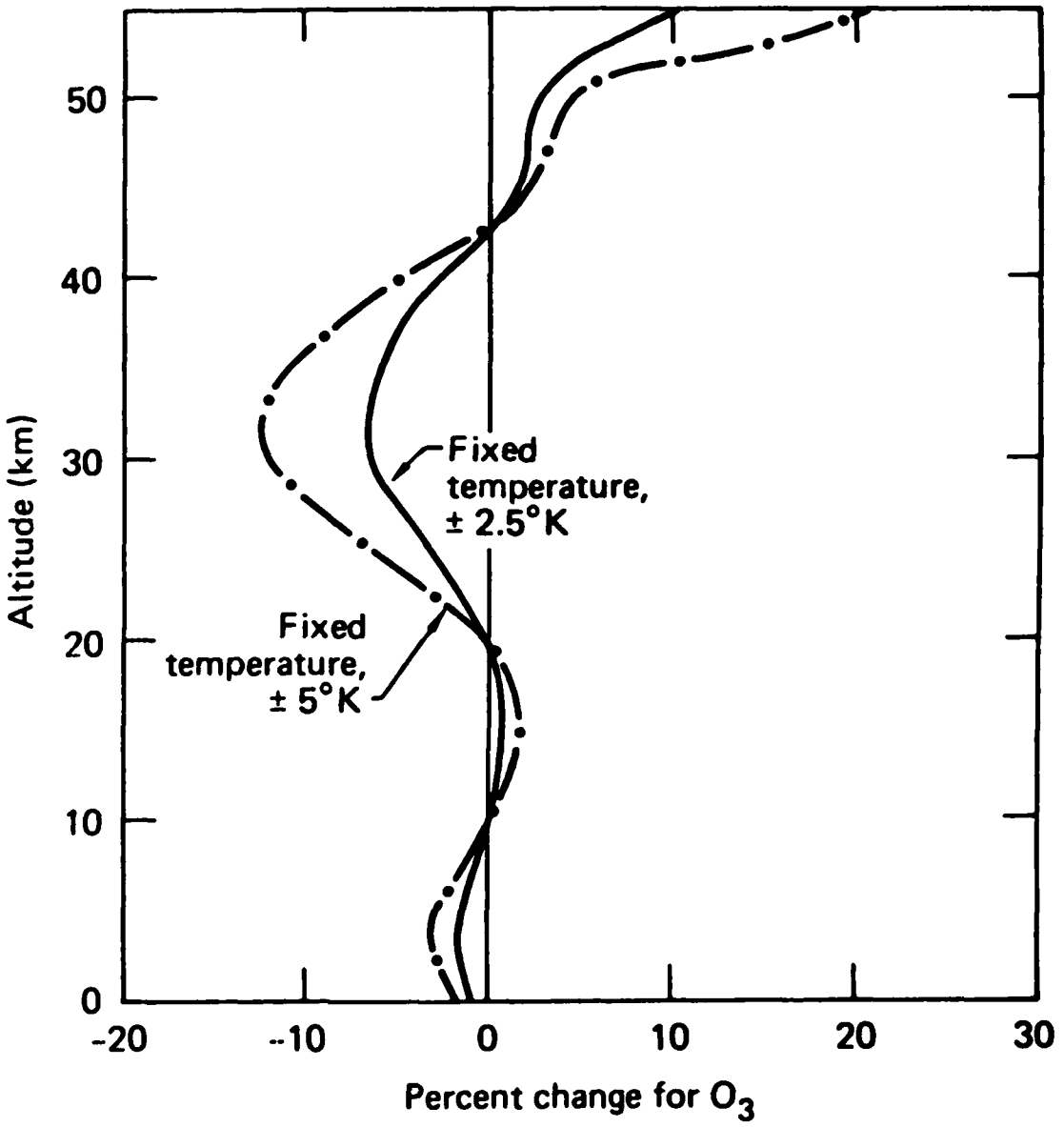

FIGURE D-7. Percent change in O_3 for a temperature perturbation of $\pm$ 1.5°K and $\pm$5.0°K above 30 km from the average calculated temperature. The temperature perturbation is decreased linearly to zero at 20 km and the background atmospheric pressure is adjusted to hydrostatic equilibrium in each case.

Stanulonis and Chamberlain (1978) looked at ozone and temperature fluctuations from 4 stations near 32°N and found positive, though small, correlations. Thus, a final conclusion in this matter must await further analysis.

LONG-LIVED TRACE SPECIES

The so-called long-lived trace species such as N_2O, CCl_4, CF_2Cl_2, $CFCl_3$, CH_3Cl, H_2O and CH_4 are destroyed in the stratosphere either by radiation at wavelengths shorter than 300 nm or by reactions with $O(^1D)$ and OH. Their time variations are in phase with the assumed 11-year variations in solar UV fluxes at altitudes above 35 km. Under the influence of the assumed variations in solar UV fluxes, CF_2Cl_2, $CFCl_3$, CCl_4 and N_2O all have variations of 40% or larger above 30 or 40 km. Since CF_2Cl_2 and $CFCl_3$ are not in steady state, their expected variations are not the same for every solar cycle. A detailed examination of their possible variations at this time is not warranted. Although CCl_4 is in quasi-steady-state, the absolute accuracies of current measurement techniques for CCl_4 ($\pm$100% (WMO, 1977)) are not adequate for detecting the estimated time variations.

The percent changes of H_2O, CH_4 anmd N_2O are shown in Fig. D-8. The calculation shows a change of less than 3% for H_2O throughout the stratosphere. Although the destruction rate of H_2O increases at solar maximum (more $O(^1D)$ and photolysis), the increase in production rate from the methane cycle more than compensates for this change in loss rate, so H_2O increases slightly at all altitudes in the stratosphere.

CH_4 shows a solar cycle variation of up to -24% (max to min) around 50 km. This is mainly the result of the variations in $O(^1D)$ and HO concentrations. Since the upward flux of CH_4 from the troposphere is fixed and the chemical lifetime of CH_4 is relatively short above 35 km, any change in the loss rate coefficients affects the local CH_4 concentrations directly. Below 50 km the reaction with HO molecules is the dominate loss mechanism for CH_4. At altitudes below 30 km, CH_4 also has very little variation since HO changes very little (Fig. D-9). Observational data of CH_4 below 40 km are highly sensitive to variations in transport (Ehhalt et al., 1975). This sensitivity and the small variations expected below 40 km make it difficult to detect CH_4 time variations below 40 km. Only rocket or satellite measurements at the top of the stratosphere offer possibilities of detecting any possible trend.

The large variations in N_2O are caused by changes in its photolysis rate. In the lower and middle stratosphere its variation over a solar cycle is very similar to that of CH_4 and is also difficult to measure. However, above 40 km it is expected

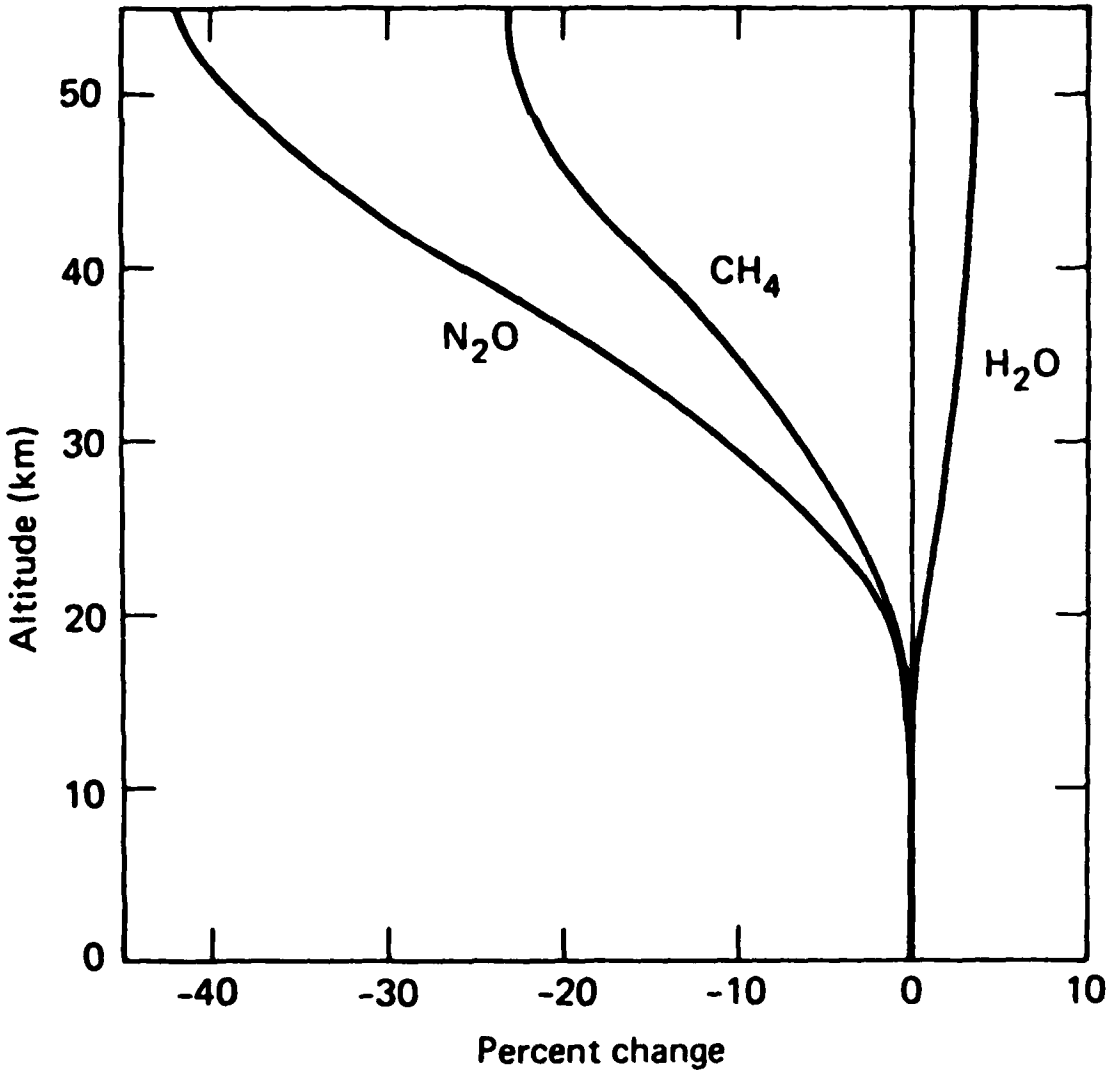

FIGURE D-8. Percent change for N_2O, CH_4, and H_2O from solar minimum to solar maximum [(max-min)/min x 100].

to vary by as much as -46% (max to min), and current measurement techniques with a gaschromatograph and grab sample have an accuracy of a few percent (WMO, 1977). Because of the large reservoir and long lifetime of N_2O in the atmosphere, its atmospheric budget is expected to remain constant for many decades. Therefore, it should be straightforward to use upper stratospheric N_2O data as a test for solar-terrestrial coupling through solar UV variations.

The time variation of N_2O concentrations for several altitudes is shown in Fig. D-10. The variation in N_2O is nearly in phase with the solar forcing function

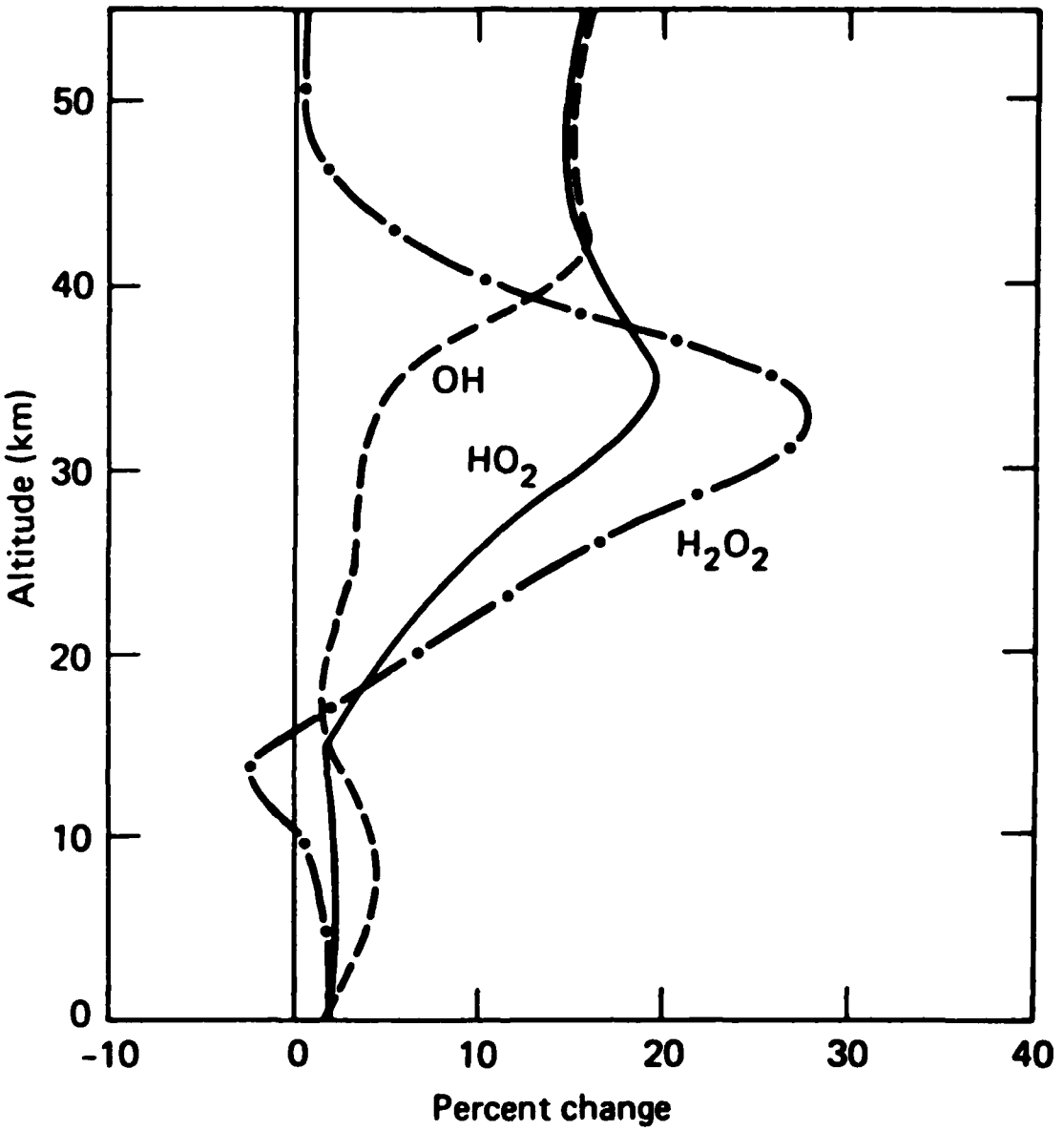

FIGURE D-9. Percent change for selected species in the HO_x family from solar minimum to solar maximum [(max-min)/min x 100].

at altitudes above 40 km. Below that level, the maximum and minimum concentrations occur well after the solar flux minimum and solar flux maximum. Near 35 km, the calculated delay is about 5 months. At 25 km it is 12 months, and below 20 km it becomes longer than 18 months, although at these levels the calculated variation is quite small (less than 1.4%). Because of this difference in

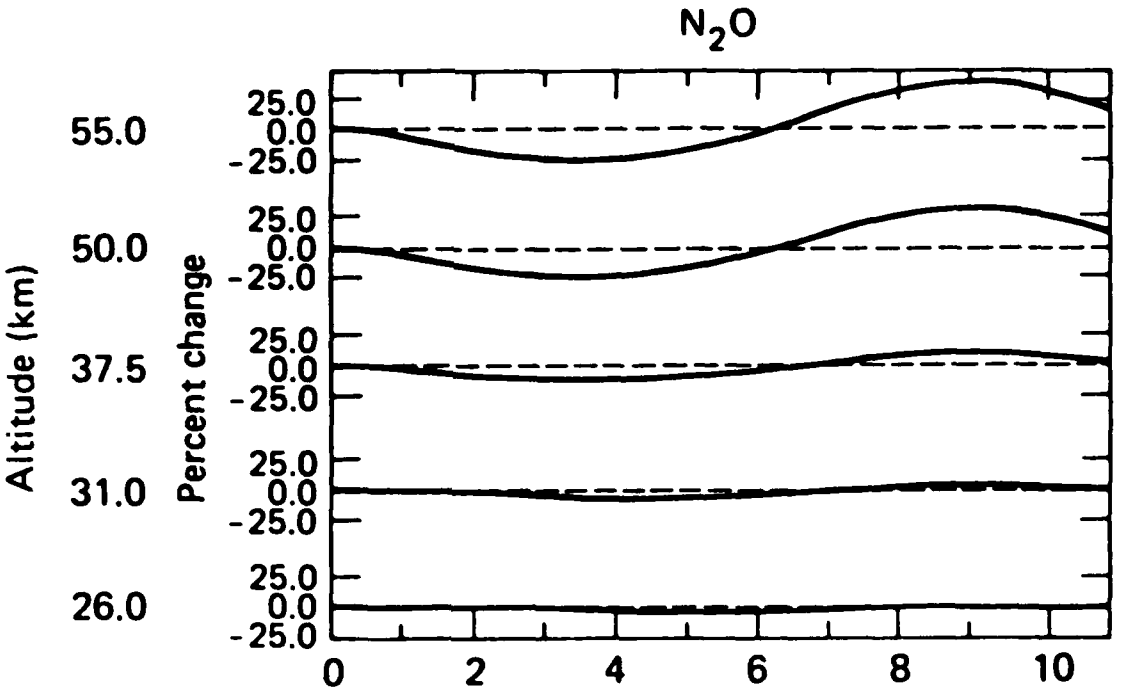

FIGURE D-10. Time variation of N_2O at selected altitudes. Solar maximum and minimum were at 2.75 and 8.25 years, respectively.

phase-lag at different altitudes, the integrated column density shows a much less clear signal for observation purposes. Similar remarks apply to the time variations of CH_3Cl and CH_4. Delays for CH_4 are somewhat longer than those of N_2O, but below 20 km the N_2O response is more delayed reflecting its longer chemical lifetime in the lower stratosphere. The delay response for CH_3Cl is less than that of either N_2O or CH_4 at all altitudes because its chemical lifetime is shorter. As with the discussion of O_3, these time lags below 30 km are a function of our one-dimensional parameterization of eddy transport and should not be interpreted as quantitative estimates of true atmospheric time lags.

OTHER TRACE SPECIES

HO_x (H + HO + HO_2 + $2H_2O_2$) is increased throughout the stratosphere as a result of the increase in $O(^1D)$. The main sources of HO_x are the reactions

$$O(^1D) + H_2O \rightarrow HO + HO \quad , \qquad k_9 \qquad (D.7)$$

$$O(^1D) + H_2 \rightarrow H + HO \quad , \qquad k_{25} \qquad (D.8)$$

$$O(^1D) + CH_4 \rightarrow CH_3 + HO \quad , \qquad k_{67} \qquad (D.9)$$

and

$$OH + CH_4 \rightarrow CH_3 + H_2O \quad , \qquad k_{64} \qquad (D.10)$$

followed by the subsequent degradation of CH_3 (see Table A-2). This results in increases for all of the species in the HO_x family throughout most of the stratosphere from solar minimum to solar maximum. The same is not true for the other families, NO_x ($N + NO + NO_2 + HNO_3 + NO_3 + 2N_2O_5 + ClONO_2$) and ClX ($Cl + ClO + HCl + ClONO_2$). The source of NO_x is approximately given by $2k_{67}[O(^1D)][N_2O]$. A comparison of the variation for $O(^1D)$ and N_2O in Figs. D-1 and D-8 shows that the net effect of increases in $O(^1D)$ and decreases in N_2O is a very slight increase in the production rate for NO_x. Total NO_x is increased by less than 4% at 40 km. The behavior of ClX is similar to that of NO_x. The enhanced photolysis coefficients for the source species, CF_2Cl_2, CCl_4, CH_3Cl, $CFCl_3$ at solar maximum is accompanied by a corresponding decrease in the source molecule concentrations resulting in only about $\pm$1% variation in ClO_x at all altitudes.

Even though the NO_x and ClX family concentrations are not greatly changed, large changes in individual trace species are calculated (Figs. D-11 and D-12). The reasons for the changes in local chemical balances among the short-lived species in each family can be fairly subtle because, in general, a large number of coupling reactions must be considered simultaneously. For example, consider the changes associated with the major NO_x species, HNO_3, NO, and NO_2. HNO_3 is decreased at solar maximum above 22 km due to increased photolysis, a major pathway for loss,

$$HNO_3 \xrightarrow{h\nu} HO + NO_2 \quad , \qquad J_7 \quad . \qquad (D.11)$$

Although the source of HNO_3, the three-body recombination of HO and NO_2,

$$HO + NO_2 + M \rightarrow HNO_3 + M \quad , \qquad k_{18} \qquad (D.12)$$

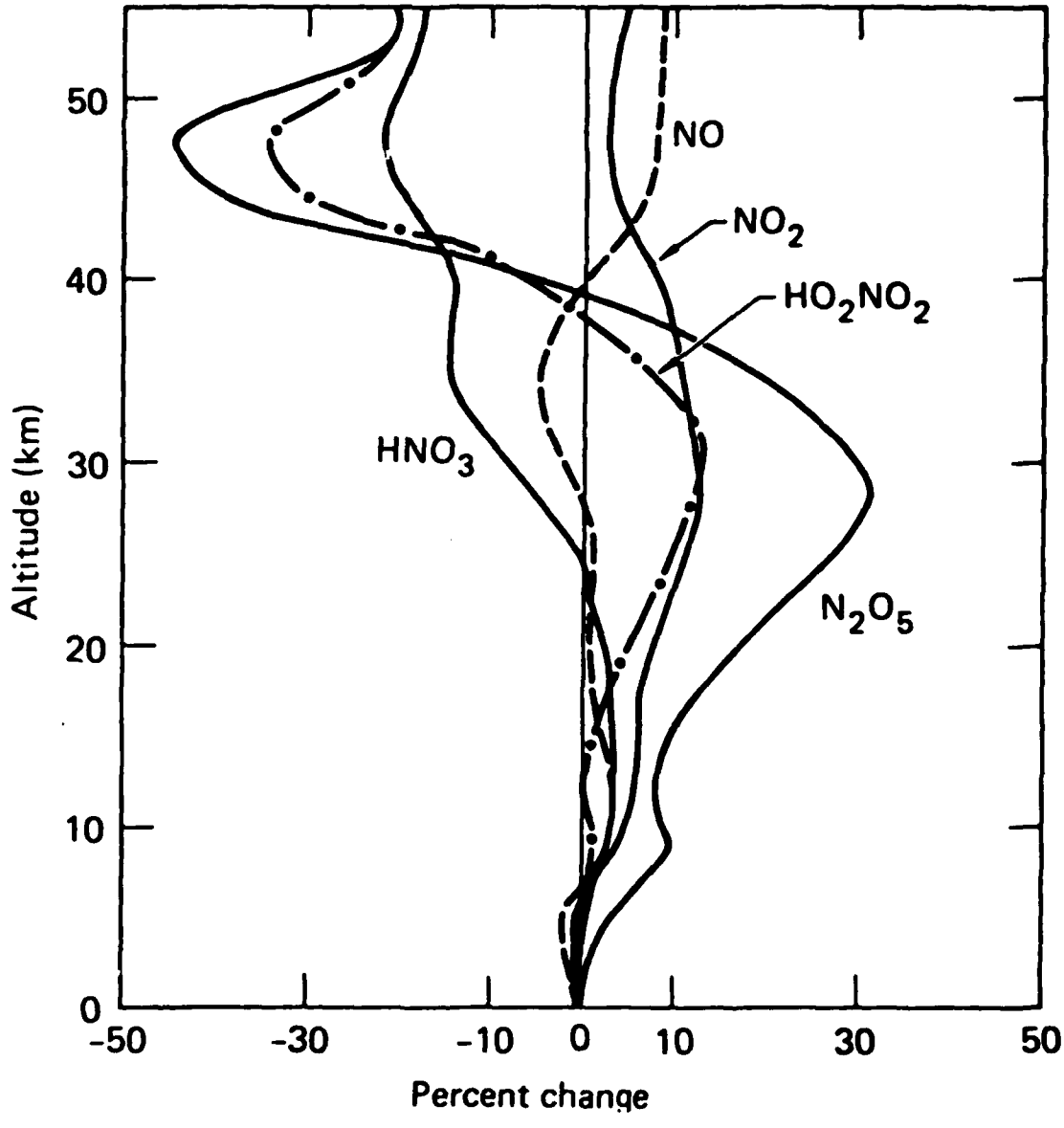

FIGURE D-11. Percent change for selected species in the NO_x family from solar minimum to solar maximum [(max-min)/min x 100].

is also larger at solar maximum (see changes in HO and NO_2 in Figs. D-9 and D-12), the increased rate of photolysis of HNO_3 actually dominates. Since total NO_x remains almost constant, a 10 to 20% decrease in HNO_3 will lead to an increase in the combined sum of NO and NO_2 above 22 km. The local partitioning of NO and NO_2 is given by

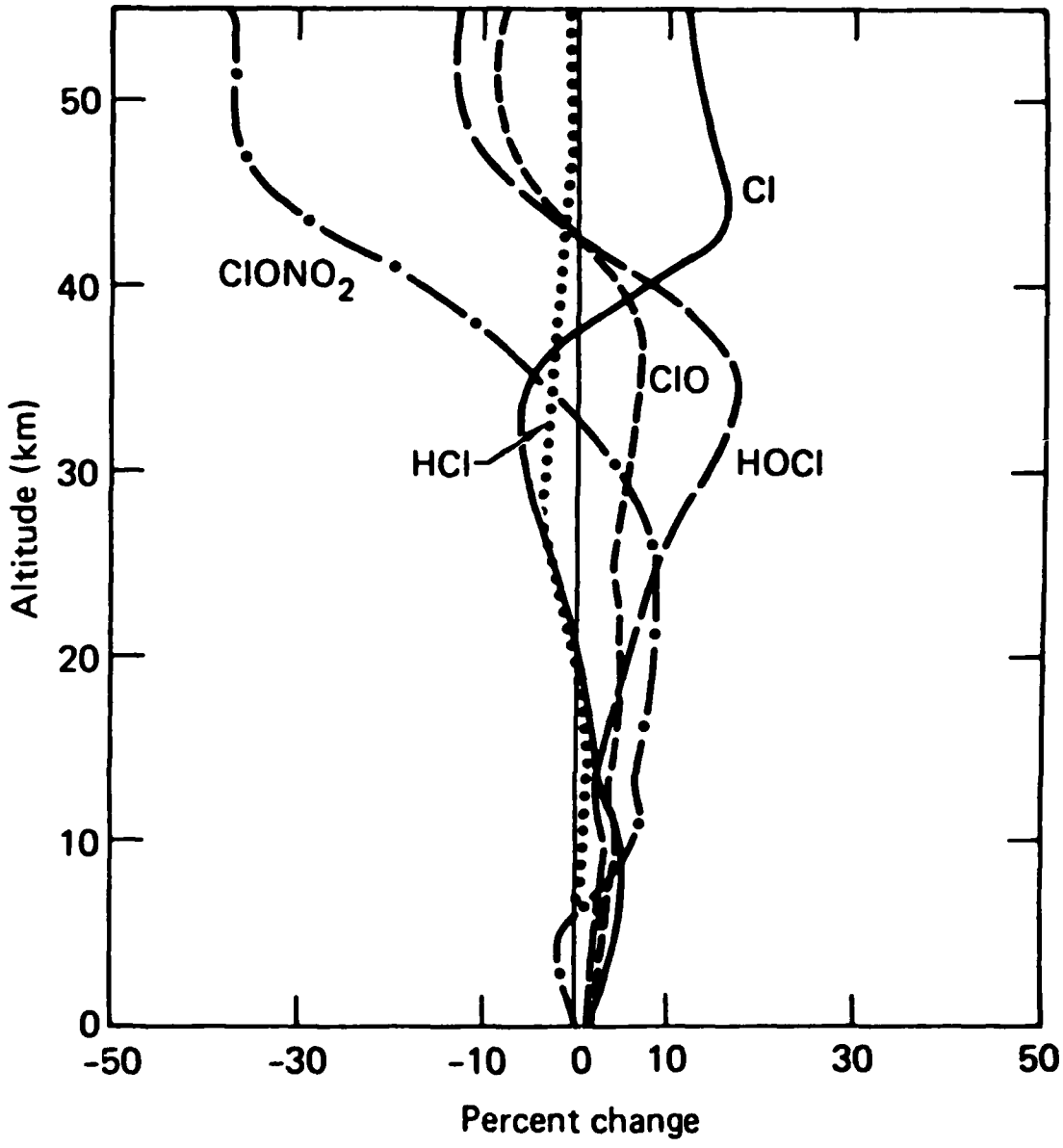

FIGURE D-12. Percent change for selected species in the ClX family from solar minimum to solar maximum [(max-min)/min x 100].

$$\frac{NO}{NO_2} = \frac{J_4 + k_4 [O]}{k_3[O_3] + k_{36}[ClO] + k_{24}[HO_2]}$$

from the reactions,

$$NO_2 + O \rightarrow NO + O_2 \quad , \qquad k_4 \qquad (D.13)$$

$$NO + O_3 \rightarrow NO_2 + O_2 \quad , \qquad k_3 \qquad (D.14)$$

$$NO + ClO \rightarrow NO_2 + Cl \quad , \qquad k_{36} \qquad (D.15)$$

$$NO + HO_2 \rightarrow NO_2 + HO \quad , \qquad k_{24} \qquad (D.16)$$

$$NO_2 + h\nu \rightarrow NO + O \quad , \qquad J_4 \quad . \qquad (D.17)$$

The net results of all the couplings are small increases for NO_2 at all altitudes and small decreases for NO between 30 and 40 km with increases above 40 km. These changes are mainly the result of the changes in O_3 concentrations and in J_4. For these species and others in the ClX and HO_x families, the magnitude of individual time variations are usually too small to be detected since they are often quite variable even on a diurnal and seasonal time scale. Even ratios such as NO/NO_2, Cl/ClO, HO/HO_2, etc. are not significantly better for long-term trend detection.

Changes in the concentrations of the major species in the ClO_x family are also driven by changes in several reactions and species. For example, increases in HO and HO_2 affect both the production and removal of HCl. Only direct fully coupled model calculations can provide the quantitative information represented in Fig. D-12. Although $ClONO_2$ shows a large percentage variation above 40 km, there is little $ClONO_2$ at these altitudes for detection. Similar general observations can also be made for the variations in HO, HO_2 and H_2O_2.

None of the short-lived species show significant solar cycle variations that are easily detectable because of the presence of all the coupling reactions and the balancing of many variations in reaction rates of similar magnitudes. Furthermore, the available instrumental accuracies for these species are in the range of 10-30% (WMO, 1977) which are either worse than or comparable to the expected maximum variations. Other species such as $ClNO_2$, NO_3, N_2O_5, H, and N included in this study are very difficult to measure. Therefore, they are of minor interest in the present analysis.

CONCLUSIONS

The variations of stratospheric trace species under the influence of hypothetical solar UV flux variations have been studied. The results may be used to guide observation strategies with a view toward verifying the validity of the assumed 11-year solar cycle influence on the earth's atmosphere. The possible candidates for this use are those species with the largest local solar cycle variations and whose response is directly due to the changing solar UV fluxes, such as N_2O, O_3, CH_4, HNO_3, CCl_4, $CFCl_3$, CF_2Cl_2, and CH_3Cl. The lifetimes for these species above 40 km are sufficiently short so their response is in phase with the changes in solar UV fluxes. Of course, seasonal varitions of these trace species in the upper stratosphere will also be fairly large and may partially obscure the expected variations. Since the seasonal change in solar conditions is well quantified, we can monitor this change and remove its effect from the trend analysis. Due to the currently available instrumental accuracy and the changing source functions for CFMs, N_2O is the best candidate.

The possibility of long-term temperature variations driving ozone variations independent of solar UV is far from settled because different data appear to give conflicting results. For this reason and in order to further validate the solar variations, long-term monitoring of high altitude (above 40 km) N_2O is particularly attractive.

REFERENCES

Angell, J. K. and J. Korshover, "Global Ozone Variations: An Update into 1976," Mon. Wea. Rev., 106, 725, 1978a.

Angell, J. K. and J. Korshover, "Recent Rocketsonde-Derived Temperature Variations in the Western Hemisphere," J. Atmos. Sci., 35, 1758-1764, 1978b.

Chandra, S., D. M. Butler and R. S. Stolarski, "Effect of Temperature Coupling on Ozone Depletion Prediction," Geophys. Res. Letters, 5, 199-202, 1978.

Ehhalt, D. H., L. E. Heidt, R. H. Lueb, and W. Pollack, "The Vertical Distribution of Trace Gases in the Stratosphere," PAGEOPH, 113, 389, 1975.

Nicolet, M., "Stratospheric Ozone: An Introduction to Its Study," Rev. Geophys. Space Phys., 13, 593-636, 1975.

Penner, J. E. and J. S. Chang, "Possible Variations in Atmospheric Ozone Related to the Eleven-Year Solar Cycle," Geophys. Res. Letters, 5, 817, 1978.

Penner, J. E. and J. S. Chang, "The Relation Between Atmospheric Trace Species Variabilities and Solar UV Variability," Lawrence Livermore Laboratory Report UCRL-83029, 1979, submitted for publication.

Quiroz, R. S., "Stratospheric Temperature During Solar Cycle 20," J. Geophys. Res., 84, 2415-2420, 1979.

Stanulonis, S. F. and J. W. Chamberlain, "Thermal Response to Ozone Fluctuations of the Stratosphere," J. Geophys. Res., 83, 6221-6223, 1978.

World Meteorological Organization, "Report of the Meeting of Experts on Measurements of Rare Species Relevant to the Ozone Budget," August 1977.

AD-A085 128 CALIFORNIA UNIV LIVERMORE LAWRENCE LIVERMORE LAB F/G 21/5
POTENTIAL ENVIRONMENTAL EFFECTS OF AIRCRAFT EMISSIONS.(U)
OCT 79 F M LUTHER, J S CHANG, W H DUEWER W-7405-ENG-48
UNCLASSIFIED UCRL-52861 FAA/EE-79-23 NL

3 · 3
AD
A085128

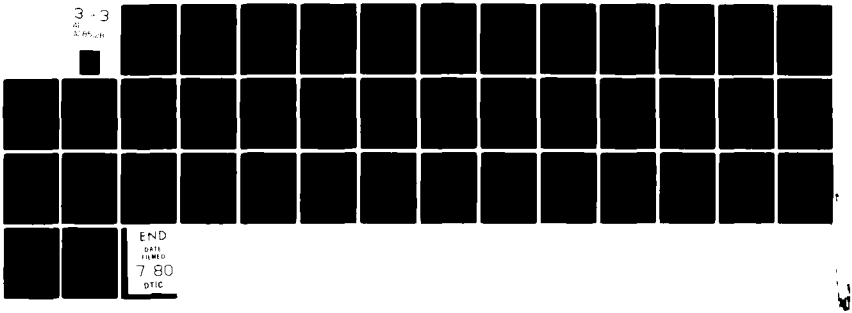

END
DATE FILMED
7 80
DTIC

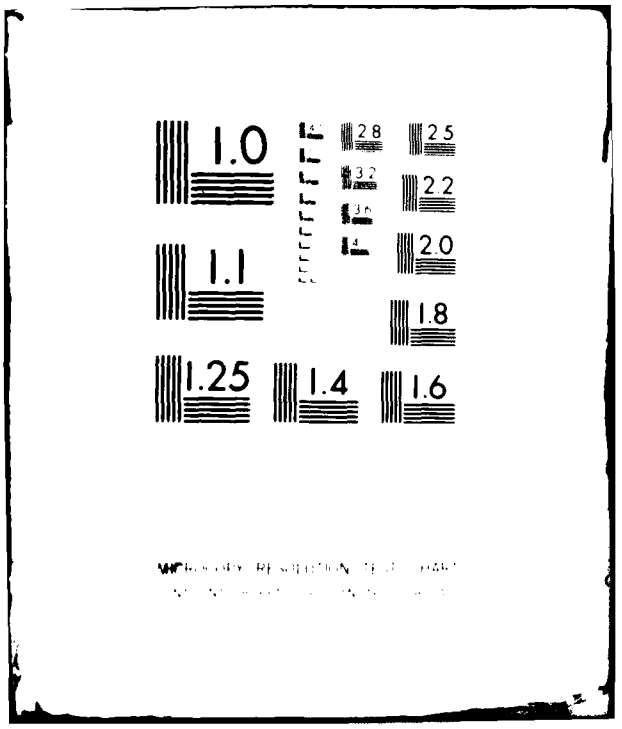
1.0
1.1
1.25
1.4
1.6
2.8
3.2
3.6
2.5
2.2
2.0
1.8

APPENDIX E.
A THEORETICAL STUDY OF STRATOSPHERIC TRACE SPECIES VARIATIONS DURING A SOLAR ECLIPSE*

INTRODUCTION

Solar eclipses are known to affect measurable quantities in the upper atmosphere. Various workers have discussed the response of ionospheric electron and positive ion densities to an eclipse (Landmark et al., 1970; Marriott et al., 1972; Anastassiades, 1970).

Other studies have investigated the possibility of changes in stratospheric and mesospheric ozone during an eclipse. Stranz (1961), using a Dobson ozonometer, measured approximately a 4% increase in total ozone shortly after the maximum phase of an eclipse in which only about 80% of totality was reached. Hunt (1965) attempted to explain this total ozone increase by using Chapman reactions and the solar flux changes expected in the path of totality. Hunt found that at most an increase of only 0.6% is to be expected, and that ozone should be affected only above 45 km. In later observations, Randhawa (1968), Ballard et al. (1969), Randhawa (1973), Grasnick et al. (1974), and Osherovich et al. (1974) had come to mutually contradictory conclusions on ozone changes during solar eclipses; some observed ozone increases while others detected no changes. Clearly inconsistencies exist in the observations and in their utilization for validating ozone-related atmospheric chemistry as it is understood at present.

In addition to ozone observations, measurements of other minor constituents during a solar eclipse could provide validation of the short-lifetime chemistry in atmospheric models. Consequently, experiments for upcoming solar eclipses, when properly supported by theoretical analysis, could contribute significantly to our understanding of atmospheric chemistry. In fact, given the proper data on trace species concentrations during an eclipse, such measurements could provide a direct demonstration that currently proposed NO_x, HO_x and ClO_x catalytic cycles are indeed concurrently functioning in the stratosphere in the manner suggested by

*See Wuebbles and Chang (1979).

laboratory chemistry. While detailed measurements of diurnal variations could provide similar knowledge, the difference in time scale between the diurnal cycle and a solar eclipse event suggests that the latter event may provide a clearer picture for understanding.

The purpose of this study is to examine theoretically the expected effect of a solar eclipse on stratospheric minor constituents. Primary emphasis is given to the total eclipse which will occur over North America on February 26, 1979 (Fiala and Lukac, 1977). Variations similar to those computed for this particular case should be expected for other total eclipses.

METHODOLOGY

Fifty degrees north is the latitude at which totality is the longest ($\sim$3 minutes) for the February 1979 eclipse. In attempting to simulate typical expected atmospheric conditions for the February 26, 1979 solar eclipse, we modified the model by setting the temperature (Louis, 1974), tropospheric water vapor (Oort and Rasmussen, 1971), and the ozone distribution (Wilcox and Belmont, 1977) to 50^{o}N winter conditions. The latitude and the solar declination angle, necessary to calculate the solar zenith angle for photodissociation coefficients, were set to 50^{o} and -8.8^{o}, respectively.

While ozone in the model was held fixed for most calculations in order to simulate February 50^{o}N conditions, the model was also run with calculated ozone to examine the expected response of ozone to an eclipse. Our analysis has shown that fixing the ozone distribution does not significantly affect the temporal variations calculated for other species during the eclipse.

Assuming fixed total odd nitrogen and odd chlorine as calculated for midlatitudes, the model was run diurnally to equilibrium. The calculated daytime total column for NO_2 at 50^{o}N of 1.9×10^{15} molecules/cm^2 is consistent with the observations of Noxon (1979). The model had approximately 1.7 ppb of ClX and 17 ppb of NO_x at 40 km.

Solar flux variations during the eclipse were parameterized based on Hunt (1965). The eclipse was assumed to start at 9:30 a.m. and end at 12:00 noon, corresponding to the February 1979 eclipse for 50^{o}N in southern Canada. Totality

was assumed to occur for three minutes beginning at 10:43:30 a.m. Based on measurements of sky brightness during an eclipse (Velasquez, 1971; Dandekar and Turtle, 1971), the solar flux at totality was uniformly reduced to 10^{-4} of the unobscured flux. During the eclipse we assumed the solar flux to be proportional to the area of the unocculted sun. Limb darkening is a secondary effect that becomes important only near totality at which time the changes in trace species concentrations that are of interest are all near completion.

RESULTS AND DISCUSSION

Those species having chemical lifetimes less than a few hours should be expected to vary significantly from normal diurnal behavior during a solar eclipse. In this study, we emphasize the variations expected for those species most important to the chemistry of stratospheric ozone. Local concentrations of the species could be quite variable, and therefore we should focus on relative effects rather than their absolute magnitudes.

The model calculated response of ozone during an eclipse essentially agrees with Hunt (1965). A significant increase in O_3 is to be expected in the upper stratosphere and in the mesosphere because of the conversion of $O(^3P)$ to ozone through the reaction $O(^3P) + O_2 + M \rightarrow O_3 + M$ accompanied by decreased photolysis of O_2 and O_3. The maximum increase in O_3, found at the end of totality, was computed to be 15% and 45% at 50 and 55 km, respectively. Larger percent changes should be expected in the mesosphere. Since most of the atmospheric ozone is at lower altitudes in the stratosphere, an insignificant change in the total ozone column is to be expected.

Figure E-1 shows the variations expected during the eclipse in the concentration of NO and NO_2 at altitudes of 20, 30, and 40 km. The solid line indicates normal behavior from 9:00 a.m. to 2:00 p.m. local time, while the dotted line shows the change in concentration expected during the eclipse. The decreased solar flux results in the NO_2 photolysis rate decreasing during the eclipse. Also the rapid conversion of $O(^3P)$ to O_3 decreases the importance of $NO_2 + O(^3P) \rightarrow NO + O_2$. NO is then rapidly converted to NO_2 during the eclipse primarily by the reactions $NO + O_3 \rightarrow NO_2 + O_2$ and $NO + ClO \rightarrow NO_2 + Cl$.

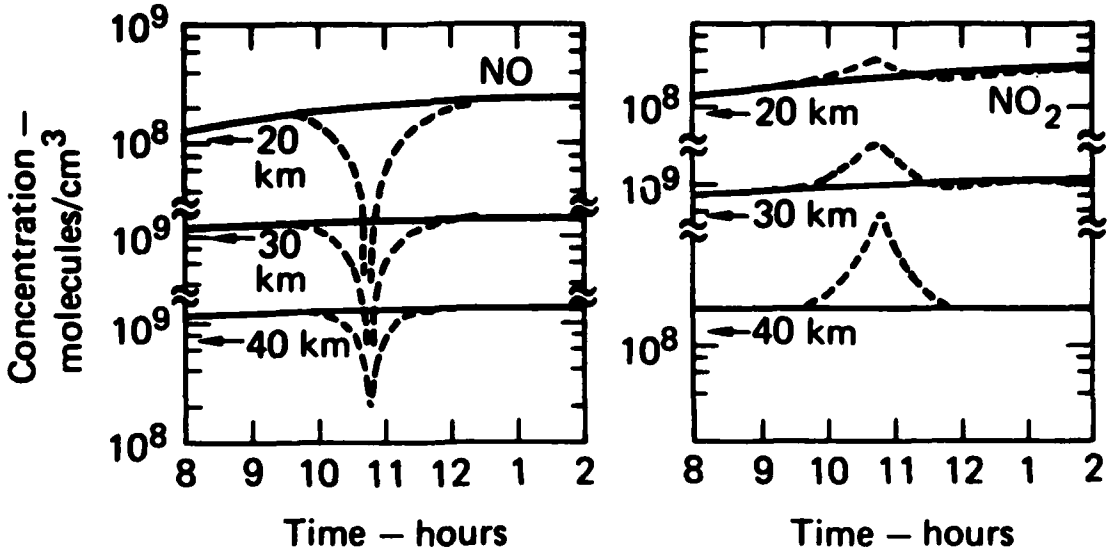

FIGURE E-1. Calculated responses of NO and NO_2 to a solar eclipse. The solid line indicates normal diurnal behavior; the dotted line shows the expected solar eclipse effect.

By the end of totality, over a factor of 10 decrease is calculated for NO at 20 and 30 km, with a factor of 6.5 decrease at 40 km. The maximum NO_2 concentration also occurs at the end of totality with values ranging from a factor of 1.4 higher than normal at 20 km to 6.4 at 40 km.

Except in the upper stratosphere (i.e., above 40 km), the NO_2 increase is not directly proportional to the NO decrease. This is due to the relatively slow, yet significant, formation rates for $ClONO_2$ and N_2O_5 from NO_2. The peak increase in the $ClONO_2$ concentration occurs approximately 15 minutes after totality due to its slow formation rate. $ClONO_2$ is increased by 20% at 20 km and 42% at 30 km. The N_2O_5 concentration increases by 11% at 20 km and 20% at 30 km. After the eclipse, the slow reconversion of stored $ClONO_2$ and N_2O_5 back to NO_2 lags behind the NO_2 to NO inversion causing the NO_2 to fall below the normal diurnal concentration. The NO to NO_2 conversion is not affected in the upper stratosphere where neither $ClONO_2$ nor N_2O_5 is important as a temporary sink for NO_2.

The expected variations for Cl and ClO are shown in Fig. E-2. Rapid conversion of Cl to ClO during the eclipse occurs primarily through $Cl + O_3 \rightarrow ClO + O_2$. However, as a result of the increased formation rate of $ClONO_2$ caused by increased NO_2 the net effect on the ClO concentration is a decrease. The

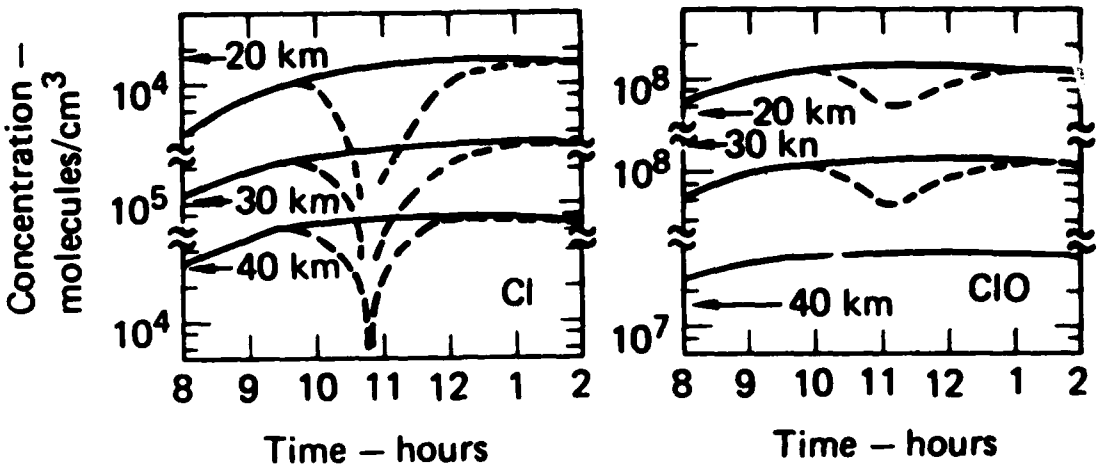

FIGURE E-2. Calculated response of Cl and ClO to a solar eclipse.

minimum in ClO occurs approximately 25 minutes after totality. This time lag is caused by the relatively slow formation rate of $ClONO_2$ when compared to the rate of change for NO_2. As the solar flux increases after totality, the ClO concentration increases due to increased photolysis of $ClONO_2$. Little change in ClO is expected at 40 km where $ClONO_2$ formulation is not important and Cl is only about 1% of ClO.

Both OH and HO_2 should decrease in concentration during an eclipse, as shown in Fig. E-3. OH concentrations were reduced relative to the normal diurnal

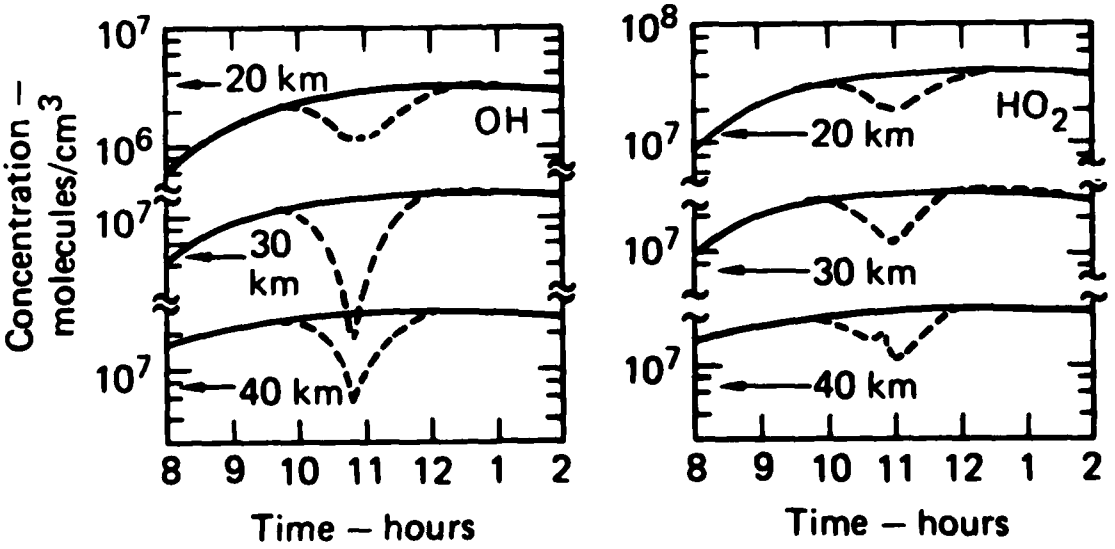

FIGURE E-3. Calculated response of OH and HO_2 to a solar eclipse.

concentrations by factors of 2.7, 17.0, and 5.9 at 20, 30, and 40 km, respectively, with the minimum occurring at the end of totality. Smaller decreases are calculated for HO_2, with the minimum in HO_2 occurring approximately 15 minutes after totality. With the decreased importance of $O(^3P)$ and NO during the eclipse, a balance between OH and HO_2 is maintained by the rapidly occurring reaction $OH + O_3 \rightarrow HO_2 + O_2$ and the slightly slower reaction $HO_2 + O_3 \rightarrow OH + 2O_2$. Odd hydrogen (OH and HO_2) loss occurs at a slower rate through conversion to H_2O ($OH + HO_2$), H_2O_2 ($HO_2 + HO_2$) and HNO_3 ($OH + NO_2 + M$). Because of the relative abundance of HNO_3 and H_2O_2 when compared to OH and HO_2, insignificant changes in the concentrations of H_2O_2 and HNO_3 were calculated. At 40 km, the relative speed of reactions for $HO_2 + O_3$ and $OH + O_3$ is at least a factor of 3 less than at 20 and 30 km. Because of this, a slight, probably artificial and not measurable, increase in HO_2 is calculated at totality (Fig. E-3).

Although we have focused mainly on the local changes at individual altitudes, clearly total column changes are also observable. Since the variations for individual species at all altitudes all follow the same general individual trends, the total column for them also varies in the same manner. For example, the ClO column shows the same approximately 25-minute delay in reaching minimum as is shown in Fig. E-2 with a factor 1.8 decrease. The NO_2 column shows a factor 2 increase at totality and the same overshoot phenomenon after totality by as much at 10%. OH and HO_2 columns at minimum are factors of 3.4 and 2.5 less with the HO_2 column showing a slight phase lag from totality. The Cl and NO columns obviously provide the most notable changes (disappear completely) and should be most easily observed.

SUMMARY AND CONCLUSIONS

The results from this study suggest that significant and detectable variations are expected for some of the important stratospheric minor constituents during a solar eclipse. Such observations, particularly simultaneous observations of trace species, would demonstrate clearly the simultaneous functioning of the various important photochemical catalytic cycles in the stratosphere. In principle, similar

information can be obtained by observations during a normal diurnal cycle, especially during sunrise and sunset. However, observations during a solar eclipse offer several advantages over that of the diurnal cycle. First, the relatively short time duration for the event allows a more clear identification of some of the major reactions in the important catalytic cycles. The same short time duration (2-3 hours) also minimizes the influence of atmospheric transport process in altering the local trace species concentrations. Measuring the full diurnal cycle would involve a much longer observation period (at least 14 and as much as 24 hours) subjecting the local chemistry to the influence of significant and usually unquantifiable mixing processes. Thus it is difficult to assess the relative role of chemistry and dynamics in determining the observation data. Also, because of the longer time scale, more interference through conversion to such temporary sinks as $ClONO_2$, N_2O_5 and HNO_3 should be expected. This increased interference makes it even more difficult to sort out the effects of the catalytic cycle reactions. Also, at sunrise and sunset there is considerable uncertainty on the proper treatment for the direct and scattered solar flux as a function of altitude. This then leads to uncertainty in the representation of photodissociation processes in the theoretical calculations. For the present calculation this will not be a limitation on the model, i.e., the eclipse takes place near local noontime.

We would like to emphasize the point that the present theoretical predictions should be viewed mostly in a qualitative sense. The relative changes in magnitudes at totality and the phase lag in maximum effect from the time of totality are the interesting parameters. Of course the precise predictions are totally dependent upon the local conditions such as temperature, total NO_x, ClO_x, HO_x, etc. direct and scattered radiation, time of the day, and local atmospheric motions (which must be measured). Depending on the measurement technique the individual data may be more dependent upon a particular set of local variables. For example, surface instruments would be highly sensitive to atmospheric transport of air masses while airborne instruments are much less so, and the rate of observed changes in NO_2 are sensitive to the yet to be measured rate of change of near ultraviolet solar fluxes while Cl and ClO are not.

We have pointed out the potential usefulness of solar eclipse events in testing our understanding of stratospheric chemistry. But the quality of the test depends upon the measurement program established. Given sufficient data on local

conditions, more precise calculations than our present preliminary results might be carried out to more fully test our understanding of stratospheric chemistry.

REFERENCES

Anastassiades, M., editor, Solar Eclipses and the Ionosphere, Plenum Press, 1970.

Ballard, H. N., R. Valenzuela, M. Izquierda, J. S. Randhawa, P. Morla, and J. F. Fettle, "Solar Eclipse: Temperature, Wind and Ozone in the Stratosphere," J. Geophys. Res., 74, 711-712, 1969.

Dandekar, B. S. and J. P. Turtle, "Day Sky Brighness and Polarization During the Total Solar Eclipse of 7 March 1970," Appl. Optics, 10, 1220-1224, 1971.

Fiala, A. D. and M. R. Lukac, "Total Solar Eclipse of 26 February 1979," U. S. Naval Observatory Circular No. 157, 1977.

Grasnick, K. H., H. Worner and P. Plessing, "Ozon Variationen uber Havanna Wahrend der Sonnenfinsternis vom 7 Morz 1970 Unter Berichsicktigung der Randverdunkelung," Geodatische und Geophysikalische Veroffentilichungen, 2, 87-101, 1974.

Hunt, G. G., "A Theoretical Study of the Changes Occurring in the Ozonosphere During a Total Eclipse of the Sun," Tellus, 18, 516-523, 1965.

Landmark, R., A. Haug, E. V. Thrane, J. E. Hall, A. P. Willmore, M. Jespersen, B. Moller Pendersen, M. Anastassiades, E. Tsagakis, and J. A. Kane, "Ionospheric Observations During the Annular Solar Eclipse of 20 May 1966 - V. Interpretation of Observed Results," JATP, 32, 1873-1883, 1970.

Louis, J. F., "A Two-Dimensional Transport Model of the Atmosphere," Ph.D. Thesis, University of Colorado, 1974.

Marriott, R. T., D. E. St. John, R. M. Thorne and S. V. Venkatesworan, "Ionospheric Effects of Two Recent Solar Eclipses," JATP, 34, 695-712, 1972.

Noxon, J. F., "Stratospheric NO_2, II. Global Behavior," to be published in J. Geophys. Res., 1979.

Oort, A. H. and E. M. Rasmussen, "Atmospheric Circulation Statistics," NOAA Professional Paper 5, 1971.

Osherovich, A. L., N. S. Shpakov, and V. T. Zarubaylo, "Measurement of Total Ozone Content During the Total Solar Eclipse of 10 July 1972," Atmos. Oceanic Phys., 10, 1221-1224, 1974.

Randhawa, J. S., "Mesospheric Ozone Measurements During a Solar Eclipse," J. Geophys. Res., 73, 493-495, 1968.

Randhawa, J. S., "An Investigation of Solar Eclipse Effects on the Subpolar Stratosphere," J. Geophys. Res., 78, 7139-7144, 1973.

Stranz, D., "Ozone Measurements During Solar Eclipse," Tellus, 13, 276-279, 1961.

Velasquez, D. A., "Zenith Sky Brighness and Color Change During the Total Solar Eclipse of 12 November 1966 at Santa Ines, Peru," Appl. Optics, 10, 1211-1214, 1971.

Wilcox, R. W. and A. D. Belmont, "Ozone Concentration by Latitude, Altitude, and Month, Near 80°W," Department of Transportation Report No. FAA-AEQ-77-13, 1977.

Wuebbles, D. J. and J. S. Chang, "A Theoretical Study of Stratospheric Trace Species Variations During a Solar Eclipse," Geophys. Res. Letters, 6, 179-182., 1979.

APPENDIX F.
THE ATMOSPHERIC NUCLEAR TESTS OF THE 1950's AND 1960's: A POSSIBLE TEST OF OZONE DEPLETION THEORIES*

INTRODUCTION

It was suggested by Foley and Ruderman (1973) that the atmospheric nuclear tests of the late 1950's and early 1960's should have caused a stratospheric ozone reduction of more than 10% if then current models of the effect on stratospheric ozone of NO_x from SST's were correct. However, their analysis failed to consider the difference in the effect to be expected from a pulse injection of NO_x in contrast to the effect of a continuous NO_x source active over a more restricted altitude range. In 1973, Chang and Duewer, using a one-dimensional time-dependent model, calculated the effect on ozone of the nuclear tests (using a production of NO_x/megaton yield about half that used by Foley and Ruderman, but spread over only the Northern Hemisphere rather than the world) and obtained a calculated Northern Hemispheric annual mean ozone reduction of roughly 4% for 1963. Using a different technique Johnston et al. (1973) had calculated a 1-6% decrease at peak ozone reduction where the range cited refers to their estimated uncertainty in NO_x production. Chang and Duewer concluded that the calculated reduction was not inconsistent with the observed variability of atmospheric ozone as analyzed by Johnston et al. (1973). The effects of the test series were also investigated by Goldsmith et al. (1973), COMESA (1975), and Bauer and Gilmore (1975). On the basis of calculations of the ozone depletion expected from operation of Concordes made with their then current models, Goldsmith et al. and the COMESA Report concluded that ozone reductions of several percent (Goldsmith et al., 1973) but less than 2% (COMESA, 1975) would have been expected, and that no reduction was apparent in the ozone record. The differences between these estimates reflected differences between their 1973 and 1975 models, largely in chemical reactions and rate coefficients. Bauer and Gilmore reviewed the calculations and analyses

*See Chang et al. (1979).

available in 1975 and concluded that the predicted ozone reductions fall within the variability of the ozone record.

In the years since 1975, significant changes have occurred in the formulation of one-dimensional models of the stratosphere and in the experimental values of chemical reaction rate constants used as model input. Also, substantially more analysis of the ozone record has been carried out. In this paper, we discuss the effect several of these advances have on the computed effect of the atmospheric nuclear test series on stratospheric ozone. Although the present discussion focuses only on the nuclear test series and the long-term ozone trend in the 1960's, there have been other studies of the near-term effect of individual nuclear NO_x clouds on ozone on the time scale of days to weeks (Christie, 1976; Johnston, 1977). Furthermore, analysis of the potential effects of large scale nuclear exchange in a doomsday scenario have been performed (Hampson, 1974; MacCracken and Chang, 1975; NRC, 1975; Whitten et al., 1975; Duewer et al., 1978).

DESCRIPTION OF THE NO_x PERTURBATION

Several workers have investigated the problem of NO_x production from a nuclear fireball (see Table F-1). The most recent and comprehensive of these are those of Gilmore (1975) and COMESA (1975). As can be seen in Table F-1, these two studies are in good agreement as to their estimates for the total NO_x produced by a nuclear explosion. However, the COMESA study included an estimate of loss of NO_x from the rising debris cloud (i.e., 20% loss). In this work we accept the COMESA estimate of the total NO_x injection per megaton, but note that this value should be considered uncertain by roughly $\pm$50%. A related question is that of the yields of the various nuclear devices. Table F-2 gives several published estimates of the total yield for the period of active testing.

We have followed the procedure of taking unclassified qualitative yield descriptions and assigning them quantitative values consistent with other available data. Our integrated yield estimate for the period 1961-1962 is consistent with the estimates given by COMESA (1975) and Foley and Ruderman (1973) but roughly 10% larger than those cited by Johnston et al. (1976) or Seitz et al. (1968).

TABLE F-1. Estimates of NO yield per MT

		10^{32} molecules/MT
Zeldovich and Razier	(1967)	0.5
Foley and Ruderman	(1972)	0.3-1.5
Johnston et al.	(1973)	0.17-1.0
Chang and Duewer	(1973)	0.5
Goldsmith et al.	(1973)	1.0
Gilmore	(1975)	0.4-1.5 (.9)
COMESA - (Goldsmith et al.)	(1975)	0.6-1.1 (.84)
COMESA - after allowance for disentrainment	(1975)	0.5-0.9 (.67)
This work uses		0.67

During the test period, a few nuclear devices were exploded in or above the stratosphere and generated clouds that stabilized in or above the mesosphere. These tests may have created more NO_x/megaton than low altitute tests because a low density fireball can be expected to depart from equilibrium composition at a higher temperature than a higher-density fireball. Thus, it might be argued (Hampson, 1977) that these devices could have produced a very high yield of NO at altitudes of 70-200 km. However, in that altitude range, NO_x has a lifetime on the order of a day (Gerard and Barth, 1977), and it is unlikely that any significant fraction of NO_x produced at high altitudes reached the stratosphere. Further, while energetic particles escaping from a high-altitude fireball might produce NO_x in the stratosphere, it is unlikely that this process had a significant effect on the yields of NO_x summed over all tests.

The model perturbations are small enough that model response to variation of the total NO_x injection is approximately linear for most chemistries. Thus, if a readjustment of the NO_x yield should be dictated by future work, our computed ozone perturbations would, to a fair approximation, scale linearly. Post-1977 one-dimensional models display near-linear response to NO_x perturbation over a more limited range than earlier models. For NO_x perturbations somewhat larger

TABLE F-2. Approximate total yield of high yield* atmospheric nuclear tests by year.

	COMESA (1975)	Foley & Ruderman (1973)	Johnston et al. (1976)	Seitz et al. (1968)	This** Work
Pre-1956	61.6	62	—	—	—
1956	26.0	26	—	—	20
1957	13.5	85	—	—	16
1958	61.9		—	—	58
1959	0	0	—	—	0
1960	0	0	—	—	0
1961	120.6	340	99.7	97	119
1962	213.5		204	206	216
1963	—	—	—	—	—
1964	—	—	—	—	—
1965	—	—	—	—	—
1966	1.4	—	—	—	—
1967	3.5	—	—	—	—
1968	7.6	—	—	—	—
1969	3.0	—	—	—	—
1970	6.1	—	—	—	—
Total 1961-62	334	340	304	303	335
Total 1956-62	435	451	—	—	429

*1 megaton TNT equivalent (4.2×10^{15} joules).
**These yield figures were estimated by taking the unclassified qualitative yield descriptions and assigning them quantitative values consistent with other available data in the open literature.

than those reported here, nonlinear feedback must be analyzed in detail. The onset of this nonlinear behavior depends on the altitude of injection, vertical diffusion coefficients, photochemical kinetics systems, rate coefficients and other model input parameters.

Foley and Ruderman (1972; 1973) gave a parameterization for the top and bottom of the stabilized cloud versus device yield such that

$$CT = 21.64Y^{(0.2)}$$

$$CB = 13.41Y^{(0.2)}$$

where CT - cloud top (km)
CB - cloud bottom (km)
Y - yield (megatons TNT equivalent)

This parameterization was largely based on direct observations of United States tests (Peterson, 1970) and was only inferred to be valid for the Soviet tests.

Seitz et al. (1968) estimated cloud tops and bases from measurements of the radioactive debris a few days after the 1961-1962 tests. Few of the debris measurements extended above 24 km, and the cloud tops for most of the higher yield tests were not directly measured. When samples were taken near 30 km shortly after a high-yield test, the cloud top was estimated to be above 30 km. However, when no data above 24 km were available, a cloud top near 24 km was given (Seitz et al., 1968). This procedure is quite arbitrary and may not be consistent with other available results. For example, from an analysis of the ratio of ^{14}C to ^{90}Sr, Telegadas and List (1969) concluded that the very large Soviet test of October 1961 probably stabilized almost entirely above the region examined by Seitz et al. Also, mesospheric lithium, ^{7}Li, increased after this test implying a cloud top above the stratopause (Martell, 1970; Sullivan and Hunten, 1964). Nevertheless, the data of Seitz et al. provide the only published systematic estimates of the debris cloud stabilization heights of the Soviet tests in the 1960's and as such must be considered along with any other choices. We believe that these data systematically underestimate (at least) the cloud tops, and we view them as probably a lower limit to the true stabilization heights.

The height parameterization of Foley and Ruderman (1973) as used in earlier reports (Chang and Duewer, 1973; MacCracken and Chang, 1975) may over-estimate the height of stabilization since it is based almost exclusively on data from the tropics. However, it provides a reasonable fit to data for moderate-yield mid-latitude tests (Telegadas, 1976). Figure F-1 presents the stabilization estimates from the two different methodologies.

We assumed the injection to result in a uniform increase in concentration between cloud top and cloud bottom. When we used Seitz et al. (1968) injection

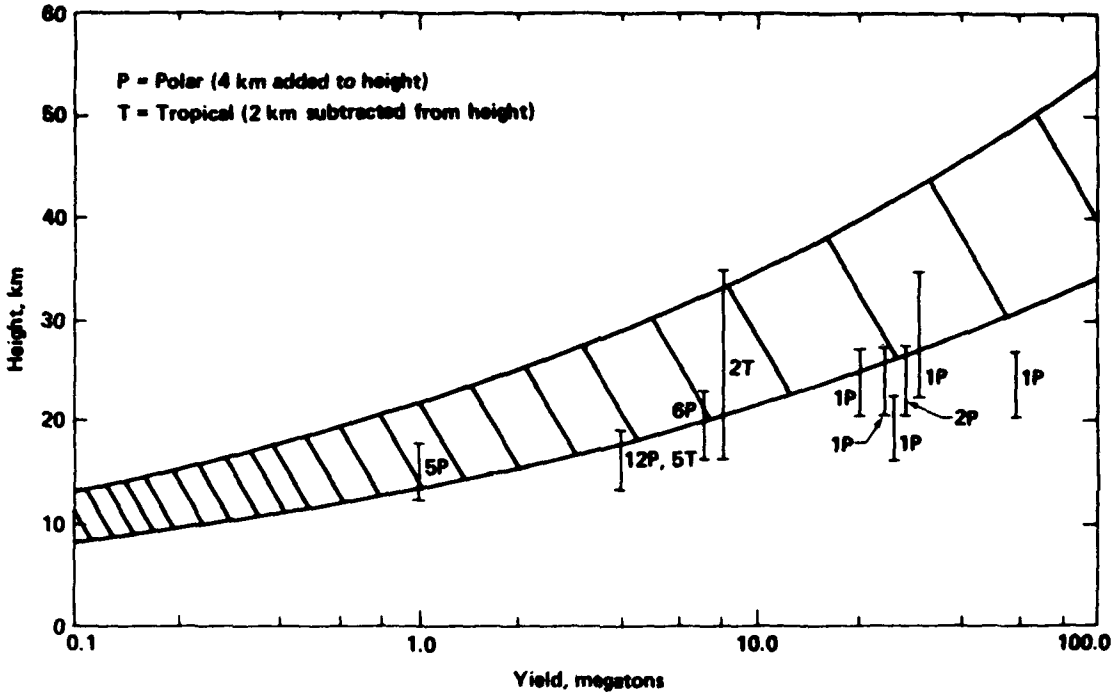

FIGURE F-1. Cloud top and cloud base vs. yield for the treatments used. The curves defining the shaded area give the cloud top and cloud base according to the parameterization of Foley and Ruderman (1972). The vertical bars extend from cloud base to cloud top for the data cited by Seitz et al. (1968) after adjustment to height above a variable tropopause as discussed in the text. The number of tests of a particular yield at high latitudes (indicated with a P) and at low latitudes (indicated with a T) is also given on the figure.

altitudes, we assumed that it was appropriate to adjust the injection to a constant height above the tropopause corrected to mid-latitude conditions (Johnston et al., 1976). Thus, we increased CT and CB by 4 km for polar tests and reduced them by 2 km for tropical tests. This was not done when the Foley and Ruderman parameterization was used because that parameterization was designed for mid-latitude applications and thus contains an implicit adjustment. We believe that these two treatments of the stabilization heights provide approximate upper and lower bounds for the stabilization altitudes of the test debris. As we will show (Fig. F-2 and Table F-3), the computed ozone reductions in the peak year (1963) are larger by about 1-2% of total O_3 when we use the Foley and Ruderman (1973) parameterization than when we use Seitz et al. (1968) estimates.

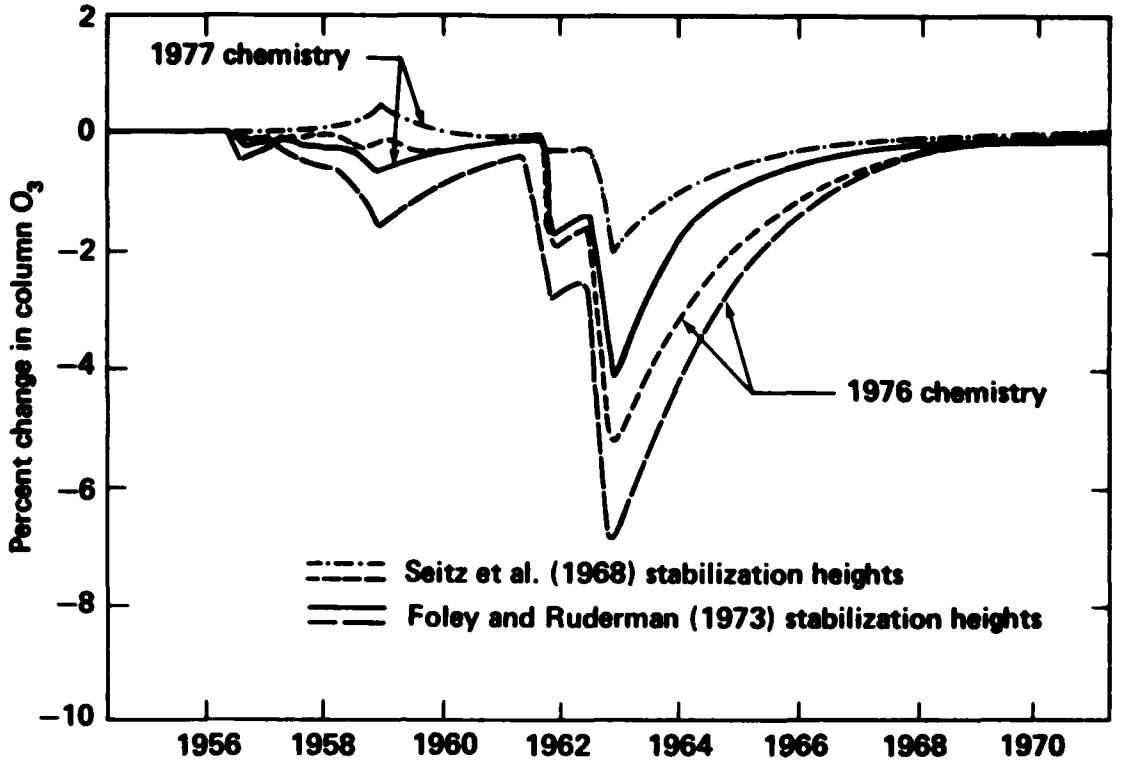

FIGURE F-2. Calculated change in O_3 vs. date showing the effect of the treatment of cloud stabilization height. - · - · - Seitz et al. (1968) stabilization height, 1977 chemistry; - - - Seitz et al. (1968) stabilization height, 1976 chemistry; _____ Foley and Ruderman (1973) stabilization height, 1977 chemistry; — — — Foley and Ruderman (1973) stabilization height, 1976 chemistry. All calculations used the Chang (1976) K_z and diurnal averaging.

In all calculations the injection was assumed to be mixed throughout the Northern Hemisphere, and no further dilution was considered. Mixing into the Southern Hemisphere might have reduced the NO_x perturbation by 15-25% in 1963-64 (Johnston et al., 1976). A simplified treatment of mixing within the Northern Hemisphere is necessary in one-dimensional models. With such approximations short-term effects (in weeks or months) of individual tests could not be analyzed. But on the time scale of years to a decade, individual initialization error in horizontal spreading would have decayed. Thus the uniform horizontal spreading approximation seems reasonable.

TABLE F-3. Effects Calculated for Various Model Inputs.

Chemistry	K_z	Stabilization Parameterization	Other Variations	$\Delta O_{3_{max}}$	$\langle \Delta O_3 \rangle_{1963}$	$\langle \Delta O_3 \rangle_{1964}$
1973	Chang (1974)	Foley & Ruderman	0.5×10^{31} NO (megaton, Bates & Hayes (1967) N_2O, NO multiple scattering)	-5.0	-4.0	-3.3
1973	Chang (1974)	Foley & Ruderman	0.5×10^{31} NO/megaton	-4.8	-3.8	-3.1
1973	Hunten (1975)	Foley & Ruderman	0.5×10^{31} NO/megaton	-5.3	-4.5	-3.9
1974	Chang (1974)	Foley & Ruderman	—	-8.2	-7.1	-6.2
1976	Chang (1976)	Foley & Ruderman	Diurnal averaging	-6.8	-4.5	-2.7
1976	Chang (1976)	Seitz et al.	Diurnal averaging	-5.1	-4.3	-2.6
1976	Chang (1976)	Foley & Ruderman	No diurnal averaging	-6.1	-4.2	-2.6
1976	Hunten (1975)	Foley & Ruderman	No diurnal averaging	-5.0	-3.9	-2.8
1976	Chang (1976)	Seitz et al.	No diurnal averaging	-4.3	-3.8	-2.5
1977	Chang (1976)	Foley & Ruderman	Diurnal averaging	-4.2	-3.0	-1.4
1977	Chang (1976)	Seitz et al.	Diurnal averaging	-1.9	-1.5	-0.8
1977	Hunten (1975)	Seitz et al.	Diurnal averaging	-1.8	-1.4	-0.7

THE MODEL

The general structure of the model used has been described elsewhere (Chang et al., 1974; Luther et al., 1978; NRC, 1976, Appendix D). We will describe only those features that have evolved significantly since 1973.

1. Model Chemistry

The model chemistry used in our 1973 calculation contained 33 reactions of HO_x, NO_x and O_x, with rate constants based primarily on Garvin and Gevantman (1972). These are given in Table F-4 as 1973 chemistry. When the CIAP calculations were carried out (1974) we incorporated the 41 reactions listed as 1974 chemistry in Table F-4. Most rate constants were taken from Garvin and Hampson (1974).

Our 1976 chemistry (Table F-4) incorporated ClX reactions and was nearly the same as was used in the NAS chlorofluoromethane report (NRC, 1976). Most of the rate constants were derived from Hampson and Garvin (1975), but several had been revised to reflect 1975 or 1976 measurements (NRC, 1976; DeMore et al., 1977). Our 1977 chemistry (Table F-4) contains the same reactions as our 1976 chemistry, but several rate constants were adjusted to reflect recent evaluations (DeMore et al., 1977: Watson, 1977) and measurements (Howard and Evenson, 1977; Burrows et al., 1977; Chang and Kaufman, 1978). There are some known processes of potential importance (e.g., HOCl and $HOONO_2$ formation) that we do not include because the important subsequent processes (e.g., photolysis rates and products) are insufficiently well characterized.

As we will show, the predicted effect of the nuclear test series is quite sensitive to model chemistry. For this study the model contained 1.1-1.3 ppb of ClX (the precise amount is a function of the transport parameterization) from CH_3Cl and CCl_4, but chlorofluoromethanes were neglected.

TABLE F-4. Chemistries Used in This Study.

Reaction	Rate 1977	Rate 1976	Rate 1974	Rate 1973
$O_2 + h\nu \rightarrow O + O$	QJ(1)*	QJ(1)	Same	QJ(1) x 2
$O_3 + h\nu \rightarrow O + O_2$	QJ(2)*	QJ(2)	Same	QJ(2) x 2
$O_3 + h\nu \rightarrow O(^1D) + O_2$	QJ(3)*	QJ(3)	Same	QJ(3) x 2
$O + O_2 + M \rightarrow O_3 + M$	$1.10\times10^{-34}\ e^{510/T}$	$1.07\times10^{-34}\ e^{510/T}$	Same	Same
$O + O_3 \rightarrow 2O_2$	$1.9\times10^{-11}\ e^{-2300/T}$	Same	Same	Same
$NO_2 + h\nu \rightarrow NO + O$	QJ(4)*	QJ(4)	Same	QJ(4) x 2
$O_3 + NO \rightarrow NO_2 + O_2$	$2.1\times10^{-12}\ e^{-1450/T}$	$9.0\times10^{-13}\ e^{-1200/T}$	Same	Same
$O + NO_2 \rightarrow NO + O_2$	9.1×10^{-12}	Same	Same	Same
$N_2O + h\nu \rightarrow N_2 + O(^1D)$	QJ(5)*	QJ(5)	Cross sections were larger	QJ(5) x 2 (larger cross sections)
$N_2O + O(^1D) \rightarrow N_2 + O_2$	5.5×10^{-11}	7×10^{-11}	1.1×10^{-10}	6.6×10^{-11}
$N_2O + O(^1D) \rightarrow 2NO$	5.5×10^{-11}	7×10^{-11}	1.1×10^{-10}	6.6×10^{-11}
$NO + h\nu \rightarrow N + O$	QJ(6)	QJ(6)	Same	QJ(6) x 2
$N + O_2 \rightarrow NO + O$	$5.5\times10^{-12}\ e^{-3220/T}$	$1.1\times10^{-14}\ T\ e^{-3150/T}$	Same	$1.02\times10^{-14}\ T\ e^{-3130/T}$
$N + NO \rightarrow N_2 + O$	$8.2\times10^{-11}\ e^{-410/T}$	2.7×10^{-11}	Same	$5.1\times10^{-11}\ e^{-170/T}$
$O(^1D) + H_2O \rightarrow 2OH$	2.3×10^{-10}	2.1×10^{-10}	3.5×10^{-10}	2.8×10^{-10}
$O(^1D) + CH_4 \rightarrow OH + CH_3$	1.3×10^{-10}	Same	4.0×10^{-10}	2.4×10^{-10}

TABLE F-4. Continued

Reaction	Rate 1977	Rate 1976	Rate 1974	Rate 1973
$HNO_3 + h\nu \rightarrow OH + NO_2$	QJ(7)*	QJ(7)	Same	QJ(7) x 2
$O_3 + OH \rightarrow HO_2 + O_2$	$1.5\times10^{-12}\ e^{-1000/T}$	$1.6\times10^{-12}\ e^{-1000/T}$	Same	$1.3\times10^{-12}\ e^{-956/T}$
$O + OH \rightarrow O_2 + H$	4.2×10^{-11}	Same	Same	Same
$O_3 + HO_2 \rightarrow OH + 2O_2$	$1.0\times10^{-13}\ e^{-1250/T}$	Same	Same	$1.0\times10^{-12}\ e^{-1875/T}$
$O + HO_2 \rightarrow OH + O_2$	3×10^{-11}	Same	$8\times10^{-11}\ e^{-500/T}$	1.0×10^{-11}
$H + O_2 + M \rightarrow HO_2 + M$	$2.08\times10^{-32}\ e^{290/T}$	Same	Same	$1.1\times10^{-32}\ e^{407/T}$
$O_3 + H \rightarrow OH + O_2$	$1.23\times10^{-10}\ e^{-562/T}$	Same	2.6×10^{-11}	2.6×10^{-11}
$HO_2 + HO_2 \rightarrow H_2O_2 + O_2$	$1.7\times10^{-11}\ e^{-500/T}$	Same	$3\times10^{-11}\ e^{-500/T}$	$3\times10^{-11}\ e^{-500/T}$
$HO_2 + OH \rightarrow H_2O + O_2$	2×10^{-11}	Same	2×10^{-10}	2×10^{-10}
$OH + NO_2 + M \rightarrow HNO_3 + M$	Parameterization given in NASA (1977)	$\frac{2.76\times10^{-13}\ e^{880/T}}{1.166\times10^{18}\ e^{222/T} + M}$	$\frac{4\times10^{-11}}{1.12\times10^{18} + M}$	$\frac{10^{-11}}{1.5\times10^{20}\ e^{-750/T} + M}$
$OH + HNO_3 \rightarrow H_2O + NO_3$	8.9×10^{-14}	Same	1.3×10^{-13}	1.3×10^{-13}
$H_2O_2 + h\nu \rightarrow 2OH$	QJ(8)*	QJ(8)	Same	Same
$H_2O_2 + OH \rightarrow H_2O + HO_2$	$1.0\times10^{-11}\ e^{-750/T}$	$1.7\times10^{-11}\ e^{-910/T}$	Same	Same
$N_2 + O(^1D) + M \rightarrow N_2O + M$	3.5×10^{-37}	2.8×10^{-36}	Same	Same
$N + NO_2 \rightarrow N_2O + O$	$2\times10^{-11}\ e^{-800/T}$	1.4×10^{-12}	9×10^{-12}	9×10^{-12}
$NO + O + M \rightarrow NO_2 + M$	$1.6\times10^{-32}\ e^{584/T}$	$3.96\times10^{-33}\ e^{940/T}$	Same	N. I.
$NO + HO_2 \rightarrow NO_2 + OH$	$4.28\times10^{-11}\ e^{-500/T}$	2.0×10^{-13}	Same	N. I.

TABLE F-4. Continued

Reaction	Rate 1977	Rate 1976	Rate 1974	Rate 1973
$H_2 + O(^1D) \rightarrow OH + H$	9.9×10^{-11}	2.9×10^{-10}	Same	N. I.
$OH + OH \rightarrow H_2O + O$	$1.0\times10^{-11}\ e^{-550/T}$	Same	Same	N. I.*
$N + O_3 \rightarrow NO + O_2$	$5\times10^{-12}\ e^{-650/T}$	5.7×10^{-13}	Same	N. I.*
$NO_2 + O_3 \rightarrow NO_3 + O_2$	$1.2\times10^{-13}\ e^{-2450/T}$	Same	$1.23\times10^{-13}\ e^{-2470/T}$	N. I.
$HO_2 + h\nu \rightarrow OH + O$	QJ(9)*	QJ(9)	N. I.	N. I.
$OH + CH_4 \rightarrow H_2O + CH_3$	$2.36\times10^{-12}\ e^{-1710/T}$	Same	N. I.	N. I.*
$OH + OH + M \rightarrow H_2O_2 + M$	$1.2\times10^{-32}\ e^{900/T}$	$2.5\times20^{-33}\ e^{2500/T}$	N. I.	N. I.
$H_2O_2 + O \rightarrow OH + HO_2$	$2.75\times10^{-12}\ e^{-2125/T}$	Same	N. I.	N. I.
$O + CH_4 \rightarrow OH + CH_3$	$3.5\times10^{-11}\ e^{-4550/T}$	Same	N. I.	N. I.
$CO + OH \rightarrow H + CO_2$	1.4×10^{-13}	Same	N. I.	N. I.*
$O(^1D) + M \rightarrow O + M$	$2.2\times10^{-11}\ e^{99/T}$	$2.2\times10^{-11}\ e^{92/T}$	5.85×10^{-11}	3.2×10^{-11}*
$NO_3 + h\nu \rightarrow NO_2 + O$	10^{-1}	10^{-1}	0.	0.
$NO_3 + h\nu \rightarrow NO + O_2$	4×10^{-2}	5×10^{-2}	1.	1.
$N + NO_2 \rightarrow 2NO$	N. I.	N. I.	6×10^{-12}	6×10^{-12}
$NO + NO_3 \rightarrow 2NO_2$	8.7×10^{-12}	N. I.	N. I.	N. I.
$NO_2 + O + M \rightarrow NO_3 + M$	1.0×10^{-31}	N. I.	N. I.	N. I.
$NO_2 + NO_3 \rightarrow NO + O_2 + NO_2$	2.0×10^{-13}	N. I.	N. I.	N. I.

TABLE F-4. Continued

Reaction	Rate 1977	Rate 1976	Rate 1974	Rate 1973
$NO_2 + NO_3 + M \rightarrow N_2O_5 + M$	$\frac{2.92\times10^{-12}}{7\times10^{21}\, e^{-2670/T} + M}$	N. I.	N. I.	N. I.
$N_2O_5 + M \rightarrow NO_2 + NO_3 + M$	$\frac{6.0\times10^{14}\, e^{-10700/T}}{7.0\times10^{21}\, e^{-2670/T} + M}$	N. I.	N. I.	N. I.
$N_2O_5 + O \rightarrow 2NO_2 + O_2$	1.0×10^{-14}	N. I.	N. I.	N. I.
$N_2O_5 + H_2 \rightarrow 2HNO_3$	1.0×10^{-20}	N. I.	N. I.	N. I.
$N_2O_5 \rightarrow 2NO_2 + O$	QJ(10)*	N. I.	N. I.	N. I.
$Cl + O_3 \rightarrow ClO + O_2$	$2.7\times10^{-11}\, e^{-257/T}$	$2.97\times10^{-11}\, e^{-243/T}$	(No ClX reactions were included in 1973 or 1974 chemistries)	
$Cl + OClO \rightarrow 2ClO$	5.9×10^{-11}	Same		
$Cl + O_2 + M \rightarrow ClO_2 + M$	N. I.	$1.7\times10^{-33}\,(300/T)$		
$Cl + CH_4 \rightarrow HCl + CH_3$	$7.3\times10^{-12}\, e^{-1260/T}$	$5.4\times10^{-12}\, e^{-1133/T}$		
$Cl + ClO_2 \rightarrow Cl_2 + O_2$	N. I.	5.0×10^{-11}		
$Cl + ClO_2 \rightarrow 2ClO$	N. I.	1.4×10^{-12}		
$Cl + NO + M \rightarrow ClNO + M$	N. I.	$1.7\times10^{-32}\, e^{553/T}$		
$Cl + ClNO \rightarrow Cl_2 + NO$	N. I.	3.0×10^{-11}		
$Cl + NO_2 + M \rightarrow ClNO_2 + M$	$6.9\times10^{-34}\, e^{2115/T}$	Same		
$Cl + ClNO_2 \rightarrow Cl_2 + NO_2$	3×10^{-12}	Same		
$ClO + O \rightarrow Cl + O_2$	$7.7\times10^{-11}\, e^{-130/T}$	5.3×10^{-11}		

TABLE F-4. Continued

Reaction	Rate 1977	Rate 1976	Rate 1974	Rate 1973
$NO + ClO \rightarrow NO_2 + Cl$	2.2×10^{-11}	$2.6\times10^{-11}\ e^{-50/T}$	(No ClX reactions were included in 1973 or 1974 chemistries	
$ClO + O_3 \rightarrow ClO_2 + O_2$	$1.0\times10^{-12}\ e^{-4000/T}$	$1.0\times10^{-12}\ e^{-2763/T}$		
$ClO + O_3 \rightarrow OClO + O_2$	$1.0\times10^{-12}\ e^{-4000/T}$	$1.0\times10^{-12}\ e^{-2763/T}$		
$ClO + NO_2 + M \rightarrow ClONO_2 + M$	$5.1\times10^{-33}\ e^{1030/T}$	Same		
$ClO + ClO \rightarrow Cl + OClO$	$2.1\times10^{-12}\ e^{-2200/T}$	$2.0\times10^{-12}\ e^{-2300/T}$		
$ClO + ClO \rightarrow 2Cl + O_2$	$1.5\times10^{-12}\ e^{-1230/T}$	$2.0\times10^{-13}\ e^{-1260/T}$		
$HCl + O(^1D) \rightarrow Cl + OH$	1.4×10^{-10}	2×10^{-10}		
$OH + HCl \rightarrow H_2O + Cl$	$3.0\times10^{-12}\ e^{-425/T}$	$2\times10^{-12}\ e^{-310/T}$		
$O + HCl \rightarrow OH + Cl$	$1.14\times10^{-11}\ e^{-3370/T}$	$1.75\times10^{-12}\ e^{-2273/T}$		
$O + OClO \rightarrow ClO + O_2$	$2\times10^{-11}\ e^{-1100/T}$	5.0×10^{-13}		
$NO + OClO \rightarrow NO_2 + ClO$	3.4×10^{-13}	Same		
$N + OClO \rightarrow NO + ClO$	6.0×10^{-13}	Same		
$H + OClO \rightarrow OH + ClO$	5.7×10^{-11}	Same		
$Cl + OH \rightarrow HCl + O$	$1.0\times10^{-11}\ e^{-2970/T}$	$2.0\times10^{-12}\ e^{-1878/T}$		
$Cl + HO_2 \rightarrow HCl + O_2$	3×10^{-11}	Same		
$Cl + HNO_3 \rightarrow HCl + NO_3$	$1.0\times10^{-11}\ e^{-2170/T}$	$4.0\times10^{-12}\ e^{-1500/T}$		
$ClONO_2 + O \rightarrow ClO + NO_3$	$4.5\times10^{-12}\ e^{-840/T}$	Same		

TABLE F-4. Continued

Reaction	Rate 1977	Rate 1976	Rate 1974	Rate 1973
$ClO_2 + HO_2 \rightarrow HCl + 2O_2$	N. I.	3.0×10^{-12}	(No ClX reactions were included in 1973 or 1974 chemistries)	
$CH_3Cl + OH \rightarrow Cl + H_2O + HO_2$	$2.2\times10^{-12}\ e^{-1142/T}$	Same		
$CH_3Cl \rightarrow 2HO_2 + CO + Cl$	QCJ(1)*	QCJ(1)		
$HCl + h\nu \rightarrow H + Cl$	QCJ(2)*	QCJ(2)		
$ClONO_2 \rightarrow ClO + NO_2$	QCJ(3)*	QCJ(3)		
$ClO + h\nu \rightarrow Cl + O$	QCJ(4)*	QCJ(4)		
$ClO + h\nu \rightarrow Cl + O(^1D)$	QCJ(5)*	QCJ(5)		
$ClNO_2 + h\nu \rightarrow Cl + NO_2$	QCJ(7)*	QCJ(7)		
$OClO + h\nu \rightarrow ClO + O(^1D)$	QCJ(8)*	QCJ(8)		
$OClO + h\nu \rightarrow ClO + O$	QCJ(9)*	QCJ(9)		
$CF_2Cl_2 + h\nu \rightarrow 2Cl$	QCJ(10)*	QCJ(10)		
$CFCl_3 + h\nu \rightarrow 2.5\ Cl$	QCJ(11)*	QCJ(11)		
$CCl_4 + h\nu \rightarrow 2Cl$	QCJ(12)*	QCJ(12)		
$CFCl_3 + O(^1D) \rightarrow 2Cl$	2.3×10^{-10}	3.0×10^{-10}		
$CF_2Cl_2 + O(^1D) \rightarrow 2Cl$	2.0×10^{-10}	2.5×10^{-10}		
$Cl + H_2 \rightarrow HCl + H$	$4.7\times10^{-11}\ e^{-2340/T}$	$5.7\times10^{-11}\ e^{-2400/T}$		
$Cl + H_2O_2 \rightarrow HCl + HO_2$	$1.6\times10^{-12}\ e^{-384/T}$	$1.0\times10^{-11}\ e^{-810/T}$		

N. I. - No included in model

*Multiple scattering effects included.

2. Rainout and Boundary Conditions

The 1973 model (Chang and Duewer, 1973) did not include rainout processes. All subsequent models included rainout losses below 8 km using rainout coefficients of 2.31×10^{-6} sec^{-1} for HNO_3, HCl and ClO (for models including chlorine chemistry) and 1.16×10^{-6} for NO_2. The major effect of rainout is to uncouple surface boundary conditions for NO_x and ClO_x from stratospheric and upper tropospheric concentrations. Calculated stratospheric perturbations are not strongly sensitive to the precise rainout rates chosen.

The model uses fixed concentration boundary conditions at the surface (Chang et al., 1974). For versions incorporating rainout, the model stratosphere has significant sensitivity to the boundary conditions for only N_2O (320 ppb), CH_4 (1.3 ppm), CH_3Cl (750 ppt), and CCl_4 (92 ppt). The 1973 model was also influenced by the surface boundary conditions for NO, NO_2 and HNO_3, which produced a nearly uniform 3.7 ppb NO_x mixing ratio in the troposphere. In current models treating rainout processes, the NO_x mixing ratio in the upper troposphere (which is about 0.1 ppb at 10 km) is dependent on the vertical transport coefficient, K_z. The upper boundary conditions are all flux boundary conditions, and all present calculations are very insensitive to them.

3. Treatment of Photolysis

In our 1973 calculation, we neglected multiple scattering effects, diurnal variation of species concentrations and used then-current values for the N_2O photodissociation cross sections (Bates and Hays, 1967). In all of the current calculations, we used Johnston and Selwyn (1975) photodissociation cross sections for N_2O. The 1974 and 1976 models approximated diurnal variations in solar flux by using 1/2 of noontime photodissociation rates. The chlorine nitrate formation rate was adjusted to be consistent with a fully diurnal calculation for the 1976 model. The 1977 model uses reaction rates at each level averaged over a diurnal cycle (Luther , 1977; Chang et al., 1978). Limited calculations were made using the 1976 chemistry and diurnal averaging. The 1976, 1977, and 1978 models included multiple scattering effects (Luther et al., 1978).

The response of the model is little affected by the change in N_2O absorption cross sections or multiple scattering (together they resulted in a 0.2% change in total ozone reduction for a calculated maximum depletion of roughly 5% using the 1973 chemistry). The incorporation of diurnal averaging of reaction rates increased the ozone reduction for 1976 chemistry by $\sim$0.5 to 1% of total ozone when the Seitz injection scheme was used (see Table F-3).

4. Parameterization of Vertical Transport

In our 1973 paper, the Chang (1974) transport coefficient K_z was used. In this paper we considered the effects of different K_z choices by performing calculations using the Chang (1974), Chang (1976), and Hunten (1975) K_z's. Only the recovery time had a strong sensitivity to K_z (see Fig. F-3 and Table F-3).

INTERPRETATION OF THE OZONE RECORD

Johnston et al. (1973) analyzed the global ozone record for 1960-1970 and found a statistically insignificant decrease of 2.2% from 1960-1962 followed by a statistically significant increase of 3.7% in 1963-1970. They viewed this increase as consistent with recovery from an ozone reduction of "a few percent" induced by the nuclear tests. The same data have been analyzed by several other authors (Komhyr et al., 1971; Angell and Korshover, 1973, 1976, 1978; Goldsmith et al., 1973; Christie, 1973; COMESA, 1975; London and Kelley, 1974). Although most of these analyses, and some analyses restricted to individual stations (e.g., Birrer, 1974; Pittock, 1974a and b, 1976, 1977) find similar trends in ozone over the decade of the 1960's, the decrease in ozone appears to have occurred before the tests (Angell and Korshover, 1976; Christie, 1973; London and Kelley, 1974; COMESA, 1975), while the subsequent increase appears to have reached ozone concentrations larger than the long-term mean. Birrer (1974) in an analysis of the Arosa data from 1926-1971 found several periods with trends comparable to those observed during the 1960's. Birrer concluded that human influence on the stratosphere could only be inferred from the analysis of all stations in the network with continuous records of at least

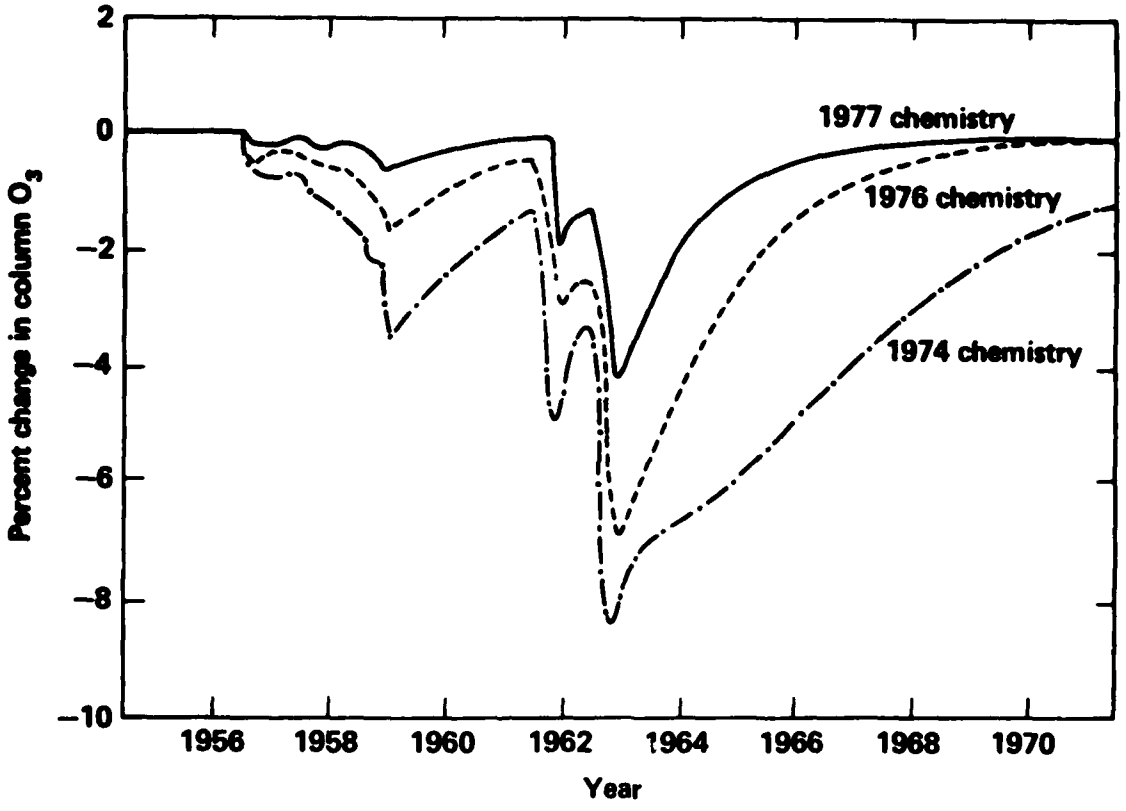

FIGURE F-3. Calculated change in O_3 vs. date showing the effect of the choice of chemistry. _____ 1977 chemistry, Chang (1976) K_z; — — — 1976 chemistry, Chang (1976) K_z; - · - · - 1974 chemistry, Chang (1974) K_z. All calculations used the Foley and Ruderman stabilization parameterization.

ten years and that a change of 5% would have to persist 10 years to be significant in the Arosa data. This viewpoint seems consistent with the analyses of Pittock, and London and Kelley, but in some contrast to the analyses of Angell and Korshover (1973, 1976, 1978), Goldsmith et al. (1973), COMESA (1975), Christie (1973), Hill et al. (1977), Johnston et al. (1973), and Komhyr et al. (1971). This is not to suggest that these studies in any group are all in total agreement. It is clear that there is considerable trend structure in the past ozone data, and existing divergent interpretations of such trend structures are yet to be resolved (e.g., Pittock, 1974a and b; Angell and Korshover, 1974, 1976, 1978; Komhyr et al., 1971; Birrer et al., 1974; Johnston et al., 1973). For the detection of possible effects on ozone from past nuclear tests, the most restrictive interpretation would appear to be that of Angell and Korshover (1976). They concluded any such effect must have been less

than 1-2%. On the other hand Johnston et al. (1973) have estimated that a perturbation of about 4-5% would be consistent with their analysis.

The 1-2% limit cited by Angell and Korshover (1976) seems to refer to the maximum trend actually found in the data. If the 2σ error bars on the data as estimated by Angell and Korshover (1978) are considered, a trend of up to about 4% would not be inconsistent. Moreover, the ozone record contains unexplained long-term fluctuations with an amplitude of roughly 5%. Some of these long-term fluctuations may be related to solar variability (Heath and Thekaekara, 1977; Callis and Nealy, 1978; Penner and Chang, 1978) volcanic activity (either as an effect on ozone or via a measurement artifact (Angell and Korshover, 1973, 1976, 1978; Cadle, 1975; Kulkarni, 1974), solar proton events (Crutzen et al., 1975), and chlorofluoromethanes (Rowland and Molina, 1974). Indeed, Johnston (1974) has suggested that the nuclear test series may account for a "missing" ozone maximum in 1963. The case for a link between ozone and solar cycle variability is somewhat ambiguous (Penner and Chang, 1978). It would appear that the data may offer some support (possibly statistically insignificant) for a 1-2% ozone reduction in 1963-1964 (with a larger reduction of unexplained origin in early 1961). Given the imprecision of the data elements as analyzed by Angell and Korshover (1978), the data would not rule out an effect of as much as 4%, and the presence of incompletely explained fluctuations in the ozone record could be used to argue for broader error bars. Although such arguments have some ad hoc character, it would appear that ozone depletions of 4-5% could be reconciled with the data, although much larger depletions (or increases) would be more difficult to reconcile with the O_3 record.

RESULTS AND DISCUSSION

1. Effect of K_z's

Calculations were carried out using the Foley and Ruderman stabilization parameterization for 1973, 1974, 1976 and 1977 chemistries. The Chang (1976) K_z was used with the 1974, 1976 and 1977 chemistries, the Chang (1974) K_z was used with the 1973 and 1974 chemistries and the Hunten K_z (1975) was used with the 1973, 1976, and 1977 chemistries. The Seitz et al. (1968) stabilization estimates

were considered using 1976 and 1977 chemistries with the Chang (1976) K_z and for the 1977 chemistry using the Hunten K_z.

In the calculation of the nuclear test series effects, the total NO_x injection is determined by the device yield and is independent of K_z. Most of the injection occurred over a fairly short time. Therefore, unlike SST calculations, the maximum change in NO_x is nearly independent of K_z. As Figure F-3 and Table F-3 show, the ozone depletions in 1963-1964 were only weakly dependent on K_z. For pre-1977 model chemistries, there is a substantial difference in recovery time based on the effective removal rate of excess stratospheric NO_x. For the 1977 model chemistry, the apparent recovery time is initially determined by the rate of vertical redistribution of the injection, although at later times recovery is controlled by the rate of removal of excess NO_x from the stratosphere. The Hunten K_z differs from the Chang K_z in that there is a sharp break at 14 km rather than a relatively slow decline in K_z values between 10 and 22 km. As a result excess NO_x between 13 and 25 km remains in excess for a longer time when the Hunten K_z is used than when the Chang K_z is used. Consequently, the ozone increases that are calculated in this altitude range persist longer, and net reductions (difference between high altitude decrease and low altitude increase, see below) disappear more rapidly. In no case would the choice of K_z alone cause the calculated perturbation to become in conflict with observation or vice versa.

2. Effect of Stabilization Estimates

As Fig. F-2 and Table F-3 show, the procedure used to estimate the stabilization altitude does have a significant effect on the calculation. However, for the model chemistries studied, the differences in the effects computed using these two stabilization estimates were less dramatic than the differences between model computations using different chemistries (Fig. F-4).

The estimated stabilization heights for the polar tests remain a significant source of uncertainty in the calculations. For reasons discussed above, we find the published information ambiguous and somewhat unsatisfactory. The two methods of estimation used provide a probable upper and lower bound to the true stabilization heights, but the Foley and Ruderman parameterization may be the more nearly accurate of the two. Chang (1975) and Mahlman (1977) have discussed the

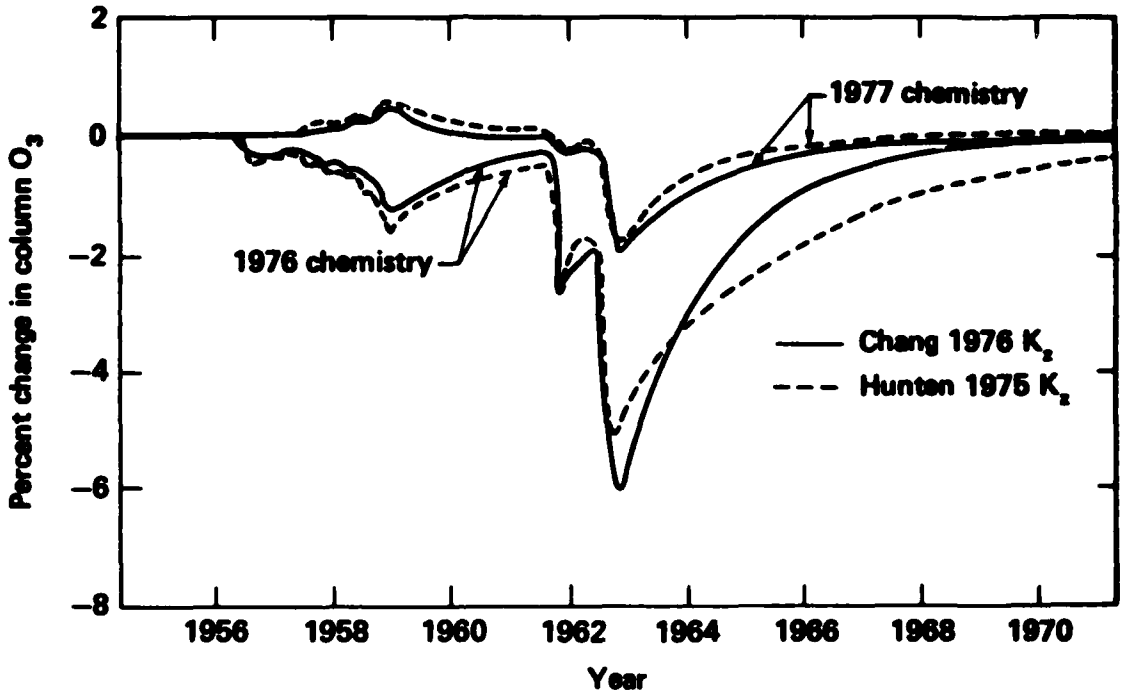

FIGURE F-4. Calculated O_3 change vs. date showing the effect of choice of K_z. - - - Hunten (1975) K_z; ——— Chang (1976) K_z. Upper curves use the 1977 chemistry and diurnal averaging. Lower curves use the 1976 chemistry without diurnal averaging.

information available from tracer calculations based on ^{14}C and ^{90}Sr. At present, we will note that these results further strengthen the need to accept the uncertainty in cloud stabilization heights as inherent uncertainties in such analysis.

3. Effect of Model Chemistries

The model representation of atmospheric chemistry has evolved substantially since early 1973. Between 1973 and 1974 several reactions involving HO_x species were added to the model, the effect of which should have been reduced model sensitivity to NO_x perturbations. However, in addition, the reaction of N atoms with O_3 was included, substantially increasing model sensitivity to high altitude NO_x injections (because of its effect on the lifetime of NO_x near 50 km). Also, the treatment of solar fluxes was modified (in 1973 we used photolysis rates characteristic of a 45^o zenith angle; in 1974 we halved the photolysis rates),

rainout processes for NO and NO_2 were neglected in 1973 but included in 1974, and the estimated NO_x injection per megaton yield was increased from 5×10^{31} to 6.7×10^{31} molecules/megaton. The net effect of these changes was that the calculated peak ozone reduction (January of 1963) increased from 4.9% to 8.2% for otherwise equivalent calculations (the 4.9% reduction for 1973 chemistry would have been 6.6% if the NO_x injections had been the same as for later calculations).

Between the calculations used in support of the CIAP Report of Findings (Grobecker et al., 1974) made with our 1974 chemistry and the NRC (1976) chlorofluoromethane report, the model was modified to include a representation of stratospheric ClX chemistry, several fairly minor reactions of HO_x were added, the rate of

$$HO + HO_2 \rightarrow H_2O + O_2 \qquad \text{(F.1)}$$

was revised (from 2×10^{-10} to 2×10^{-11} cm^3 sec^{-1}), and numerous comparatively minor changes in rate constants were entered (see Table F-4). As a result of these changes, the computed effects declined by roughly 30% of the computed change, but remained larger than 5% of the total ozone.

Our 1977 chemistry reflects the measurement of Howard and Evenson (1977), i.e., the rate of

$$HO_2 + NO \rightarrow NO_2 + OH \qquad \text{(F.2)}$$

was increased by roughly a factor of 40. Also, there were a few comparatively minor changes in other rate coefficients (see Table F-4). The dramatic results of these changes were almost completely due to reation (2). Reaction (2) strongly couples NO_x and HO_x reaction systems. As a result of the large change in the rate constant for reaction (2) used in the model, the interference by NO_x with HO_x catalyzed ozone destruction, important between 10-25 km, became much stronger.

Recently, Howard (1978) has reported a negative activation energy for reaction (2) and has also reported a first direct measurement for the reaction

$$HO_2 + O_3 \rightarrow OH + 2O_2 \quad . \qquad \text{(F.3)}$$

When this is considered along with the measurement of Cox (1978) for the rate constant for the reaction

$$HO_2 + HO_2 \rightarrow H_2O_2 + O_2 \quad , \tag{F.4}$$

the above-mentioned coupling becomes stronger and further enhances the role of HO_x in the lower stratosphere. A preliminary estimate indicates that the calculated best estimate of O_3 change in 1963 would be more positive and may even be a small increase in ozone. This new development is very complex, and a full analysis of it may demand a better understanding of stratospheric and tropospheric exchange processes that have been heavily parameterized in all current models as well as further refinement of the chemical reaction rate data.

4. Calculated Ozone Trend

The sharp decrease immediately following the large tests is due to the initialization procedure used. The source term consisted of pulse injections primarily at high latitudes, most of them in a period of $\sim$4 months in late 1962. Thus, at least for the several months before horizontal mixing in the Northern Hemisphere became extensive, the one-dimensional approximation is expected to be poor and to overestimate the ozone depletions (Bauer and Gilmore, 1975). When the Foley and Ruderman (1973) stabilization height estimates were used with 1977 chemistry, we computed ozone decreases for all years during the period of active atmospheric testing, and the reductions calculated in 1963 (3% annual average ozone reduction in the Northern Hemisphere) are slightly larger than the limit to the perturbation cited by Angell and Korshover (1976) but consistent with Johnston et al. (1973) or Angell and Korshover (1978). The effect we now predict is smaller than the error bars in the ozone data as estimated by Angell and Korshover (1978) and should not be detectible in any case.

The model calculation can provide estimates of the local ozone changes at each altitude. Figure F-5 presents the ozone changes computed at various altitudes when we use 1977 chemistry, the Foley and Ruderman injection parameterization and the Chang (1976) K_z. Because these detailed trends are very sensitive to

variations in the input parameters, all such details should only be viewed qualitatively.

Figure F-5 does show several features of qualitative importance, however. Although recent chemistries predict net perturbations in column ozone that are small relative to the changes predicted using earlier chemistries, these small column changes result from the partial cancellation of larger local changes in ozone. That is, there are local increases in ozone below ∿ 24 km, and local decreases in ozone

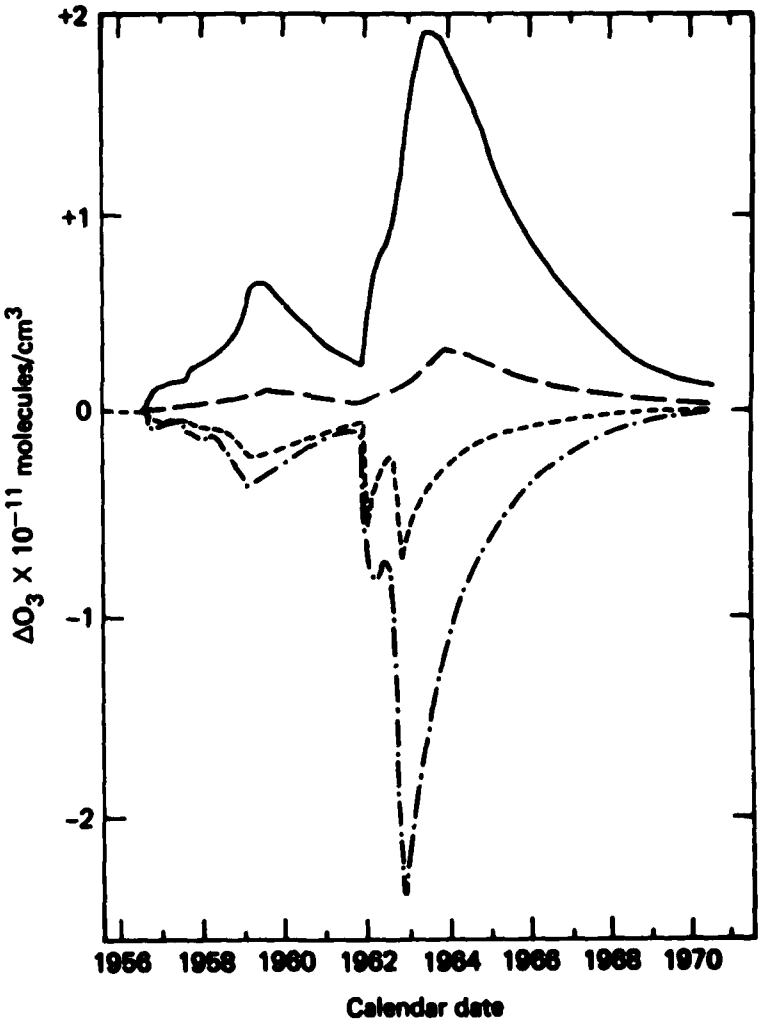

FIGURE F-5. Calculated change in local ozone concentration vs. date for several altitudes. — — — 10 km; _____ 20 km; - · - · - 30 km; - - - 40 km. The Chang (1976) K_z, Foley and Ruderman stabilization parameterization and our 1977 chemistry were used in this calculation.

above ~ 25 km, and the magnitudes of these local changes are comparable (but of opposite sign). The ozone decreases at higher altitudes result largely from the well known NO_x catalyzed ozone destruction via the reactions

$$NO + O_3 \rightarrow NO_2 + O_2 \qquad (F.5)$$

and

$$NO_2 + O \rightarrow NO + O_2 \quad . \qquad (F.6)$$

The ozone increases at lower altitudes result because

1. in the lower stratosphere there is a comparatively low oxygen atom concentration which makes the rate of reaction (6) very slow relative to

$$NO_2 \xrightarrow{h\nu} NO + O \qquad (F.7)$$

so that the efficiency of NO_x catalyzed ozone destruction is low.

2. Reactions such as

$$HO + O_3 \rightarrow HO_2 + O_2 \qquad (F.8)$$

and

$$HO_2 + O_3 \rightarrow HO + 2O_2 \qquad (F.9)$$

that result in an HO_x catalyzed ozone destruction have a reduced efficiency if HO_2 reacts with NO by reaction (2) (and this is followed by reaction (7)) rather than reacting with ozone via reaction (3).

3. The reactions

$$HO + NO_2 \xrightarrow{M} HNO_3 \qquad (F.10)$$

and

$$HO + HNO_3 \rightarrow H_2O + NO_3 \qquad (F.11)$$

are a major sink for HO_x radicals in the lower stratosphere.

4. The reactions

$$ClO + NO \rightarrow Cl + NO_2 \qquad (F.12)$$

and

$$ClO + NO_2 \overset{M}{\rightleftharpoons} ClONO_2 \qquad (F.13)$$

are analogs to reactions (2) and (10) involving chlorine species. The net effect of the slow direct catalysis of ozone destruction by NO_x via reactions 5 and 6 (and some other processes) and the interference with ozone destruction catalyzed by HO_x and ClX species is that ozone increases are calculated in portions of the lower stratosphere.

However, the magnitude and vertical extent of this increase are quite strongly dependent on the ambient concentrations of HO_x species and precursers, the details of exchange between the troposphere and the stratosphere, and the rate constants for several difficult to study chemical reactions. Unfortunately, there are no published measurements of HO or HO_2 in the 12-27 km region, and most reactive species that have been measured in this region seem highly variable. Thus, model results continue to be quite sensitive to poorly known input parameters, and the possibility that future models will have significantly different sensitivity to NO_x than our current model is quite real.

It should be noted that the problems related to high latitude injections (i.e., much of the injected material may be removed from the stratosphere before it affects middle or low latitudes) and the initial dispersion of pollutant are also present in calculations of the effects of SST flight since more than half of projected SST emissions occur north of 50°N (Oliver et al., 1977). Thus, some of the potential sources of error introduced by the use of one-dimensional models in the calculation of the test series effects also exist for calculations of SST's.

It may appear that the difficulty of dealing with initial cloud spread could be dealt with in two-dimensional models. However, for the simple reason that all two-dimensional models derive their transport from long-term averaged observation data of stratospheric tracers, it is not clear that such models can correctly represent transport on the time scale of weeks to months. Furthermore, limited spatial resolution in two- and three-dimensional models as required by practical computational considerations also requires parameterization of initial debris cloud spread and its effects are yet to be studied. Nevertheless, two- or three-dimensional calculations of both effects are to be desired, but present

multi-dimensional models are expensive to run, and the likely rapid evolution of model chemistry may act to discourage extensive calculations.

CONCLUSIONS

Several conclusions may be drawn from these calculations. Most important is that our current (1977) one-dimensional model calculates ozone depletions that seem reconcilible with observations, and that the 1960's tests may provide a useful if largely negative test of stratospheric models (i.e., a test that some past models could have met only by presuming all uncertainties near their limits, and that some future calculations might encounter similar difficulties in meeting). The calculations reported here demonstrate that a one-dimensional calculation of the effects of the nuclear tests is relatively insensitive to K_z and only moderately sensitive to the treatment of cloud stabilization heights. Unexpected changes in model chemistry have produced major reductions in the predicted effects on atmospheric ozone of nuclear weapons and SST's (Luther, 1977; Broderick, 1977), more than five years after major programs designed to predict the effects of NO_x on ozone were instituted and more than two years after reports of findings were issued. These major changes came as a result of measurements of parameters not affecting the major NO_x catalytic cycles directly.

The calculations reported here reflect current best estimates of many input parameters, some of which (especially reaction rate constants involving HO_2) are admittedly rather uncertain (DeMore et al., 1977; Duewer et al., 1977). Thus, when new measurements become available, it is likely that some model inputs and model predictions will change again.

The major changes in model chemistry, and those changes that most strongly affect model sensitivities have been in the treatment of reactions that affect HO_x species or link NO_x to minor species other than odd oxygen, rather than in the major catalytic odd oxygen destruction cycles involving NO_x (see also Duewer et al., 1977). Because this secondary chemistry has such a strong effect on one-dimensional model sensitivity to NO_x injection, it will be necessary to closely examine the representation of the chemistry used in multi-dimensional models when interpreting their results.

We believe that ozone changes of the magnitude of 4% are reconcilable with observation if one accepts the analysis of either Angell and Korshover (1978) or Johnston et al. (1973). Any model that predicts a response to the nuclear weapons tests of the 1950's and 1960's significantly larger than 4% (Northern Hemisphere annual average) may be in error in a way that seriously affects its reliability in other prognostic applications, although the case for this may be rendered ambiguous by the possible existence of other sources of long-term O_3 variability. In the above application model errors could result from the basic model formulation (e.g., dimensionality, resolution, numerical method), the detailed representation of chemistry or transport (e.g., input rate constants), or the treatment of the perturbation (e.g., NO_x yield, stabilization heights). In the case of the calculations described here using 1973, 1974 and 1976 chemistries, relatively large perturbations were predicted, and new measurements of chemical rate constants have led to a much smaller predicted response to the nuclear tests.

As the above discussion indicates, the nuclear test series do not appear to provide a positive test or calibration point for models of the stratosphere. However, they would appear to provide a negative test of such models. This test may be overly stringent when applied to steady-state effects, such as those from SST and CFM's. However, if any current or future stratospheric model should predict large ozone changes from the tests of the 1950's and 1960's, it would be necessary to understand this apparent conflict with observation before accepting other predictions of that model.

REFERENCES

Angell, J. K. and J. Korshover, "Quasi Biennial and Long-Term Fluctuations in Total Ozone," Mon. Wea. Rev., 101, 426-443, 1973.

Angell, J. K. and J. Korshover, "Reply to Pittock," Mon. Wea. Rev., 102, 86-87, 1974.

Angell, J. K. and J. Korshover, "Global Analysis of Recent Total Ozone Fluctuations," Mon. Wea. Rev., 104, 63-75, 1976.

Angell, J. K. and J. Korshover, "Global Ozone Variations: An Update into 1976," Mon. Wea. Rev., 106, 725-737, 1978.

Bates, D. R. and P. B. Hays, "Atmospheric Nitrous Oxide," Planetary and Space Science, 15, 189-197, 1967.

Bauer, E. and F. R. Gilmore, "Effect of Atmospheric Nuclear Explosions on Total Ozone," Rev. Geophys. and Space Phys., 13, 451-457, 1975.

Birrer, W. M., "Some Critical Remarks on Trend Analysis of Total Ozone Data," Pageoph, 112, 523-532, 1974

Broderick, A. J., "Stratospheric Effects from Aviation," presented at the AIAA/SAE 13th Propulsion Conference, Orlando, Fla., July 1977.

Burrows, J. D., G. W. Harris and B. A. Thrush, "Roles of Reaction of HO_2 with HO and O Studied by Laser Magnetic Resources," Nature, 267, 233-234, 1977.

Cadle, R. D., "Volcanic Emissions of Halides and Sulfur Compounds to the Troposphere and Stratosphere," J. Geophys. Res., 80, 1650-1652, 1975.

Callis, L. B. and J. E. Nealy, "Solar UV Variability and Its Effect on Stratospheric Thermal Structure and Trace Constituents," Geophys. Res. Let., 5, 249-252, 1978.

Chang, J. S., "Simulations, Perturbations, and Interpretations," Proceedings of the 3rd CIAP Conference, Report DOT-TSC-OST-74-15, pp. 330-341, U.S. Department of Transportation, Cambridge, MA, February 1974.

Chang, J. S., "Uncertainties in the Validation of Parameterized Transport in One-Dimensional Models of the Stratosphere," pp. 175-182 in Proceedings of the Fourth CIAP Conference, Report DOT-TSC-OST-75-38, U.S. Department of Transportation, Cambridge, MA, February 1975.

Chang, J. S., Eddy diffusion profile described in "First Annual Report of Lawrence Livermore Laboratory to the High Altitude Pollution Program," F. M. Luther (ed.), Lawrence Livermore Laboratory Report UCRL-50042-76, 1976 and in NRC, 1976.

Chang, J. S. and W. H. Duewer, "On the Possible Effect of NO_x Injection in the Stratosphere Due to Past Atmospheric Nuclear Weapons Tests," paper presented at the AIAA/AMS Meeting, Denver, CO, June 1973; Lawrence Livermore Laboratory Report UCRL-74480, 1973.

Chang, J. S. and F. Kaufman, "Upper Bound and Probable Value of the Rate Constant of the Reaction $OH + HO_2 \rightarrow H_2O + O_2$," J. Physical Chem., 82, 1683-1687, 1978.

Chang, J. S., A. C. Hindmarsh, and N. K. Madsen, "Simulation of Chemical Kinetics Transport in the Stratosphere," in Stiff Differential Systems, edited by R. A. Willoughby, pp. 51-65, Plenum, N. Y., 1974.

Chang, J. S., D. J. Wuebbles, and R. Tarp, "Fully Diurnal Averaged Model of the Stratosphere," presented at IAGA/IAMAP Joint Session, Seattle, WA, August 1977 and MS in preparation, 1978.

Chang, J. S., W. H. Duewer, and D. J. Wuebbles, "The Atmospheric Nuclear Tests of the 1950's and 1960's: A Possible Test of Ozone Depletion Theories," J. Geophys. Res., 84, 1755-1765, 1979.

Christie, A. D., "Secular or Cyclic Change in Ozone," Pageoph, 106, 1000-1009, 1973.

Christie, A. D., "Atmospheric Ozone Depletion by Nuclear Weapons Testing," JGR, 81, 3583-2594, 1976.

Cox, R. A., "Kinetics of HO_2 Radical Reactions of Atmospheric Interest," Proceedings of the WMO Symposium on the Geophysical Aspects and Consequences of Changes in the Composition of the Stratosphere, WMO #511, 1978.

Crutzen, P. J., I. S. A. Isaakson and G. C. Reid, "Solar Proton Events: Stratospheric Sources of Nitric Oxide," Science, 189, 457-459, 1975.

COMESA, "The Report of the Committee on Meteorological Effects of Stratospheric Aircraft (1972-1975)," U. K. Meteorological Office, Bracknell, 1975.

DeMore, W. B., L. Steif, R. T. Watson, R. Hampson, D. Garvin, J. Margitan, M. Molmer, D. Golder, "Laboratory Measurements," pp. 1-50 in Chlorofluoromethanes in the Stratosphere, R. D. Hudson (ed.), NASA reference publication 1010. National Aeronautical and Space Administration, Greenbelt, MD, 1977.

Duewer, W. H., D. J. Wuebbles, and J. S. Chang, "The Effects of a Massive Pulse Injection of NO_x into the Stratosphere," presented at the WMO Symposium on Geophysical Aspects and Consequences of Changes in the Composition of the Stratosphere, Toronto, Canada, June 26-30, 1978; also available Lawrence Livermore Laboratory Report UCRL-80397, 1978.

Duewer, W. H., D. J. Wuebbles, H. W. Ellsaesser and J. S. Chang, "NO_x Catalytic Ozone Destruction: Sensitivity to Rate Coefficients," J. Geophys. Res., 82, 935-942, 1977; see also Reply to Comment, J. Geophys. Res., 82, 2599-2605, 1977.

Foley, H. M. and M. A. Ruderman, "Stratospheric Nitric Oxide Production from Past Nuclear Explosions and Its Relevance to Projected SST Pollution," Paper P-894, Institute for Defense Analysis, JASON, Arlington, VA, pp. 1-25, 1972.

Foley, H. M. and M. A. Ruderman, "Stratospheric NO Production from Past Nuclear Explosions," J. Geophys. Res., 78, 4441-4450, 1973.

Garvin, D. and T. H. Gevantman, "Chemical Kinetics Data Survey. III. Selected Rate Constants for Chemical Reactions of Interest in Atmospheric Chemistry," NBS Report 10867, June 1972.

Garvin, D. and R. F. Hampson, "Chemical Kinetics Data Survey. VII. Tables of Date and Photochemical Data for Modeling of the Stratosphere," (Revised) NBSIR-74-430, National Bureau of Standards, Washington, D. C., 1974.

Gerard, J. C. and C. A. Barth, "High Latitude Nitric Oxide in the Lower Thermosphere," J. Geophys. Res., 82, 674-681, 1977.

Gilmore, F. R., "The Production of Nitrogen Oxides by Low Altitude Nuclear Explosions," J. Geophys. Res., 80, 4553-4554, 1975.

Goldsmith, P., A. F. Tuck, J. S. Foot, E. L. Simmons and R. L. Newson, "Nitrogen Oxides, Nuclear Weapon Testing, Concorde and Stratospheric Ozone," Nature, 244, 545-551, 1973.

Grobecker, A. J., S. C. Coroniti and R. H. Cannon, Jr., "Report of Findings," Report DOT-TSC-75-50, U. S. Department of Transportation, Washington, D. C., December 1974.

Hampson, J., "Photochemical War on the Atmosphere," Nature, 250, 189-191, 1974.

Hampson, J., "A Model for Iterative Interaction Between Atmospheric Chemistry, Heating, and Circulation to Explain Perturbation of Weather and Climate by Solar Activity and Anthropogenic Change," paper presented at the IAGA/IAMAP Joint Assembly, Seattle, WA, August 1977.

Hampson, R. F. and D. Garvin, "Chemical Kinetic and Photochemical Data for Modeling Atmospheric Chemistry," Technical Note 866, National Bureau of Standards, Washington, D. C., 1975.

Heath, D. F. and M. P. Thekaekara, "The Solar Spectrum Between 1200 and 3000 A," pp. 193-213 in The Solar Output and its Variation, O. R. White (ed.) Colorado Associated University Press, Boulder, CO, 1977.

Hill, W. J., P. N. Sheldon, J. J. Tiede, "Analyzing Worldwide Total Ozone for Trends," Geophys. Res. Letters, 4, 21-24, 1977.

Howard, C. J., "Recent Developments in Atmospheric HO_2 Chemistry," presented at the WMO Symposium on the Geophysical Aspects and Consequences of Changes in the Composition of the Stratosphere, Toronto, Canada, June 26-30, 1978.

Howard, C. J. and K. M. Evenson, "Laser Magnetic Resonance Study of HO_2 Chemistry," Geophys. Res. Letters, 10, 437-440, 1977.

Hunten, D. M., "Estimates of Stratospheric Pollution by an Analytic Model," Proceedings of the National Academy of Sciences, U. S., 72, 4711-4715, 1975.

Johnston, H. S., "Pollution of the Stratosphere," Environmental Conservation, 1, 163-176, 1974.

Johnston, H. S., "Expected Short-Term Local Effect of Nuclear Bombs on Stratospheric Ozone," J. Geophys. Res., 82, 3119-3124, 1977.

Johnston, H. S., G. Whitten, and J. Birks, "Effect of Nuclear Explosions on Stratospheric Nitric Oxide and Ozone," J. Geophys. Res., 78, 6107-6135, 1973.

Johnston, H. S. and G. S. Selwyn, "New Cross Sections for the Absorption of Near-Ultraviolet Radiation by Nitrous Oxide (N_2O), Geophys. Res. Letters, 2, 549-551, 1975.

Johnston, H. S., D. Kattenhorn, and G. Whitten, "Use of Excess Carbon 14 Data to Calibrate Models of Stratospheric Ozone Depletion by Supersonic Transports," J. Geophys. Res., 81, 368-380, 1976.

Komhyr, W. D., E. W. Barrett, G. Slocum, and H. K. Weickmann, "Atmospheric Total Ozone Increase During the 1960's," Nature, 233, 390-391, 1971.

Kulkarni, R. N., "Ozone Trends Over Australia," Environ. Conservation, 346, 1974.

London, J. and J. Kelley, "Global Trends in Total Atmospheric Ozone," Science, 184, 987-989, 1974.

Luther, F. M. (ed.), "Annual Report of Lawrence Livermore Laboratory to the High Altitude Pollution Program," Lawrence Livermore Laboratory Report UCRL-50042-77, 1977.

Luther, F. M., D. J. Wuebbles, W. H. Duewer, and J. S. Chang, "Effect of Multiple Scattering on Species Concentrations and Model Sensitivity," J. Geophys. Res., 83, 3563-3570, 1978.

MacCracken, M. C. and J. S. Chang (eds.), "A Preliminary Study of the Potential Chemical and Climatic Effects of Atmospheric Nuclear Explosions," Lawrence Livermore Laboratory Report UCRL-51653, April 1975.

Mahlman, J. P., "Application of General Circulation Models to Stratospheric Transport Problems," IAGA/IAMAP Joint Assembly, Seattle, WA, August 1977.

Martell, E. A., "Transport Patterns and Residence Times for Atmospheric Trace Constitutents vs. Altitude," pp. 138-156 in Radionuclides in the Environment, E. C. Freeling (Ed.), Advances in Chemistry, 93, 1970.

NASA Reference Publication 1010, "Chlorofluoromethanes and the Stratosphere," R. D. Hudson, Ed., National Aeronautics and Space Administration, 1977.

National Research Council, Long-Term Worldwide Effects of Multiple Nuclear Weapons, National Academy of Sciences, Washington, D. C., 1975.

National Research Council, Halocarbons: Effects on Stratospheric Ozone, National Academy of Sciences, Washington, D. C., 1976.

Oliver, R. C., E. Bauer, H. Hidalgo, K. A. Gardner and W. Wasylkiwskyj, "Aircraft Emissions: Potential Effects on Ozone and Climate, A Review and Progress Report," Report FAA-EQ-77-3, U. S. Department of Transportation, Washington, D. C., March 1977.

Penner, J. E. and J. S. Chang, "Possible Variation in Atmospheric Ozone Related to the Eleven-Year Solar Cycle," Geophys. Res. Letters, 5, 817, 1978.

Peterson, K. R., "An Empirical Model for Estimating World-Wide Deposition from Atmospheric Nuclear Detonations," Health Physics, 18, 357-378, Pergamon Press, Northern Ireland, 1970.

Pittock, A. B., "Ozone Climatology Trends and the Monitoring Problem," FAMAP/IAPSO Melbourne Meeting, January 1974a.

Pittock, A. B., "Comments on 'Quasi-Biennial and Long-Term Fluctuations in Total Ozone," Mon. Wea. Rev., 102, 84-86, 1974b.

Pittock, A. B., "Trends in the Vertical Distribution of Ozone Over Australia," Nature, 249, 641-643, 1976.

Pittock, A. B., "Climatology of the Vertical Distribution of Ozone Over Aspendale (38°S, 145°E)," Quart. J. R. Met. Soc., 103, 575-584, 1977.

Rowland, F. S. and M. J. Molina, "Chlorofluoromethanes in the Environment," AEC Report 1974-1, University of California, Irvine, CA, 1974.

Seitz, H., B. Davidson, J. P. Friend, and H. W. Feely, "Numerical Models of Transport Diffusion and Fallout of Stratospheric Radioactive Materials," Final Report on Project STREAK, USAEC Report NYO-3654-4, 1968.

Sullivan, H. M. and D. M. Hunten, "Lithium, Sodium, and Potassium in the Twilight Air-Glow," Can. J. Phys., 42, 937-956, 1964.

Telegadas, K., "Radioactivity Distribution in the Stratosphere from the Chinese High Yield Nuclear Test of June 27, 1973," ERDA Report HASL-298, Health and Safety Laboratory, January 1976.

Telegadas, K. and R. J. List, "Are Particulate Radioactive Tracers Indicative of Stratospheric Motions?" J. Geophys. Res., 74, 1339-1350, 1969.

Whitten, R. C., W. J. Borucki, and R. P. Turco, "Possible Ozone Depletions Following Nuclear Explosions," Nature, 257, 38-39, 1975.

Watson, R. T., "Rate Constants of ClO_x of Atmospheric Interest," J. Phys. Chem. Ref. Data, 6, 871, 1977.

Zeldovitch, Y. and Raizen, Y., Physics of Shock Waves and High Temperature Phenomena, p. 565, Academic Press, New York, 1967.

☆U.S. GOVERNMENT PRINTING OFFICE: 1980-311-588/114


FILM
7-8